19th World Congress of Soil Science

Symposium 1.3.1
Pedogenesis: ratios and ranges of influence

Soil Solutions for a Changing World,

Brisbane, Australia

1 – 6 August 2010

Table of Contents

Table of Contents (Cont.)

A holistic and universal view of soil

Donald L Johnson[A,B] and Diana N. Johnson[B]

[A]Department of Geography, University of Illinois, Urbana, Illinois, USA, Email dljohns@illinois.edu
[B]Geosciences Consultants, 713 So. Lynn St., Champaign, Illinois, USA, Email dn-jhnsn@illinois.edu

Abstract

The best scientific definition of any entity is one that is most useful and comprehensible to a spectrum of scientists and the lay public. It especially should be simply expressed, scientifically sound, easily explainable, and cover all cases. In sum, it should be clear, simple, logical, unequivocal, broad, and ideally universal. A definition of soil that meets these criteria that is applicable to soil on Earth and all other generally lithic-composed or non-gaseous celestial bodies is: *Soil is substrate at or near the surface of Earth and similar bodies altered by biological, chemical, and/or physical agents and processes.*

Key Words

Planetary-soils, biomantle, biota, bioturbation, pedogenesis, astropedology

Introduction

In the Elkhorn Slough Visitor's Center at the head of Monterey Bay, California, is a diorama titled "A Bountiful Bucket of Mud," showing a shore bird feeding in a bucket of mud from the adjacent slough. The diorama asks: "What lives in this much mud? 500 billion bacteria, 500 million diatoms, 50,000 protozoa, 50,027 worms, 5,000 crustaceans, 39 clams" (Figure 1). While we cannot vouch for the accuracy of the estimate, what we have learned over the last few decades about soil organisms and numbers suggests it may be low. But, aside from questions about biota, in pondering the diorama several other questions are raised. Does slough mud qualify as soil? If so, what is soil, and how should we define it? Should our definition apply only to Earth, or to Earth and all other generally lithic-composed planets and satellites – even biologically inert ones?

Figure 1. Marbled godwits feeding in slough soil, Elkhorn Slough, California (right photo by Robert Morris).

Does slough mud qualify as soil?

Yes, slough mud with its myriad organisms does qualify as soil, but it qualifies more in a natural state -- before being slurried as mud. While the conventional idea that soil forms on land has a long tradition, the idea that it might also form underwater also has long been espoused (e.g., Post, 1862; Dokuchaev, 1883; Robinson, 1930, and others). Such expressions as 'submerged soils,' submarine soils,' 'ocean soils,' 'freshwater soils,' and 'subaqueous soils' follow on this tradition, and now garner validity (Buurman, 1975; Soil Survey Staff, 1999, p. 9; Demas and Rabenhorst, 2001). However, while most above observers used the word "soil," they more likely were alluding to its normally organic-rich upper part – its biomantle, where most organisms live, metabolize, bioturbate, die, and re-assimilate.

What is soil?

Views and paradigms of soil have been in flux, not only for agronomists, soil scientists, and pedologists, but also for archaeologists, astropedologists, biologists, cosmologists, ecologists, foresters, geographers, geologists, oceanographers, and many others. Such a community of scientists must deal with a broad concept of soil, one that embraces both applied and pure science research, transcends multiple disciplines, and encompasses all environmental and disciplinary contexts. A definition of soil that is compatible with such an agenda is a necessary step. In advance of this task -- and to gain a sense of the entrenched mindsets that might resist such a broadened view of soil, we must briefly examine the gardener-farmer-agronomic practical traditions that underlie conventional views of soil, and that link traditional soil science tenuously to pedology, the two disciplines that claim soil as an object of study. Soil science has a broad societal practical agenda-domain that includes crop yields, soil amendments (fertilizers, pesticides, herbicides, fungicides), plant diseases, soil survey-classification-mapping, soil genesis, soil quality, soil and natural resources conservation and management, extension-outreach services, etcetera. The thematic domain of pedology, clearly overlapping somewhat, is narrower and less practical, with a focus on a scientific understanding of the nature of soil, how it forms, its properties, depth (thickness), its environmental functionality, and similar attributes -- subtle though very basic distinctions. (Some would include within the focused domain of pedology -- understandably, and with historic and philosophical justification -- soil survey, classification, and mapping.)

The question “What is soil?” was asked by Hungarian Professor Gorjanovic-Kramberger during a field excursion of the First International Conference on “Agrogeology” held in Budapest in 1909. As reported by Yarilov (1936), the professor “obtained a whole gamut of answers” by scientists from various countries, each revealing their different approaches and ethnic backgrounds. As most soil scientists and pedologists know, a general widely acceptable soil definition has been elusive, most reflecting the specialty and specific interests of the definer.

Two Gatekeeper Soil Documents

For most soil scientists, agronomists, horticulturalists, gardeners, farmers, and probably most ecologists, the answer to “What is soil?” may be simply that soil is what plants grow in. This was in fact a common definition in the 19th and 20th Century literature of soil in the agricultural sciences, and still is. Several similar, though more specific and lengthier, definitions are given in recent editions of two gatekeeper soil compendia, *Soil Survey Manual* (Soil Survey Division Staff, 1993, pp. 7-8), and *Soil Taxonomy* (Soil Survey Staff, 1999, p. 9), both hereafter referred to as *Manual* and *Taxonomy*. Both are conceptual and operational 'reference bibles' for many soil specialists and practitioners. Both also foster, in the first instance, a practical agronomic agenda where soil survey, classification, and mapping -- not necessarily ecologic functionality or biospherical understanding -- are principal stated goals. This practical focus defines the traditional domain of soil science, and is what separates it from pedology, whose focus, as stated, is a more purely scientific study of soil.

The 1999 *Taxonomy* has a distractingly long definition of soil, 360-plus words, very similar to *Manual’s* – both notable for their conceptual narrowness and limitations. First, like many definitions of soil, both are extensions of Dokuchaev’s late 19th Century ‘five factors’ model, updated in 1941 by Jenny, where Soils form as functions of climate, organisms, relief, and parent material over time: or S = f(clorpt). Even though the definition implicitly equates the ‘o’ factor to plants, built-in provisos limit soil depth on land to 2 m for purposes of survey and classification -- a strictly utilitarian (and arbitrary) contrivance. Depth of rooting, however, is actually far deeper for many plants (Nepstad *et al.*, 1994; Schenk and Jackson, 2002). Also for substrate to be considered soil, according to the agronomic definition, it must show evidence of horizonation and be capable of supporting rooted plants in natural environments. Substrates lacking either are "not-soil" or "non-soil". The definition includes shallow water substrates as soil, but only if plants are rooted in them, and then only to 2.5 m water depth. However, vascular plants in marine environments may root at water depths of 10-40 m, occasionally even 90 m (Hartog, 1970). In sum, soil depth in *Manual* and *Taxonomy* is arbitrarily set at 2 meters on land and 2.5 meters underwater -- all for the practical need to survey, map, and classify soils.

Such arbitrariness for defining the domain of soil, initiated in the late 1920s, understandable and perhaps necessary for its practical agenda, has created conceptual confusion, uncertainty, and even misinformation amongst pedologists. Additionally, such a plant based, agronomically inspired definition inadequately serves those in the broader Earth, marine, planetary, and environmental-ecological-ecosystemic sciences. Even amongst soil scientists, the definition inadequately explains many meters-thick biomantles in some humid tropical-subtropical soils (*Taxonomy*, p. 36; Fey 2009; van Breeman and Buurman 2002, p. 81; Johnson 1995; Johnson *et al.*, 2005; Morrás *et al.*, 2009), and their far deeper subsoil weathering zones and saprolites. Rooted plants can also grow in many different environments in totally non-soil contexts -- in air (on building roofs, parapets, gutters, walls, abandoned autos, as epiphytes on power lines, tree-trunks, and branches), as free-floating plants in water (aquatic hydrophytes, some with dangling water-roots), on animals (three-toed sloths, other animals), in quartz or gypsum sand, on rocks, under translucent quartzose-type rocks (even within some porous rocks), on freshly exposed bedrock cores of bulldozed mountains, on fresh unweathered quarry spoil, on vertical walls of bedrock quarries and buildings, and so on. Furthermore, emphasizing plants as a major -- or the major -- condition for defining soil sends two messages: Firstly, it underscores the deep gardener-farmer-agronomic pragmatic roots of the *Manual* and *Taxonomy* definitions. Secondly, it conceptually suppresses all other non-plant life forms that also play key roles – in many cases more important roles -- in producing soil. Such life forms comprise the deep, rich, and enormously diverse reservoir of organisms that, with plants, power Earth's ecosystems. Most of the myriad non-plant life forms on Earth spend at least part of their life cycles on or in soils and substrates, and to which most contribute their metabolic products while alive – and all contribute their bodies upon death. Non-plant life forms collectively far outnumber plants in both species and total numbers, by many orders of magnitude (Brussard *et al*., 1997; Nardi, 2007; Wall *et al*., 2001).

In fact, many members of all life form groups are involved in forming soil and likewise modifying substrate, and animals in bioturbationally sorting it to produce texturally distinct biomantles. No question exists regarding the role of plants in soil formation; the issue is the traditionally lopsided 'clorpt' emphasis on their role to the conceptual suppression of other biota. The 'o' in 'clorpt' is for all soil organisms, but its meaning in conventional-practical soil science has traditionally (and philosophically) meant plants. We submit that the consequence of linking the 'o' factor mainly with plants, plus the near-exclusive reliance on the 'clorpt' model for soil studies and teaching, has severely limited the kinds of questions we can ask to expand our understanding of soil genesis and the way Earth-systems operate. Further, regarding the condition that soils must display horizons or layers produced by pedogenic processes, we must remember that pedogenesis includes bioturbation, a preeminent upper soil process (Fey, 2009; Johnson *et al.,* 2005; Paton *et al.,* 1995; Schaetzl and Anderson, 2005; Wilkinson and Humphreys, 2005; Wilkinson *et al.,* 2009). Bioturbation can mix and destratify geogenic stratifications, plus mix preexistent soil horizons and create new ones in the process. Pedogenesis can alter any substrate, and its products should be considered soil even if only nannometers thick. But calling nannometer-altered substrate a soil or horizon, especially if disturbed and micromixed, falls outside of practical agronomic conventions of what soils and horizons are. (This raises technical questions of how might soil horizons and 'horizonation' be defined, and even what might constitute pedogenesis?) Further, in light of active space explorations and the search for extraterrestrial life, should a definition of soil be exclusively Earth-bound?

Universal Definition of Soil

So, how should we define soil insofar as it technically is the 'skin' of landforms, an integument of planets, and in the case of Earth primarily biophysically-biochemically produced with an epidermal biomantle? The best scientific definition is one that is most useful and comprehensible to a spectrum of scientists and the lay public. It should be simply expressed, scientifically sound, easily explainable, and cover all cases (Johnson *et al.* 1997), and ideally have universality. Being applicable to soil on Earth and on all other generally lithic-composed planets and planetoids, a definition that fits these criteria is: *Soil is substrate at or near the surface of Earth and similar bodies altered by biological, chemical, and/or physical agents and processes*.

The definition is brief and applies broadly and universally. The qualifier "or near" acknowledges that soil on at least one planet, Earth, has variable depth. It also covers subaqueous soils and their biomantles, for such -- even where applied to lacustrine and marine substrates, are still relatively near Earth's planetary surface. The two words also embrace notions of "suspended soils" (Kevan, 1962), and "soil body extensions" (Hole, 1981), which cover temporary aboveground pockets of organic-rich soil in rainforest canopies, and soil incorporated into nests of birds, wasps, termites, and other aboveground contexts. The words "or near" also cover wind-deposited soil on rooftops and other human structures (in which plants, insects, and other soil life invariably live), as well as temporary islands and rafts of vegetation-bound soil floating on rivers, estuaries, and lakes. The definition also covers soil that washes into bedrock cavities, caves, joints, fractures, and vugs in carbonate (limestone) and other rocks. Further, it focuses attention on the fact that one celestial body, Earth, is the only one that uniquely hosts all three agents and processes. The definition also accommodates the fact that 'soil' is now being increasingly applied to extreme substrate environments on Earth and other planets, including 'exotic' soils formed on such materials as ice, solid methane, and so on. Finally, the definition reminds us that soil is not simple, that we must recalibrate our thinking about soils, planetary soils, and soil in general, and that on Earth it is -- in the first instance, a predominantly biophysical and biochemical entity.

References

Brussard L, 17 co-authors (1997) Biodiversity and ecosystem functioning in soil. *Ambio* **26,** 563-570.

Demas GP, Rabenhorst MC (2001) Factors of subaqueous soil formation: a system of quantitative pedology for submerged environments. *Geoderma* **102**, 189-204.

Fey MV (2009) *Soils of South Africa*. Stellenbosch University, Stellenbosch, South Africa. (Craft Printing International, Ltd: Singapore).

Hartog C den (1970) The Sea-Grasses of the World. (North-Holland Publishing Co: Amsterdam)

Hole FD (1981) Effects of animals on soils. *Geoderma* **25**, 75-112.

Johnson, DL (1995) Reassessment of early and modern soil horizon designation frameworks and associated pedogenetic processes: are midlatitude A E B-C horizons equivalent to tropical M S W horizons? In Soil *Science (Trends in Agricultural Science).* (Ed. J Menon), pp. 77-91. (Council of Scientific Research Information, Trivandrum, India).

Johnson DL, Ambrose SH, Bassett TJ, Bowen ML, Crummey DE, Isaacson JS, Johnson DN, Lamb P, Saul M, Winter-Nelson AE (1997) Meanings of environmental terms. *Journal of Environmental Quality* **26**, 581-589.

Johnson DL, Domier JEJ, Johnson DN (2005) Animating the biodynamics of soil thickness using process vector analysis: a dynamic denudation approach to soil formation. *Geomorphology* **67**, 23-46.

Kevan DK, McE (1962) *Soil Animals.* (HF & G Witherby, Ltd: London).

Morrás H, Moretti L, Pícolo G, Zech W (2009) Genesis of subtropical soils with stony horizons in NE Argentina: autochthony and polygenesis. *Quaternary International* **196**, 137-159.

Nardi JB (2007) *Life in the Soil: A Guide for Naturalists and Gardeners*. (University of Chicago Press: Chicago).

Nepstad DC, de Carvalho CR, Davidson EA, Jipp PH, Lefebvre PA, Negreiros GH, da Silva ED, Stone TA, Trumbore SE, Vieira S (1994) The role of deep roots in the hydrological and carbon cycles of Amazonian forests and pastures. *Nature* **372**, 666-669.

Paton TR, Humphreys GS, Mitchell PB (1995) *Soils, A New Global View*. (Yale University Press: New Haven, London).

Schaetzl RJ, Anderson S (2005) *Soils -- Genesis and Geomorphology*. (Cambridge University Press: Cambridge UK).

Schenk HJ, Jackson RB (2002) Rooting depths, lateral root spreads and below-ground/above-ground allometries of plants in water-limited ecosystems. *Journal of Ecology* **90**, 480-494.

Soil Survey Division Staff (1993) *Soil Survey Manual*. US Department of Agriculture Handbook No. 18. (US Department of Agriculture, Washington DC).

Soil Survey Staff (1999) *Soil Taxonomy.* US Department of Agriculture, Natural Resources Conservation Service Handbook No. 436. (US Department of Agriculture, Washington DC).

Van Breeman N, Buurman P (2002) *Soil Formation* (2nd ed.). (Springer-Kluwer Academic Publishers: Dordrecht, Boston, London).

Wall DH, Adams G, Parsons AN (2001) Soil biodiversity. In 'Global Biodiversity in a Changing Environment: Scenarios for the 21st Century'. *Ecological Studies* **152**, 47-82.

Wilkinson MT, Humphreys GS (2005) Exploring pedogenesis via nuclide-based soil production rates and OSL-based bioturbation rates. *Australian Journal of Soil Research* **43**, 767-779.

Wilkinson MT, Richards PJ, Humphreys, GS (2009) Breaking ground: pedological, geological, and ecological implications of soil bioturbation *Earth Science Reviews* **97**, 257-272.

Yarilov AA (1936) A quarter of a century in the service of soil science and of propaganda amongst soil scientists. *Soil Research* **5**,184-186.

Characteristics and genesis of placic horizon in subalpine montane forest soils in northeastern Taiwan

Tzu-Yu Huang[A], Yu-Fang Chang[B], and **Chen-Chi Tsai**[C]

[A]Department of Forestry and Natural Resources, National Ilan University, Ilan, TAIWAN, Email roooykimo@yahoo.com.tw
[B]Department of Forestry and Natural Resources, National Ilan University, Ilan, TAIWAN, Email r9320005@yahoo.com.tw
[C]Department of Forestry and Natural Resources, National Ilan University, Ilan, TAIWAN, Email cctsai@niu.edu.tw

Abstract

Placic horizons occurred between the overlying E horizon and the underlying argillic or cambic horizon in the two subalpine forests, Chilanshan (CLS) and Szyuanyakou (SY) area. The thickness of the placic horizon in CLS area (Hapludults) was 20 mm, while that in SY area (Placorthods and Dystrudepts) was 30 to 60 mm. Redoximorphic features are evidence of wetness and of leaching and translocation of Fe. In both pedons, Fe_o/Fe_d ratios were much higher in the placic horizons compared with the other horizons. High clay contents in both pedons inhibited the downward movement of surface water. Reduction and oxidation processes associated with various favorable hydrological conditions are considered to be the main pedogenic processes that formed the placic horizons in soils in CLS area. Subsequent evolution of the landscape of the original soils in SY1 area, with partial truncation of the original soil and emplacement of a younger and deeper depositional material on the eroded surface, created the modern soil, which is classified as an Inceptisols. The environmental conditions, such as relatively flat landscape, clayey soil, and very high precipitation have enhanced this process.

Key Words

Placic horizon, temperate forest, soil characteristics, soil genesis, soil classification

Introduction

Placic horizons occur in a wide range of landscapes from temperate to tropical zones but are always associated with udic or perudic moisture regimes. Taiwan is located at the tropical and subtropical climatic zones. The subalpine forest regions are suitable for the formation of Podzolic soils, including Ultisols, Inceptisols, Entisols and Spodosols (Chen and Tsai, 2000). The Podzolic soils were formed at the elevation that is higher than 1900 m, cool and humid climate, high precipitation (3000 mm/year) mostly from April to October and with dominant coniferous vegetation type in Taiwan (Chen *et al*., 1989; 1995; Liu *et al*., 1994; Li *et al*., 1998; Hseu *et al*., 1999). However, in addition to sandstone, parent materials of subalpine forest areas of Taiwan also include shale or slate, which are easily weathered to a finer texture soil. In this condition, the water slowly flows into the soil and provides the cycling of reduced and oxidized (or wet and dry) conditions. The cycling of reduced and oxidized conditions is one of the important factors for the genesis of placic horizon in Taiwan (Chen *et al*., 1989, 1995; Clayden *et al*., 1990; Hseu *et al*., 1999). Therefore, the objectives of this study were (i) to evaluate and interpret the morphological and chemical characteristics of placic horizons occurring in subalpine forest in Taiwan and (ii) to explain the genesis of the placic horizons in these forest soils.

Methods

Site description

In northeastern Taiwan, three Ultisols with placic horizons in the Chilanshan (CLS) area and one Inceptisols and one Spodosols with placic horizons in the Szyuanyakou (SY) areas were selected (Table 1). The major parent materials of soils in the area are sandstone and shale, with minor amounts of slate. The slope of selected subalpine forest soils ranged from 3° to 20°, and the elevation of five soils ranged from 1840 to 1940 m above sea level (asl). The soil temperature regime in both pedons is mesic. The moisture regime in CLS area is perudic having a mean annual precipitation (MAP) of 3700 mm and in SY area is udic with 2280 mm MAP. However, the microrelief of the sampling sites appears to have modified the moisture regime toward perudic or aquic. The dominant vegetation in both sites is coniferous, composed of Taiwan red cypress (*Chamaecyparis formosensis* Matsum), Taiwan cypress [*Chamaecyparis obtusa* (Siebold & Zucc.)], Ranta fir (*Cunninghamia konishii* Hayata), and Willow fir (*Cryptomeria japonica* Hassk.). An herbaceous plant, Alpine silver grass (*Miscanthus transmorrisonensis* Hay.), is also common around SY area. In each study site, soil pits were excavated for the description of macromorphological soil characteristics as well as for the collection of soil samples according to standard procedures (Soil Survey Staff, 1993).

Table 1. Environmental characteristics and soil classification of five selected soil pedons in this study.

Pedon	Elevation (m)	Slope (degree)	Landscape position	Soil drainage	Parent material	STR[a]	SMR[b]	Soil classification[c]
					Chilanshan			
CLS-1	1840	3	summit	good	slate	mesic	udic	Typic Hapludults
CLS-3	1840	31	shoulder	good	slate	mesic	udic	Typic Hapludults
CLS-4	1880	20	shoulder	good	slate	mesic	udic	Typic Hapludults
					Szyuanyakou			
SY1	1940	10	summit	good	slate	mesic	udic	Typic Dystrudepts
SY3	1940	9	summit	good	slate	mesic	udic	Typic Placorthods

[a] STR = soil temperature regime

[b] SMR = soil moisture regime

[c] Based on Keys to Soil Taxonomy (Soil Survey Staff, 2006)

Laboratory analysis

Soil samples were collected from each horizon of five soil pedons for physical and chemical analyses. Soil samples were air dried and slightly ground to pass a 2-mm sieve. Bulk density was measured by cold method. Particle size distribution was determined by pipette method. Soil pH was determined with a soil/water ratio of 1:1 and soil/1 M KCl ratio of 1:2.5. Organic C was determined by the Walkley-Black wet combustion method. Cation exchange capacity (CEC) and exchangeable bases were measured using ammonium acetate extraction. Different forms of Fe and Al were extracted by dithionite-citrate- bicarbonate (DCB, Fe_d and Al_d), ammonium oxalate (pH 3.0, Fe_o and Al_o) and sodium pyrophosphate (pH 10.0, Fe_p and Al_p). Optical density of the oxalate extract (ODOE) of soils was also determined by ammonium oxalate. Potassium, Na, Ca, Mg, Fe, and Al were quantified by atomic absorption spectrometry.

Results

Soil macromorphology

All pedons have soil properties associated with Podzols and suggest strong eluviation and illuviation of soluble salts, Fe, Mn, and other materials. All albic E horizons have a massive structure that is enhanced by wet soil conditions and was identified as a redoximorphic feature. The poor drainage condition was further enhanced by current climate conditions characterized by high annual rainfall, low air temperature, and low evapotranspiration rate. The abundant coniferous vegetation is believed to have contributed to the climate. Gleyzation of the albic material was apparently affected by the poor drainage resulting from the underlying placic horizon (Hseu *et al*., 1999; Wu and Chen, 2005).The thickness of the placic horizons ranged from 2 to 6 cm. The placic horizon had colors of 2.5YR 5/8 in pedon CLS-1, 5YR 4/6 in pedon CLS-3, 7.5YR 5/8 in pedon CLS-4, and 5YR 5/8 in pedon SY1 and SY3. Two distinct phases were found in these placic horizons. A dark hard iron pan occurred in the upper part of the Bs horizon of pedon CLS-1, 3, and 4 accompanied by less-dense plasma immediately below the main pan. In the placic horizon of pedons SY1 and SY3, darker red iron bands and lighter dense plasma paralleled each other. The placic horizon in SY area was more brittle than the one in CLS area, as revealed by field test. The placic horizon is too dense to be penetrated by roots. The soil between E horizon and Bw horizon have an abrupt texture change. This change of clay content may affect vertical water movement and relate to the formation of the placic horizons of three pedons.

Pedogenesis of placic horizon in CLS and SY area

In soil of CLS area, the original dense plasma formed a thin layer that grew progressively as a result of Fe accumulation in the upper margins of the Bs horizons (Table 2). This probably reduced the percolation rate of surface water. The generally flat land surface (with minor irregularities and a 5% slope) and its continuity across the landscape could have enhanced perching of water on the surface of the clay soil. This may have in turn produced the irregular surface of albic horizon as well as the abrupt and wavy lower boundary of the placic horizon. These site and soil morphological features help to explain why water could have perched on top of the soil, saturating it and reducing Fe, which was then translocated vertically down through the E horizon. Reoxidization and precipitation of Fe occurred in the placic horizon. The chroma the Bs horizon of Pedon CLS-1, 3, and 4 suggests that the water did not stay long in this horizon. The growth of iron pan gradually impeded the normal water flow into the Bs horizons. Thus, the reducing condition occurred only within the eluvial horizon above the placic horizon and not in the Bs horizons. This is supposed by the barrier imposed by the pan to have retarded further precipitation of Fe, and this may account for the limited thickness the placic horizon in Pedon 1. In addition, the placic horizon further impeded the deposition of Fe, Al, or Mn in the lower B horizon.

Table 2. Results of selective dissolution analysis of selected soils in Chilanshan and Szyuanyakou area.

	DCB		Oxalate		Pyrophosphate		Al_o	$Fe_{p/o}$	$Fe_{o/d}$	$Al_{p/o}$	$Al_{o/d}$	ODOE[a]
Horizon	Fe_d	Al_d	Fe_o	Al_o	Fe_p	Al_p	$+1/2Fe_o$					
			g/kg				%					
						CLS-1						
A	8.40	2.64	4.06	1.90	3.72	2.62	0.39	0.91	0.48	1.38	0.72	1.67
E	2.08	2.07	0.89	1.79	0.40	2.53	0.22	0.45	0.43	1.41	0.86	0.40
Bsm	123	8.72	80.3	5.18	43.6	5.71	4.53	0.54	0.65	1.10	0.59	2.01
Bt	36.4	9.28	10.2	3.65	8.18	5.43	0.87	0.80	0.28	1.49	0.39	0.60
BC	33.4	10.8	7.31	3.08	6.16	3.27	0.67	0.84	0.22	1.06	0.29	0.36
Saprolite	18.7	6.78	7.73	4.40	5.99	4.36	0.83	0.77	0.41	0.99	0.65	1.27
						CLS-3						
OA	ND	1.26	2.55	1.41	1.70	2.05	0.27	0.67	ND[b]	1.45	1.12	0.29
A	25.3	3.49	27.2	2.51	23.9	2.91	1.61	0.88	1.08	1.16	0.72	2.69
AE	4.36	2.03	6.24	2.20	4.82	2.86	0.53	0.77	1.43	1.30	1.08	0.85
Bsm	195	10.8	161	7.96	94.3	7.02	8.85	0.59	0.83	0.88	0.74	--[c]
Bt	27.2	8.32	23.6	5.99	30.8	7.71	1.78	1.31	0.87	1.29	0.72	1.27
2E	17.9	2.49	5.29	1.55	8.10	2.52	0.42	1.53	0.30	1.63	0.62	0.40
2Bsm	122	10.1	115	7.27	56.3	6.61	6.48	0.49	0.94	0.91	0.72	0.78
2Bt	25.6	7.97	21.6	5.35	22.1	8.08	1.62	1.02	0.84	1.51	0.67	0.97
2BC	27.1	5.50	17.4	4.06	17.1	5.50	1.27	0.98	0.64	1.36	0.74	1.58
						CLS-4						
A	11.3	3.37	6.76	3.04	7.17	3.84	0.64	1.06	0.60	1.27	0.90	1.87
E1	5.19	0.59	4.25	1.14	4.14	1.21	0.33	0.98	0.82	1.06	1.93	0.42
E2	8.20	0.98	3.48	1.36	1.97	1.33	0.31	0.57	0.42	0.98	1.38	0.67
Bsm	111	4.82	75.8	3.05	41.9	2.75	4.10	0.55	0.68	0.90	0.63	--
Bt1	40.9	3.38	10.6	2.36	9.35	2.78	0.76	0.89	0.26	1.18	0.70	1.85
Bt2	27.0	7.34	15.5	5.11	16.8	5.76	1.29	1.08	0.57	1.13	0.70	2.92
BC	24.0	6.90	12.1	4.86	10.2	4.98	1.09	0.84	0.51	1.02	0.70	2.53
						SY1						
O	11.7	1.97	6.17	1.52	3.76	2.21	0.46	0.61	0.53	1.45	0.77	1.76
A	21.4	3.96	12.0	3.03	8.86	4.94	0.90	0.74	0.56	1.63	0.77	1.43
Bw	24.9	2.92	6.34	1.63	3.78	2.07	0.48	0.60	0.25	1.27	0.56	0.25
2E1	22.0	3.97	6.80	2.49	5.42	3.25	0.59	0.80	0.31	1.30	0.63	0.44
2Bsm	155	7.26	40.3	2.28	3.28	1.42	2.24	0.08	0.26	0.63	0.31	1.71
2E2	34.1	4.36	3.16	2.04	4.16	3.00	0.36	1.31	0.09	1.47	0.47	1.59
2Bw1	35.2	5.67	3.80	1.72	3.91	2.00	0.36	1.03	0.11	1.16	0.30	0.30
2Bw2	32.3	4.90	6.28	1.64	3.49	1.65	0.48	0.56	0.19	1.00	0.33	0.58
2BC	33.7	4.44	7.38	1.79	3.84	1.75	0.55	0.52	0.22	0.97	0.40	0.26
						SY3						
O	16.5	2.74	4.87	1.67	3.32	1.84	0.41	0.68	0.30	1.10	0.61	--
A	22.3	4.06	5.33	1.94	4.15	2.30	0.46	0.78	0.24	1.19	0.48	0.69
E	22.0	4.83	7.53	2.92	6.72	3.78	0.67	0.89	0.34	1.29	0.61	0.66
Bsm	--	--	--	--	--	--	--	--	--	--	--	--
Bw	34.3	4.86	6.85	2.35	7.66	3.24	0.58	1.12	0.20	1.38	0.48	0.24
BC	31.9	4.20	7.88	2.73	7.27	3.50	0.67	0.92	0.25	1.28	0.65	0.17

[a] optical density of oxalate extraction.

[b] ND = not detected

[c] -- = no data

In SY area, the landscape once had fairly uniform parent materials beneath it, much like the soil materials found in the horizons below the Bsm horizons. Classic podzolization processes, complexing of Fe, Al, and organic matter in well drained, very acid soil environments, mobilized Fe and C and translocated them together into subsoil horizons. A spodic horizon began to form in the original soils. Then, the landscape became unstable, perhaps due to climate change. Erosion stripped away the surface soils above the 2E1 horizon. The placic horizon effectively armored the landscape and prevented erosion from removing any of the soil beneath the placic horizon. New soil materials, perhaps colluvium washed down from higher landscapes, blanketed the landscape and rested above the erosion surface. The hydrological barrier caused by the placic horizon created a perched water table, saturating the younger soils above it, and leading to the reduction of Fe in 2E horizons of Pedon SY1. Lateral flow through the soil landscape above the placic horizon caused much of the reduced, mobile Fe to be removed via downslope leaching process. The 2Bsm horizon and the weakly developed 2Bw horizons beneath it are relic feature of an earlier cycle of soil genesis and landscape evolution. The soil horizons that provided the source of Fe to concentrate in the placic horizon are long gone. Therefore, the horizons currently above the placic horizon are much younger soil materials, and the development of redoximorphic features in them is also a much younger phenomenon.

Conclusion

Placic horizons occurred between the overlying E horizon and the underlying argillic or cambic horizon in the two subalpine forests, Chilanshan and Szyuanyakou area. Bifurcated iron pans occurred mixed with dense plasma within the placic horizon. The thickness of the placic horizon in CLS area (Hapludults) was 20 mm, while that in SY area (Placorthods and Dystrudepts) was 30 to 60 mm. Organo-Fe complexes in the placic horizon of Pedon CLS-1, 3, and 4 formed isotropic plasma separated by planar voids. Redoximorphic features are the evidence of wetness and by leaching and translocation of Fe. Pedons in CLS area had maximum Fe and organic C content in the placic horizon, whereas in SY area had only a maximum Fe content in the placic horizon. In both pedons, Fe_o/Fe_d ratios were much higher in the placic horizons compared with the other horizons. High clay contents in both pedons inhibited the downward movement of surface water. Reduction and oxidation processes associated with various favorable hydrological conditions are considered to be the main pedogenic processes that formed the placic horizons in soils in CLS area. Subsequent evolution of the landscape of the original soils in SY1 area, with partial truncation of the original soil and emplacement of a younger and deeper depositional material on the eroded surface, created the modern soil, which is classified as an Inceptisols. The environmental conditions, such as relatively flat landscape, clayey soil, and very high precipitation have enhanced this process.

Acknowledgements

The authors would like to thank National Science Council, Taiwan, for financially supporting this research under Contract No. NSC 95-2313-B-197-006-.

References

Chen ZS, Lin KC, Chang JM (1989) Soil characteristics, pedogenesis, and classification of Beichateinshan Podzolic soils, Taiwan. *Journal of the Chinese Agricultural Chemical Society* **27**, 145-155.

Chen ZS, Liu JC, Chiang HC (1995) Soil properties, clay mineralogy, and genesis of some alpine forest soils in Ho-Huan Mountain area of Taiwan. *Journal of the Chinese Agricultural Chemical Society* **33**, 1-17.

Chen ZS, Tsai CC (2000) Morphological characteristics and classification of Podzolic soils in Taiwan. *Soil and Environment* **3**, 49-62. (In Chinese, with English abstract tables and figures).

Clayden B, Daly BK, Lee R, Mew G (1990) The nature, occurrence and genesis of placic horizons. In ‘Proceedings of the Fifth International Soil Correlation Meeting (V-ISCOM) Characterization, Classification and Utilization of Spodosols’. (Eds JM Kimble, RD Beck), pp. 88-104. (1–14 Oct. 1988. Natl Soil Survey Lab, USDA-SCS: Lincoln, NE).

Hseu ZY, Chen ZS, Wu ZD (1999) Characterization of placic horizons in two subalpine forest Inceptisols. *Soil Science Society of American Journal* **63**, 941-947.

Li SY, Chen ZS, Liu JC (1998) Subalpine loamy Spodosols in Taiwan: Characteristics, micromorphology, and genesis. *Soil Science Society of American Journal* **62**, 710-716.

Liu JC, Yang JH, Chiang HC, Guo HY, Chen ZS (1994) Properties, clay mineralogy and pedogenic processes of two montane forest soils in Chi-lan area, Taiwan. *Journal of the Chinese Agricultural Chemical Society* **32**, 612-626.

Soil Survey Staff (1993) Soil Survey Manual. (USDA Agric. Handb. 18. U.S. Gov. Print. Office: Washington, DC).

Soil Survey Staff (2006) Keys to Soil Taxonomy. (10th ed., US Dept. Agric. - Nat. Res. Cons. Serv.: Washington, DC).

Wu SP, Chen ZS (2005) Characteristics and genesis of Inceptisols with placic horizons in the subalpine forest soils of Taiwan. *Geoderma* **125**, 331-341.

Characterization of Placic Horizons in Central Louisiana, USA

David C. Weindorf[A], Noura Bakr[A], Yuanda Zhu[A], Beatrix Haggard[A], Stephanie Johnson[A], and Jerry Daigle[B]

[A]LSU AgCenter, 307 MB Sturgis Hall, Baton Rouge, LA, 70803, USA, dweindorf@agcenter.lsu.edu
[B]USDA-NRCS, 3737 Government Street, Alexandria, LA, 71302, USA, jerry.daigle@la.usda.gov

Abstract

Placic horizons, indurated subsoil horizons of cemented iron and organic matter, have been scarcely recognized in soils of the United States. They have been described in highly leached, acid soils of Alaska, Washington, and Hawaii. A soil with similar morphology and physicochemical properties in central Louisiana was evaluated for possible placic recognition. Results conclusively indicate that the described pedon contains placic horizons. The moisture regime of the sampling location is important to its taxonomic classification. Presently, *US Soil Taxonomy* would define the soil as a Fine-loamy, siliceous, subactive, thermic, Placic Petraquept. However, if the site is found to be udic, adjustments to *US Soil Taxonomy* may be warranted to recognize this soil's unique properties within the taxonomic structure.

Key Words

Placic horizon, ironstone, ortstein, petroferric contact

Introduction

The placic horizon is defined by the Soil Survey Staff (2006a) as "a thin, black to dark reddish pan that is cemented by iron (or iron and manganese) and organic matter." A petroferric contact represents "a boundary between soil and a continuous layer of indurated material in which iron is an important cement and organic matter is absent or present only in traces (Soil Survey Staff, 2006a)." Ortstein is essentially an indurated spodic horizon or spodic materials of >25mm in thickness (Soil Survey Staff 2006a). A query of 23,543 soil series in the Soil Survey Staff's (2009) official soil series description database identified only seven soil series in the United States containing placic horizons; all occurring in Washington, Alaska, or Hawaii. While disparate in their location, they share several common features: 1) moderately to very strongly acid conditions, 2) average annual precipitation >177 cm, and 3) similar soil colors (very red). The thickness of the placic horizons in the seven soil series ranges from 2.5 cm to 10 cm, with finite gradations in hardness and color.

The presence of plinthite, fractured ironstone ledges, strong leaching conditions, and acidic, sandy soils in parts of Louisiana are conducive to placic horizon formation. The objectives of this study were to: 1) evaluate and interpret the morphological and chemical characteristics of suspected placic horizons occurring in a pedon in central Louisiana, 2) explain the pedogenesis of this soil, and 3) propose an appropriate classification of such soils per *US Soil Taxonomy* (Soil Survey Staff, 1999).

Methods

Description of study area

The study was conducted in Vernon Parish, LA in the Kisatche National Forest. The area falls within major land resource area (MLRA) 133B, the Western Coastal Plain (Soil Survey Staff, 2006b). The pedon described occurs along the high wall of a large sand/gravel pit at 31.0599 °N and 92.8954°W. Elevation at the site is ~95 m (LSU CADGIS, 2006). Climate of the area is characterized as moist subtropical, with both continental and marine influences. Summers are hot and humid and winters are cool with precipitation often caused by frontal passage. Average annual precipitation is approximately 150 cm. Soils mapped in the area include the Malbis (Fine-loamy, siliceous, subactive, thermic Plinthic Paleudult) and Ruston (Fine-loamy, siliceous, semiactive, thermic Typic Paleudult) soil series (Soil Survey Staff, 2009). Parent materials in the area consist of sandy and gravelly Pleistocene alluvium. The described pedon was on a convex, linear shoulder slope with a gradient of 1-5%. The site appears to be moderately well drained, with no evidence of flooding and none to slight erosion of natural habitat. The area is dominated by mixed hardwood (post oak) and coniferous (loblolly pine and longleaf pine) forest and mixed mid- and tall grasses such as little bluestem. Coarse fragments, in the form of gravel and cobbles, were estimated to cover ~35% of the surface.

Laboratory analysis

Particle size analysis was conducted using the hydrometer method with 24 h clay determination and sieved sands (53 µm) (Gee and Bauder, 1986). Sands were fractionated using nested sieves on a Ro-Tap sieve shaker.

Bulk density was determined using ring cores for disaggregated soil, and volume displacement for indurated horizons (Blake and Hartge, 1986). Soil reaction (pH) was determined via saturated paste, after equilibration for 24 h, using an Orion 2 Star pH meter (Thermo Scientific, Waltham, MA)(Salinity Laboratory Staff 1954). Electrical conductivity was evaluated on the soil paste using a model 4063CC digital salinity bridge (Traceable Calibration Control Company, Friendswood, TX)(Salinity Laboratory Staff, 1954). Loss on ignition organic matter was determined after 16 h at 400°C (Nelson and Sommers, 1996). Organic carbon was determined via titration following the Walkley-Black dichromate oxidation method (Nelson and Sommers, 1996; Walkley and Black, 1934). Poorly crystalline Fe (Fe_o) and Al (Al_o) were extracted via acid ammonium oxalate (Loeppert and Inskeep, 1996; McKeague and Day, 1966). Elemental quantification was conducted using a Ciros model inductively coupled plasma atomic emission spectrometer (Spetro Analytical, Marlboro, MA).

Results

Physical properties

Condensed results of soil physicochemical analysis are presented in Table 1. A number of key differences were observed between placic horizons (Bsm, Bsm', Bsm'', and Bsm''') and noncemented horizons. In the Bsm, Bsm'', and Bsm''' horizons, sand percentage was higher and clay percentage was lower than the immediately overlying horizons. Fractionated sands showed similar trends. Very coarse sand increased by >13% for each Bsm horizon compared to each overlying horizon. Given the macropores present in very coarse sands, the contrast in particle size between Bsm horizons and immediately overlying horizons likely served as a restrictive layer, limiting soil solution percolation. With downward movement of the soil solution stalled, dissolved iron and organic compounds would have begun to precipitate, triggering placic horizon formation. This mode of formation supports Clayden *et al.'s* (1990) theories on placic horizon genesis. The contrasting particle sizes within the pedon are relic features of ancient alluvial deposition. Soil bulk density was higher in the Bsm (3.25 Mg/m^3) and Bsm''' (2.84 Mg/m^3) horizons than the adjacent Bv2 (1.45 Mg/m^3) and 2C (1.59 Mg/m^3) horizons. Soil color varied dramatically throughout the pedon due to stratification of alluvial materials, plinthite, and differential oxidation of iron in relation to the Bsm horizons. With the exception of the A and Bw horizons, all other horizons were structureless (massive or single grain). Consistency of all Bsm horizons was very rigid as these horizons had to be broken from the profile with a hammer.

Chemical properties

Soil reaction (pH) ranged from extremely acid in the A (4.46) and Bv2 horizons (4.31) to very strongly acid in all other disaggregated horizons (4.60 to 4.86). A general trend of increasing pH with depth was observed (4.46 to 4.86). However, pH of each Bsm horizon was substantially higher than adjacent horizons above or below it. The placic nature of Bsm horizons in this pedon, however are dramatically defined by the loss on ignition organic matter (LOI_{OM}) levels. In each Bsm horizon, LOI_{OM} increases by ~3% to 6% compared to the overlying horizon. Organic carbon (OC) levels determined via Walkley Black methodology show the same pattern among horizons as the LOI_{OM} levels, but at a different magnitude. Cation exchange capacity (CEC) was low throughout the pedon, with all horizons ≤3.76 $cmol_c/kg$, and generally decreased with depth. The Bsm', Bsm'' and Bsm''' horizons, however, all showed higher CEC than adjacent horizons above or below them, owing to the elevated levels of organic material in these horizons. Acid ammonium oxalate extractable Fe and Al were inversely proportional to one another. In each Bsm horizon, Fe levels increased and Al levels decreased compared to overlying and underlying adjacent horizons.

Morphological properties and taxonomic classification

The wavy nature of the Bsm horizon formed semi-polygon features (large, rounded, oblong-shaped segregations of soil surrounded by hardened Bsm material) within the pedon (Figure 1A); the interiors of which were characterized by 7.5YR or 10YR hues while the exteriors (most susceptible to downward wetting fronts) were much redder with hues of 2.5YR or 10R. The indurated organo-Fe placic horizon varied in thickness from 0.5-4.0 cm and extended laterally for ~ 25 m. Scanning electron migrographs of the placic horizon show a nodular surface lamination (Figure 1B). Classification of the soil at this site rests largely on moisture regime. If the site is locally aquic, the proposed *US Soil Taxonomy* classification of the pedon would be Fine-loamy, siliceous, subactive, thermic, Placic Petraquept. Conversely, if the site is found to be udic, a larger quandary presents itself. Under the Udepts suborder in *US Soil Taxonomy*, Durudepts is a possible great group. However, examination of the language defining Durudepts clearly favors duripan recognition. It is noteworthy that 'Durudepts' occupy the same taxonomic position under Udepts that 'Petraquepts' occupy under Aquepts. Results from this study indicate that the introduction of a 'Petraudepts' great group (between Sulfudepts and Durudepts) may be warranted.

Table 1. Physicochemical soil properties of a pedon containing placic horizons in central Louisiana, USA.

		Munsell color						
Horizon	Depth	Soil	REDOX	Gravel	Texture†	Structure	Dry Consistence	Boundary
	----cm----			---%---				
A	0-51	2.5YR 4/6		4.4	SCL	W,M,SBK	MH	CW
Bv1	52-122	10R 4/8	7.5YR 6/8	-	SCL	MA	VH	CW
Bv2	123-267	2.5YR 5/6	7.5YR 6/8	7.2	SCL	MA	VH	AS
Bsm	268-274	2.5Y 2.5/1		-	LS	MA	VR	AW
C	275-280	10YR 5/8		12.9	S	SG	SH	AW
Bsm'	281-282	2.5Y 6/6		-	S	MA	VR	AW
Bw	283-301	5YR 5/6		2.3	LS	W,F,PL	SH	AW
Bsm''	302-303	10YR 4/4		-	S	MA	VR	AW
C'	304-332	5YR 5/6		3.2	LS	SG	SH	AS
Bsm'''	333-335	5YR 4/6		-	S	MA	VR	AS
2C	336-390	5YR 6/4		5.6	S	SG	SO	-

Horizon	pH	EC	OC	LOI_{OM}	CEC	BS	Fe_o	Al_o
		µs/cm	-------------%----------		$cmol_c$/kg	------%-----	------------mg/kg----------	
A	4.46	227	0.017	1.45	3.45	32.4	921	1280
Bv1	4.74	173.5	ND	0.84	2.65	20.0	507	1472
Bv2	4.31	134	ND	0.82	3.29	18.2	866	1378
Bsm	4.96	285	0.055	3.84	0.55	42.4	2034	665
C	4.72	150	ND	0.29	1.46	25.8	643	1149
Bsm'	5.87	444	0.151	6.48	2.37	10.9	1573	668
Bw	4.72	145.7	ND	0.43	1.04	42.1	624	940
Bsm''	5.11	260	0.119	6.44	2.58	7.9	1784	858
C'	4.60	74.5	ND	0.50	2.29	22.7	879	1565
Bsm'''	5.15	265	0.032	6.98	3.76	7.9	1691	599
2C	4.86	61.4	ND	0.18	0.54	59.5	256	711

†Soil Survey Staff (2002)

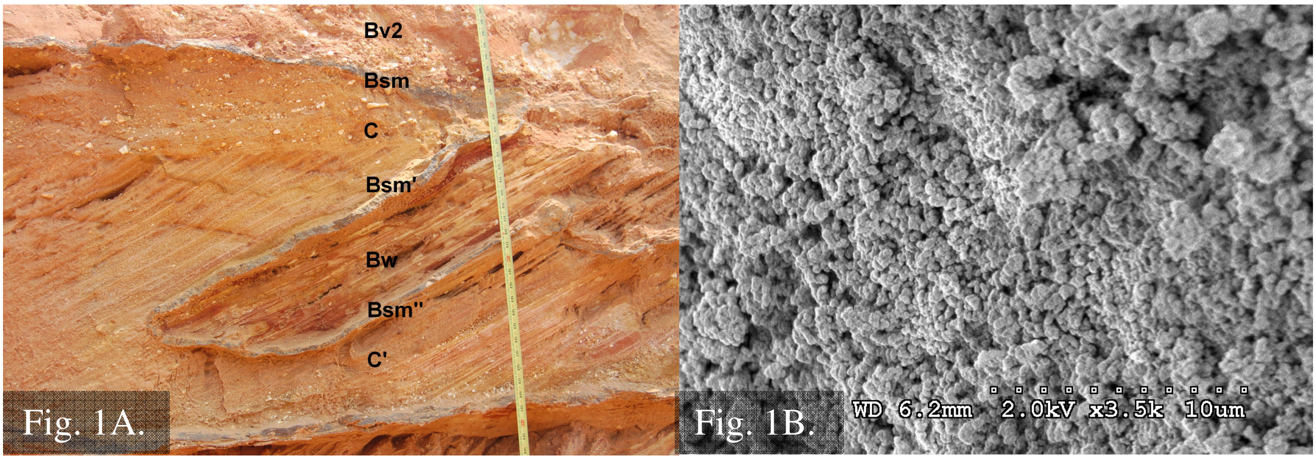

Figure 1. A) Soil profile containing wavy placic horizons, and B) scanning electron micrograph of the Bsm horizon in a pedon from central Louisiana, USA.

Conclusion

A pedon containing ironstone features in Vernon Parish, LA was evaluated to determine if its properties qualify as placic horizons. Results from soil physicochemical analysis confirm that multiple horizons within the pedon do qualify as placic horizons. This is highly significant since no soils with placic horizons have been mapped in the southern United States. The mode of formation is similar to findings by previous researchers (i.e. strong leaching conditions of acidic soils with placic horizon formation triggered by discontinuity in soil physical or chemical properties). Future research will focus on the spatial distribution of such soils in Louisiana and the southern United States to determine their extent.

References

Blake GR, Hartge KH (1986) Bulk density. In 'Methods of soil analysis, Part 1- Physical and mineralogical methods 2nd ed'. (Ed. A Klute) pp. 363-375. (Soil Science Society of America: Madison).

Clayden B, Daly BK, Lee R, and Mew G (1990) The nature, occurrence and genesis of placic horizons. In 'Proceedings of the Fifth International Soil Correlation Meeting (V-ISCOM) Characterization, Classification, and Utilization of Spodosols'. (Eds JM Kimble, RD Beck RD), pp. 88-104. (Natl Soil Survey Lab, USDA-SCS, Lincoln, NE).

Gee GW, Bauder JW (1986) Particle-size analysis. In 'Methods of soil analysis, Part 1- Physical and mineralogical methods 2nd ed'. (Ed. A Klute), pp. 383-411. (Soil Science Society of America: Madison).

Loeppert RH, Inskeep KP (1996) Iron. In 'Methods of soil analysis, Part 3 – Chemical methods'. (Ed. DL Sparks), pp. 639-664. (Soil Science Society of America: Madison).

LSU CADGIS (2006) Atlas: The Louisiana Statewide GIS [online]. LSU CADGIS Research Laboratory, Baton Rouge, LA. Available at http://atlas.lsu.edu.

McKeague JA, Day JH (1966) Dithionite- and oxalate-extractable Fe and Al as aids in differentiating various classes of soils. *Can. J. Soil Sci.* **46,** 13-22.

Nelson DW, Sommers LE (1996) Total carbon, organic carbon and organic matter. In 'Methods of soil analysis, Part 3 – Chemical methods'. (Ed. DL Sparks) pp. 961-1010. (Soil Science Society of America: Madison).

Salinity Laboratory Staff (1954) Diagnosis and improvement of saline and alkali soils. Agriculture Handbook No. 60. USDA. (US Government Printing Office: Washington).

Soil Survey Staff (1999) Soil taxonomy 2nd ed. USDA. (US Government Printing Office: Washington).

Soil Survey Staff (2002) Field book for describing and sampling soils version 2.0. USDA-NRCS. (US Government Printing Office: Washington).

Soil Survey Staff (2006a) Keys to soil taxonomy 10th ed. USDA-NRCS. (Pocahontas Press: Blacksburg).

Soil Survey Staff (2006b) Land resource regions and major land resource areas of the United States, the Caribbean, and the Pacific Basin. USDA-NRCS. Agriculture Handbook No. 296. (US Government Printing Office: Washington).

Soil Survey Staff (2009) Official soil series descriptions [online]. USDA-NRCS. Available at http://ortho.ftw.nrcs.usda.gov/cgi-bin/osd/osdquery.cgi.

Walkley A, Black IA (1934) An examination of the Degtjareff method for determining soil organic matter and a proposed modification of the chromic acid titration method. *Soil Sci.* **37,** 29-38.

Direct determination of allophane and imogolite in Andosols using nuclear magnetic resonance spectroscopy

Syuntaro Hiradate[A], Hideaki Hirai[B], Hitoshi Hashimoto[C]

[A]Biodiversity Division, National Institute for Agro-Environmental Sciences, Tsukuba, Ibaraki, Japan, Email hiradate@affrc.go.jp
[B]Faculty of Agriculture, University of Utsunomiya, Utsunomiya, Tochigi, Japan, Email hirai@cc.utsunomiya-u.ac.jp
[C]Agro-environmental Science Division, Hokkaido Central Agricultural Experiment Station, Yubari, Hokkaido, Japan, Email hasimoht@agri.pref.hokkaido.jp

Abstract

Allophane and imogolite are the major weathering products of volcanic materials at early stage of the soil formation processes of Andosols. In general, the amounts of allophane plus imogolite in soils are determined by a selective dissolution methods using acid-oxalate, although the accuracy of the indirect method is not well understood. In the present study, the amounts of allophane plus imogolite in Andosol profiles were determined directly by using solid-state ^{29}Si nuclear magnetic resonance (NMR) spectroscopy and compared the results with those by the selective dissolution method. The result suggested that the amounts of allophane plus imogolite determined by the both methods were roughly correlated for many Andosol samples. For soil samples containing large amount of pumice and organic materials, however, it was suggested that the acid-oxalate would underestimate and overestimate the amounts of allophane plus imogolite, respectively. Acid-oxalate is a convenient and well studied reagent to dissolve allophane and imogolite from soils, but it might not always be reliable depending on the properties of samples. Non-destructive determination by ^{29}Si NMR could validate the acid-oxalate analysis.

Key Words

Acid-oxalate, NMR, allophanic constituents, selective dissolution methods, volcanic ash soils, weathering

Introduction

Many soil properties have been characterized by responses to the addition of chemicals. For example, the amounts of allophane plus imogolite, which are poorly crystalline aluminosilicates, have been estimated from acid-oxalate extractable Si (Si_{OX}: Parfitt *et al*., 1983; Parfitt and Wilson, 1985; Wada, 1989; Parfitt, 1990; Dahlgren, 1994). However, if the acid-oxalate dissolves Si not only from allophane and imogolite but also from other soil components, then the amount of allophane plus imogolite could be overestimated. On the other hand, it is possible that not all allophane and imogolite are completely dissolved and the amount of allophane plus imogolite could be underestimated. Therefore, a non-destructive and direct analysis that can characterize soil samples without any chemical treatment would be helpful in characterizing soil properties and in confirming analyses determined by such chemical dissolution techniques.

Nuclear magnetic resonance (NMR) is one of the most powerful non-destructive and direct analytical tools used in the characterization and speciation of atoms. To characterize soils without any chemical treatment, NMR instruments should be optimized for the solid-state measurement, although their resolutions are much worse than those of liquid-state NMR (Hiradate, 2004). In the present study, the authors determined the amounts of allophane plus imogolite in soil samples from three representative allophanic Andosols in Japan by using solid-state ^{29}Si NMR, and the results were compared with those by the acid-oxalate extraction method.

Methods

Soil samples

Soil samples from the horizons of three allophanic Andosol profiles were collected in Tochigi Prefecture, Japan: Funyu (FF) soil at a broad-leaved and red pine mixed forest in Funyu Experimental Forests of Utsunomiya University in Shioya town; Kiwadashima (KF) soil at a broad-leaved forest in Imaichi city; and Kawaraya-cho (KO) soil at a reclaimed orchard land in an experimental field of Tochigi Prefectural Agricultural Experimental Station in Utsunomiya city. All of the three soils were classified into Silandic Andosols (FAO *et al*., 1998).

Chemical analyses

Soil samples were air-dried and sieved (< 2 mm). The amounts of acid-oxalate extractable Si (Si_{OX}) were determined following the method described by Blakemore *et al.* (1981).

Solid-state ^{27}Al and ^{29}Si NMR analyses

Solid-state NMR spectra of soil samples were recorded with an FT NMR system (Alpha 300, JEOL, Tokyo). Soils were finely ground with a mortar, and ~200 mg was tightly packed into a high-speed spinning NMR tube. Signals of ^{27}Al were recorded at 78.2 MHz in a single-pulse experiment without decoupling, and with a flip angle of $\pi/2$ for ^{27}Al (0.9 μs as a pulse width), an observation band of 80 kHz, a number of observation points of 4096 (resolution; 19.5 Hz), an acquisition time of 0.013 s, a pulse interval of 2 s, a number of scans of 600-22,000 (0.5-13 h), and 8 kHz of magic angle spinning (MAS). The standard chemical shift (0 ppm) was adjusted externally using 1 mol/L $AlCl_3$ solution. Signals of ^{29}Si were recorded at 59.6 MHz in a single-pulse experiment without decoupling, and with a flip angle of $\pi/2$ for ^{29}Si (5.0 μs as a pulse width), an observation band of 50 kHz, a number of observation points of 4096 (resolution; 12.2 Hz), an acquisition time of 0.082 s, a pulse interval of 10 s, a number of scans of 6,000-35,000 (16-99 h), and 6 kHz of MAS. Chemical shifts were quoted with respect to tetramethylsilane but were determined by referring to an external sample of silicon rubber (-22 ppm). A broadening factor of 100 Hz was employed in the Fourier transform procedure for all NMR experiments.

Results

Solid-state ^{27}Al NMR is able to differentiate tetrahedral ^{IV}Al (resonated at around 50 ppm) from octahedral ^{VI}Al (ca. 0 ppm). In Andosols, ^{IV}Al is incorporated in volcanic glasses, feldspars, and 2:1 aluminosilicates with isomorphic substitution in Si tetrahedral sheets containing Al, such as micaceous minerals, vermiculite, and beidellites, whereas ^{VI}Al is contained in Al-humus complexes, allophane, imogolite, gibbsite, and aluminosilicates having Al octahedral sheets such as micaceous minerals, montmorillonite, vermiculite, and kaolins (Hiradate, 2004). In solid-state ^{29}Si NMR spectra of Andosols, three major signals are detectable: allophane plus imogolite at -78 ppm, layer silicates at around -90 ppm, and SiO_2 including volcanic glass, quartz, cristobalite, opal phytoliths, and silica gel-like constituents at around -105 ppm (Hiradate, 2004). Fresh volcanic ash is composed mainly of volcanic glass (Shoji *et al.*, 1993), which gives resonance peaks at around 50 ppm in ^{27}Al NMR (corresponds to ^{IV}Al) and at around -105 ppm in ^{29}Si NMR (Hiradate and Wada, 2005). Although all the three soils analysed in the present study are younger than 25,000 ^{14}C y old, the major portion of these soil materials had been weathered and secondary components had been formed, as indicated by intensive resonance peak for ^{VI}Al than ^{IV}Al (Figure 1). Solid-state ^{29}Si NMR also suggested the rapid weathering of volcanic glass (ca. -105 ppm) into other components in the soils (Figure 1).

Barron *et al.* (1982) showed that imogolite in soils could be determined quantitatively by solid-state ^{29}Si NMR. It has also been shown that Si in allophane has identical chemical surroundings as those in imogolite, i.e., comprising isolated Si tetrahedron coordinated with three ^{VI}Al on gibbsite sheet and one H through O bonds, resulting in the same chemical shift (-78 ppm) in ^{29}Si NMR spectrum (Hiradate and Wada, 2005). Therefore, solid-state ^{29}Si NMR can detect both allophane and imogolite at -78 ppm. In the present study, it was clarified that allophane and imogolite were abundant in B horizons for all the tested soil profiles (Figure 1), probably because allophane and imogolite had been mainly formed in the B horizons. In the humus-rich A horizons, the amounts of allophane plus imogolite were much lower than those in the B horizons.

It has been believed that Si in allophane and imogolite is selectively dissolved by acid-oxalate. Therefore, the amount of allophane plus imogolite in soils has been estimated by multiplying the amount of Si dissolved by acid-oxalate (Si_{OX}) by a factor which had been determined from the chemical composition of allophane in soils, which is typically 7 for Al-rich allophane (Parfitt and Henmi, 1980; Parfitt and Wilson, 1985; Parfitt, 1990; Dahlgren, 1994; Dahlgren *et al.*, 2004). In the present study, the Si_{OX} values were compared with the amounts of Si determined by ^{29}Si NMR at -78 ppm (Si_{-78ppm}) which can be also assigned for allophane plus imogolite (Figure 2). It was shown that many of the Si_{OX} values were roughly correlated with Si_{-78ppm} values, but some samples deviated from 1:1 relationship. Soil samples from three horizons of KF soil, 4Bw, 4Bw2, and 4Bw3 horizons (Figure 2, ▲), which were composed mainly of Imaichi pumice, tend to show lower Si_{OX} values (44.1, 27.9, and 36.1 g/kg, respectively) than Si_{-78ppm} values (50.2, 68.0, and 56.0 g/kg, respectively), indicating that at least a part of Si in allophane and imogolite in these samples was not dissolved by acid-oxalate. For the uppermost horizons of FF, KF, and KO soils (Figure 2, ●), Si_{OX} values (11.7, 9.8, and 22.2 g/ kg, respectively) were significantly higher than Si_{-78ppm} values (4.2, 5.4, and 7.1 g/kg, respectively). It might be possible that acid-oxalate dissolves Si not only from allophane and imogolite but also from other soil components.

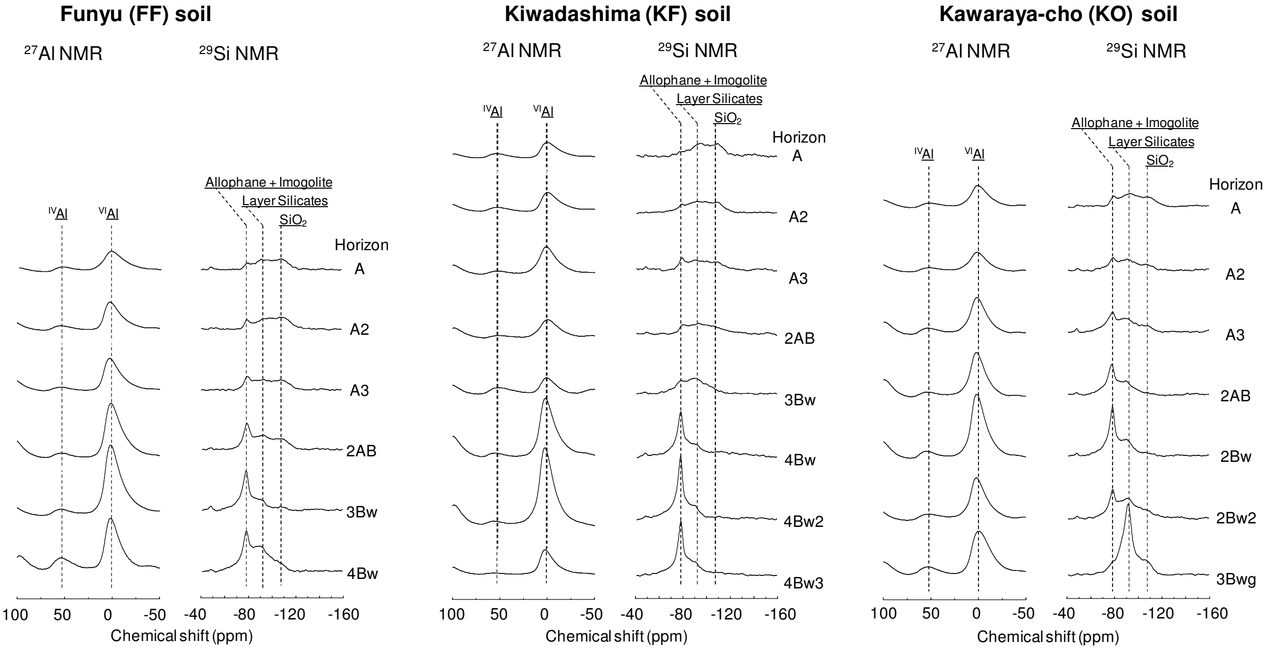

Figure 1. Solid-state MAS ^{27}Al and ^{29}Si NMR spectra of soil samples from three allophanic Andosols, named Funyu (FF), Kiwadashima (KF), and Kawaraya-cho (KO) soils. The y-axes of NMR spectra for each nuclide are adjusted to the same scales.

The acid-oxalate is a convenient and well-studied reagent to dissolve allophane and imogolite from soils, but it might not always be reliable depending on the properties of samples. Non-destructive determination by ^{29}Si NMR could validate the acid-oxalate analysis.

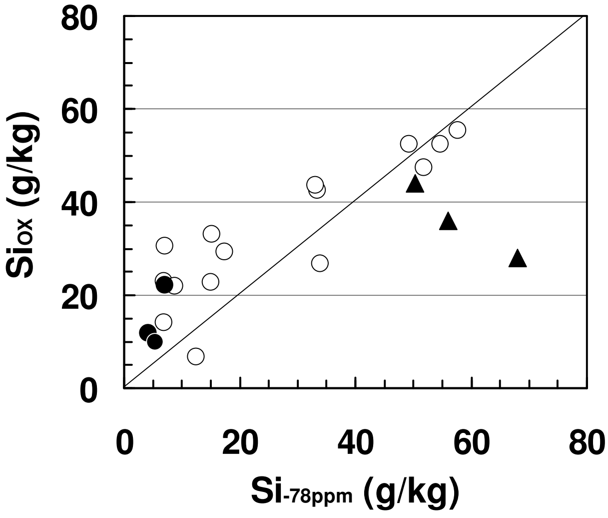

Figure 2. Comparison of the amount of Si dissolved by acid-oxalate (Si$_{OX}$, y-axis) and the amount of Si determined at -78 ppm by solid-state MAS ^{29}Si NMR (Si$_{-78ppm}$, x-axis) for soil samples from Funyu (FF), Kiwadashima (KF), and Kawaraya-cho (KO) soils. ●; uppermost horizons, ▲; 4Bw, 4Bw2, and 4Bw3 horizons of Kiwadashima (KF) soil (composed mainly of Imaichi pumice), ○; other horizons.

Conclusion

Atomic status of Al and Si in three allophanic Andosol profiles from Japan were non-destructively analysed with solid-state ^{27}Al and ^{29}Si NMR. It was observed that ^{IV}Al in volcanic glass was weathered into ^{VI}Al and Si was converted into allophane and imogolite especially in B horizons. For some samples, the amounts of allophane and imogolite determined by the acid-oxalate dissolution method were significantly different from those by ^{29}Si NMR. It might be possible that the acid-oxalate method might not always be reliable depending on the properties of samples. Non-destructive determination by ^{29}Si NMR could validate the acid-oxalate analysis.

References

Barron PF, Wilson WA, Campbell AS, Frost RL (1982) Detection of imogolite in soils using solid state ^{29}Si NMR. *Nature* **299,** 616-618.

Blakemore LC, Searle PL, Daly BK (1981) Methods for chemical analysis of soils. New Zealand Soil Bureau Scientific Report **10A**, DSIR, New Zealand.

Dahlgren RA (1994) Quantification of allophane and imogolite. In 'Quantitative Methods in Soil Mineralogy'. (Eds. Amonette E, Zelazny LW), pp. 430-451. (Soil Science Society of America: Madison).

Dahlgren RA, Saigusa M, Ugolini FC (2004) The nature, properties and management of volcanic soils. *Advances in Agronomy* **82,** 113-182.

FAO, ISRIC, ISSS (1998) World Reference Base for Soil Resources. In 'World Soil Resources'. Reports 84. (FAO: Rome).

Hiradate S (2004) Speciation of aluminum in soil environments; application of NMR technique. *Soil Science and Plant Nutrition* **50,** 303-314.

Hiradate S, Wada S-I (2005) Weathering process of volcanic glass into allophane determined by ^{27}Al and ^{29}Si solid state NMR. *Clays and Clay Minerals* **53,** 401-408.

Parfitt RL (1990) Allophane in New Zealand; a review. *Australian Journal of Soil Research* **28,** 343-360.

Parfitt RL, Henmi T (1980) Structure of some allophanes from New Zealand. *Clays and Clay Minerals* **28,** 285-294.

Parfitt RL, Wilson AD (1985) Estimation of allophane and halloysite in three sequences of volcanic soils, New Zealand. *Catena* **7,** 1-8.

Parfitt RL, Russell M, Orbell GE (1983) Weathering sequence of soils from volcanic ash involving allophane and halloysite, New Zealand. *Geoderma* **29,** 41-57.

Shoji S, Nanzyo M, Dahlgren RA (1993) Volcanic Ash Soils. Elsevier Science Publishers, Amsterdam.

Wada K (1989) Allophane and imogolite. 2nd edition. In 'Minerals in Soil Environments'. (Eds JB Dixon, SB Weed) pp. 1051-1087. (Soil Science Society of America; Madison).

Distribution and formation conditions of gibbsite in the upland soils of humid Asia: Japan, Thailand and Indonesia

Tetsuhiro Watanabe[A], Shinya Funakawa[B] and Takashi Kosaki[C]

[A]Graduate School of Agriculture, Kyoto University, Kyoto, Japan, Email nabe14@kais.kyoto-u.ac.jp
[B]Graduate School of Agriculture, Kyoto University, Kyoto, Japan, Email funakawa@kais.kyoto-u.ac.jp
[C]Graduate School of Urban Environmental Sciences, Tokyo Metropolitan University, Tokyo, Japan, Email kosakit8@tmu.ac.jp

Abstract

Gibbsite is considered to be an ultimate product of weathering. However, soils in temperate regions such as Japan usually contain gibbsite, whereas some strongly weathered soils in tropical regions do not. We investigated gibbsite distribution in humid Asia (Japan, Thailand and Indonesia) and the relationship between gibbsite and soil solution to explain distribution according to soil forming factors. Clay mineralogy was determined by X-ray diffraction and differential thermal analyses. The chemical composition of soil water extract (indicative of field soil solution) was determined to evaluate minerals' thermodynamic stability. Relatively large amounts of gibbsite were found in the Japanese soils, and no or small amounts in the soils from Thailand and the Java-Sumatra and East Kalimantan region of Indonesia. In Japanese soils the distribution of gibbsite, in which $H_4SiO_4^0$ activity was high enough to be in the kaolinite stability field, was explained by 1) rapid precipitation or formation of gibbsite, and its conservation due to low temperature, which retards resilication to more stable kaolinite under a given $H_4SiO_4^0$ activity, or 2) intense leaching resulting in low $H_4SiO_4^0$ activity. In Thailand and the Java-Sumatra region, high temperatures may enhance formation of the more stable minerals kaolinite and smectite. In contrast to Thai and Indonesian soils, Japanese soils are characterized by an abundance of Al hydroxides or gibbsite, as well as amorphous Al hydroxides and interlayered Al hydroxides between 2:1 layers.

Key Words

$H_4SiO_4^0$ activity; stability diagram; soil solution; weathering.

Introduction

It is widely accepted that gibbsite is "the ultimate end product of weathering", and is usually present in high concentrations in old and weathered soils such as Oxisols and Ultisols. Gibbsite is also found commonly in young soils, i.e. Inceptisols and Andisols. The occurrence of gibbsite in these young soils is usually ascribed to the rapid desilication that occurs in very permeable materials under high rainfall or to paleoclimate. In contrast, Green and Eden (1971), Herrmann *et al.* (2007) and Vazquez (1981) have determined gibbsite occurrence in soils in the initial stages of weathering in southwest England, northern Spain and northern Thailand, respectively. In humid Asian regions such as Japan, Thailand and Indonesia, information on gibbsite distribution is still scarce. The geological conditions of these regions, characterized by steep topography caused by intense orogenesis and small areas of Oxisols, differ significantly from those of the South American and African shield areas, and differences in gibbsite distribution patterns is to be expected. Characterizing gibbsite distribution and formation conditions will deepen our understanding of soils in these regions.
Thermodynamic analysis and weathering indices help to elucidate the formation conditions of clay minerals. Thermodynamic analysis of soil solution is useful for the theoretical understanding of clay mineral distributions and weathering trends (Watanabe *et al.* 2006). $H_4SiO_4^0$ activity controls mainly the relative stability of gibbsite, kaolinite and smectite: gibbsite is most stable under strong leaching conditions with low $H_4SiO_4^0$ activity, whereas kaolinite is stable under moderate $H_4SiO_4^0$ activity conditions and smectite is stable under restricted drainage with high $H_4SiO_4^0$ activity conditions. Among soil weathering indices, total reserve in bases (TRB) and the relative content of crystalline iron oxides are most common.

The objective of this study is to investigate soil gibbsite distribution in extensive regions of Japan, Thailand and Indonesia, and to discuss gibbsite formation conditions through thermodynamic analysis and weathering indices, which will increase our understanding of soils in these regions.

Materials and methods

Soils

We collected soil samples from Japan, Thailand and Indonesia, according to the soil distribution patterns in the respective regions based on geology and climate. Climatic conditions differ between the regions and soil temperature and moisture regimes are mesic/thermic-udic in Japan, isohyperthermic-ustic in Thailand, and isohyperthermic-udic in Indonesia. Soil parent materials reflect their geological conditions. Parent materials of soils from Japan, where volcanic belts are distributed, include felsic igneous and sedimentary rocks, and tephra. The soils in Thailand are formed on sedimentary and felsic igneous rocks. The soils from Java and Sumatra, where volcanic belts are also distributed, are formed on andesite, tephra, sedimentary rocks, and limited areas of felsic rocks. Most of East Kalimantan, Indonesia is underlain by sedimentary rocks, there are no active volcanoes, and soils are more weathered on stable rolling landscapes.

Types of soils investigated were common in each region. Japanese soils consist mostly of Udepts, Thai soils Ustults and Humults, Java-Sumatra's Udepts and Udults, and East Kalimantan's Udults. Oxisols are restricted to very limited areas of humid Asia and were not included in the samples.

Analytical methods

Clay minerals were identified by X-ray diffraction (XRD). Gibbsite and kaolin minerals in the clay fraction were quantified by differential thermal analysis (DTA). Before DTA, iron oxides were removed by citrate-dithionite-bicarbonate treatments. Fe (Fe_o) was extracted with ammonium oxalate in the dark. Fe (Fe_d) was also extracted with citrate-dithionite-bicarbonate. Total elemental analysis was made with HF and HClO.

The weathering indices, TRB and (Fe_d-Fe_o)/Fe_{total} ratio were calculated; TRB is the sum of basic cations (Ca+Mg+K+Na) and gives a chemical estimation of weatherable minerals, and the (Fe_d-Fe_o)/Fe_{total} ratio indicates the relative content of crystalline iron oxides.

For thermodynamic analysis on the stability of minerals, soil water extracts, of which composition gives an indication of soil solution composition in the field, were collected by continuously shaking the soils for 1 week at 25°C and 1 atm with a soil to water ratio of 1:2. In these samples, pH and Si, Al, Ca, Mg, Na, K concentrations were determined. Inorganic monomeric Al species were determined by the method of Driscoll (1984). Ionic activities were calculated by the extended Debye-Hükel equation.

Results

Gibbsite detection by XRD and DTA

Results of XRD show that gibbsite was detected in most Japanese soils, whereas a gibbsite peak was usually very small or not detected in the other study regions (Figure 1a). In XRD analysis, a large part of Al hydroxide between the 2:1 layers remained even after heat treatment up to 350°C for Japanese, Thai and Java-Sumatra samples, while a small part remained for the East Kalimantan ones. The gibbsite content measured by DTA was high in Japanese samples, low in Thai and Java-Sumatra samples, and not detected in most East Kalimantan soils (Figure 1b).

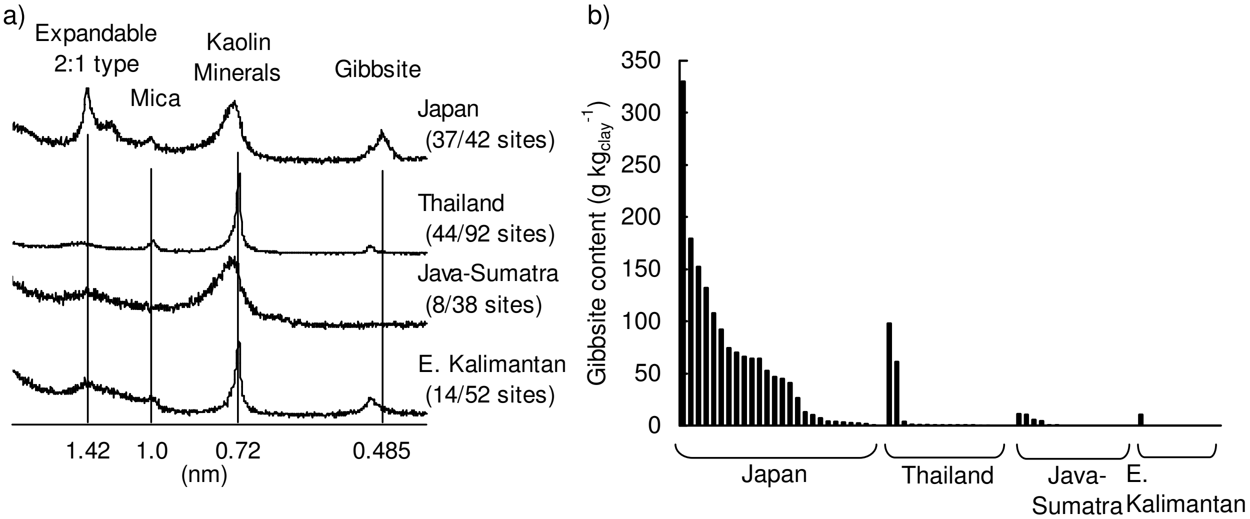

Figure 1. Gibbsite detection by X-ray diffraction (a) and differential thermal analysis (b). Number of sites where gibbsite was detected by X-ray diffraction is in the parentheses.

Weathering indices

Weathering indices indicated that Japanese and Java-Sumatra soils were younger than those in Thailand and East Kalimantan (Figure 2). The (Fe_d-Fe_o)/Fe_{total} ratio, indicating the relative content of crystalline iron oxides, was low in Japanese and Java-Sumatra soils (mostly less than 0.6), and high in Thai and East Kalimantan soils (mostly more than 0.6). TRB values, giving a chemical estimation of weatherable minerals, were high in Japanese, Java-Sumatra and Thai soils, with averages of 128, 136 and 106 $cmol_c\ kg^{-1}$, respectively. The TRB values in East Kalimantan soils were smaller than in the other regions, with an average of 69 $cmol_c\ kg^{-1}$. The high values of TRB (Figure 2) and presence of 2:1 type minerals (Figure 1a) indicate that all the investigated soils still contain some amount of weatherable minerals, and are not as strongly weathered and desilicated as Oxisols or Ferralsols.

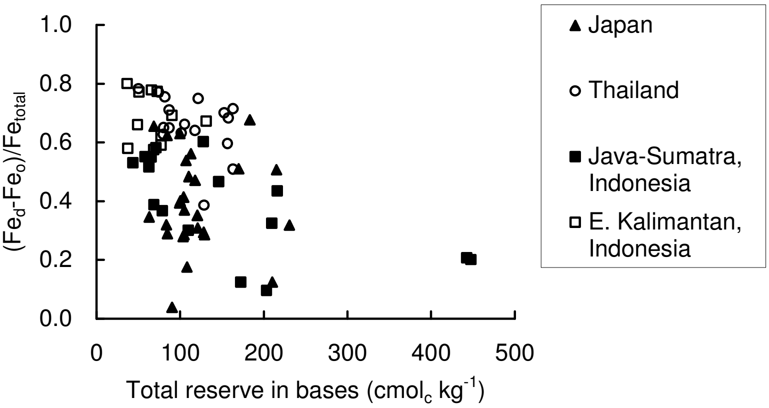

Figure 2. Weathering indices of the soils: total reserve in bases and relative content of crystalline iron oxides.

Composition of soil water extract

Most of the water extracts for Japan, Thailand and Java-Sumatra were supersaturated with gibbsite, indicating the possibility of gibbsite precipitation (Figure 3a). In contrast, East Kalimantan water extracts were undersaturated, indicating dissolution or non formation of gibbsite. Judging from $H_4SiO_4^0$ activity in the soil water extracts, kaolinite was considered to be the most stable mineral in most of the soils (Figure 3b). For the Java-Sumatra region, $H_4SiO_4^0$ activity in the soil water extracts was high and the extract compositions are close to or within the stablity field of smectite (Figure 3b). Composition of soil water extract indicated that gibbsite can form in Japanese soils where the composition is supersaturated with gibbsite (Figure 3a), but is unstable compared with kaolinite (Figure 3b).

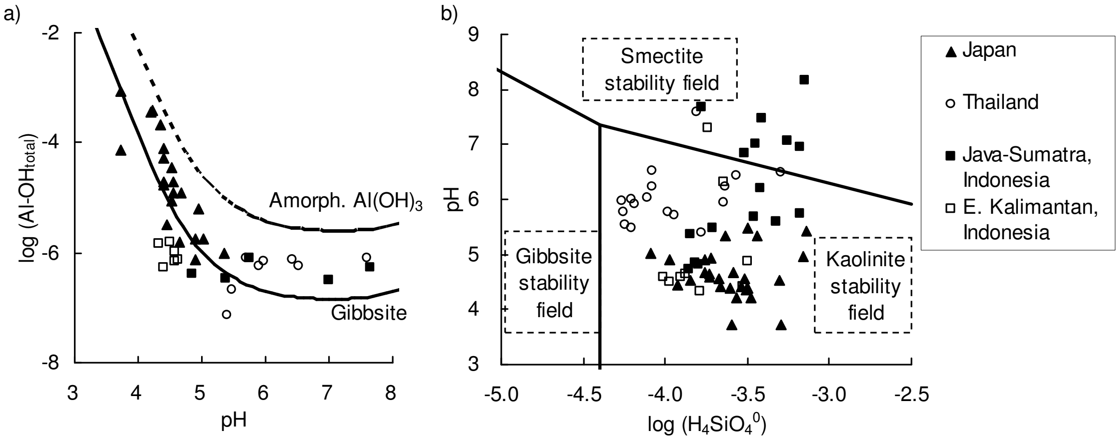

Figure 3. Composition of soil water extract plotted on a solubility diagram with gibbsite and amorphous $Al(OH)_3$ solubility lines (a) and a stability diagram representing relative stability of gibbsite, kaolinite and smectite.

Discussion

Gibbsite formation conditions in humid Asia

The presence of gibbsite in weakly weathered soils where soil water extract indicated that kaolinite or smectite is most stable can be explained by 1) a higher precipitation rate of gibbsite as a transient mineral than that of kaolinite in soil solutions supersaturated with gibbsite, or 2) low $H_4SiO_4^0$ activity due to rapid removal of soil solution or a high leaching rate. Both explain the formation of gibbsite in young soils that are not strongly desilicated. The former is demonstrated by May *et al.* (1986) as gibbsite formation under high $H_4SiO_4^0$ activity of the smectite stable range, which is explained by *Gay-Lussac-Ostwald Step Rule* (Sposito 1994). Synthesis of gibbsite in laboratory experiments is easy and rapid compared to that of kaolinite (Nagy 1995). The second factor is assumed in weathering saprolites and soils derived from volcanic ash (Huang *et al.* 2002).

Depending on gibbsite's precipitation rate, the regional differences in the amount of gibbsite between Japan and the tropical regions of Thailand and Java-Sumatra were presumably due to the difference in temperatures: high temperature in tropical regions stimulates chemical reactions and results in dominance of the most stable mineral or kaolinite, which may consume gibbsite, if present, precipitated as less stable mineral. Thus, the lifetime of gibbsite in tropical regions with high $H_4SiO_4^0$ activity, where kaolinite or smectite is stable, is short. On the other hand, the low temperatures in Japan are considered to inhibit the formation of kaolinite, and gibbsite remains as a transient mineral. Rapid removal of soil solution resulting in low $H_4SiO_4^0$ activity did not explain well the regional distribution pattern of gibbsite. The content of gibbsite in Japanese soils is higher than that in Indonesian soils, although the leaching in Indonesian soils seems to be as strong as or stronger than Japanese soils. The above explanations for the presence of gibbsite in young soils under cool temperature conditions seen in this study cannot be applied to the presence of gibbsite in Oxisols. The presence of gibbsite in highly weathered soils such as Oxisols on the shields in South America and Africa is supposed to be caused by strong desilication, where gibbsite is present as the most stable mineral.

Importance of Al hydroxides in Japanese soils

The occurrence of gibbsite as well as the other Al hydroxides, i.e. amorphous Al hydroxides and interlayered Al hydroxides (Watanabe *et al.* 2006) characterize Japanese soils in comparison to Indonesian and Thai soils. These Al hydroxides affect soil properties; amorphous Al and gibbsite contribute to acid neutralization in soils (Watanabe *et al.* 2008), cancel the negative charge in 2:1 layers (Funakawa *et al.* 2008), adsorb phosphorus (Huang *et al.* 2002) and accumulate soil organic matter (Imaya *et al.* 2007).

References

Driscoll CT (1984) A procedure for the fractionation of aqueous aluminum in dilute acidic waters. *International Journal of Environmental Analytical Chemistry* **16**, 267-283.

Funakawa S, Watanabe T, Kosaki T (2008) Regional trends in the chemical and mineralogical properties of upland soils in humid Asia: With special reference to the WRB classification scheme. *Soil Science and Plant Nutrition* **54**, 751-760.

Green CP, Eden MJ (1971) Gibbsite in weathered Dartmoor granite. *Geoderma* **6**, 315-317.

Herrmann L, Anongrak N, Zarei M, Schuler U, Spohrer K (2007) Factors and processes of gibbsite formation in Northern Thailand. *Catena* **71**, 279-291.

Huang PM, Wang MK, Kampf N, Schulze DG (2002) Aluminum hydroxides. In 'Soil Mineralogy with Environmental Applications'. (Eds JB Dixon, DG Schulze) pp. 261-289. (Soil Science Society of America: Madison).

Imaya A, Inagaki Y, Tanaka N, Ohta S (2007) Free oxides and short-range ordered mineral properties of brown forest soils developed from different parent materials in the submontane zone of the Kanto and Chubu districts, Japan. *Soil Science and Plant Nutrition* **53**, 621-633.

May HM, Kinniburgh DG, Helmke PA, Jackson ML (1986) Aqueous dissolution, solubilities and thermodynamic stabilities of common aluminosilicate clay-minerals - kaolinite and smectites. *Geochimica Et Cosmochimica Acta* **50**, 1667-1677.

Nagy KL (1995) Dissolution and precipitation kinetics of sheet silicates. In 'Chemical weathering rates of silicate minerals'. (Eds W A.F., SL Brantley) pp. 173-233. (Mineralogical Society of America: Washington, D.C.).

Sposito G (1994) Mineral solubility. In 'Chemical equilibria and kinetics in soils' pp. 93-137. (Oxford University Press, Inc.: New York).

Vazquez FM (1981) Formation of gibbsite in soils and saprolites of temperature-humid zones. *Clay Minerals* **16**, 43-52.

Watanabe T, Funakawa S, Kosaki T (2006) Clay mineralogy and its relationship to soil solution composition in soils from different weathering environments of humid Asia: Japan, Thailand and Indonesia. *Geoderma* **136**, 51-63.

Watanabe T, Ogawa N, Funakawa S, Kosaki T (2008) Relationship between chemical and mineralogical properties and the rapid response to acid load of soils in humid Asia: Japan, Thailand and Indonesia. *Soil Science and Plant Nutrition* **54**, 856-869.

Downward Thinking: Rethinking the “Up” in Soil Bioturbation

Alan F. Halfen[A], Stephen T. Hasiotis[B]

[A]Department of Geography, University of Kansas, 1475 Jayhawk Blvd., Rm. 213, Lawrence, Kansas, USA, Email afhalfen@ku.edu
[B]Department of Geology, University of Kansas, 1475 Jayhawk Blvd., Rm. 120, Lawrence, Kansas, USA, Email: hasiotis@ku.edu

Abstract

The nests of western harvester ants (*Pogonomyrmex occidentalis*) are extensive structures usually capped by a large conical mound. These ants have been documented to translocate significant amounts of soil and sediment to the surface; however, subsurface mixing patterns have not been investigated and documented. One thousand western harvester ants were added to a glass enclosure filled with discrete layers of homogeneous sediment to document this mixing. A 12-week experiment on nest development was conducted, during which (remarkable) translocation and mixing of sediment occurred. At the end of the experiment the distance and quantity of material translocated was measured. In sum, the ants excavated ~16% of the enclosure. Large amounts of this sediment were moved upward and significant amounts of material were moved down into the nest. Notably, ~51% of all excavated sediment was shown to be incorporated into the nest as backfill or tunnel lining. This material was neither translocated to the surface nor incorporated into the nest mound as traditionally thought. Our study demonstrates the significance of downward movement of sediments within soil. It also emphasises the underestimated role of soil-dwelling organisms, specifically the ant, in soil bioturbation and pedogenesis.

Keywords

Burrowing, pedogenesis, formicidae, soil biota, sediment mixing

Introduction

The acknowledgement that soil-dwelling organisms play a significant role in bioturbation, and thus pedogenesis, has been ascribed since the late nineteenth century (Darwin, 1881). Since Darwin’s initial observations, a wide range of related studies have been conducted examining soil biota’s role in pedogenesis. Many have recognized soil-dwelling social insects, particularly termites and ants, to be the most effect soil bioturbators found in soils today (e.g. Hasiotis, 2003). Some researchers have attempted to quantify the quantity of material excavated by ants (e.g. Baxter and Hole, 1967; Eldridge and Pickard, 1994; Humphreys and Field, 1998; Richards, 2009), while others have explored how excavated material influence the creation of soil mantels (biomantles) (e.g. Johnson, 1990). Other than Humphreys and Field (1998), these studies lack any observations of how ants move and mix sediment below the surface within and throughout subsurface. Understanding and quantifying the subsurface mixing of sediment by ants is important for understand the role soil-dwelling organisms play in soil pedogenesis. This paper quantifies and demonstrates the unobserved significance of the ant in the downward movement and subsurface mixing of sediments and soils.

Methods

Layers of sand, gravel, carbonate shells, and silty clay sediment were added to a 64 cm long x 120 cm high x 10.7 cm wide glass enclosure constructed as a three-sided wood frame with inset slots cut into the wood to hold two panes of glass, sealed with silicon caulk. Sediment was layered from the bottom of the enclosure as follows: 0-2 cm—carbonate shells, 2-12 cm—alluvial sand, 12-14 cm—red sand, 14-23 cm—alluvial sand, 23-24 cm—alluvial gravel, 24-32 cm—alluvial sand, 32-34 cm—green sand, 34-43 cm—alluvial sand, 43-44 cm—pink gravel, 44-54cm —alluvial sand, 54-56 cm—yellow sand, 56-64 cm—alluvial sand, 64-65 cm—blue gravel, 65-71 cm—alluvial sand, and 71-77 cm—silty clay top soil. Carbonate shells were coarse sand to granular in size; alluvial sand, medium to coarse; gravels, granular to pebble; and colored sand, medium to coarse. All layers were flattened and compacted before the next layer of material was added. Vegetation was transplanted with the silty clay top layer. Once filled, the entire enclosure was wetted. An ultra-violet (UV) light was placed atop the enclosure, and the grass was allowed to grow within the enclosure for 21 days. After 21 days, ~ 1000 western harvester ants were introduced to the enclosure. The ants were allowed to excavate uninterrupted for 12 weeks.

Sediment Mixing

A combination of digital images and traced gridded transparencies were used to estimate the quantity and distance of colored sediment moved from its respective horizons within the enclosure (see above for original depths and thicknesses). A digital image of the front side of the enclosure was loaded in Adobe Illustrator ® and calibrated so that a 64 x 80 cm, 1 cm grid accurately fit the image. The image size was constrained, relative to the grid, so that actual distance was maintained. Translocated sediment was marked on the digital grid with different colors representative of the different sediment layers (e.g. yellow for yellow sand, blue for blue pebbles). In some cases not all translocated sediments were visible in the digital image (e.g. yellow versus green sand). Therefore, these sediments were traced on a 1 x 1 cm gridded transparency and then added to the digital grid. Once all translocated sediment was added to the digital grid, the grid was printed on 11 x 17 paper the occurrence and depth of movement was recorded. The same procedure was used for the rear side of the enclosure.

The distance of translocated sediment was measured by counting the occurrence of a specific sediment in cm from the original horizon. Because it was not possible to accurately count individual grains of colored sand, the 1 x 1 cm grid was counted whenever colored sand was present as one occurrence, regardless of how full this area was. This method is acceptable since we are only measuring the distance grains were transported, not the volume of sediment transported. For shell, blue gravel, and pink gravel, individual pieces were counted as single occurrences because they could be visually differentiated.

The occurrence and depth of red sand, green sand, yellow sand, carbonate shells, blue gravel, and pink gravel was documented for both sides of the enclosure. Because the enclosure was 10.7 cm thick, 85% of the fill could not be seen through the front or rear glass sides. To account for translocated material not visible, the front side and rear side measurements were averaged and applied to the remaining unseen sediment. This provided an accurate estimate of the distance and number of occurrences of specific translocated sediment. In using this estimation we assume that sediment-mixing patterns observed from the front and rear of the enclosure are the same in the middle of the enclosure.

Volumetric Calculations

The total volume of excavated sediment for each layer in the enclosure was also estimated allying the procedure describe above. Digital images and gridded transparencies were used to trace open and backfilled galleries and chambers visible through the front and rear of the enclosure on a digital 64 x 80 cm, 1 x 1 cm grid. Once all passageways were traced, they were printed at a 1:1 scale and measured using a nylon string. The total distance of all passageways, backfilled and opened, were tabulated for each sediment horizon (see previous sections for depths and thicknesses) for the front and the rear of the enclosure (Table 1). We then assumed a network of galleries and chambers in the middle sediment comparable to the averaged length of those tunnels visible in from the front and rear of the enclosure. In doing so, we created an equation to estimate the total volume of sediment excavated during nest construction (Eq. 1). Sediment mixing rates were also calculated based on the volumetric measurements and assumed average bulk density measurement of ~1.60 g cm^{-3}.

$$v = \left(\left(\frac{L_f + L_r}{2} \right)_h \times \left(\frac{10.7}{x} \right) \right) \pi \left(0.5x\right)^2$$

Equation 1: L_f represent the total distance of passageways, in cm, on the front size of the enclosure and L_r the rear of the enclosure. h serves as a delineator of individual horizons or any cumulative total of horizons. x represents the mean diameter, in cm, of all galleries and chambers in the nest.

Results

In general, the majority of all sediment was translocated upwards towards the surface, although the ants did not always place the sediment at the surface. Sediment was moved a maximum distance of 84 cm, from the lowest reaches of the enclosure to the surface of the nest mound. Vegetation was also moved down into the nest 82 cm from the surface. Some degree of mixing occurred in all colored sediment layers with carbonate shells being moved up 84 cm; red sand being moved 72 cm upwards and 10 cm down; river gravel being moved upwards 62 cm and 21 cm down; green sand being moved upwards 52 cm and 30 cm down; pink gravel being moved upwards 40 cm and 42 cm down; yellow sand being moved upwards 28 cm and 52 cm down; blue gravel being moved upwards 20 cm and 42 cm down (Figure 1). All colored sediments appear to have a bimodal distribution with sediment displaced to the surface and sediment normally distributed above and below the position of the original sediment layer (Figure 1).

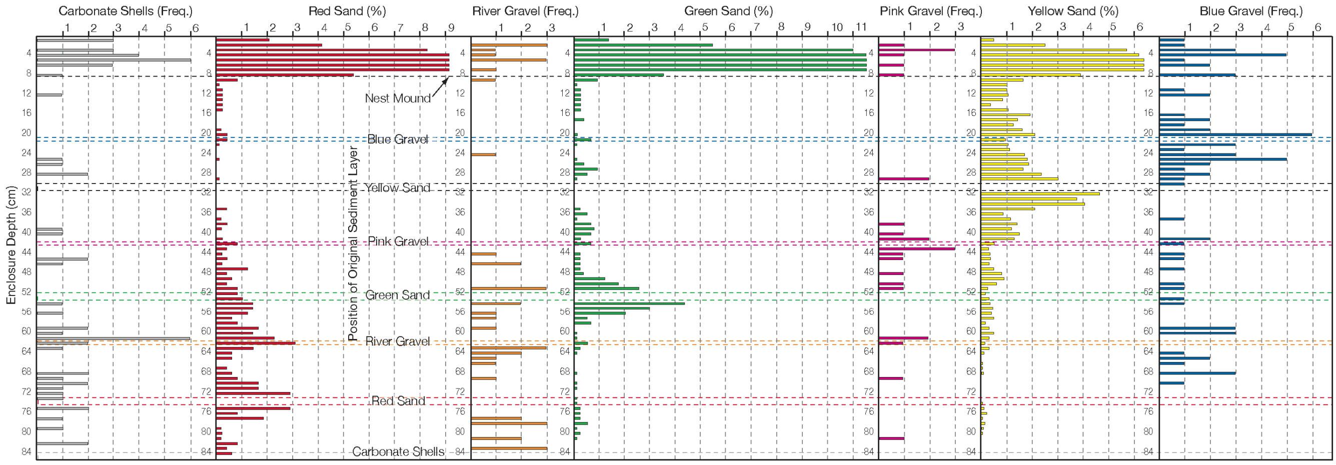

Figure 1. Distribution of colored sediment deposited at the end of the experiment. Depths are in cm and calibrated to the top of the nest mound. Original colored sediment horizons are marked with horizontal dashed boxes. Colored sand is represented as percent distributed of total. Colored gravel and carbonate shells are represented by frequency count of individual particles.

The calculated volume results show that 15.75% of the total 54,099.20 cm^3 sediment was excavated during the experiment (Table I). Considering individual sediment layers, most excavation took place in upper horizons (i.e., yellow sand and above) (Table I). The volume of the constructed nest mound was measured to be ~4,150 cm^3 and the total volume of excavated sediment was estimated to be 8,523.18 cm^3, indicating that ~51% of all sediment excavated in the nest was not placed at the surface and incorporated into the nest mound, but placed elsewhere in the nest below the surface. Simple sediment-mixing rates can be calculated with these data as well. A sediment-mixing rate of 28.55 kg yr^{-1} was calculated if examining the mound sediment alone. When incorporating the subsurface mixing, the rate of mixing increases to 58.64 kg yr^{-1}.

Discussion

Our experiment shows four significant results: 1) sediments were moved from all horizons to the surface, from horizons to other horizons, and from the surface back into the nest; 2) the distance of movement appears to be limited by the experiment, not the ants; 3) ~51% of all excavated material was either incorporated in the nest directly or after being deposited at the surface, not the mound; and 4) sediment-mixing rates can be calculated based on our results and indicate a much higher rates after accounting for surface and subsurface mixing of sediments.

It has been known that ants could bring material to the surface from deep in their nest, but no studies to our knowledge have observed the deliberate downward movement of sediment by ants. This multidirectional movement of sediment significantly alters the perceived sediment-mixing rates of ants. To begin with, mixing rates of ants are difficult to quantify because ants do not ingest the soil like earthworms, a measurable behaviour. Baxter and Hole (1967) quantified the rate of soil turnover at 35 ha-cm over a period of 3500 years, Eldridge and Pickard (1994) estimated that ants contributed 0.28 mm to the thickness of a soil per year, and Humphreys and Field (1998) showed that over a period of 17 years, 127 t ha^{-1} y^{-1} of sediment was mixed by ants. Only the mixing rate provided by Humphreys and Field (1998) is based in part on subsurface mixing, although the actual method of analysis is unclear. When considering past estimates of mixing rates, our experiment clearly demonstrates that sediment-mixing rates are much higher when subsurface sediment mixing is quantified. Ants not only play a significant role is soil formation and soil turnover by adding sediment to the surface, but also by directly altering and adding soil to lower horizons. This behaviour has a direct influence on soil pedogenesis.

Table 1. Volumetric estimates of excavated sediment for each horizon.

Sed. Horizon	Thickness (cm)	Total Volume (cm^3)[a]	Side 1 Galleries (cm)[b]	Side 2 Galleries (cm)[c]	Mean Galleries (cm)	Total Galleries (cm)[d]	Total Galleries Volume (cm^3)[e]	Material Excavated (% of each)[f]	Material Excavated (% of total)[g]
White Shells	2.00	1369.600	12.50	5.10	8.80	104.622	66.558	4.86%	0.13%
Reg. Sand	8.00	5478.400	77.70	84.60	81.15	964.783	613.769	11.20%	1.18%
Red Sand	2.00	1369.600	6.40	10.10	8.25	98.083	62.398	4.56%	0.12%
Reg. Sand	10.00	6848.000	81.70	76.70	79.20	941.600	599.020	8.75%	1.15%
Reg. Gravel	1.00	684.800	10.90	4.80	7.85	93.328	59.373	8.67%	0.11%
Reg. Sand	8.00	5478.400	60.30	65.10	62.70	745.433	474.224	8.66%	0.91%
Green Sand	2.00	1369.600	8.30	17.80	13.05	155.150	98.702	7.21%	0.19%
Reg. Sand	9.00	6163.200	131.80	114.70	123.25	1465.306	932.187	15.13%	1.79%
Pink Gravel	1.00	684.800	2.30	3.30	2.80	33.289	21.177	3.09%	0.04%
Reg. Sand	10.00	6848.000	194.60	218.20	206.40	2453.867	1561.083	22.80%	3.00%
Yellow Sand	2.00	1369.600	99.50	62.70	81.10	964.189	613.391	44.79%	1.18%
Reg. Sand	8.00	5478.400	193.60	211.50	202.55	2408.095	1531.964	27.96%	2.94%
Blue Gravel	1.00	684.800	27.60	5.30	16.45	195.572	124.418	18.17%	0.24%
Reg. Sand	6.00	4108.800	113.80	118.20	116.00	1379.111	877.353	21.35%	1.69%
Silty Clay	6.00	4108.800	114.70	120.00	117.35	1395.161	887.563	21.60%	1.71%
Total	**76.00**	**52044.800**	**1135.70**	**1118.10**	**1126.90**	**13397.590**	**8523.179**	**16.38%**	**16.38%**

[a] Total volume calculated: horizon thickness x 10.7 x 64, [b] Total tunnel length network visible from side 1, [c] Total tunnel length network visible from side 2, [d] Total tunnel length network (see text for details)
[e] Calculated usign equation 1 (see text for details), [f] Percent material excavated from each respective sediment horizon, [g] Percent material excavated from total enclosure volume

Conclusions

Quantities and distance of sediment moved by ants was estimated. In general, most movement was upward. Sediment was moved downward to the bottom of the nest as well. The volume of excavated sediment was calculated and shows that most excavated material was not placed at the surface and incorporated in the mound, but mixed and incorporated into the subsurface nest. This paper shows the significance of the ant in the deliberate downward movement and subsurface mixing of sediments and soils. This mixing plays an unobserved but present and important role in soil bioturbation and soil pedogenesis. More studies, specifically those that explore the mixing patterns of subsurface sediment, should be conducted on ants and other soil-dwelling organisms to further demonstrate their significance is soil pedogenesis.

References

Baxter FP, Hole FD (1967) Ant (Formica cinerea) pedoturbation in a prairie soil. *Proceedings of the Soil Science Society of America* **31**, 425-428.

Darwin, C (1881) ‘The formation of vegetable mould through the action of worms, with observations on their habits.’ (John Murray, London).

Eldridge DJ, Pickard, J (1994) Effects of ants on sandy soils in semi-arid eastern Australia: Relocation of nest entrances and consequences for bioturbation. *Australian Journal of Soil Research* **32**, 323-333.

Hasiotis ST (2003). Complex ichnofossils of solitary to social soil organisms: under- standing their evolution and roles in terrestrial paleoecosystems. *Palaeogeography, Palaeoclimatology, Palaeoecology* **192**, 259-320.

Humphreys GS, Field R (1998) Mixing, mounding and other aspects of bioturbation: implications for pedogenesis. *16th World Congress of Soil Science Abstracts*.

Johnson DL (1990) Biomantle evolution and the redistribution of earth materials and artifacts. *Soil Science* **149**, 84-102.

Richards PJ (2009) *Aphaenogaster* ants as bioturbators: Impacts on soil and slope processes. *Earth-Science Reviews* **96**, 92-106.

Formation of volcanic ash soils in the Matese Mountains of southern Italy

V.M., Sellitto[a] , G. Palumbo[a], C.Colombo[a], F. Terribile[b]., D. G. Schulze[c]

[a]Dip. di Scienze Animali, Vegetali e dell'Ambiente, Via De Sanctis, 86100 Campobasso, Italy colombo@unimol.it
[b] Dip di Scienze del Suolo , della Pianta e dell'Ambiente Via Università, 100 - 80055 Portici Italy
[c] Agronomy Dept., Purdue University, Lilly Hall of Life Sciences, 915 W. State St., West Lafayette, IN 47907-2054

Abstract

Over the past 40 ka, there have been many explosive eruptions in southern Italy from Campi Flegrei that have dispersed pyroclastic material in the southern Apennines surrounding the Matese Massif . A detailed mineralogical study was conducted on 5 pedons sampled on the Matese Massif to study volcanic ash soil genesis. All pedons contained vermiculite, mica, kaolinite and some interstratified mica-kaolinite. The diffraction patterns presented weak peaks, indicating a low mineral content and the presence of materials that did not diffract strongly, most likely allophane and unweathered volcanic glass and sanidine. The mica was most likely primary mica that crystallized along with the sanidine. The vermiculite was a weathering product of the mica. We assume that the finest ash cools faster, resulting in a glass, whereas the larger particles cool slower, resulting in sanidine and mica. Sanidine and mica weathering released K and Na ions, which leached from the profile, resulting in halloysite crystallization. We also identified gibbsite in the deepest horizons of 2 profiles. The sequence of pyroclastic deposits and the mineralogical evidence demonstrate the important contribution of the Campi Flegrei pyroclastic products on volcanic ash soil genesis in the southern Apennines.

Key words

Andic properties, halloisite, volcanic ash soils, aluminium oxides.

Introduction

The Matese Massif represents a wide calcareous relief located in southern Italy. The highest peaks are Mt. Miletto (2050 m), La Gallinola (1923) and Mt. Mutria (1823 m). The Matese Massif is part of the Mesozoic-Cenozoic carbonate platform domain. The geomorphologic features which characterize the Matese Massif and its northern border range from those typical of an upper mountain environment (glacial to periglacial landforms and deposits) to those of a fluvial to lacustrine environment. Its geomorphologic evolution appears strongly linked to tectonic and litho-structural controls, as well as to the high solubility of the carbonatic succession that has produced a rich karst landscape and diffuse endokarst phenomena. The Matese Massif represents one of the main karst aquifers of the Central-Southern Apennines. Groundwater percolates about 1500 m since it reaches the basal karst level. Over the past 40 ka, many eruptions of volcanoes in southern Italy were explosive and largely related to the Campi Flegrei and Somma-Vesuvius activity. During the Campi Flegrei, the higher magnitude eruptions produced the Campanian Ignimbrite (39 ka) and the Neapolitan Yellow Tuff (13 ka) as the result of several plinian and subplinian eruptions that resulted in a large amount of pyroclastitic material. The Campi Flegrei pyroclastic products were dispersed mainly eastward and north-eastward by the prevailing stratospheric wind regime and they mantle the southern Apennine Mountains surrounding the Matese Massif . The general sequence of pyroclastic deposits and dispersion, and the chemical and lithological evidence suggest an important contribution from Neapolitan Yellow Tuff (Tufo Giallo Napolitano) in this area. On the basis of paleoreconstructions, besides the described glacial deposits, two morainic arcs are present along the southern border of the Campitello plain. Older moraine deposits of pre-Würmian age are present along the northern border of the Matese Massif and reach minimum altitudes of about 800 m a.s.l. In this research a detailed chemical and mineralogical study was conducted on 5 pedons sampled on a selected area of the Matese Massif to study the characteristics of the volcanic ash in soil genesis and also to investigate the influence of the parent material and time on pedogenic processes under a Mediterranean climate.

Methods

Studied area

Five pedons were described by standard soil survey methodology. All analyses were performed on air-dried <2 mm soil (MIPAF, 2000). The Campitello Matese study site is characterized by small to large-scale surface karst features including bare rock outcrops, small karstic depressions (dolines), and sinkholes. The MAT 8, MAT10 and MAT13 profiles occur at an elevation of 1624 m a.s.l. in a large doline.

The climatic condition is moist (1874 mm) and cool (lowest medium annual temperatures of 7.2°C). MAT7 occurs in the same climate zone, but at 50 m lower elevation on a 37 % slope and in a different landscape. The present vegetation and land use are similar in MAT8, MAT10 and MAT13. The MAT9 profile was characterized by lacustrine sediments derived from pyroclastic material redeposited by turbidity currents. Mineralogical and geochemical analyses allow one to assign these pyroclastic materials to trachytes-trachyandesites. The criteria for andic soil properties were examined for the whole pedon and classified as Aluandic Andosols (WRB 2006).

Selective Dissolution

Iron, Al, and Si were extracted by ammonium oxalate (Fe_o, Al_o , Si_o); Fe and Al were also extracted by sodium pyrophosphate (Fe_p, Al_p). Iron, Al, and Si in solution were determined by ICP. Poorly crystallized aluminosilicate minerals (allophane and imogolite) were estimated by pH 3 NH_4-oxalate extraction.

Mineralogical data

The soil samples were treated with pH 5 Na-acetate to destroy carbonates and pH 8.5 Na-hypochlorite to remove organic matter before being dispersed ultrasonically in distilled water. They were then fractionated into <2 µm, 2 - 50 µm, and >50 µm fractions by sieving and repeated gravity sedimentation in distilled water adjusted to pH 10 with NaOH. The <2 µm fraction was used for X-ray diffraction (XRD) and differential X-ray diffraction (DXRD), as well as for selective dissolution by acid ammonium oxalate. Diffraction patterns were obtained using a PANalytical X'Pert PRO MPD x-ray diffraction system (PANalytical, Almelo, The Netherlands) equipped with a PW3050/60 θ-θ goniometer and a Co-target x-ray tube operated at 40 KeV and 35 mA. The diffraction patterns were collected from 2.1 to 80° 2θ at 0.05° steps with 60 sec measurement time per step. The data were analyzed with the X'Pert High Score Plus software package (PANalytical, Almelo, The Netherlands).

Results

Pedon characteristic

Pedons MAT7, MAT 8, MAT 10 and MAT13 are located in Campitello Matese on calcareous material. All soils are usually rich in organic carbon, with saturation base below to 50%, and with acidic pH.

The MAT 8 and MAT 10 pedons are deep and most likely reflective of repeated colluvial deposition in a doline environment. MAT8 has thick, black to dark brown granular A horizons, weakly-expressed Bw horizons with subangular blocky structure, and a long sequence of CB horizons. These horizons are quite homogeneous. In this pedon, the A is dark and granular while the Bw horizons have subangular blocky structure. Both the A and Bw horizons are very friable, highly permeable, and contain stratification.. The soil surface has thick, black to dark brown granular A horizons and weakly-expressed Bw horizons with subangular blocky structure. The permanent vegetation changes at higher altitudes (1650-1700 m. a.s.l.) from beech forest (Fagus sylvatica) to oak forest (Quercus pubescens), to chestnut forest (Castanea sativa) at 1000- 800 m. a.s.l. and follow the change from a udic to ustic pedoclimate. Soil temperature regimes change accordingly from thermic to mesic.

Chemical aspects

All horizons of pedons MAT7, MAT8, MAT13, MAT10 have oven-dry bulk densities of <0.80 kg dm^3 and a sand texture . This is typical for volcanic ash soils strongly influenced by non-crystalline materials and high soil organic matter concentrations (Shoji *et al.* 1993; Colombo *et al.* 2007). Water pH values range from 5.0 to 7.1 and are generally higher in surface horizons than in subsurface horizons. For all profiles and for all horizons, the sum (Al + 1/2Fe) extracted by oxalate is near the diagnostic 2% limit used to define andic soil properties in WRB and Soil Taxonomy. In profiles MAT8 and MAT13 the Al_p/Al_o ratio ranges from 0.38 to 0.85, suggesting the presence of active Al-humus complexes. The relative amounts of Al extracted by sodium pyrophosphate are correlated with Al-organo complexs. The Al_o concentrations are negatively correlated with pH in water (Figure 1). The values of Si_o are positively correlate with pH in NaF, indicating an increasing amount of allophane (<5 %) in some horizons. Ferrihydrite is also common but in low amount, with Fe_o ranging from 0.5% to 1 %.

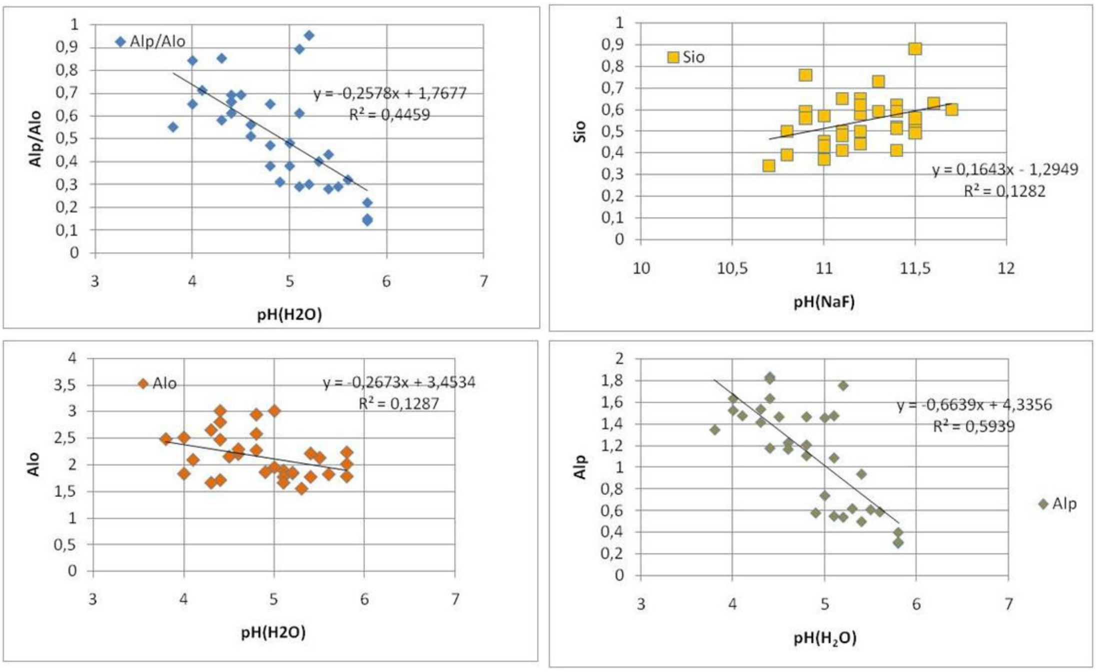

Figure 1. Correlation between Al and Si extracted by oxalate (in per cent), Al extracted with pyrophosphate (Al_p) and Al_p/Al_o ratio vs pH.

Mineralogical aspects

The clay minerals in the MAT7, MAT8 and MAT 13 profiles consist usually of vermiculite, mica and kaolinite and/or halloysite. Some hydroxy- interlayered vermiculite was also observed in the clay fraction. Mica and plagioclase are also present in all horizons. The highly ordered nature of the mica suggests its inheritance from the parent material, while the poor crystallinity of the 1.4-nm intergrade suggests a pedogenic origin (Vacca *et al.* 2003). Sanidine inherited from the parent material is revealed by a small peak at 0.62 nm present in many horizons of the MAT8, MAT13 and MAT10 profiles. The mica peaks are very weak in all patterns, while the vermiculite seems stronger in the MAT7 pedon in comparison with horizons above it. The presence of gibbsite in some horizons of MAT7 and MAT8 indicates intense (or long) leaching of these horizons compared to the ones above it. Again, the fact that these horizons were identified as buried horizons in the field is consistent with the presence of gibbsite. Presumably, these horizons were exposed to weathering for quite some time before they were buried by an additional ash fall. Some hydroxy interlayering in many pedons is indicated by a weak peak at 1.49 nm after heating to 100 C. The clay fraction of the MAT9 profile is dominated by kaolinite, mica, and vermiculite. In addition, the Bb2 horizon contains interstratified mica-kaolinite, a situation in which mica layers and kaolinite layers are stacked together in a random sequence. This is confirmed by the presence of a hump at about 0.80 nm that gets stronger on heating, but disappears after heating to 550 C. The interstratified mica-kaolinite is a weathering produce of mica. Traces of a partially dehydrated halloysite are also present in the CBb7 horizon and crystallized from the Al and Si released from the weathering of the sanidine and mica. The weathering of the sanidine and mica would have released K and Na ions, which have leached from the profile (Ugolini and Dahlgren 1991) This is consistent with the well-drained nature of the profile and the site. Primary minerals remaining in the < 2 µm fraction include K-feldspars (sanadine) and quartz. In the BW1 horizon some XRD lines also suggest the presence of analcime, a zeolite mineral.

Conclusion

The pedogenic environment of the studied soils is especially complex because of the heterogeneity of the stratified pyroclastic materials. Such stratification is a general condition in many volcanic areas (such as in the soils from the southern Apennine), it produces very different pedogenic way. The five profiles show different degrees of soil development, ranging from moderately weathered MAT7, MAT8, and MAT10, to poorly weathered MAT9. Despite such differences, all the soils exhibit common features such as the pedogenic redistribution of fine material.

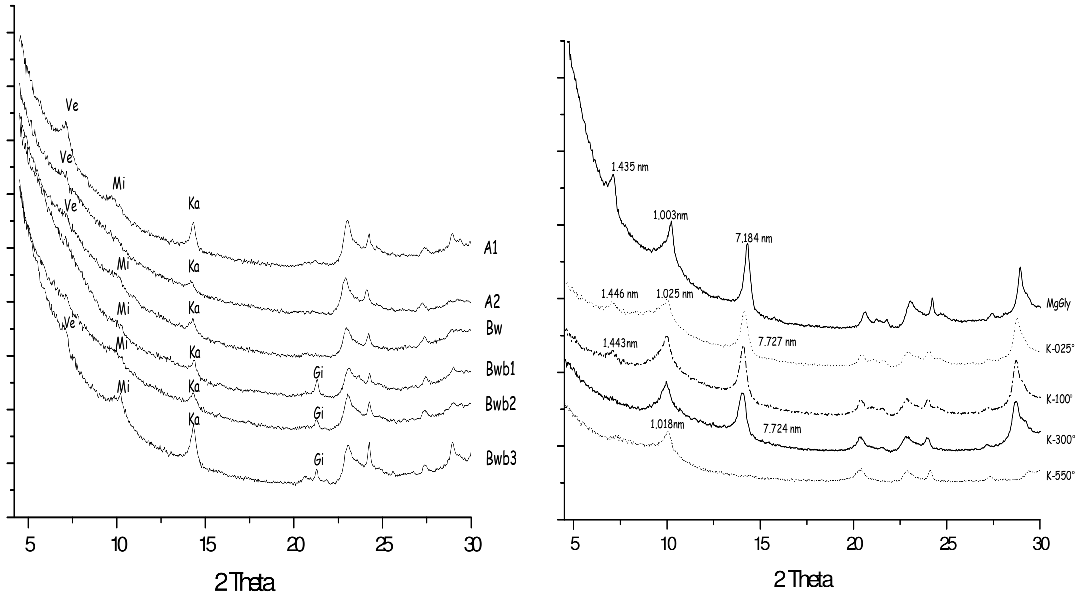

Figure 2. X-ray diffraction patterns (Co-Kα radiation) of the clay fraction of the 2Bb horizon of profile MAT 7 and MAT 13 (a) Ve_ vermiculite, Mi = mica, Ka = kaolinite.

The diffraction patterns presented weak peaks, indicating a low mineral content and the presence of materials that do not diffract strongly, most likely allophane and unweathered volcanic glass and sanidine. The mica is most likely primary mica that crystallized along with the sanidine. The vermiculite is a weathering product of the mica. We assume that the finest ash cools faster, resulting in a glass, whereas the larger particles cool slower, resulting in sanidine and mica. Sanidine and mica weathering released K and Na ions, which leached from the profile and resulted in halloysite crystallization. We also observed that some gibbsite occurred in the deepest horizons of profiles (MAT7 and MAT8). The sequence of pyroclastic deposits and the mineralogical evidence demonstrated the important contribution of the Campi Flegrei pyroclastic products on volcanic ash soil genesis in the Matese Mountains.

References

Colombo C, Sellitto MV, Palumbo G, Terribile F, Stoops G (2007) Characteristics and genesis of volcanic soils from South Central Italy: Mt Gauro (Phlegraean Fields, Campania) and Vico lake (Latium). In ‘Soils of Volcanic Regions in Europe’ (Eds O Arnalds, F Bartoli, P Buurman, H Oskarsson, Stoops G, Garcia-Rodeja E). pp.197-229. (Springer, Berlin, Heidelberg, New York).

Shoji S, Nanzyo M, Dahlgren R (1993) Volcanic ash soils: Genesis, properties and utilization. *Developments in Soil Science 21*. pp.288. (Elsevier, Amsterdam).

Ugolini FC, Dahlgren RA (1991) Weathering environments and occurrence of imogolite/allophane in selected Andisols and Spodosols. *Soil Sci. Soc. Am. J.* **55,** 1166–1171.

Vacca A, Adamo P, Pigna M, Violante P (2003) Genesis of Tephra-derived Soils from the Roccamonfina Volcano, South Central Italy. *Soil Sci. Soc. Am. J.* **67,** 198–207.

WRB (2006) World Reference Base for Soil Resources, 2nd edn. World Soil Resources Reports 103, FAO, Rome. 118 pp

Forms of energy involved in soil formation

Winfried EH Blum

Institute of Soil Research, University of Natural Resources and Applied Life Sciences Vienna, Austria, Europe, Email winfried.Blum@boku.ac.at

Abstract

Four different forms of energy involved in soil formation are described: gravity, orogenic energy, solar energy and anthropogenic energy, in order to understand and to measure soil formation under different physio-geographic and environmental conditions.

Key Words
Soil formation, forms of energy, weathering, critical zone research

Introduction

Soils are providing goods and services of paramount importance for sustaining human societies and the environment (Blum, 2005; Frossard *et al*., 2006; Costanza *et al*., 1997).
In view of the world wide losses of soil, e.g. through erosion, information about the time scale of soil formation becomes increasingly important (European Commission 2006). Until today, we have measurements and assessments regarding soil losses, but no solid data about the pace of soil formation. Therefore, the question arises: How much soil is formed with time, under different climatic, geological, topographical, hydrological and biotic conditions, under the influence of human activities, including climate change. An international research group on critical zone processes is targeting this issue (Chorover *et al*., 2007).

Methods

For answering this question, a first approach could be to identify the basic forms of energy involved in soil forming processes. With such an approach, it would also be possible to develop a comprehensive concept, which would allow to describe processes of soil formation as well as methods to measure them, e.g. weathering of rock parent material and the development of the regolith zone, as well as the further development from regolith to soil. This concept could also allow to define indicators for the different characteristics of rock, regolith and soil.

Results

Soil formation is driven by four main forms of energy: gravity, orogenic energy, solar energy and anthropogenic energy. Gravity influences all movements of solid, liquid and gaseous materials. It is an inherent form of energy and influences the vector and the velocity of fluxes within soils as well as at their surface. – Gravity is also the main factor of morphogenesis.
Orogenic energy is the second form of energy and is herited from the rock parent material, which was formed through orogenesis, an endogenic process which created very diverse types of rocks and minerals under high temperature and pressure. This endogenic energy, which can also be called orogenic energy, is still contained in rocks and in the rock forming minerals. This energy is normally not renewed for a long time, except in cases such as volcanic activities and others. – Through exogenic forces, derived from solar energy, e.g. through processes of weathering and transport (e.g. erosion), this orogenic energy pool is constantly lowered. Primary minerals, such as micas and feldspars contain more energy, derived from orogenesis as their weathering products, e.g. clay minerals and oxides. Moreover, the resistance of different minerals against weathering or the buffer capacity of soils against acidification can also be explained by orogenic energy. Orogenic energy is manifest in the texture and structure of rocks and the crystallography of minerals and their resistance to exogenic forces, which is mainly explained by the form and density of the mineral package in the rocks or the element package in the crystal structure of minerals. – Orogenic energy is also manifest in the chemical composition of minerals, which plays an important role, e.g. through the content of alkaline and earth alkaline cations in relation to silica, aluminium and metals such as iron, manganese, copper, zinc and others.

Solar energy is the third form of energy, deriving directly from solar radiation or from diffuse radiation through reflection and indirectly from organic matter and biomass, which can be considered as a secondary form of solar energy, with a different dimension in space and time. Both, direct and indirect forms of solar energy e.g. organic matter are the basis of exogenic forces, driving biochemical and physico-chemical processes in soils. – Solar energy also influences the velocity of bio-physico-chemical reactions. – In the past, soils developed under different climatic conditions (paleoclimates), especially in the tropics and sub-tropics, which makes it difficult to use current climatic data, such as temperature and/or precipitation to explain soil formation.

Anthropogenic energy is the fourth form of energy, deriving from anthropogenic activities. It is a mixture of different energy forms, including human labour, and is mainly based on fossil energy and non-renewable resources, such as oil, coal, rocks and minerals.

Since the end of the 18th century, anthropogenic influences on terrestrial and aquatic ecosystems have been exceeding the natural impacts (Crutzen, 2002; Blum and Eswaran, 2004).

Conclusions

In order to understand soil formation under different environmental, social, economic, technical and cultural conditions, it seems to be interesting to use the energy concept in order to make soil formation understandable and measurable. This is the current task of the critical zone approach.

References

Blum WEH (2005) Functions of Soil for Society and the Environment. *Reviews in Environmental Science and Biotechnology* **4**, 75-79.

Blum WEH (2008) Forms of energy involved in soil and sediment processes. *J. Soils Sediments* **8**(1), 1-2.

Blum WEH, Eswaran H (2004) Soils and sediments in the anthropocene. *J. Soils Sediments* **4**(2) 71.

Costanza R, d'Arge R, de Groot R, Farber S, Grasso M, Hannon B, Limburg K, Naeem S, O'Neill RV, Paruelo J, Raskin RG, Sutton P, van den Belt M (1997) The value of the world's ecosystem services and natural capital. *Nature* **38**, 253-260.

Chorover J, Kretzschmar R, Garcia-Pichel F, Spraks DL (2007) Soil biogeochemical processes within the Critical Zone. *Elements* 321-326.

Crutzen PJ (2002) Geology of mankind. Nature 415, 23.

European Commission (2006) Thematic Strategy for Soil Protection. COM(2006)231 final.

Frossard E, Blum WEH, Warkentin BP (Eds.) (2006) Function of Soils for Human Societies and the Environment. Special Publication No. 266, Geological Society, London (ISBN 978-1-86239-207-6).

Warr B, Ayres R (2004): Accounting for soils: Towards an integrated sustainability and productivity asessment for soils. INSEAD, CMER, 1-11, Fontainbleau, France.

Genesis of ferruginous concretions in a ferric soil and implications for past and present iron mobility

S. Löhr[A,B], M. Grigorescu[A] and M. Cox[A,B,C]

[A]Discipline of Biogeosciences, Queensland University of Technology, Brisbane, QLD, Australia, Email s.loehr@qut.edu.au
[B]Institute for Sustainable Resources, Queensland University of Technology, Brisbane, QLD, Australia.
[C]National Centre for Groundwater Research and Training.

Abstract

Theories on the genesis of ferruginous concretions in soils and weathering profiles continue to be debated. In particular, whether concretions represent *in situ* pedogenesis or are transported residues of 'laterite' weathering or ferricrete formation is unclear. In this study we use detailed field, micromorphological, geochemical and mineralogical investigations of a ferric soil profile from the Fraser Coast of Queensland to show that ferruginous concretions are of transported origin, and have been modified since deposition. The study found no evidence for a postulated Miocene 'laterite' weathering episode in this area; preserved primary minerals such as microcline show that the concretions are derived from reworked ferricrete rather than laterite.

Key Words

Pisolith, transport, ferricrete, laterite, iron mobilisation, in situ.

Introduction

As defined in the Australian Soil Classification (Isbell 2002), soils or soil horizons which contain a high proportion of ferruginous concretions (pisoliths) are 'ferric'. However, considerable controversy surrounds the origin of ferruginous concretions in soils and weathering profiles, in particular whether they have formed *in situ* or have been transported to their present locations (Bourman 1993b). Workers such as Tardy and Nahon (1985) and Muller and Bocquier (1986) propose *in situ* concretion formation. In this model the progressive formation of concretions in laterite weathering profiles can be traced from the mottled subsurface horizons to the surface. In contrast, other studies emphasise the role of erosion in the formation of concretions. Here, concretions result from the physical breakup of iron (Fe) duricrusts and ferruginised mottles, and their transport and modification in the soil and surface environments. In effect, this latter model considers concretions to be the breakdown product of either ferricrete or laterite materials (Bourman 1993a). These are dissected, eroded and redeposited at a lower landscape position, forming a new generation of mechanically accumulated ferricrete (Widdowson 2008). The current study investigates the genesis and processes currently affecting ferruginous concretions in the ferric soils of a coastal catchment in Australia. The concretions are considered the largest Fe reservoir in the surficial soils and sediments of the study area. Consequently, their genesis has clear implications for the past and current mobility of Fe. The potential for Fe remobilisation throughout the catchment has down-stream implications for coastal seawater chemistry and possible detrimental environmental ramifications. To this end, we determine field relationships, micromorphology, geochemistry and mineralogy of a soil profile exposed in an 'iron-stone gravel' quarry.

Setting

The 2.5 m deep soil profile investigated here is located in the Poona Creek catchment, on the Fraser Coast of Queensland (Figure 1A). The region lies 300 km north of Brisbane, and has a subtropical climate. Bedrock is quartzose sandstone of the Late Triassic-Early Jurassic Dunkinwilla Group (Cranfield 1994), which has been deeply weathered since the Miocene. Limited previous investigations suggest that soils in the study area are varied, but a sequence of Red Kandosols and Kurosols on hilltops, Red and Yellow Kandosols or Kurosols (often ferric) at midslope to footslope positions and Redoxic Hydrosols or Semi-Aquic Podosols in poorly drained valleys and on creek margins has been observed (Coaldrake 1961). Soils commonly feature a ferric horizon or, more rarely, a cemented ferruginous duricrust. In a recent survey of the catchment 60% of samples of the top 30 cm of the soil contained ferruginous concretions, ranging from 3-47 wt% (Löhr *et al.* 2010). The ubiquity of the ferruginous concretions and duricrust within the soil profile has previously been explained by resorting to a hypothetical 'laterisation' episode in the Miocene, which is thought to have led to the development of a deep weathering profile featuring extensive laterite duricrust (Cranfield 1994). Other workers have interpreted them as recent features of in situ pedogenesis (Coaldrake 1961).

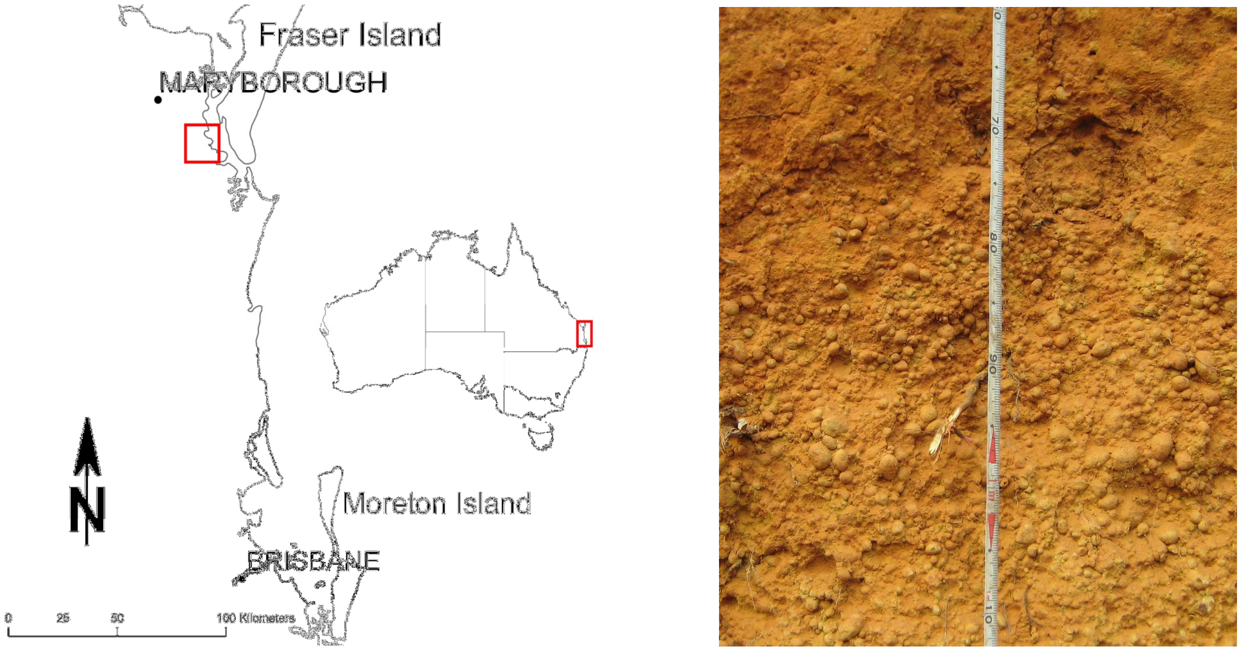

Figure 1. A) Location of the study area B) Soil profile showing ferruginous concretions in ferric horizon.

Results

The profile has been classified as a Ferric, Brown Kandosol. It features a 1 m thick ferric horizon at a depth of 75 cm (Figure 1B), as well as a surface horizon with up to 30 % concretions (Table 1). Angularity increases with depth in the ferric horizon, and occasional elongate concretions are dipping at less than 30° or are clast supported. Ferruginised rock fragments only occur at the bottom of the profile.

Table 1. Soil profile description. Terminology after Australian soil and land survey field handbook (National Committee on Soil and Terrain, 2008).

Depth (cm)	Horizon	Colour	Description
0-15	A1	2.5 YR 4/6	Clay loam, sandy. Platy structure. Fine roots, faunal channels, bioturbation. Some concretions on surface, concentrated on bottom of horizon. 30 % concretions, matrix supported, 0.5-2 cm diameter. Subrounded –rounded. Sharp, smooth boundary.
15-55	A2	2.5 YR 4/6	Sandy clay loam. Massive, very firm structure. Fine-thick roots. Few concretions, < 5 %, 0.2-1.2 cm. Rounded, high sphericity. Diffuse boundary.
55-75	B1	2.5 YR 4/8	Clay loam. Concretions 10 % with gradual increase to bottom. 0.5 to 2 cm. Rounded, med-high sphericity. Clear, wavy boundary.
75-175	B2	7.5 YR 4/6	Clay loam. Ferric horizon. Concretions 80-90 %, clast supported. Decrease from rounded-well rounded at top, to angular-subrounded. Mostly medium-high sphericity. Elongate concretions horizontal or clast supported. Clear, irregular boundary.
175-210	CB	10 YR 5/6	Clay loam, sandy. Massive structure. Up to 50 % poorly sorted, ferruginised rock fragments, 4-8 cm in size. Sub angular-angular.
> 210	C	10 YR 5/6	As above, smaller and less frequent rock fragments. (Sandy) light-medium clay.

Concretions can be sorted into two types, based on their appearance. Most concretions are brown, with a burnished outer surface. These range from <2 mm to > 16 mm in diameter. Black concretions which are harder and often magnetised are also common. These are typically much smaller than the brown concretions and do not exceed 8 mm in diameter. The fine earth fraction, the black and the brown concretions are characterised by distinct mineralogy and composition (Table 2). Major differences are the low concentration of iron oxides and total iron in the fine earth fraction compared to the concretions, and the higher concentration of siderophile trace elements in the concretions. Polished thin sections of undisturbed material collected from all horizons, as well as representative concretions, show evidence of four types of internal arrangement. This includes: a) concentric concretions (alternating bands of distinctly coloured cementing material, sharp boundaries between bands), b) uniform concretions (uniform texture and colour, or diffuse changes), c) nucleic concretions (formed around a nucleus or incorporating a fragment or another concretion) and d) ferruginised rock fragments. Concentric and uniform concretions are most common.

Micromorphological study of the undisturbed samples and selected concretions shows: a) compound concretions, b) incomplete or broken surface coatings, c) laminae free of quartz grains, d) lenses featuring quartz grains of different size to core, surrounded by quartz-free cement. Angular concretions at depth display iron and aluminium oxyhydroxide overgrowths.

Table 2. Mineralogical (A) and selected compositional data (B) of fine earth fraction, black concretions and brown concretions. Data shown are ranges, compiled from multiple samples. Mineralogy obtained by XRD and Rietveld pattern refining, compositional data obtained by XRF.

A	Quartz^A	Microcline^A	Anatase^A	Kaolinite^A	Maghemite^A	Hematite^A	Goethite^A	Gibbsite^A	Amorph^A
Fine Earth <2mm	57-60	0-5.5	1	17-27	0	1-1.5	0-2	2-11	4-9
Black	38-39	0-1.4	0	6	17	26-31	0-2	1	5-11
Brown	28-36	0-7	0-1	16-23	0-6.5	2-7	17-24	4-12	7-20

B	SiO_2^{A}	Al_2O_3^{A}	Fe_2O_3^{A}	MnO^A	MgO^A	Ti^B	V^B	Cr^B	Mn^B	Co^B	Ni^B	Cu^B	Zn^B	Pb^B
Fine Earth <2mm	71.3-78.9	10.9-15.3	2.5-3.47	0.01	0.24	6524-8794	80-102	82-95	<4-15	<2-5	6-8	<3	13-14	<10
Black	40.1-43.9	11.8-12.7	36.7-41.5	0.01	0.24-0.25	5255-5391	643-752	378-439	50-52	<2-6	19-21	<3	9-10	86-100
Brown	37.7-46.5	16.4-22.1	19-28.6	0.01	0.22-0.23	4103-5927	456-557	177-321	<4-19	<2-12	12-18	<3	11-15	26-53

^{a} wt %; ^{b} mg/kg

Discussion

Field-based evidence such as a high proportion of elongate concretions lying horizontally, as well as a high proportion of sub-rounded to rounded clasts indicate a transported origin for the concretions investigated here. This is further supported by the marked differences between fine earth fraction and concretions. However, the compositional and mineralogical differences between morphologically distinct concretions suggest a different origin or source for different concretion types. The multiple bands or concentric rings which are typical of the larger, brown concretions also suggest a complex growth history, while the smaller concretions generally show less structural variation.

Coventry *et al.* (1983) used a range of micromorphological features to distinguish *in situ* from transported concretions. Those features which indicate a transported origin include a) incomplete or broken surface coatings, b) different particle size distributions of sand and silt grains in concretions and non-cemented matrix, c) different particle size distributions of sand and silt grains in adjacent concretions and d) compound or nucleic concretions. Milnes *et al.* (1987) also described a series of depositional multiple laminar goethite rinds on concretions, with occasional gibbsite, incorporating individual quartz grains or lenses between them as evidence of their accretionary origin. Micromorphological study of the concretions in the Poona Creek soil profile shows many of the same features, consistent with a transported origin. In fact, Milnes *et al.* (1987) suggested that deposition of the laminae and incorporation of the quartz occurs in a succession of pedogenic environments, which would be consistent with a long history of exposure, transportation and weathering.

We do not, at present, have sufficient data from other profiles to fully place this study into a landscape context (i.e. toposequence). Nevertheless, based on the micromorphological, geochemical, mineralogical and field evidence presented here, it is likely that the concretions have been transported prior to deposition and that they were formed by the physical break-up of pre-existing ferruginous materials. There is also sufficient evidence to identify the original type of ferruginous material. Microcline is a relatively unstable mineral, especially in the aggressive weathering conditions of the upper laterite weathering profile in which residual laterite duricrust forms. The fact that microcline has been identified in some of the concretions suggests that the concretions are the reworked residuum of earlier generations of ferricrete, in which microcline was preserved by coating with Fe oxides, rather than a lateritic residuum (Widdowson 2008). Comparison of the chemical composition and mineralogy of the concretions in this study with those in other studies (mostly formed by lateritic weathering) show that the Poona catchment Fe-concretions are similar in mineralogy but relatively poor in most trace elements.

They are, however, within the compositional range expected, assuming that they have formed through ferruginisation by allochthonous inputs of iron into the Duckinwilla Group parent material. 'Laterisation' is very unlikely to have been widespread in the study area, as the quartz- and kaolinite-rich sandstones of the Duckinwilla Group are unlikely to have contained sufficient iron for laterite duricrust formation (Widdowson 2008).

Based on this information and the evidence that the concretions are indeed transported residuum, it is unlikely that the study area has in fact been subject to a deep lateritic weathering event, as previously suggested (Cranfield 1994). A more suitable explanation is perhaps that of Bourman (1993b), which provides a model of long-term continual weathering that leads to ferruginisation and the formation of ferricrete in lower landscape positions. Bourman argues that this better explains the occurrence of ferruginous materials in much of southern and eastern Australia. There is also evidence of more recent mobilisation of iron within the profile. The increase in angularity of concretions at lower levels of the ferric horizon, as well as the occurrence of ferruginised rock clasts in the bottom horizons, suggests that mobilisation of iron has occurred since deposition of the concretions, and has resulted in overgrowths and ferruginisation of the rock fragments.

Conclusions

The concretions are most likely to be of transported origin and can be regarded as clastic components, which formed outside the material in which they are currently found. They have been modified since their deposition by re-mobilisation of iron and re-precipitation further down the profile. These processes have resulted in iron oxyhydroxide overgrowths on some concretions and the ferruginisation of rock fragments in lower horizons. Thus, the concretions are contributing to Fe cycling processes in many ferric soils. Mineralogical and geochemical evidence suggests the concretions are originally derived from reworked ferricrete duricrust, rather than reworking of laterite duricrust. There is therefore no evidence for a Miocene 'laterite' weathering episode preserved in the study area.

References

Bourman RP (1993a) Modes of ferricrete genesis-evidence from southeastern Australia. *Zeitschrift für Geomorphologie* **37,** 77-101.

Bourman RP (1993b) Perennial Problems in the Study of Laterite-A Review. *Australian Journal of Earth Sciences* **40,** 387-401.

Coaldrake JE (1961) 'The Ecoystem of the Coastal Lowlands ("Wallum") of Southern Queensland'. (CSIRO: Melbourne)

Coventry RJ, Taylor RM, Fitzpatrick RW (1983) Pedological significance of the gravels in some red and grey earths of central North Queensland. *Australian Journal of Soil Research* **21,** 219-240.

Cranfield LC (1994) '1:250000 Geological Series-Explanatory Notes. Maryborough, Queensland. Sheet SG56-6'. (Geological Survey of Queensland: Department of Minerals and Energy).

Isbell RF (2002) 'The Australian Soil Classification'. (CSIRO Publishing: Melbourne).

Löhr SC, Grigorescu M, Hodgkinson JJ., Cox ME, Fraser SJ (2010). Iron occurrence in soils and sediments of a coastal catchment. A multivariate approach using self organising maps. Geoderma **156,** 253- 266.

Milnes AR, Bourman RP, Fitzpatrick JW (1987) Petrology and mineralogy of 'laterites' in southern and eastern Australia and southern Africa. *Chemical Geology* **60,** 237-250.

Muller JP, Bocquier G (1986) Dissolution of kaolinites and accumulation of iron oxides in lateritic-ferruginous nodules: mineralogical and microstructural transformations. *Geoderma* **37,** 113-136.

National Committee on Soil and Terrain (2008) 'Australian soil and land survey field handbook'. (CSIRO Publishing: Melbourne).

Tardy Y, Nahon D (1985) Geochemistry of laterites, stability of Al-goethite, Al-hematite and Fe-kaolinite in bauxites and ferricretes: an approach to the mechanism of concretion formation. *American Journal of Science* **285,** 865-903.

Widdowson M (2008) Laterite and Ferricrete. In 'Geochemical Sediments and Landscapes'. (Eds DJ Nash, SJ McLaren) pp. 46-94. (Wiley-Blackwell: Chichester).

Geochemical mass-balance in intensely weathered soils, Darling Range, Western Australia

Xin Du [A, B], Andrew W. Rate[A], Mary Gee[A]

[A]School of Earth and Environment, The University of Western Australia, Crawley, 6009 WA, Australia
[B]School of Environmental Studies, China University of Geosciences, 430074 Wuhan, China, Email dux01@student.uwa.edu.au;

Abstract

Chemical weathering, one of the major processes that modify the earth's surface, exerts important controls on the geochemical cycling of elements. The behavior of elements in rock weathering processes, especially in intensely weathered regolith profiles, is not very well understood. In addition, rigorous calculation of the mass fluxes during intense weathering is seldom performed. This study aimed to determine geochemical mass balance for regolith profiles subject to intense chemical weathering. Two lateritic profiles in Western Australia with different weathering intensity were studied, to investigate influence of weathering intensity on element loss or gain. GE lateritic profile (CIA values 90.8~99.2), with kaolinite and gibbsite as main weathering products, is more intensely weathered than MQ profile (CIA from 63.6 to 83.9). Calculating mass balance with Zr as the immobile element, Na, Ca, Sr, Rb and Ba were almost completely depleted in the GE profile, while in MQ profile, only Ca loss as high as 95%. Aluminium, Ti and Fe accumulate at 0.6 m depth MQ profile, which also has the highest clay content; in the GE profile, Fe is significantly enriched from 3.5-7 m, forming haematite and goethite in duricrust and ferruginous matrix.

Key Word

Laterite, weathering, geochemical anomalies, modelling, major elements

Introduction

Chemical weathering of rocks is one of the major processes that modify the earth's surface and is one of the critical processes in the geochemical cycling of elements (Ji *et al.,* 2004). Weathering intensity exerts important influence on mobilization and redistribution of different elements in a regolith profile. As the result of intense weathering, deposition, and modified by later soil-forming (pedogenic) processes on near-surface rocks, laterite (lateritic soil) represents one of the most common superficial formations in the tropics and covers long periods of time, extending over tens of millions of years (Dequincey *et al.,* 2006). Although much research on the laterization process and element mobilization has been performed worldwide (e.g. Beauvais, 1999; Beyala *et al.,* 2009; Ma *et al.,* 2007), the precise sequence of events and behavior of elements in rock weathering process and laterite formation are still not unambiguously understood. In Western Australia, high rainfall and humid weathering conditions have further enhanced rock weathering and element leaching, and form notable duricust (ferricrete) due to accumulation of iron. The purpose of this paper is to investigate the element mobilization and redistribution during intense weathering in lateritic profiles. Two lateritic profiles with different weathering intensity were studied, to investigate influence of weathering intensity on element loss or gain.

Material and Methods

Description of the study areas

The first profile is located in Mountain Quarry (31°54′54″S, 116°3′44″E), on the southern slope of Greenmount Hill, Western Australia. Here, granites typical of the Darling Range are intruded by a number of dolerite dykes. The profile is developed overlying granite with stonelines preserved from quartz veins implying in-situ weathering. The profile is 2 m-deep, samples from five depths were collected on 29th, May, 2009. The potential parent rocks, including granite and intrusive dolerite dyke were also sampled. The second profile is adjacent to Great Eastern Highway, Western Australia (31°22'30.95"S, 118°41'26.74"E) with very good bedrock (granitoid/dolerite dyke) exposure and a very deep weathered profile. The profile is 12 m deep, including saprolite, mottled clay, duricrust, and topsoil. Detailed sample information is listed in Table 1.

Analytical methods

Pretreatment of the soil samples included sieving through 2-mm plastic mesh for separation of gravel and roots/rhizomes from the -2 mm soil fraction. Part of the subsamples of the -2 mm fraction was used to determine the pH and particle size distribution. Soil pH was determined potentiometrically in the supernatant in a 1: 5 suspension of soil: 0.01 M $CaCl_2$, and particle size distribution of soil samples were determined by the pipette method. Other soil subsamples and crushed rock samples were grounded to less than 100 meshes prior to fusion to determine major and trace elements: 0.7 g of finely ground soil was mixed with 12:22 Norrish flux (lithium metaborate/ lithium tetraborate) in a muffle furnace at 1050 °C to prepare fusion beads for determination of major elements by Philips PW1404 XRF. Two standard reference materials (OREAS and stsd-2) were analyzed together with the samples to check the accuracy and precision of the analyses. Primary minerals were identified in the thin sections of the rocks by optical microscopy; secondary minerals in the weathering products and the soil were identified by means of random powder X-ray diffraction. Relevant physical and chemical properties of the samples are listed in Table 1.

Table 3. Selected physical and chemical properties of samples from each profile.

Sample ID [1]	Depth (m)	soil pH [2]	clay%	silt%	sand%	CIA	C%	Description
MQ15	0.08	4.88	18.39	10.29	71.32	71.0	2.04	Horizon A topsoil
MQ14	0.25	5.16	30.47	1.75	67.79	75.7	0.28	Horizon A topsoil
MQ13	0.60	4.83	50.31	0.76	48.93	83.9	0.32	
MQ12	1.10	4.75	25.56	1.98	72.46	75.7	0.11	
MQ11	1.60	4.62	23.25	2.45	74.30	68.5	0.09	
MQ10	2.00	4.65	18.00	0.83	81.16	63.6	0.07	saprolite
GEA1	0.09	5.09	1.91	3.20	94.89	90.8	4.66	Horizon A topsoil
GEA2	0.12	5.03	1.46	2.84	95.70	94.0	1.46	Horizon A topsoil
GEA3	0.23	5.33	1.86	2.91	95.23	93.3	0.80	Horizon A topsoil
GE6	3.50	6.12	2.30	6.98	90.72	99.2	0.38	ferricrete
GE5	7.00	5.96	19.30	2.27	78.43	97.6	0.21	ferruginous matrix
GE4	8.40	5.75	18.85	9.69	71.46	94.3	0.04	mottled clay
GE3	10.00	5.52	22.56	8.12	69.31	98.9	0.03	mottled clay
GE2	11.40	5.26	22.64	7.68	69.67	97.8	0.03	saprolite
GE1	12.50	4.77	24.67	12.59	62.74	94.6	0.07	low saprolite

[1] The first two letters of sample codes identify each profile: Mountain Quarry (MQ) and Great Eastern Highway (GE).

[2] pH was determined in a 1:5 suspension of soil: 0.01 M $CaCl_2$

Results and discussion

Weathering intensity and mineral composition

To quantitatively evaluate the intensity of chemical weathering, the Chemical Index of Alteration (CIA, Nesbitt and Young 1982) was used. The CIA values of regolith samples are in Table 1. In the MQ profile, CIA decreases from MQ13 to saprolite, ranging from 63.6 to 83.9. For the GE profile, CIA varies substantially from the regolith-bedrock interface to the top of the profile, with two peaks at GE6 and GE3; the regolith is more intensely weathered than MQ profile, with CIA values 90.8~99.2. Weathering indices of topsoils in both profiles (MQ15, MQ14, GEA1, GEA2 and GEA3) are lower than the subsoils, which may be because the original weathered topsoil has been eroded.

The main minerals present in the samples collected from MQ profile are quartz, plagioclase, muscovite, microcline and clay minerals. In contrast, the main minerals in GE regolith samples (Table 1) are kaolinite and gibbsite. In GE6 (duricrust), the iron oxides haematite and goethite were identified.

Chemical composition

To quantify the net result of pedogenic weathering, a geochemical mass balance calculation was used in this study. The formula (Equation (1) assumes an immobile element behaves conservatively and corrects mobile element concentrations for volumetric strain during weathering and pedogenesis).

$$\tau_{i,j} = \left(\frac{C_{i,p}}{C_{i,w}}\right)\left(\frac{C_{j,w}}{C_{j,p}}\right) - 1 \qquad (1)$$

Where C represents concentration, with subscript i for immobile element, j for element of interest, w for weathered material and p for parent rock. If $\tau_{i,j} = -1$, the element i is completely depleted during weathering.

Although this equation provides a tool for estimating elemental loss or gain of a profile, the mass balance equations have several critical assumptions. First, there should be a genetic relationship between regolith and its parent material. Second, since the calculations are highly dependent on immobile elemental concentrations, the reference element should be conservative in its real sense. The chosen immobile element for this analysis is Zr, because Zr primarily resides in zircon, which is resistant to chemical weathering and inter-sample variations in Zr are less than for Ti.

Alkalis and alkaline earths – In the GE profile, the weathering is complete and extreme, while in the MQ profile, the weathering and leaching process is still in progress. The alkali and alkaline earth elements in both profile are highly depleted, especially in the GE profile; calcium (Ca), sodium (Na), strontium (Sr), barium (Ba) and rubidium (Rb) were almost completely depleted; 83%~97% potassium (K) and 66%~85% magnesium (Mg) were also leached from the profile relative to its assumed parent rock (Figure 1).

In the MQ samples, Ca is the element with highest loss (80%~95%), reflecting minimal anorthite feldspar remaining in the profile; followed by Na (25%~80%), Mg (40%~60%) and K (30%~50%). Rb, Sr and Ba losses were 40%~53%, 60%~75%, 25%~55% respectively (Figure 1). Hence, with continued weathering of MQ profile, anorthitic plagioclase will progressively be replaced by clay minerals (kaolinite in this study). Alkali- and alkaline-earth elements may also be fixed by exchange and adsorption onto secondary clay minerals, or incorporation into structural sites of clays (Nesbitt *et al.,* 1980).

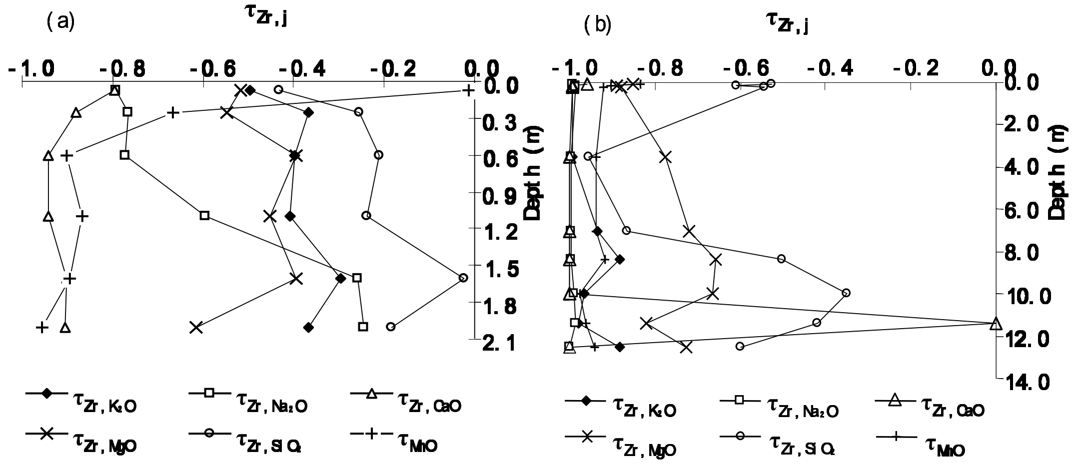

Figure 2. Depth profiles for geochemical mass-balance (τ = solute gain or loss) of Ca, Na, K, Mn, Mg and Si for (a) the Mountain Quarry (MQ) profile and (b) the Great Eastern Highway (GE) profile.

Translocation of aluminum and iron –in the MQ profile, mass balance calculations suggest that iron, aluminum and titanium accumulate in regolith samples, all peaking in sample MQ13 (Figure 3(a)). Sample MQ13 also had highest clay proportion, which accounted for enrichment of aluminum. It is likely that, with intense weathering, mafic silicates (e.g. biotite) broke down, and Fe(II) is released and transferred downwards, rapidly oxidized and precipitated as hydrous oxides in the subsoil, or adsorbed by clay minerals.

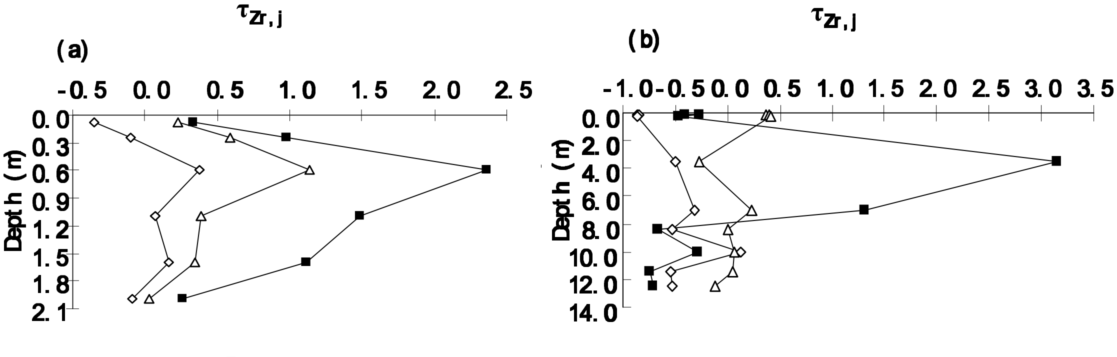

Figure 3. Depth profiles for geochemical mass-balance (τ = absolute gain or loss) of Al, Fe, and Ti for (a) the Mountain Quarry (MQ) profile and (b) the Great Eastern Highway (GE) profile.

For GE samples, iron showed enrichment mid-profile with depletion in the topsoil and at depth (Figure 3(b)). Aluminum was leached from the GE profile, and titanium behaves approximately conservatively (Figure 3(b)). Except for the GE3 mottled clay sample, aluminum was depleted by approximately 50%. Haematite and goethite were identified in samples GE5 and GE6 (ferricrete) which showed addition of iron. This depth (GE6) may be the original groundwater table; iron leached from the topsoil, transferred downwards by rainfall, with the groundwater slowly decreasing, iron was oxidized and precipitated as Fe(III) oxyhydroxides. The Ti: Zr ratio was relatively constant (0.1~0.4) in most of samples in GE profile, except possible depletion in GE6 (duricrust) and GE1 (saprolite). While it is generally considered that Ti is a conserved element, Ti is mobile in extreme weathering conditions. Further work using scanning electron microscopy will examine physical evidence for weathering of Ti-bearing minerals (e.g. biotite, or even refractory minerals such as titanite and anatase), which may have resulted in Ti translocation.

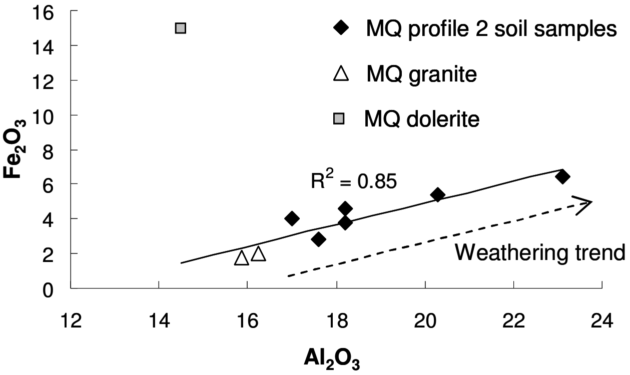

Figure 4. Plot of Fe_2O_3 vs. Al_2O_3 for regolith and parent rocks from Mountain Quarry (MQ), showing evidence confirming the assumed parent material of the profile.

Conclusion

Some trends are apparent in the mobilization and redistribution of elements in intensely to extremely weathered profiles developed on granite in Western Australia. Losses of elements based on mass balance calculations are consistent with the degree of weathering calculated by weathering indices, and mineralogy of the weathered regolith. Fe, Al, and Ti show variable behaviour, with the most intensely weathered profile only showing evidence of Fe accumulation in ferruginous duricrust. The less weathered profile has accumulations of Fe, Al and Ti; the contents of these elements (e.g., Al: Fe ratio) provide geochemical confirmation of the parent material.

References

Beauvais A (1999) Geochemical balance of lateritization processes and climatic signatures in weathering profiles overlain by ferricretes in Central Africa. *Geochimica et Cosmochimica Acta* **63**, 3939-3957.

Beyala VKK, Onana VL, Priso ENE, Parisot JC, Ekodeck GE (2009) Behaviour of REE and mass balance calculations in a lateritic profile over chlorite schists in South Cameroon. *Chemie Der Erde-Geochemistry* **69**, 61-73.

Dequincey O, Chabaux F, Leprun JC, Paquet H, Clauer N, Larque P (2006) Lanthanide and trace element mobilization in a lateritic toposequence: inferences from the Kaya laterite in Burkina Faso. *European Journal of Soil Science* **57**, 816-830.

Ji HB, Wang SJ, Ouyang ZY, Zhang S, Sun CX, Liu XM, Zhou DQ (2004) Geochemistry of red residua underlying dolomites in karst terrains of Yunnan-Guizhou Plateau I. The formation of the Pingba profile. *Chemical Geology* **203**, 1-27.

Harnois L (1988) The CIW Index: a new chemical index for weathering. *Sedimentary Geology* **55**, 319-322.

Ma JL, Wei GH, Xu YG, Long WG, Sun WD (2007) Mobilization and re-distribution of major and trace elements during extreme weathering of basalt in Hainan Island, South China. *Geochimica et Cosmochimica Acta* **71**, 3223-3237.

Nesbitt HW, Markovics G, Price RC (1980) Chemical processes affecting alkalis and alkaline earths during continental weathering. *Geochimica et Cosmochimica Acta* **44**, 1659-1666.

Nesbitt HW, Young GM (1982) Early Proterozoic climates and plate motion inferred from major element chemistry of lutites. *Nature* **299**, 715-717.

Geochemical processes in Latosols on the geomorphic surfaces from Brazilian Central Plateau

Adriana Reatto[A], Ary Bruand[B], Luiz Roberto Guimarães Guilherme[C], Eder de Souza Martins[A], Euzebio Medrado[D], Michel Brossard[E] and Fabrice Muller[B]

[A]Empresa Brasileira de Pesquisa Agropecuária (Embrapa Cerrados), BR 020, km 18, 73310-970, Planaltina, Distrito Federal, Brazil, Email reatto@cpac.embrapa.br, eder@cpac.embrapa.br
[B]Institut des Sciences de la Terre d'Orléans (ISTO) UMR6113 CNRS/Université d'Orléans 1A, rue de la Férollerie 45071 Orléans, France Cedex 2, Email Ary.Bruand@univ-orleans.fr, Fabrice.Muller@univ-orleans.fr
[C] Universidade Federal de Lavras, Departamento de Ciência do Solo, Setor de Mineralogia e Química do Solo. Campus Universitário UFLA 37200-000 - Lavras, MG - Brasil - CP: 3037, Email guilherm@ufla.br
[D] Consultor Técnico, Brasília-Brasil, Email euzebio.medrado@gmail.com
[E] Institut de Recherche pour le Développement (IRD), Unité Valpédo, BP 64501, 34394 Montpellier Cedex 5, France, Email Michel.Brossard@ird.fr

Abstract

Latosols are deeply weathered soils characteristic of the most Tropics. These soils represent 1/3 of the Brazilian National Territory and occupy about 40% of the Brazilian Central Plateau. The objective of this study was to discuss the distribution of the Latosols on the geomorphic surfaces from Brazilian Central Plateau based on geochemical process. Ten Latosols (L) developed in different parent materials were selected along an approximately 350km long regional toposequence across the South American Surface (L1 to L4) and Velhas Surface (L5 to L10) from Brazilian Central Plateau. The main conclusion is that there is a close relation between the occurrence of gibbsite(Gb), kaolinite (K) and hydroxy-Al interlayered vermiculite (HIV) in the soil-solution phase versus their presence in the equilibrium soil-solid phase for these Latosols independently of the geomorphic surface. The presence of HIV is not consistent with the weathering process in the tropical areas where the tendency is the progressive loss of Si and the enrichment of Al consequently Gb.

Key Words

Oxisols, pedogenesis, clay mineralogy, soil solution equilibria, geomorphology.

Introduction

The Latosols represent 1/3 of the Brazilian National Territory and occupy about 40% of the Brazilian Central Plateau surface area. These soils correspond to the end of a geochemical sequence of weathering (Pédro 1968). Most Latosols in the Brazilian Taxonomy (Embrapa 2006) correspond to Oxisols in the Soil Taxonomy (Soil Survey Staff 2006) and Ferralsols in the World Reference Base (IUSS Working Group WRB 2006). The Latosols are defined in Brazilian Taxonomy by the presence of a diagnostic Bw horizon somewhere between the top surface and 200-cm depth (Embrapa 2006). The main geochemical process occurring in Latosols is hydrolysis (Melfi and Pédro 1977, 1978) causing a release of cations from the primary minerals thus resulting in the formation of minerals depleted of silica such as 1:1 clay minerals or without silica such as iron oxyhydroxides and aluminum hydroxide. Thus, the clay fraction of the Bw horizon is characterized by the presence of kaolinite, gibbsite, goethite, and hematite in variable proportions, according to the parental material, geomorphic position, and prevailing moisture conditions (Curi and Franzmeier 1984; Macedo and Bryant 1987; Ker 1998; Schaefer *et al.* 2008; Reatto *et al.* 2008). The objective of this study was to discuss the distribution of the Latosols on the geomorphic surfaces from Brazilian Central Plateau based on geochemical process, such as chemical and mineralogical characteristics of the solid phase (soil and parent material) and chemical composition of the soil-solution phase equilibrium.

Methods

Soil selection

Ten Latosols (L) were selected along an approximately 350-km long regional toposequence across the Brazilian Central Plateau, thus enabling to explore a large range of mineralogical soil composition. They were located either on the South American Surface (SAS), (Latosols L1 to L4) or on the Velhas Surface (VS) (Latosols L5 to L10) as shown in Figure 1.

Soil characterization

Samples were collected in the diagnostic horizon (Bw) for every Latosol selected in this study. Physico-chemical analysis were performed on the air-dried <2-mm material according to the Brazilian standard procedures (Embrapa 1997) which in general follow the international procedures (Klute, 1986; Page *et al.* 1982). X-ray diffractions (XRD) patterns were performed using oriented samples of the < 2-µm fraction using Thermo Electron ARL`XTRA diffractometer. Oriented samples were studied after Mg^{2+} saturation (i) at room temperature, (ii) after heating at 110°C, 220°C, 350°C and 550°C, (iii) and at room temperature after glycerol solvatation (Robert and Tessier, 1974). X-ray diffractions patterns were also recorded as transmission for samples collected in the saprolite, which corresponds to the parent materials of the Latosols, using an INEL XR3000 diffractometer. Every sample was grinded and installed within a capillary tube 0.5-mm in diameter. Soil solution extracts were obtained in triplicate for every B*w* horizon following the saturation extract method (Embrapa 1997; Sparks 2003). The concentrations of Si, Al, Ca, Mg, Fe and K were determined using ICP-AES.

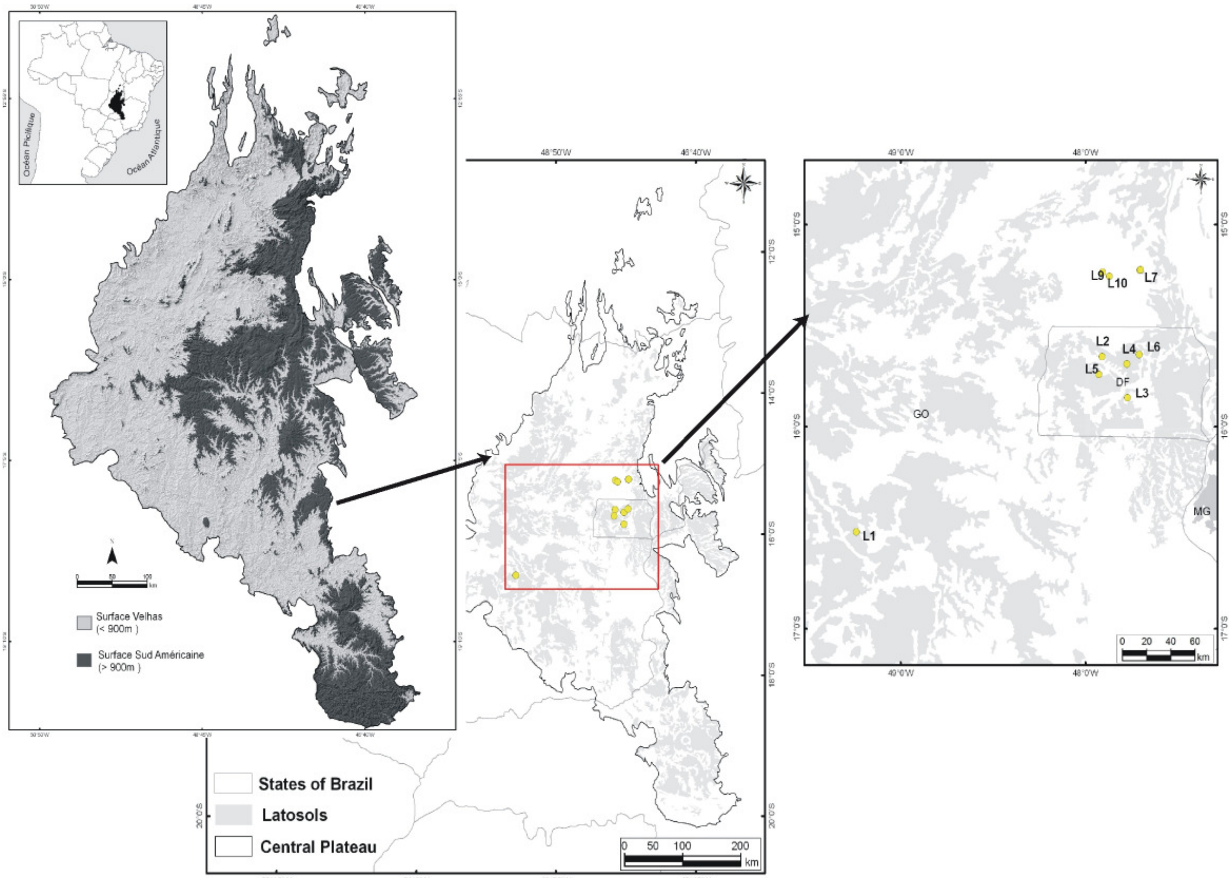

Figure 1. Spatial distribution of the Latosols (L) on the geomorphic surfaces from Brazilian Central Plateau: South American Surface (> 900-m high) represented by L1 to L4, and Velhas Surface (< 900-m high) represented by L5 to L10.

Results

General physical and chemical properties

The Bw horizons of the Latosols studied showed a variation of clay content ranging from 300 to 780 g/kg, smallest for L4 from quartzite parent material. The pH_w ranged from 4.8 to 5.3 and the pH_{KCl} from 4.00 to 6.20. The pH_w and pH_{KCl} of Latosols was greater on the SAS ($5.2 \leq pH_w \leq 5.3$ and $5.7 \leq pH_{KCl} \leq 6.2$) for the Latosols (L1, L2, L3, and L4) than on the VS ($4.8 \leq pH_w \leq 5.2$ and $4.0 \leq pH_{KCl} \leq 5.5$) for the Latosols (L5, L6, L7, L8, L9, and L10). The organic carbon content ranged from 0.01 to 0.62 g/kg. The cation exchange capacity (CEC) ranged from 1.73 to 10.60 $cmol_c$/kg and the high values of CEC were correlated with high ($H^+ + Al^{3+}$) content as observed in L2, L6, and L8. The Al_2O_3 content removable by H_2SO_4 in the Bw horizons was greater in the Latosols on the SAS (528 to 651 g/kg) than in those on the VS (440 to 514 g/kg). On the other hand, the SiO_2 content removable by H_2SO_4 in the Bw horizons was smaller in the Latosols on the SAS (112 to 239 g/kg) than in those on the VS (226 to 341 g/kg). In general the Fe_2O_3 and TiO_2 content removable by H_2SO_4 in the Bw horizons were greater in the Bw horizons on the SAS than in those on the VS with exceptions.

Mineralogical properties

The Table 1 summarizes the main minerals found in the Bw horizons (in different fractions; < 2 mm and

< 2 µm) as well as in the saprolite-rocks of the Latosols investigated. In general, the minerals identified were kaolinite (K), gibbsite (Gb), goethite (Gt), and hematite (Hm) in all Bw horizons in the two soil-fractions analyzed, except for L4 concerning to Hm. Quartz (Q) was also found, except in the < 2 – µm fraction (oriented sample). Hydroxy-Al interlayered vermiculite (HIV) and muscovite (M) were observed respectively in the < 2 µm fraction (oriented sample) and the saprolite-rocks for Latosols L5, L7, L8, L9, and L10.

Table 1. Clay mineralogy of the Latosols (L) studied.

Latosol	Samples identification		Minerals identification						
			K	Gb	Gt	Hm	Q	HIV	M
L1	saprolite	granulite (powder)	x	-	-	-	x	-	-
	soil	< 2 – mm fraction (powder)	x	x	x	x	x	-	-
		< 2 – µm fraction (powder)[1/]	x	x	x	x	x	-	-
		< 2 – µm fraction (oriented)	x	x	x	x	-	-	-
L2	saprolite	sandy metarithimite (powder)	x	-	-	-	x	-	-
		lateritic crusts (powder)	x	x	x	x	x	-	-
	soil	< 2 – mm fraction (powder)	x	x	x	x	x	-	-
		< 2 – µm fraction (powder)[1/]	x	x	x	x	x	-	-
		< 2 – µm fraction (oriented)	x	x	x	x	-	-	-
L3	saprolite	sandy metarithimite (powder)	x	-	-	-	x	-	-
		lateritic crusts (powder)	x	x	x	x	x	-	-
	soil	< 2 – mm fraction (powder)	x	x	x	x	x	-	-
		< 2 – µm fraction (powder)[1/]	x	x	x	x	x	-	-
		< 2 – µm fraction (oriented)	x	x	x	x	-	-	-
L4	saprolite	quartzite (powder)	-	-	-	-	x	-	-
		lateritic crusts (powder)	x	x	x	x	x	-	-
	soil	< 2 – mm fraction (powder)	x	x	x	-	x	-	-
		< 2 – µm fraction (powder)[1/]	x	x	x	x	x	x	-
		< 2 – µm fraction (oriented)	x	x	x	x	-	x	-
L5	saprolite	clayed metarithimite (powder)	x	-	-	-	x	-	x
	soil	< 2 – mm fraction (powder)	x	x	x	x	x	-	-
		< 2 – µm fraction (powder)[1/]	x	x	x	x	x	x	-
		< 2 – µm fraction (oriented)	x	x	x	x	-	x	-
L6	saprolite	metapelite (powder)	x	-	-	-	x	-	x
	soil	lateritic crusts (powder)	x	x	x	x	x	-	-
		< 2 – mm fraction (powder)	x	x	x	x	x	-	-
		< 2 – µm fraction (powder)[1/]	x	x	x	x	x	-	-
		< 2 – µm fraction (oriented)	x	x	x	x	-	-	-
L7	saprolite	metapelite (powder)	x	-	-	-	x	-	x
	soil	< 2 – mm fraction (powder)	x	x	x	x	x	-	-
		< 2 – µm fraction (powder)[1/]	x	x	x	x	x	-	-
		< 2 – µm fraction (oriented)	x	x	x	x	-	x	-
L8	saprolite	metapelite (powder)	x	-	-	-	x	-	x
	soil	< 2 – mm fraction (powder)	x	x	x	x	x	-	-
		< 2 – µm fraction (powder)[1/]	x	x	x	x	x	-	-
		< 2 – µm fraction (oriented)	x	x	x	x	-	x	-
L9	saprolite	metapelite (powder)	x	-	-	x	x	-	x
	soil	< 2 – mm fraction (powder)	x	x	x	x	x	-	-
		< 2 – µm fraction (powder)[1/]	x	x	x	x	x	-	-
		< 2 – µm fraction (oriented)	x	x	x	x	-	x	-
L10	saprolite	limestone (powder)	-	-	-	x	x	-	x
	soil	< 2 – mm fraction (powder)	x	x	x	x	x	-	-
		< 2 – µm fraction (powder)[1/]	x	x	x	x	x	-	-
		< 2 – µm fraction (oriented)	x	x	x	x	-	x	-

[1/] Reatto *et al.* (2008), saprolite-rocks = parent material, soil = Bw horizon of the Latosols, (x) = presence of the minerals and (-) absence of the minerals, K = Kaolinite, Gb = Gibbsite, Gt = Goethite, Hm = Hematite, Q = Quartz, HIV = Hydroxy-Al interlayered vermiculite, M = Muscovite.

Soil-solution composition

The values of soil-solution pH (pHs-s) ranged from 4.28 to 6.42. These values of pHs-s for the Latosols on the SAS presented higher values (pH 5.16 to 6.42) than in those on the VS (4.28 to 4.84). The activities of the major ionic species (pCa, pMg, pK, pAl and pH_4SiO_4) in the soil-solution composition for these Latosols ranged from: 4.91 to 5.12 (pCa); 5.15 to 6.03 (pMg); 4.78 to 5.49 (pK); 6.14 to 6.55 (pFe); 5.34 to 5.71 (pAl) and 4.21 to 4.73 (pH_4SiO_4). The ion-activity product for the minerals gibbsite (pQ_{Gb}), kaolinite (pQ_K) and hydroxy-Al interlayered vermiculite (pQ_{HIV}) in the soil-solution composition for almost all Bw horizons investigated were more negative than the thermodynamic equilibrium constant of these minerals. These findings indicate supersaturation or precipitation conditions before equilibrium is reached, except for the L7, L9, and L10, in which undersaturation or dissolution condition prevailed.

Conclusions

There is close relation between the occurrence of Gb, K, and HIV in the soil-solution phase versus its presence the equilibrium soil-solid phase in a short-time scale for the Latosols studied. The presence of HIV in these Latosols is not consistent with the weathering process in the tropical areas where the tendency is the progressive loss of Si and the enrichment of Al, consequently Gb (pedogenesis time).

References

Curi N, Franzmeier D (1984) Topossequence of Oxisols from Central Plateau of Brazil. *Soil Sci. Soc. Am. J.* **48,** 341–346.

Embrapa (1997) ‘Manual de métodos de análise de solo’. 2ed. rev. atual. (Empresa Brasileira de Pesquisa Agropecuária: Rio de Janeiro-RJ).

Embrapa (2006) ‘Sistema Brasileiro de Classificação de Solos’. (Empresa Brasileira de Pesquisa Agropecuária: Rio de Janeiro-RJ).

IUSS Working Group WRB. (2006) ‘World Reference Base for Soil Resources 2006’. (FAO: Rome)

Ker JC (1998) Latossolos do Brasil: uma revisão. *Geonomos.* **5,** 17-40.

Klute A (1986) In ‘Methods of Soil Analysis. Part 1. Physical and Mineralogical Methods’. (Ed A Klute) pp. 383–411. (American Society of Agronomy Inc.: Madison, WI)

Macedo J, Bryant RB (1987) Morphology, mineralogy, and genesis of a hydrosequence of Oxisols in Brazil. *Soil Sci. Soc. Am. J.* **51,** 690-698.

Melfi AJ, Pédro G (1977) Estudo geoquímico dos solos e formações superficiais do Brasil. Parte 1 – Caracterização e repartição dos principais tipos de evolução pedogeoquímica. *R. bras. Geociências.* **7,** 271 – 286.

Melfi AJ, Pédro G (1978) Estudo geoquímico dos solos e formações superficiais do Brasil. Parte 2 – Considerações sobre os mecanismos geoquímicos envolvidos na alteração superficial e sua repartição no Brasil. *R. bras. Geociências.* **8,** 11 – 22.

Page, A. L., Miller, R. H. and Keeney, D. R. (1982) *Methods of Soil Analysis, Part 2, Chemical and Microbiological Properties.* Amer. Soc. Agronomy and Soil Sci. Soc. Amer., Madison, Wisconsin, USA. 1159 pp.

Pédro G (1968) Distribution des principaux types d`altération chimique à la surface du globe. *Rev. Géogr. Phys. Géol. Dyn.* **X,** 457-470.

Reatto A, Bruand A, Martins ES, Muller F, Silva EM, Carvalho Jr OA, Brossard M (2008) Variation of the kaolinite and gibbsite content at regional and local scale in the Latosols of the Brazilian Central Plateau. *C. R. Geoscience* **340,** 741-748.

Robert M, Tessier D (1974) Méthode de préparation des argiles des sols pour des études minéralogiques. *Ann. Agron.* **25,** 859–882.

Schaefer CEGR, Fabris JD, Ker JC (2008) Minerals in the clay fraction of Brazilian latosols (Oxisols): a review. *Clay Minerals.* **43,** 1-18.

Soil Survey Staff (2006) ‘Keys to Soil Taxonomy.’ 10th edn. (USDA–Natural Resources Conservation Service: Washington, DC)

Sparks DL (2003) ‘Environmental Soil Chemistry’. (Academic Press: London).

Geochemical translocation of trace metals in iron-manganese cutans and matrices of subtropical soils in China

Li Huang[A], Fan Liu[A], Wenfeng Tan[A] and Ming Kuang Wang[B]

[A]Key Laboratory of Subtropical Agriculture Resources and Environment, Ministry of Agriculture, Huazhong Agricultural University, 430070, Wuhan, Hubei Province, China. Email huang_li62@yahoo.com.cn, liufan@mail.hzau.edu.cn, tanwf@mail.hzau.edu.cn
[B]Department of Agricultural Chemistry, National Taiwan University, Taipei, 10617, Taiwan, Email mkwang@ntu.edu.tw

Abstract

The geochemical translocation of trace elements in iron-manganese cutans and the corresponding matrix soils of Fragiudalfs (FRA), Ferrudalfs (FER) and Hapludult (HAP) in Subtropical China, were subjected to selective dissolution with 0.1 mol/L $NH_2OH·HCl$ (HAHC) and dithionite-carbonate-citrate (DCB) solutions, respectively. The MnO_2, Fe_2O_3, Ba, Co, Pb, Li, Cu, Zn, Ni, Cd contents in iron-manganese cutans are notable higher than those in corresponding matrix soils. Iron contents extracted by HAHC solutions is less than 3% of that by aqua regia solution, but the extractable manganese contents is over 80% in cutans. The Ba, Zn, Cd, Co, Cu, Ni and Pb mainly enrich in manganses minerals, and majority of Cr, Li and Mo exist in iron minerals of cutans. Selective extraction shows that the trace elements translocated from matrix soils and enriched in cutans along with the illuviation of iron- and manganese oxides during the formation of cutans.

Key Words

Geochemical translocation, iron oxide, iron-manganese cutan, manganese oxide, matrix soil, trace metal.

Introduction

Trace metals have different geochemical actions in the process of mineral weatherings and soil developments. The translocation abilities of trace metals in soils are different due to the diversity of properties among elements (Galán *et al.* 2008). Soil iron-manganese cutan is product of movement and precipitation of the special soil materials, such as iron and manganese oxides and clays (Brewer 1976). It could enrich lots of trace metals (Jongmans *et al.* 1996; Manceau *et al.* 2007). Their special material compositions reflected the geochemical information of elemental migration, deposition and transformation in the soil-forming process, and indicated the new combination and existing form of trace elements after translocation and transformation from bulk soils (Sullivan and Koppi 1993; Liu *et al.* 2002). Iron-manganese cutans are widely distributed in Alfisols and Ultisols in subtropical area in China. Although base ions are massively leached, the iron-manganese oxides and other trace metals are in the stage of frequent migration and deposition (Huang *et al.* 2007, 2008). Therefore, this article analysed the composition of iron and manganese oxides of the iron-manganese cutans in the Alfisols and Ultisols, studied the translocation characteristic of trace elements in the cutans, and gained the geochemical relationship between these trace elements and iron and manganese oxides of iron-manganese cutans in these subtropical Chinese soils.

Methods

Three representative soils with iron-manganese cutans in B horizons from different subtropical regions in central China, were collected for this study. They are Fragiudalf, Ferrudalf and Hapludult, according to Key to Soil Taxonomy (Soil Survey Staff, 2006), from Xinyang city in Henan Province, Wuhan City in Hubei Province and Taoyuan City in Hunan Province, respectively. There were collected 54 soil samples from the three pedons for physicochemical and statistical analyses. These soils were all from barren lands on the upper part of slopes in hilly area with good drainage conditions. The subangular blocky peds (matrix soils) containing cutans were collected from the B horizon at the depth about 20-50 cm. The cutan samples were black or brown materials collected lightly with a sterile blade under a microscope from soil blocks. Matrix soils (i.e., at least 25-30 kg) were sampled from adjacent ped interior blocks that were scraped off cutans. The air-dried matrix soils and cutans were ground to pass 10-, 20-, 60- and 100-mesh sieves, respectively. Table 1 is shown the climatic data and description of the selected sample tested. The cutan samples were dissolved in 0.1 mol/L $NH_2OH·HCl$ (HAHC) at pH 3.0 with a sample weight/ solution volume ratio of 1:100 to selectively reduce and dissolve manganese oxides in samples, and shaken at 25°C for 2 h (Tokashiki *et al.* 1986). The supernatant was collected after centrifugation for analysis. The total elements (Fe, Mn, Cu, Zn, Co, Pb, Li, Cr, Cd, Ni, Mo, Ba) were determined by Varian Vista-MPX ICP-OES, after acid digestion with aqua regia (HNO_3: HCl = 1:3) (125°C). Samples were extracted with dithionite-carbonate-citrate (DCB) (Mehra and Jackson 1960) and HAHC to determine free Fe-oxide (Fed) bound and iron-manganese oxide bound metals, respectively.

Table 1. Climate data and description of the selected samples tested.

No.	Sample	Location	Parent material	MAR[A] mm	MAT[B] °C	SM & TR[C]	Description
1-C	Cutan of FRA[D]	Xinyang (32°22'N, 114°39'E)	Quaternary (Q_3)	670	12.8-15.5	Udic-mesic	Reddish black moist color (10R 2/1)
1-B	Matrix of FRA						Strong brown (7.5YR 5/6); light clay; weak/moderate subangular blocky structure; very firm; some cutans
2-C	Cutan of FER[E]	Wuhan (30°42'N, 114°24'E)	Quaternary (Q_3)	1269	15.8-17.5	Udic-thermic	Yellowish block moist color (5Y 2/1)
2-B	Matrix of FER						Yellowish red (5YR 5/8); clay; weak/moderate subangular blocky structure; very firm; many cutans
3-C	Cutan of HAP[F]	Taoyuan (28°52'N, 111°27'E)	Quaternary (Q_2)	1437	16.0-16.5	Udic-thermic	Reddish black moist color (10R 2/1)
3-B	Matrix of HAP						Reddish yellow (7.5YR 6/8); clay; moderate subangular blocky structure; very firm; many cutans

[A] MAR = Mean annual rainfall; [B] MAT = Mean annual temperature; [C] SM&TR = Soil moisture and temperature regime; [D] FRA = Fragiudalf; [E] FER = Ferrudalf; [F] HAP = Hapludult.

Results

The basic properties and HAHC-extracted iron and manganese of cutan and matrix

The pH, organic matter (O.M.), base saturation (B.S.), Fe_2O_3, MnO_2, and clay contents of cutans are higher than that of matrix soils in horizon B (Table 2). Especially the MnO_2 contents in the iron-manganese cutans are 8.83-19.31 times higher than that in the relevant matrix soils. This indicates that iron-manganese cutans of Fragiudalf, Ferrudalf and Hapludult contain more clay, organic matter and iron-manganese oxides than the corresponding matrix soils. Vermiculite, illite and kaolinite are the major clay compositions in both cutans and matrix soils. Hydroxy-interlayered vermiculite (HIV) exists in matrix soils of Fragiudalf and Ferrudalf. Goethite is the main Fe-oxide mineral in cutans and matrix soils. Low amounts of birnessite and lithiophorite are present in cutans, but they cannot be detected in corresponding matrix soils (Huang *et al,* 2007, 2008).

Table 2. Selected soil chemical and physical properties.

No.	pH[a]	O.M.[b]	B.S.[c]	Fe_2O_3	MnO_2	Clay	Mineralogy of samples (Huang *et al,*2007, 2008)	
		g/ kg	%	g/ kg	g/ kg	g/ kg	Clay mineralogical composition[d]	Fe and Mn oxides[e]
1-C	6.70	18.01	50.02	57.96	16.41	526.4	V(++), I(++++), K(+)	G, B, L
1-B	6.54	12.70	55.74	48.63	0.94	424.0	V(++), H(+), I(++++), K(++)	G
2-C	5.93	3.35	45.06	62.37	10.04	514.8	V(++), I(++++), K(++),	G, B, L
2-B	5.81	3.01	53.65	45.56	0.52	457.7	V(+), H(+), I(++++), K(++)	G
3-C	4.41	3.61	35.85	60.76	5.83	547.8	V(+), H(+), I(++++), K(++)	G, B, L
3-B	4.25	3.24	34.15	56.53	0.66	462.5	V(+), H(+), I(++++), K(+++)	G

[a] Soil:H_2O = 1:2.5. [b] O.M. = organic matter. [c] B.S.= base saturation. [d] V = vermiculite, H = hydroxy-interlayered vermiculite(HIV), I = illite, K = kaolinite. Symbols of +: <100 g/ kg, ++: 100-250 g/ kg, +++: 250-500 g/ kg, ++++: 500-750 g/ kg. The semiquantitative mineralogical compositions were estimated by peak areas of XRD to phyllosilicate. [e] G = goethite, B = birnessite, L = lithiophorite.

Table 3. Manganese and iron oxides extracted by HAHC solutions.

No.	Fe_2O_3			MnO_2		
	Total content g/ kg	HAHC-extracted g/ kg	% extracted	Total content g/ kg	HAHC-extracted g/ kg	% extracted
1-C	57.96	1.40	2.42	16.41	13.69	83.42
2-C	62.37	1.56	2.50	10.04	10.01	99.70
3-C	60.76	1.27	2.09	5.83	5.08	87.14

The iron-manganese cutans were treated with 0.1mol/L HAHC solution at pH 3 .0 (Table 3). The iron extracted by HAHC is less than 3% of that by aqua regia solution, but the extractable manganese is over 80%. This indicates that HAHC selectively reaction with Mn is stronger that of Fe. Thus, it can extract the majority of manganese from iron-manganese cutans.

The form of trace metals in cutan and matrix after different selective dissolution

Compared with the matrix soils, the cutans enrich in trace elements (excepted Cr and Mo) (Table 4). This shows that a great deal of the trace elements move out of matrix soils and deposit in iron-manganese cutans. The contents of Ba, Co and Pb in cutans are especially higher than those in matrices. Ba, Zn, Cd, Co, Cu, Ni and Pb dissolve with HAHC in cutans are notably higher than those in the corresponding matrices that indicate these metals mainly enrich in Mn-oxides. Cr, Li and Mo dissolve in HAHC are obviously lower than those extracted with DCB and aqua regia solutions in cutans. Thus, Cr, Li, and Mo elements mainly exist in Fe-oxides in cutans.

Table 4. The contents of trace metals dissolved with aqua regia, HAHC and DCB solutions.

Sample	Ba (μg/g)			Zn (μg/g)			Cd (μg/g)			Co (μg/g)		
	AR[A]	HAHC[B]	DCB[C]	AR	HAHC	DCB	AR	HAHC	DCB	AR	HAHC	DCB
Cutan	156.73	67.49	98.73	51.07	2.17	30.10	0.45	0.06	0.21	11.90	7.44	9.44
Matrix	436.23	366.74	421.95	68.97	58.98	66.08	0.79	0.47	0.59	166.43	125.38	164.71

Sample	Cr (μg/g)			Cu (μg/g)			Li (μg/g)		
	AR	HAHC	DCB	AR	HAHC	DCB	AR	HAHC	DCB
Cutan	21.91	1.34	14.48	27.33	1.41	4.22	18.57	3.49	4.95
Matrix	15.31	0.20	10.04	41.35	28.53	34.72	21.61	7.48	18.05

Sample	Mo (μg/g)			Ni (μg/g)			Pb (μg/g)		
	AR	HAHC	DCB	AR	HAHC	DCB	AR	HAHC	DCB
Cutan	2.26	0.20	1.60	26.34	1.32	5.08	7.82	5.66	6.47
Matrix	1.78	0.20	1.14	47.43	27.51	40.21	124.30	106.85	119.37

[A] AR = aqua regia extraction; [B] HAHC =0.1mol/L $NH_2OH\cdot HCl$ extraction; [C] DCB = dithionite-carbonate-citrate extraction.

The molar ratio of trace metals in cutans and matrix soils

The metals respectively in the pairs of Mn and Fe, Cu and Zn, Zn and Cd, Co and Ni, Pb and Co have shown the similar chemical behaviors, and the mean molar rations of those elements are listed in Table 5. The molar rations of Mn/Fe, Cu/Zn, Co/Ni and Pb/Co in cutans all are greater than those of the matrices, but Zn/Cd molar ration is shown the reversed trend. This indicates that Mn, Cu, Co, Pb and Cd are easy to translocate in soils and deposit in cutans, respectively. Molar ratios of Mn to Fe and Co to Ni in cutans are respective 8.00 and 7.80 times higher than those in matrices, and the molar ratios of Cu/Zn, Zn/Cd and Pb/Co in cutans are respective 1.11, 0.77 and 1.14 times higher than those in matrices. It indicates that the differentiations of Mn and Fe, Co and Ni between cutans and matrices are greater than those of Cu/Zn, Pb/Co and Zn/Cd, respectively.

Table 5. The molar ratios of some trace metals in cutans and matrix soils.

Sample	Mn/Fe	Cu/Zn	Zn/Cd	Co/Ni	Pb/Co
Cutan	0.08	0.60	87.30	3.51	0.75
Matrix	0.01	0.54	113.49	0.45	0.66

The standard redox potential (Eh°) of manganese system is generally higher than that of the iron system, such as Eh° is 1.23 V for MnO_2-Mn (□) system and 0.77 V for Fe (□)-Fe (□) system (McKenzie 1989; Huang 1991). Therefore, manganese is generally more sensitive than iron to the change of wetting and drying. This led that the molar ratio of Mn to Fe in cutan is higher than that of matrix soil. MnO_2 contents show positive correlation with Co (R=0.72, n=54) and Ni (R=0.55, n=54) in matrices (Table 5). In cutans, the correlation of Ni and MnO_2 (R=0.40, n=54) changes a little bit compared with that of matrices, but the correlation of Co and free Fe-oxide (Fed) (R=0.45, n=54) obviously improved beside that Co and MnO_2 shows high correlation(R=0.71, n=54). There are shown positive correlations of Cu and Zn (R=0.75, n=54), Pb and Co (R=0.38, n=54), Zn and Cd (R=0.46, n=54) in matrices, respectively. There are also shown positive correlations in cutans. These metals all also show positive correlations with MnO_2 in cutans. Therefore, the differentiation degrees of Mn/Fe, and Co/Ni are higher, but those of Cu/Zn, Pb/Co and Zn/Cd molar rations are low in the process of translocation from matrix soils to cutans, respectively.

Table 6. Correlation coefficient (R) of selected elemental concentrations in cutans and matrix soils.

	MnO_2		Fed[a]		Co		Pb		Cu		Zn		Ni	
	C[b]	M[c]	C	M	C	M	C	M	C	M	C	M	C	M
MnO_2	1	1												
Fed	0.46[d]	-0.24	1	1										
Co	0.71	0.72	0.45	-0.45	1	1								
Pb	0.75	0.38	0.58	0.11	0.94	0.38	1	1						
Cu	0.22	-0.35	0.06	0.29	0.22	-0.40	0.20	-0.19	1	1				
Zn	0.34	-0.35	0.02	0.18	0.21	-0.50	0.20	-0.42	0.11	0.75	1	1		
Ni	0.40	0.55	-0.37	-0.42	0.00	0.61	-0.11	0.29	-0.01	-0.03	0.25	-0.04	1	1
Cd	0.66	-0.40	0.20	0.04	0.27	-0.36	0.29	-0.53	0.12	0.27	0.23	0.46	0.49	-0.39

[A]Fed = Fe soluble in dithionite-carbonate-citrate; [B]C = Cutan; [C]M = Matrix soil; [D]The underlined datum was a significant statistical correlation at $P < 0.05$ or 0.01(n=54, r0.05= 0.27, r0.01= 0.35).

Conclusions

The tested traces elements, especial Ba, Co and Pb, enrich in the iron-manganese cutans. These trace elements move from matrix soils to cutans with Fe- and Mn-oxides abundantly. Ba, Zn, Cd, Co, Cu, Ni and Pb mainly enrich in Mn-oxides, but Cr, Li and Mo mostly exist with Fe-oxides. Mn/Fe and Co/Ni molar rations show higher differentiation degrees than those of Cu/Zn, Pb/Co and Zn/Cd molar rations in the cutans compare with those in matrix soils. Iron-manganese cutans are possible geochemical information carriers of trace elements translocated in pedons during pedogenesis.

Acknowledgements

This research was supported by the National Natural Science Foundation of China (Grant No. 40971143).

References

Brewer R (1976) Fabric and mineral analysis of soils. pp. 205-233. (Robert E. Krieger Publishing, Huntington, NY)

Galán E, Fernández-Caliani JC, González I, Aparicio P, Romero A (2008) Influence of geological setting on geochemical baselines of trace elements in soils. Application to soils of South–West Spain. *Journal of Geochemical Exploration* **98,** 89-106.

Huang L, Hong J, Tan WF, Hu HQ, Liu, F, Wang MK (2008) Characteristics of micromorphology and element distribution of iron-manganese cutans in typical soils of subtropical China, *Geoderma* **146,** 40-47.

Huang L, Tan WF, Liu F, Hu HQ, Huang QY (2007) Composition and transformation of 1.4 nm minerals in cutan and matrix of Alfisols in central China. *Journal of Soils and Sediments* **7,** 240-246.

Huang PM (1991) Kinetics of redox reactions on manganese oxides and its impact on environmental quality. In 'Rate of Soil Chemical Processes'. (Eds DL Sparks, DL Suarez) pp.191-230.(SSSA Spec. Publ. 27. SSSA Madison. WI.)

Jongmans AG, Mulder J, Groenesteijn K, Buurman P (1996) Soil surface coatings at Costa Rican recently active volcanoes. *Soil Science Society of America* **60,** 1871-1880.

Liu F, Gilkes RJ, Hart RD, Bruand A (2002) Differences in potassium forms between cutans and adjacent soil matrix in a grey clay soil. *Geoderma* **106,** 289-303.

Manceau A, Lanson M, Geoffroy N (2007) Natural speciation of Ni, Zn, Ba, and As in ferromanganese coatings on quartz using X-ray fluorescence, absorption, and diffraction. *Geochimica et Cosmochimica Acta* **71,** 95-128.

McKenzie RM (1989) Manganese oxides and hydroxides. In 'Minerals in Soil Environments. 2nd edn.'. (Eds JB Dixon, SB Weed) pp. 439-465. (SSSA, Madison, WI, USA)

Mehra OP, Jackson ML (1960) Iron oxide removal from soils and clays by a dithionite-citrate system buffered with sodium bicarbonate. *Clays and Clay Minerals* **7,** 317-327.

Soil Survey Staff (2006) Keys to Soil Taxonomy. 10th ed., United States Department of Agriculture. Washington D.C., USA

Sullivan LA, Koppi AJ (1993) Manganese oxide accumulations associated with some soil structural pores. II. Composite coatings and translocation. *Australian Journal of Soil Research* **31,** 227-233.

Tokashiki Y, Dixon JB, Golden DC (1986) Manganese oxide analysis in soils by combined X-ray diffraction and selective dissolution methods. *Soil Science Society of America* **50,** 1079-1084.

Holocene volcanic soils in the Mt. Gambier region, South Australia

Hiroshi Takesako[A], David J. Lowe[B], Jock Churchman[C] and David Chittleborough[D]

[A]School of Agriculture, Meiji University, Kawasaki, Kanagawa, Japan, Email takesako@isc.meiji.ac.jp
[B]Dept Earth and Ocean Sciences, School of Science and Engineering, University of Waikato, Hamilton, New Zealand, Email d.lowe@waikato.ac.nz
[C]School of Earth and Environmental Scs., University of Adelaide, Adelaide, SA, Australia, Email jock.churchman@adelaide.edu.au
[D]School of Earth and Environmental Scs., University of Adelaide, Adelaide, SA, Australia, Email david.chittleborough@adelaide.edu.au

Abstract

Volcanic soils derived from mid-Holocene basaltic tephra in the Mt. Gambier region of South Australia have developed in a xeric moisture regime. We studied two soils, one at Mt Gambier (MTG) and the other at nearby Mt Schank (MTS). Both volcanoes were active ca. 6000 cal. years ago. The MTG soil has a high content of $CaCO_3$ (incorporated during eruption through limestone) and other exotic materials intermixed with basaltic tephra containing low amounts of glass. The MTS soil is derived mainly from basaltic tephra with high glass content and much less $CaCO_3$ than at MTG. These parent mineralogies have led to markedly different clay compositions and chemical properties: the MTS soil contains abundant allophane (mainly) and ferrihydrite with few layer silicate clays, whereas the MTG soil is dominated by layer silicate clays and low allophane or ferrihydrite. Both soils are near neutral or alkaline. The MTS soil has a melanic horizon and andic properties and is classed as a Melanoxerand. The MTG soil has weak andic properties with insufficient glass to enable it to be classed in the Andisols, and is instead a Calcixeroll.

Key Words

Andic properties, Xerands, Xerolls, basaltic tephra, limestone, humus composition.

Introduction

The youngest volcanoes in Australia comprise the Mt Gambier (MTG) and Mt Schank (MTS) basalt complexes, ~10 km apart, in southeast South Australia. The area is characterised by xeric moisture and mesic temperature regimes. Volcanic soils and on around these complexes are derived mainly from basaltic tephra materials erupted ca. 6,000 cal. years ago. Tephra erupted from the craters at MTG contains considerable quantities of $CaCO_3$ and quartz, chert, and siliceous sponge spicules derived from thick Tertiary limestone, and calcareous sands, through which the basalt was erupted. Previous work has shown that glass content in MTG soils is comparatively low (<20%), and that much of the glass is altered. Tephra (scoria) from MTS contains much less exotic material (only from underlying calcareous sands) and has a higher glass content (≥50%), most unaltered. Volcanic crystals in both cases include olivine, labradorite, titanaugite, and Fe-Ti oxides (Lowe and Palmer 2005). Although the glass at both sites is basaltic, and hence low in SiO_2 (~50 wt %) and high in Al_2O_3 (~17 wt %), extra SiO_2 occurs at Mt Gambier by inclusion of the exotic minerals. We studied differences in physical, mineralogical, and chemical properties for two soils, one at MTG (near Blue Lake) and the other at MTS (on scoria). We also analysed humic materials because both soils have deep, dark A horizons.

Methods

Soil analytical methods were based on ISRIC (1986). Humus compositions were analyzed using the Nagoya method (Kumada 1987). Allophane and ferrihydrite contents were estimated from oxalate and pyrophosphate-soluble Al, Si, and Fe (Parfitt and Wilson 1985). Layer silicate clays were estimated using XRD.

Results

The MTS soil has physical properties typical of pedogenesis of tephra including low bulk density (≤ 0.7 g/cm^3) and low solid phases. A high porosity with warm, dry summers and moist winters accelerated the weathering of the material to form a relatively high clay content in upper horizons (~30%) in comparison with that of the MTG soil (~20%) (Table 1). Total soil analyses match the primary mineralogies: the MTS soil has a typical basaltic composition whereas the MTG soil has a high content of SiO_2 in upper horizons and a high content of CaO in lower horizons, commensurate with the incorporation of limestone and silica polymorphs into its parent material (Table 2). The 2Bk horizons have high base/Al ratios because of minimal losses of CaO by leaching compared with losses from upper horizons. A1 and A2 horizons of both soils have high soil organic

Table 1. Physical properties.

	Horizon	Depth	Munsell	Bulk density	Three phase distributuion (%)			Particle size distribution (%)				Txture
		(cm)	color	(g/cm^3)	Solid	Liquid	Air	C. sand	F. sand	Silt	Clay	
Mt. Gambier	A1	0-20	10YR1.7/1	0.86	34.7	30.4	34.9	30.1	32.2	16.4	21.3	SCL
	A2	20-45	10YR2/1	0.97	38.8	27.4	33.8	35.9	31.2	13.6	19.3	SCL
	AB	45-60	10YR2/2	1.14	45.8	25.8	28.4	38.9	30.1	11.9	19.1	SCL
	Bw	60-75	10YR3/4	1.18	42.2	25.8	32.0	39.0	29.7	13.5	17.7	SCL
	2BCk	75-91	10YR4/3	1.33	50.2	23.6	26.2	48.2	30.1	10.8	10.8	LS
	2Ck1	91-130	10YR5/3	1.48	58.0	21.2	20.8	53.4	26.5	7.1	13.0	SL
	2Ck2	130-	10YR5/2	1.45	56.7	16.6	26.8	44.9	31.1	10.1	14.0	SL
Mt. Schank	A1	0-11	10YR1.7/1	0.52	22.4	40.6	37.0	26.4	17.8	26.2	29.6	LiC
	A2	11-22	10YR2/1	0.72	28.9	43.0	28.1	26.2	18.1	25.4	30.4	LiC
	AB	22-35	10YR2/3	0.72	26.6	40.8	32.6	29.3	20.2	23.5	27.1	LiC
	Bw	35-55	10YR4/4	0.66	24.9	36.6	38.5	39.3	24.3	20.0	16.4	LiC
	2A	55-75	10YR3/3	0.97	36.7	38.4	24.9	46.8	30.0	13.8	9.5	LS
	2C	75-100	10YR2/1	1.39	52.5	29.6	17.9	44.9	40.5	8.0	6.6	LS

Table 2. Total analysis of <2 mm fraction (% of 900 °C base).

	Horizon	SiO_2	Al_2O_3	Fe_2O_3	Ti_2O	MnO_2	CaO	MgO	K_2O	Na_2O	P_2O_5	SiO_2/Al_2O_3	$^aB/Al_2O_3$
Mt. Gambier	A1	75.34	8.45	5.55	1.13	0.07	4.92	2.03	1.07	0.69	0.75	15.1	1.94
	A2	81.42	6.84	4.83	0.93	0.06	2.41	1.50	0.85	0.63	0.53	20.2	1.48
	AB	81.57	7.43	4.90	0.96	0.06	1.65	1.50	0.87	0.59	0.48	18.6	1.17
	Bw	78.49	8.17	5.88	1.11	0.06	1.86	2.05	0.90	0.99	0.49	16.3	1.37
	2BCk	57.63	7.08	4.62	0.94	0.06	23.28	4.39	0.66	0.78	0.57	13.8	7.83
	2Ck1	59.15	6.60	4.16	0.80	0.05	22.69	4.68	0.62	0.76	0.49	15.2	8.34
	2Ck2	58.65	6.51	4.42	0.89	0.05	23.00	4.40	0.68	0.86	0.53	15.3	8.46
Mt. Schank	A1	51.14	12.89	12.73	3.15	0.17	6.83	7.20	1.04	1.52	3.35	6.7	2.66
	A2	49.51	13.44	13.42	3.30	0.18	6.81	7.61	1.01	1.60	3.12	6.3	2.63
	AB	47.72	14.65	14.17	3.50	0.17	6.67	7.80	0.96	1.56	2.80	5.5	2.42
	Bw	46.25	15.63	14.34	3.64	0.16	6.89	7.43	1.20	1.93	2.53	5.0	2.29
	2A	44.95	14.59	13.52	3.42	0.16	7.75	7.82	1.91	3.41	2.46	5.2	2.85
	2C	45.99	13.37	12.62	3.17	0.15	8.02	7.82	2.58	3.88	2.40	5.8	3.26

$^aB/Al_2O_3$: Base/Aluminum ratio;$(CaO+MgO+K_2O+Na_2O)/Al_2O_3$

matter contents (>10%), but a relatively lower content of N in the MTG soil relates to its high pH. The base saturation is >100% in horizons of the MTG soil, higher than for the MTS soil because of the limestone-bearing parent material. Values are also high in the MTS soil (~100%) because of the accumulation of bases by upward capillary movement during warm and dry summers. The values of phosphate absorption coefficients (equivalent to P retention) in horizons of the MTS soil are higher than those of the MTG soil because the MTS soil has much more allophane and ferrihydrite (Tables 3 and 4).

Table 3. Chemical properties.

	Horizon	pH			Org. C	Ino. C	T-N	C/N	Humus	CEC	Exchangeable cations (cmol/kg)				Base	P-Abs.
		H_2O	KCl	NaF	(g/kg)	(g/kg)	(g/kg)	(org. C)	(%)	(cmol/kg)	Ca	Mg	K	Na	satu. (%)	coeffi.
Mt. Gambier	A1	8.08	7.36	9.55	72.7	2.6	2.2	33.0	12.53	45.00	57.57	5.03	5.53	10.22	174	1179
	A2	7.98	7.38	9.67	56.6	1.8	1.7	33.3	9.76	37.44	46.14	3.65	0.77	1.16	138	1074
	AB	7.93	7.31	9.81	35.9	nd	1.1	32.6	6.19	32.54	30.58	2.85	0.50	1.41	109	947
	Bw	7.98	7.18	9.88	19.0	nd	0.6	31.7	3.28	24.48	24.88	3.91	1.32	3.25	136	920
	2BCk	8.29	7.60	10.5	11.8	41.2	0.3	39.3	2.03	14.91	36.20	3.98	0.83	3.50	298	765
	2Ck1	8.46	7.71	10.7	8.1	40.8	0.2	40.5	1.40	13.39	34.65	3.99	1.27	3.92	327	638
	2Ck2	8.66	7.70	10.5	5.1	51.2	0.1	51.0	0.88	12.68	30.71	2.63	0.61	1.65	281	703
Mt Schank	A1	6.57	5.72	10.3	112.8	nd	8.2	13.8	19.45	58.28	32.02	12.08	4.54	2.16	87	1670
	A2	6.84	5.81	10.7	60.2	nd	4.1	14.7	10.38	42.36	26.08	7.26	2.97	2.00	91	1635
	AB	6.96	5.90	10.5	40.0	nd	3.1	12.9	6.90	37.73	23.70	6.07	3.89	4.92	102	1769
	Bw	7.26	6.16	10.4	16.6	nd	1.3	12.8	2.86	29.28	18.49	5.27	2.41	3.05	100	2157
	2A	7.69	6.49	10.3	21.9	nd	1.6	13.7	3.78	25.23	16.92	5.18	2.42	3.06	109	1216
	2C	7.70	6.68	9.94	5.0	nd	0.4	12.5	0.86	10.04	6.44	2.00	1.18	1.27	109	433

P-Abs. coeff., is Japanese traditional metod for p-retension. Max value is 2687mg P_2O_5/100g soil at pH 7.0, nd: not detected.

The dominant clay minerals in the MTG soil are kaolinite, smectite, illite, irregular mixed layer smectite-illite, minor kaolin-smectite (indicated by asymmetric 0.7nm peaks), all of which originated from the limestone, and in the MTS soil the main clay is allophane with subordinate ferrihydrite (Figure 1). Allophane formation in the MTS soil is governed by Si leaching from upper horizons during winter and early spring when precipitation is at a maximum and evaporation is low, thereby promoting the formation of Al-rich allophane (Al: Si ratios are ~1.6-1.9) (Table 4). Around 280 mm of water on average drains through upper horizons for typically three to ten weeks in this period (out of a total annual rainfall of ~700 mm) (Lowe and Palmer, 2005). The MTS soil fulfills the andic properties requirements of both Soil Taxonomy and WRB to qualify for Andisols (Andosols), but the MTG soil has only weak andic properties and insufficient glass (<~20% required) to meet the thresholds for Andisols (Table 4). At some other sites in the MTG area, however, some soils had sufficient glass to just meet criteria required for Andisols (Lowe and Palmer 2005)

Table 4. Selective dissolution analysis and allophane content.

	horizon	^{A}OX (g/kg)			^{B}DC (g/kg)		^{C}PY (g/kg)		(Alo-Alp)/Sio	^{D}SRO	SRO/	Ferrihyd
		Sio	Alo	Feo	Ald	Fed	Alp	Fep	(molar)	(%)	Clay(%)	rite(%)
Mt. Gambier	A1	2.36	3.96	5.38	2.88	14.15	0.93	0.57	1.33	1.4	6	9
	A2	3.06	5.39	6.28	2.44	15.35	1.08	0.74	1.47	1.9	10	11
	AB	2.59	4.97	7.02	1.33	13.18	1.31	0.84	1.47	1.6	8	12
	Bw	3.11	6.79	9.22	2.72	13.69	1.08	0.73	1.91	2.3	13	16
	2BCk	3.55	4.58	6.92	2.00	9.14	0.25	0.14	1.27	2.0	19	12
	2C1k	3.33	3.65	5.34	1.33	8.75	0.25	0.10	1.06	1.7	13	9
	2C2k	3.01	2.25	5.71	1.02	7.66	0.12	0.11	0.74	1.3	9	10
Mt. Schank	A1	12.91	26.89	11.38	5.22	16.93	3.89	0.92	1.85	9.2	31	19
	A2	15.51	30.56	13.60	5.04	16.57	3.13	0.90	1.84	11.0	36	23
	AB	21.51	38.62	15.70	5.34	23.17	2.58	0.66	1.74	14.8	54	27
	Bw	24.72	39.42	17.73	5.58	21.99	1.22	0.52	1.61	16.1	98	30
	2A	16.38	24.91	13.58	4.70	22.87	0.87	0.47	1.53	10.4	109	23
	2C	6.98	11.19	7.31	1.28	5.55	0.47	0.24	1.60	4.5	69	12

^{A}Oxalate soluble Si, Al, Fe ^{C}Pyrophosphate soluble Al, Fe, Ca

^{B}Dithionite soluble Al, Fe ^{D}SRO: Short Range Order minerals; mainly allophane

Humic acids for all soil horizons from both MTS and MTG soils are classified as “A type”, the most highly humified type (Figure 2). Properties associated with these humic acids in surface to subsurface horizons of both soil are very similar (Table 5). We found it difficult to distinguish beween the soils using ^{13}C solid NMR spectra (data not shown). The accumulation and high degree of humification of the soil organic matter in both soils are probably promoted by formation of Ca-humus complexes in the MTG soil and of Al-humus complexes in the MTS soil. It is possible that Aboriginal ‘fire-stick’ farming has promoted strong humification and ‘melanisation’ in upper horizons through the addition of charcoal from burning and from regular bracken fern growth that follows (Lowe and Palmer, 2005). The upper horizons of the MTS soil form a melanic horizon and those of the MTG soil a mollic horizon (Tables 4 and 5).

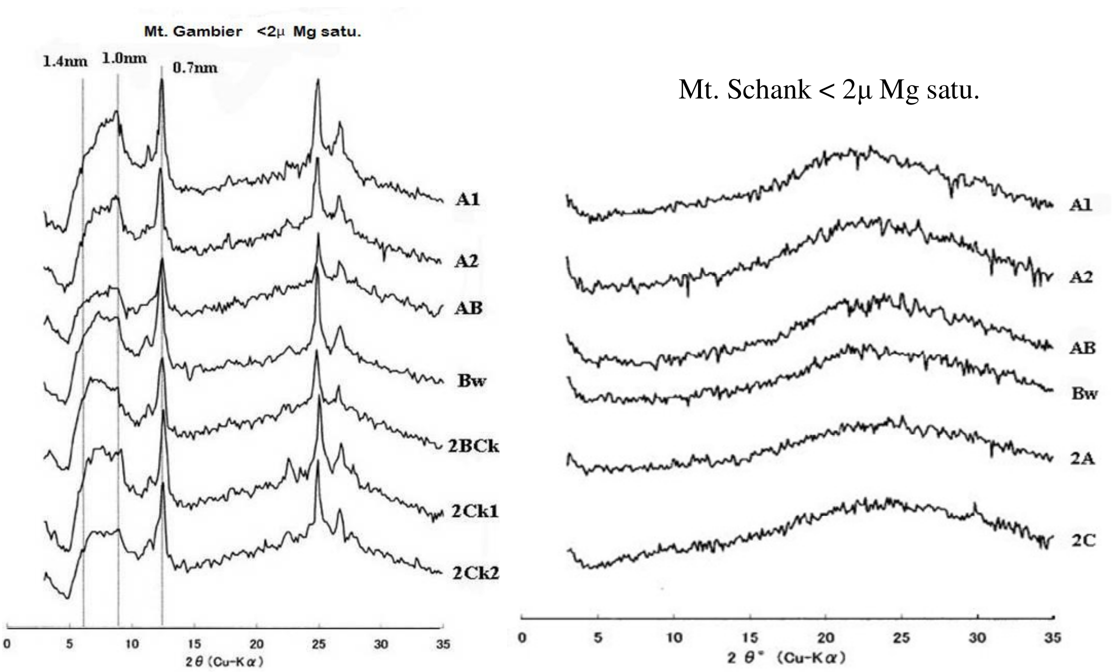

Figure 1. XRD patterns of Mg-saturated clay fractions.

Soil classification

The MTS soil we studied is a Typic Melanoxerand in Soil Taxonomy and a Silandic, Melanic Andosol (Eutric, clayic) in the WRB system. (Thaptic Haploxerands were also reported at MTS by Lowe and Palmer 2005.) The MTG soil we studied is a Typic Calcixeroll in Soil Taxonomy and a Haplic Chernozem in the WRB system. (Both Humic Vitrixerands and Calcic Haploxerands were additionally reported at MTG by Lowe and Palmer 2005.) At a site midway between the two volcanic complexes, a soil on fine basaltic ash was classed as an Alfic Humic Vitrixerand by Lowe and Palmer (2005). Xerands make up only ~4% of Andisols and hence are rare globally because andisolization tends to be favoured by strong leaching in cool, udic moisture regimes. The Xerands in the Mt Gambier area are the only Andisols currently known in Australia (they are Andic, Chernic Tenosols in the Australian Soil Classification).

Table 5. Humus composition.

	Horizon	HT	HE	HE/HT(%)	a	b	PQ(%)	RF	⊿-logK
Mt Gambier	A1	137.1	67.5	49	51.4	16.1	76	112.7	0.557
	A2	92.0	57.7	63	44.9	12.8	78	131.0	0.538
	AB	85.1	42.0	49	28.7	13.4	68	136.9	0.530
	Bw	48.4	19.4	40	9.5	9.9	49	125.9	0.535
	2BCk	15.8	8.7	55	3.5	5.2	40	98.3	0.538
	2C1k	7.0	3.6	52	1.5	2.1	41	94.0	0.554
	2C2k	2.1	1.6	76	0.7	0.9	45	116.7	0.591
Mt. Schank	A1	222.9	94.1	42	64.9	29.2	69	88.1	0.623
	A2	137.7	64.2	47	40.0	24.2	62	156.2	0.512
	AB	96.2	39.6	41	19.8	19.8	50	138.8	0.552
	Bw	36.8	17.3	47	6.7	10.5	39	140.2	0.554
	2A	30.9	16.2	53	6.5	9.7	40	120.0	0.520
	2C	10.9	6.0	55	1.9	4.1	32	103.0	0.503

HT: total humus; ml of 0.1N $KMnO_4$ consumed by 1g soil. (converted rate using dry combastion is 1ml = 0.4mg C)

HE; extracted humus; the sum of 0.1N $KMnO_4$ (ml) consumed by HA and FA of the two extracts per 1g soil.

a and **b**: the amount of HA(humic acid) and FA(fuvic acid, respectively, calculated as ml of 0.1N $kMnO_4$ consumed by HA and FA of each extract corresponding to 1g soils.

PQ: a/(a+b) * 100; percent of HA in extracted humus(HA + FA)

RF: K600 * 1000/c; where c is ml of 0.1N $KMnO_4$ consumed by 30ml of HA solution used for determining absorption spectrum.

⊿-log K: log k 400 - log K 600, where K is the optical density at 400 or 600 nm

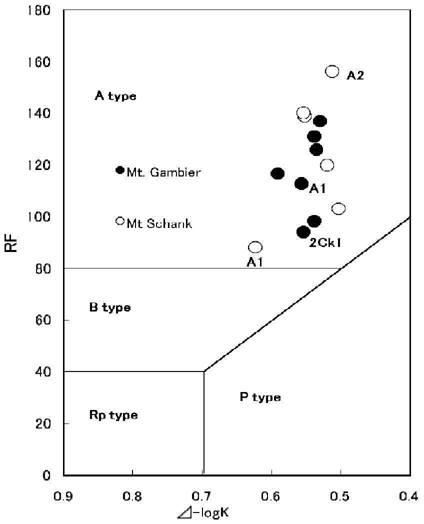

Figure 2. Classification diagram of humic acid

Conclusion

Contrasts in parent materials of two soils of similar mid-Holocene age at MTG and at MTS in southeast South Australia, which has a xeric moisture regime, have led to markedly different soil physico-chemical properties and clay compositions. Soils at MTS, on basaltic tephra (scoria) with common glass and relatively few limestone-derived minerals, contain much more allophane and ferrihydrite but few layer silicate clays. Soils at MTG, on basaltic tephra with intermixed limestone and other exotic materials including silica polymorphs, contain low allophane and ferrihydrite and abundant layer silicate clays including kaolinite, smectite, and illite. Organic matter in both soils is similar in accumulation and humification (both A type) and meets melanic or mollic epipedon requirements. The MTS soil in our study is Typic Melanoxerand (or Silandic, Melanic Andosol), and the MTG soil in our study is a Typic Calcixeroll (or Haplic Chernozem).

Selected reference

Lowe DJ, Palmer DJ (2005) Andisols of New Zealand and Australia. *Journal of Integrated Field Science* 2, 39-65.

Micromorphological identification of selected lithogenic features in soils developed from Lower Triassic deposits in the Holy Cross Mountains (S Poland)

Sylwia Brzychcy, **Zbigniew Zagórski**

Division of Soil Science, Department of Soil Environmental Sciences, Warsaw University of Life Sciences-SGGW, Nowoursynowska 159, 02-776 Warszawa, Poland e-mail: zbigniew_zagorski@sggw.pl, sylwia_brzychcy@wggw.pl

Abstract

Areas with red soils developed from Lower Triassic (Buntsandstein) deposits cover about 500 km^2 of the Holy Cross Mountains area (S Poland). Application of modern techniques such as microscopic studies and computer image analysis allow us to identify the lithogenic features of these soils and establish their systematic position. Micromorphological analysis revealed the occurrence of such lithogenic soil substrate features as the presence of hematite and muscovite in the microskeleton, diagenetic features of the quartz grains or fissuring. Based on these data the soils were classified as Leptosols or Cambisols.

Key Words

pedogenesis, lithogenesis, sandstones, siltstones, clays

Introduction

One of the most crucial problems in soil science is the determination of mutual relationships between such factors as the geological origin of the parent rock, the pedogenic process and the soil properties. This issue is particularly significant in cases when the parent material is represented by deposits with specific or variable mineralogical-petrographic properties. In present-day research trends, the most objective indicators of the *in situ* soil environment are micropedological methods. Based on analysis of unchanged soil samples using microscopic and ultramicroscopic techniques, these methods allow us to identify various elements of the soil environment, determining their mutual relationships in space (pedons), as well as indicating their succession in time (Zaniewski, Van der Meer, 2005; Todisco, Bhiry, 2008). In case of micromorphological studies, the application of optic microscopy methods in polarized transmitted and reflected light allows the observation of many features and properties of the soil substrate that are imperceptible to the naked eye (e.g. size, shape and distribution of coarse grains, distribution of fine elements and pores, presence of organic remains), and which compose the soil microstructure (soil fabrics; Brewer, 1976). Detailed recognition of the microstructure elements allows to evaluate the transformations taking place in the parent material under pedogenic processes. Determination of the scale of these transformations, e.g. based on the analysis of lithorelicts, may have crucial significance in interpreting soil properties and origin (Fitz Patrick, 1993; Stoops 2003). Application of digital registration of micromorphological images and advanced computer software for data processing allow an objective evaluation of the determined features and phenomena (Zaniewski, Van der Meer, 2005; Eliot, Heck, 2007).

The present studies were focused on recognition and quantification of characteristic lithogenic elements in the substrate of soils developed from the Lower Triassic (Buntsandstein) sandstone-clay sediments of the Holy Cross Mountains (S Poland). The obtained results allowed to verify macroscopic data on the range and course of pedogenic processes, origin of some soil horizons and explanation of the specific properties of these soils. They were also an important factor used in classifying the studied soils.

Material and methods

The Holy Cross Mountains are a hilly area in southern Poland. Palaeozoic folds surrounded by Mesozoic strata were exposed after tectonic uplift in Tertiary times (Mizerski, 1995). A large variety of rocks resulted in the complexity of the spatial distribution of many soil types. The Lower Triassic Buntsandstein deposits occur in the Holy Cross Mountains in an area of about 500 km^2 and are developed as clays, sandstones and conglomerates (Senkowiczowa, 1970). Soils developed from these sediments have unique features and properties, unknown in other genetically and typologically similar rocks. One of the dominating features is the characteristic red colour, resulting from the presence of hematite in the substrate (Szafranek, 1989; Zagórski, Kaczorek, 2002). The study area was located in the Holy Cross Mountains near Wrzosy, Skrzelczyce, Osiny and on Brzuśnica Hill. Profiles of soils developed from Lower Triassic Buntsandstein conglomerates, sandstones, clays and siltstones were made. The micromorphological studies were made on thin sections from

all genetic horizons with application of the Olympus BX-41 polarized microscope.
The terminology applied for micromorphological features is after Stoops (2003) and Bullock (Bullock *et al.*, 1985). Image analysis was made with AxioVision 4.5 software with Auto Measure module; each thin section was covered with 8 photographs made at identical light exposure and magnification, which were next combined into an entire thin section (Zaniewski, Van Der Meer, 2005).

Discussion of results

In soils located near Brzuśnica Hill the crucial problem was to explain whether the specific gravel-clay horizons at 50-90 cm are illuvial horizons Bt or lithogenic horizons C or R. Microscopic analysis of thin sections indicated that many micromorphological features of the soil substrate from these horizons show similarities to the petrographic-lithological features of Lower Triassic conglomerates. The main microskeleton elements $c_{(> 1\ mm)}$ are rather well rounded clasts of various rocks – sandstones, quartzites and siltstones. Rarer are fine quartz grains $c_{(1 - 0.01\ mm)}$ and muscovite plates. Fine elements $f_{(< 0.01\ mm)}$ comprise clay minerals and they generally fill up voids between the grains (Figure 1). The micromorphological features of this fraction indicate that it is of lithogenic character and represents the primary matrix-type component. The characteristic red colour indicates the presence of hematite, which evidences its relationship with the Triassic clay rocks (Bullock *et al.*, 1985; Zagórski, Kaczorek 2002; Tawornpruek *et al.*, 2006). The analysis of clay concentrations did not reveal the presence of specific incrustations pointing to processes of clay fraction translocation. Thus, elluvial-illuvial processes responsible for the formation of horizon Bt are not present. Based on these results the soils were assigned to Cambisols.

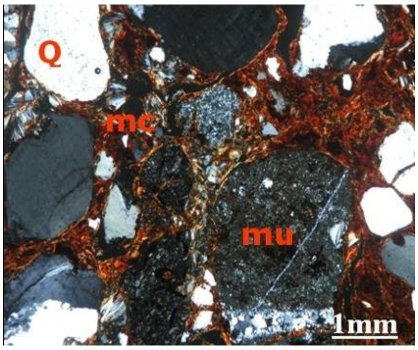

Figure 1. Mikroskeleton differentiated with size of grains and mineral composition; Q – quartz, mc – muscovite, mu - mudstone. Brzuśnica Hill profile, gravel-clay horizon (XPL).

In soils developed from sandstones (Skrzelczyce profile), an important issue was the small thickness of the soil profile. The location of soils in the topmost parts of the hills showed the possibility of erosional processes as factors influencing their formation. Micromorphological analysis showed that most quartz grains derive from the weathering sandstones. This is evidenced by their small size $c_{(1 - 0.01\ mm)}$ and lack of rounding (Figure 2A). The lithogenic origin of the quartz grains is indicated also by the fact that a large number of grains showed characteristic optical features e.g. microsegment relief (Figure 2B) and regeneration rims. These are typical diagenetic features of the Lower Triassic sandstones (Barczuk, 1979). The obtained results unequivocally indicate that the soils developed from Lower Triassic sandstones are shallow soils, and their soil material is not the result of accumulation (glacial, eolian) processes but is formed in situ due to weathering of rocks. Thus the soils were classified as Leptosols.

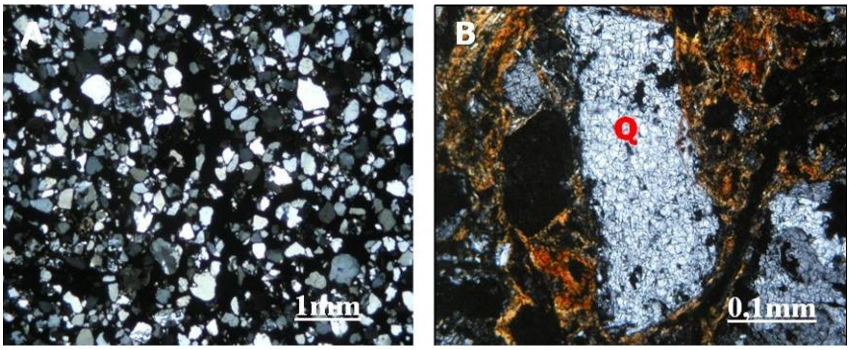

Figure 2. A – unrounded quartz grains in mikroskeleton; B - mikrosegment relief of quartz grain. Skrzelczyce profile (XPL).

In soils developed from siltstones (Wrzosy profile), micromorphological analysis of the lithogenic features allowed us to distinguish the lower range of the pedogenic processes. The specific character of these soils (fine-grained soil substrate and uniform red colour) caused difficulties in macroscopic distinguishing of the genetic horizons. Microscopic analysis of thin sections in subsequent samples allowed to determine that the prevalence of lithogenic features is evident below 80 cm of the soil substrate. The small diameter of the microskeleton grains c $_{(0.1-0.01\ \mathrm{mm})}$ directly corresponds to the siltstone fraction and comprises unrounded quartz grains and small muscovite plates (Figure 3). The most important lithogenic indicator is the characteristic red colour of the fine elements f $_{(< 0.01\ \mathrm{mm})}$ comprising the clay fraction. It occurs in form of laminas (or forms zonal concentrations), what evidences the preservation of sedimentary features of the deposit. Deep table of the parent rock allows to classify these soils as Cambisols.

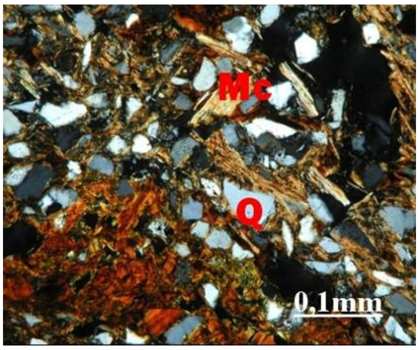

Figure 3. Microskeleton with unrounded quartz grains and small muscovite plates. Wrzosy profile, depth 80cm (XPL).

In soils developed from clays (Osiny profile), an important issue was the presence of a characteristic structure in the middle and lower part of the soil profile. The soil substrate was disintegrated into sharp-edged prisms. This is probably a lithogenic feature. Microscopic analysis showed that the clay soil substrate is sub-divided by numerous fissures (craks structure; Bullock *et al*., 1985), whereas voids in form of channels and chambers are absent. A characteristic feature is the lack of changes in the organization of clay domains near the fissures (vosepic structure; Brewer, 1976). Detailed measurements of the microscopic images was made with application of computer image analysis. It showed that the fissures occurring in the soil substrate are 200-400µm long and organized in a network with meshes approximately at 90° (Figure 4). The fissures are of secondary character, typical of the Lower Triassic clays from the Holy Cross Mountains area and interpreted as the result of post-diagenetic relaxation of the clay sediment (Barczuk 1979). The presented lithogenic features testify for the assignment of these soils to Cambisols.

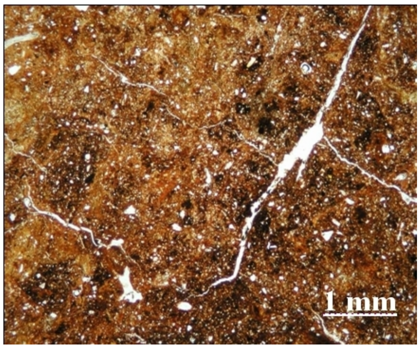

Figure 4. The fissures organized in a network with meshes approximately at 90°. Osiny profile (PPL).

Summary

Micromorphological studies have shown that soils may preserve the lithogenic features of the parent substrate. They include: the presence of hematite and muscovite in the mineralogical-petrographic microskeleton and soil plasma, the diagenetic regeneration rims on quartz grains as well as secondary fissuring. The identification of these features allowed a precise determination of the systematic position of the studied soils: Leptosols in the case of the Skrzelczyce profile and Cambisols in the case of the Wrzosy, Osiny and Brzuśnica Hill profiles.

References

Barczuk A (1979) Geological study of Buntsandstein in NE part of Holly Cross Mountains. (In polish) *Mineralogical Archive* **35**, 1-156.

Brewer R (1976) Fabric and mineral analyses of soil. 2-nd printing. Kreiger Publishing Co., Huntington, New York.

Bullock P, Fedoroff N, Jongerius A, Stoops T, Tursina T (1985) Handbook for soil thin section description. Waine Research Publication. Wolverhampton, England.

Elliot TR, Heck J (2007) A comparison of optical and CT techniques for void analysis in soil thin sections. *Geoderma* **141**, 60-70.

Fitzpatrick EA (1984) Micromorphology of Solis. Champman and Hall. London.

Łyczewska J (1971) Quaternary on Holly Cross Mountains Region. (In polish) Works PIG **64**, 5-98.

Mizerski W (1995) Geotectonic evolution in the Holy Cross Mts. in Central Europe. *Bulletin of Polish Geological Institute* **372**, 51-75.

Mycielska-Dowgiałło E (1988) Genesis of sediments and soils in electron microscope researches. (In polish). Publishing Warsaw University: 57-62.

Senkowiczowa H (1970) Trias In: Stratygraphy of Mesozoic in are around The Holly Cross Mountains. (In polish) *Bulletin of Polish Geological Institute* **56**, 21-35.

Stoops G (2003) Guidelines for analysis and description of soil land regolith thin section. Soil Science Society of America. Madison, Wisconsin, USA.

Szafranek A (1989) Influence of relief and parent material on soil formed from Devon and Triasic sandstone in Holly Cross Mountains. (In polish) *Polish Annual of Soil Science* **40**, 2, 59-81.

Tawonpruek S, Kheoruenromne I, Suddhiprakarn A, Gilkes RJ (2006) Properties of red Oxisols on calcareous sedimentary rocks in Thailand. *Geoderma* **136**, 477-493.

Todisco D, Bhiry N (2008) Micromorphology of peryglacial sediments from the Tayara site, Qikirtaq Island, Nunavik (Canada). *Catena* **76**, 1-21.

WRB (2006) Word Reference Base for Soil Resources 2006. Food and Agriculture Organization of the United Nations. Rome.

Zaniewski K, Van Der Meer JJM (2005) Quantification of plasmic fabric trough image analysis. *Catena* **63**, 109-127.

Zagórski Z, Kaczorek D (2002) Haematite – a lithogenic form of iron in soils from the southern part of the Holy Cross Mountains. Annual of Warsaw Agricultural University, Agriculture **43**, 78-96.

Pedogenesis in a fluvial terrace chronosequence in the Pacific Northwest, USA

Katherine Lindeburg[A], **Peter Almond**[B], Joshua Roering[C], and Oliver Chadwick[D]

[A]Graduate student of Crop and Soil Sciences, Pennsylvania State University, University Park, USA, Email klindeburg@gmail.com
[B]Faculty of Soil and Physical Sciences, Lincoln University, Canterbury, New Zealand, Email peter.almond@lincoln.ac.nz
[C]Faculty of Geological Sciences, University of Oregon, Eugene, USA, Email jroering@uoregon.edu
[D]Faculty of Geography, University of California, Santa Barbara, USA Email oac@geog.ucsb.edu

Abstract

We evaluated pedogenic properties in a river terrace chronosequence in the Oregon Coast Range with the purpose of identifying pathways and rates of soil genesis. Knowledge of time-dependent changes in soil properties enables approximations of residence times to be made for soils of unknown ages. We also used a mass balance analysis to determine how rates and forms of mass losses change over the course of soil development. Changes in soil properties observed in the soil chronosequence include an increase in profile thickness, soil redness, and accumulation of secondary minerals. Losses of weatherable minerals and total Si, Na, Ca, and K increase with terrace age. Fe is conserved in secondary crystalline oxides, and elemental Al is conserved in Al-Si clay minerals. The largest changes in soil physical and chemical properties occur within the first five terraces. The advancement of the weathering front to depths of nine meters in the two oldest terraces contributes to the large mass loss of Si.

Key Words

Quantitative pedogenesis, desilication, podzolization, marine terraces.

Introduction

Bockheim *et al.* (1992) developed a model of pedogenesis for the udic moisture regime (mean annual rainfall of 1900 mm), isomesic temperature regime (mean annual air temperature 11.7˚C) region of coastal Oregon, USA, from chronosequences of soils across flights of coastal marine terraces. The soils formed in surficial deposits of sand derived from in situ and reworked beach and beach face sediments under predominately Sitka spruce in the younger (80 to 125 ky) and Douglas-fir in the older (240 to >500 ky) terraces. The marine terrace model of Bockheim *et al.* (1992) suggests that in-situ clay formation and podzolization dominate early in pedogenesis, leading to development of Inceptisols and Spodosols; after intermediate periods of soil formation, podzolization and argilluviation act concurrently to form spodic and argillic horizons in soils classified as Ultisols; in late stages of soil development, argilluviation and clay neoformation are the dominant soil-forming processes and form strongly expressed Ultisols.

In this paper we test the general validity of this model in coastal Oregon, recognising that the soil sequences it is based on form in a quartz-rich, coarse-textured parent material, have relatively low temporal resolution, and receive high accessions of marine aerosols. Our test is based on morphological, chemical and mineralogical characterisation of a chronosequence of soils formed on fluvial terraces of the Siuslaw River in the Oregon Coast Range (OCR). A key question centres on the absence of Spodosols in the OCR chronosequence whereas this soil order features prominently in the coastal and marine terraces of Oregon and California and in the marine terrace model (Bockheim *et al.* 1992; Bockheim and Langley-Turnbaugh 1997; Langley-Turnbaugh and Bockheim 1997; 1998).

Methods

Site description

The OCR chronosequence comprises seven fluvial terraces formed along a ridge on the inside of a meander bend of the Siuslaw River in Lane County of western Oregon. The lower five terraces (T1 through T5, Table 1) have an obvious broad, planar form and are underlain by silty to sandy alluvium and some colluvium derived from Eocene Tyee sandstone. The highest two sites (T6 and T7) are terrace remnants recognisable only as benches in the ridge and denudation has removed the alluvial coverbeds, although deeply weathered soils persist. Ages of the two youngest terraces were determined by radiocarbon dating of detrital charcoal in the soil pits of Terraces 1 and 2; and, ages of the five other terraces were calculated using elevation above modern river

1 – 6 August 2010, Brisbane, Australia. Published on DVD.

valley and incision rate (Almond *et al.* 2007). The terraces range in age from several thousand to ~990 ky.

Table 1. Study site properties.

Terrace	Terrace age (ky)[†]	Elevation (m)[‡]	Depth of weathering (cm)	Soil suborder
T1	3.5	85.5	25	Psamment
T2	20	89.0	109	Udept
T3	69	94.3	260	Udult
T4	140	106.9	310	Udult
T5	200	117.6	460	Udult
T6	908	248.9	>910	Humult
T7	990	263.8	>1100	Humult

[†]Terrace ages and [‡]elevations from Almond *et al.* 2007. Ages of terrace 1 and 2 determined from radiocarbon dating of detrital charcoal; ages of terraces 3 through 7 calculated from uplift rates and terrace elevations.

Field sampling

Soil pits were dug to at least 1.4 meters in the first five terraces, and roadside exposures were used in the two remnant and oldest terraces. Soils were described by genetic horizon using the standard methods (Milne *et al.* 1995) and sampled in 10 cm increments. An auger was used to collect samples deeper than the exposed pits either to the parent material or the maximum extent of the auger. Bulk density was calculated using a soil sleeve of known volume in the top two meters and a bucket auger of known volume in deeper locations.

Laboratory analyses

All laboratory procedures were performed according to standard USDA methods (Soil Survey Staff 2004). Soils were air-dried and sieved to <2 mm at University of Oregon at Eugene. Representative subsets of samples were sent to ALS Chemex (Sparks, NV) for total elemental analysis and to University of California at Santa Barbara for soil physical and chemical analyses. Base cations were extracted at pH 7 with 1M NH_4oac and analysed by flame atomic absorption spectrometry. Cation exchange capacity (CEC-7) was determined with 1M KCl and a colorimetric autoanalyzer analyser. Electrical conductivity (mS/cm) and pH were measured on the supernatant of a 2:1 water to soil solution with handheld and bench-top meters. Soils were extracted for Fe and Al with 0.1M sodium pyrophosphate (McKeague 1967), 0.2M ammonium acid oxalic acid buffered at pH 3 (McKeague and Day 1966), and dithionite-citrate-bicarbonate (Mehra and Jackson 1960). Extracts were analysed by flame atomic absorption spectroscopy and correspond to the crystalline, non-crystalline, and organically-complexed Fe and Al oxides. Percent C and N were determined by the combustion method utilizing a Carla-Erba analyser after samples were ground to a fine mesh. Particle size distribution was determined by the pipette method on samples pre-treated for organic matter using H_2O_2 and for iron oxides using dithionite-citrate-bicarbonate (Jackson 1954). Sand fractions were wet sieved prior to sedimentation and prepared for analysis by XRD via random powder mounts. A qualitative analysis was performed using the relative intensities of diagnostic diffraction peaks to determine relative abundances of quartz, potassium feldspars, and plagioclase feldspars in sand-sized fractions (Moore and Reynolds 1997). Diffractograms were obtained with a Bruker D8 Advance diffractometer with a CuKα beam, scan range of 4° to 60° 2θ, step size of 0.015° 2θ, and step time of 0.5 seconds.

Results

Soils change from Entisols (T1) to Inceptisols (T2), to Ultisols (T3 and older). The most striking feature of soil morphological evolution is reddening. Soil hues are 2.5Y on T1 and progressively redden to 10R on the oldest two terraces (Figure 1). Reddening is associated with progressive increase in clay, expression of clay cutans, and formation of concretions. Strongly developed topsoils or surface organic (L, F, H) horizons are not strong features of any of the soils apart from a clear cumulate A horizon on T1.

Other than on T1, all soils are strongly acid, depleted in exchangeable base cations, and have low cation exchange capacities (Table 2). Pedogenic oxides of both Al and Fe accumulate over time and generally decrease in concentration with soil depth. Whereas pedogenic Al oxides comprise only a small fraction of total Al in all terraces, pedogenic Fe comprises an increasing amount of total Fe, with increasing degree of crystallinity, as soils age (Figure 2).

Table 2. Depth-weighted average chemical properties.

Terrace	pH	Soil Moisture (%, θ_g)	Ca	K	Na	Mg	CEC	Σ Cats
			---------------------------------- cmolc/kg ----------------------------------					
1	5.4	1.00	3.4	0.21	0.21	1.5	11.5	5.32
2	4.9	4.09	0.60	0.31	0.10	0.34	30.2	1.35
3	4.9	2.64	0.16	0.16	0.10	0.31	17.5	0.74
4	5.1	2.67	0.25	0.20	0.14	0.38	19.4	0.98
5	4.9	2.45	0.05	0.13	0.07	0.15	16.7	0.39
6	4.8	2.94	0.32	0.14	0.14	0.32	20.7	0.92
7	4.9	2.66	0.13	0.12	0.11	0.16	17.6	0.53

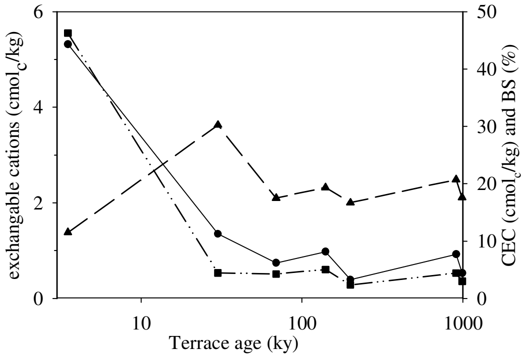

Figure 1. Chemical properties of B horizons. The youngest aside, all soils are depleted in exchangeable base cations (Σ cations, ●) and have low base saturations (BS, ■). Maximum cation exchange capacity (CEC, ▲) in the chronosequence soils occurs in terrace 2, and all others have relatively similar and low CECs.

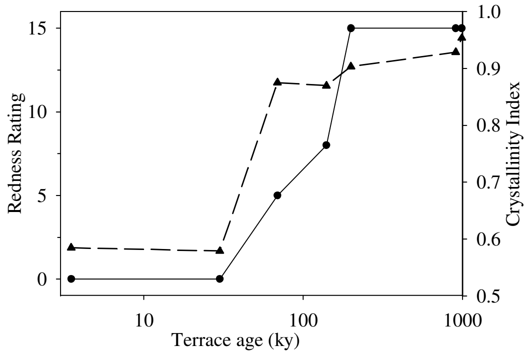

Figure 2. Crystallinity and redness ratings of B horizons. Crystallinity (●) was calculated as [1-(Fe_{ox}/Fe_{dcb})]. Redness rating (▲) was calculated from field-moist colors as [(10-H)x(C/V)] where H is hue, C is chroma, and V is value, and H was converted from Munsell hues of 10R, 2.5YR, 5YR, 7.5YR, and 10YR to 0, 2.5, 5, 7.5, and 10, respectively (Torrent *et al.* 1983).

Temporal mineralogical changes of the sand fraction include an increase in the abundance of quartz at the expense of plagioclase and K-feldspars on increasingly older terraces. Soil chemical and physical properties, pedogenic Fe- and Al-oxide contents, sand mineralogy, and bulk-soil elemental analyses suggest progressive pedogenesis results in transformation of the primary minerals muscovite, biotite, Mg-chlorites, andesine, plagioclase feldspars, and K-feldspars to gibbsite, hematite, goethite, vermiculite, smectite, and kaolinite.

The dominant effects of pedogenesis are (1) depletion of Si, Na, Ca, K, and Mg; (2) conservation and redistribution of Al and Fe; and (3) transformation of Al and Fe from the parent material to secondary pedogenic oxides. Losses of Si represent the largest and most progressive net elemental depletion. Losses range from -28.7 g/cm^2 at 40 ky to -219 g/cm^2 by 990 ky. In contrast, Na and Ca losses are supply-limited and reach maximum depletion by 140 ky with net elemental losses of 5.62g/cm^2 and 3.41 g/cm^2, respectively. Maximum elemental depletion of K and Mg is reached by 200 ky, and losses subsequently lessen with age. Mineral analyses corroborate mass-balance results of Na and Ca removal with increasing age, and shifts of Si, Mg, and K from sand to clay-sized particles. Overall, the chronosequence data suggest a shift from depletion of bases and acidification as the dominant processes for the first 200 ky, to production and redistribution of secondary oxides and clay minerals thereafter, whilst Si is continually leached.

Conclusion

Important differences between the pedogenic evolution of the soils on marine terraces described by Bockheim *at al.* (1992) and our river terrace sequence include (1) an absence of Spodosols and (2) a rapid accumulation of clay in our chronosequence. After only 20 ky, B horizons contain >30% clay; in contrast, 105 ky is required to form this amount of clay in well-drained marine terrace soil sequence. The soil parent materials derived from the Tyee formation contain an abundance of pre-weathered and easily-weatherable minerals and the fluvial deposition processes have resulted in less textural and mineralogical sorting than the beach and eolian processes forming the parent materials of the marine terrace soils. Clays inherited from the parent material and formed by weathering appear to have a moderating effect on podzolization, allowing clay – Fe oxide complexes to form, and inhibiting strong redistribution of Fe and Al characteristic of podzolization. We speculate that as Fe oxides accumulate, organic chelating agents become saturated with Fe and are rendered immobile. Relatively rapid organic matter turnover in the dry, warm environment then prevents these compounds from accumulating. The net result is a pedogenic pathway that favours the accumulation of Fe oxides and clay. The pedogenic pathways represented by the coastal marine terrace chronosequences and the OCR chronosequence therefore probably reflect a bifurcation resulting from a subtle shift in the balance of formation of complexing organic compounds and secondary Fe oxides and clays. The shift in this balance may result from any combination of subtle differences in vegetation, marine aerosol inputs, parent materials, and bioturbation regimes.

References

Almond P, Roering JJ, Hales TC (2007) Using soil residence time to delineate spatial and temporal patterns of transient landscape response. *Journal of Geophysical Research-Earth Surface* **112**.

Bockheim JG, Kelsey HM, III JMM (1992) Soil development, relative dating, and correlation of late Quaternary marine terraces in southwestern Oregon. *Quaternary Research* **37**, 60-74.

Bockheim JG, Langley-Turnbaugh S (1997) Biogeochemical cycling in coniferous ecosystems on different aged marine terraces in coastal Oregon. *Journal of Environmental Quality* **26**, 292-301.

Jackson ML (1954) 'Soil Chemical Analysis: Advanced Course.' (Parallel Press: Madison).

Langley-Turnbaugh SJ, Bockheim JG (1997) Time-dependent changes in pedogenic processes on marine terraces in Coastal Oregon. *Soil Sci. Soc. Am. J* **61**, 1428-1440.

Langley-Turnbaugh SJ, Bockheim JG (1998) Mass balance of soil evolution on late Quaternary marine terraces in Coastal Oregon. *Geoderma* **84**, 265-288.

McKeague JA (1967) An evaluation of 0.1 M Pyrophosphate and pyrophosphate-dithionite in comparison with oxalate as extractants of the accumulation products in podzols and some other soils. *Can. J. Soil Sci* **47**, 97-99.

McKeague JA, Day JK (1966) Dithionite- and oxalate-extractable Fe and Al as aids in differentiating various classes of soils. *Can. J. Soil Sci* **46**, 13-22.

Mehra OP, Jackson ML (1960) Iron oxide removal from soils and clays by a dithionite-citrate system buffered with sodium bicarbonate. *Clays and Clay Minerals* **7**, 317-327.

Milne JDG, Clayden B, Singleton PL, Wilson AD (1995) 'Soil description handbook.' (Manaaki-Whenua Press: Lincoln, New Zealand).

Moore DM, Reynolds RC (1997) 'X-Ray Diffraction and the Identification of Clay Minerals.' (Oxford University Press: New York).

Soil Survey Staff (2004) Soil survey laboratory methods manual. (U.S. Gov. Print. Office: Washington, DC).

Torrent J, Schwertmann U, Fetcher H, Alferex F (1983) Quantitative relationships between soil color and hematite content. *Soil Science* **136**, 354-358.

Pedogenesis of gypsum soils from gypseous materials

Hudnall W, Boxell J

Plant and Soil Science, Email wayne.hudnall@ttu.edu

Abstract

This paper focuses on the pedogenesis of soils which have formed in the Permian Castile formation; a deep water evaporite deposit constituted of varved gypsum and calcite. Soils selected for study were located in Culberson and Hudspeth counties in West Texas and formed from gypsic bedrock (Permian, Castile Formation). Thin sections, SEM analysis, XRD, along with features observable in hand specimen were utilized in order to ascertain the processes of formation. Preliminary analysis of thin sections showed an alteration of the crystal structure and habit from the parent material, which appears to undergo a discernible series of changes as pedogenesis progresses. For soils forming on the Castile Formation, the dissolution of interlocking crystals and the formation of lenticular gypsum crystals, which are commonly associated with pedogenic processes, were observed to occur in soils that had greater degrees of pedogenesis.

Past work by researchers in Spain and the United States has attempted to correctly classify and identify gypsum in soils and geologic materials. Previous research has shown that gypsum can be estimated using specific criterion in the field and by utilizing proper laboratory methodology. However, experience has shown that many researchers continue to handle samples and materials in a manner which leads to erroneous data or costly mistakes. Thus it is vitally important to understand the proper handling procedures in the laboratory and the proper field methods for identification and application. It is also very important to know the pedogenic processes and geologic process which gypsum materials undergo.

Introduction

Gypsum in soils and geologic materials has been studied by many scientists for a wide array of purposes. It is found in both geologic material and soils and is utilized in many different ways. The correct identification and distinction of gypsum from other materials is important for understanding potential uses and limitations. Misidentification can lead to many problems including the misclassification of plants; improper land use; failure of engineered structures; and many other problems. In spite of the necessity of correctly identifying and understanding the properties of gypsum, there remain many hurdles to the proper identification, classification, and utilization of gypsum bearing materials. In soils, the recognition of pedogenic gypsum from geologic gypsum in parent materials, which are predominantly gypsum, can prove extremely difficult or impossible in the field.

This study aims to focus on the pedogenesis of gypsum soils that form in gypsum rich parent materials in order to determine the processes and morphological features that would aid in the correct identification and utilization of gypsum soils. Soils were selected that formed on the Permian-aged Castile formation; a varved, deep water evaporite consisting of greater than 95% gypsum and containing minor components of calcite and miniscule amounts of silicate minerals. The residual formation of soils on the Castile gypsum appears to be occurring as the original material is weathered in situ and to secondary products, chiefly pedogenic gypsum. Distinguishing secondary gypsum from primary gypsum has been difficult for other researchers working with different parent materials, but the morphology of the Castile formation gypsum allows for a more easy determination of secondary gypsum to be made. This distinction is easier due to the very apparent varves, interlocking crystals, and relatively low porosity of the Castile formation (Figure 1).

Methods

Pedons were selected are thought to represent a series of soils in varying stages of pedogenic development. At this point in the project there are no quantifiable constraints on age, but depth to bedrock, horizonation, and silicate accumulation serve as proxies for the determination of length of time of soil development. Soils with a greater depth to bedrock, have a greater number of horizons, have horizons that are more fully developed, or have a greater amount of silicate material overlying the gypsum soil material are considered to be more well developed than those that have a shallow depth to bedrock, few horizons, poorly developed horizonation, or no veneer of silicate material. Sites used in this paper were located in Culberson County in West Texas, USA, southwest of Texas Tech University, which is located in Lubbock, Texas and northwest of Pecos County where

1 – 6 August 2010, Brisbane, Australia. Published on DVD.

further research sites may be located (Figure 2).

Soil mineralogy and morphology was determined using thin sections, SEM, and XRD techniques. The relatively high solubility of the gypsum necessitated special care during the preparation of the thin sections to ensure that dissolution of the original soil fabric did not occur. Oil was used when cutting the soil peds and for the grinding of the final thin section to the appropriate thickness. Thin section slides were then examined using a Nikon Eclipse LV100POL polarizing light microscope equipped with a digital camera and monitor. Soils were prepared for the XRD by first being ground to pass a 60 mesh sieve (>.250 mm) and then were placed onto discs for analysis. Soil samples were analyzed on XRD equipment at Texas A&M University in the Soil Mineralogy Lab. Samples were scanned from 4 to 70˚ 2 θ with a step size of 0.017˚ with a scan time of one second for each step. Care was taken when placing the samples into the disks to ensure that the surface was uniformly prepared so as to ensure a random orientation of the soil particles. Soil bulk density, cation exchange capacity, electrical conductivity, calcium carbonate equivalent, and gypsum content were determined by the USDA-NRCS national characterization laboratory in Lincoln, Nebraska, USA using their standard analytical procedures.

Results

Soil thin section analysis showed a progressive dissolution and reprecipitation of gypsum from the parent material and the soil profile. Gypsum material appeared to have been reworked numerous times and was evident in the thin sections (Figure 3). SEM images showed the dissolution that was occurring along crystal planes in the Castile formation and the subsequent formation of lenticular gypsum crystals (Figure 4). XRD analysis showed a change in the mineral assemblages according to the depth in the soil profile. Soil chemical data determined that most of the nutrient availability for these soils was derived from the silicate material which has accumulated above the highly gypsiferous material. This was easily observable in the field as well where soil productivity is easily correlated to the depth of silicate material at the surface.

Conclusions

Soil formation from highly gypsiferous parent materials such as the Castile formation shows a discernible progression of alteration of the original material to secondary pedogenic products. The rates of formation were not calculated from this study, but a set of dissolution and reprecipitation could be discerned. The original rock fabric first undergoes a dissolution process in which porosity increases and secondary crystals are reprecipitated in voids. Next an innumerable and unknown set of dissolution and reprecipitation cycles advances the weathering of the parent material until a soil texture resembling flour results. This flour-like material then appears to become denser and more tightly packed until a petrogypsic horizon is formed. The petrogypsic horizon does not appear to be a result of cementation of materials together but instead seems to result from a closest packing arrangement of the soil (gypsum) particles.

Figure 1. Varves in the Permian Castile formation are very apparent as the alternating light and dark bands in hand specimen and as the brownish band running horizontally in the inset photo.

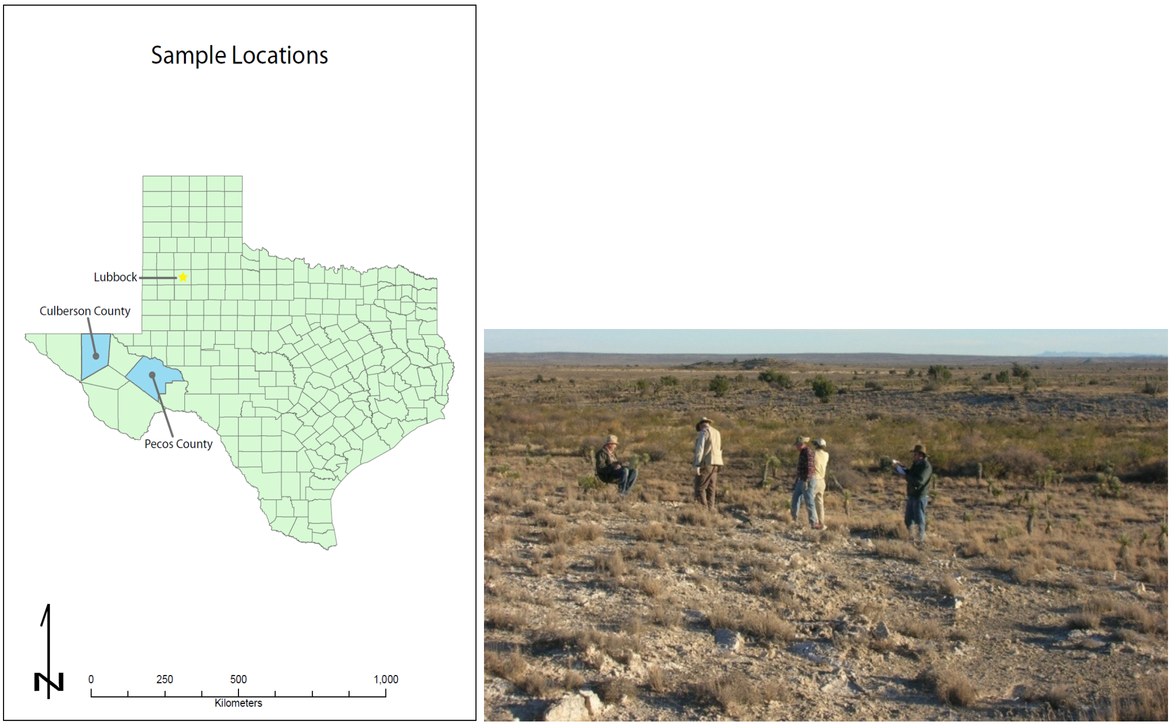

Figure 2. Sites for this study were located in Culberson County on what is locally referred to as the gypsum plain. The photo on the right shows the topography and plant cover typical of the area.

Figure 3. This thin section was taken from a gypsic horizon (10-20 cm depth) and shows a lenticular gypsum crystal, which is disintegrating as a result of pedogenic processes (arrow).

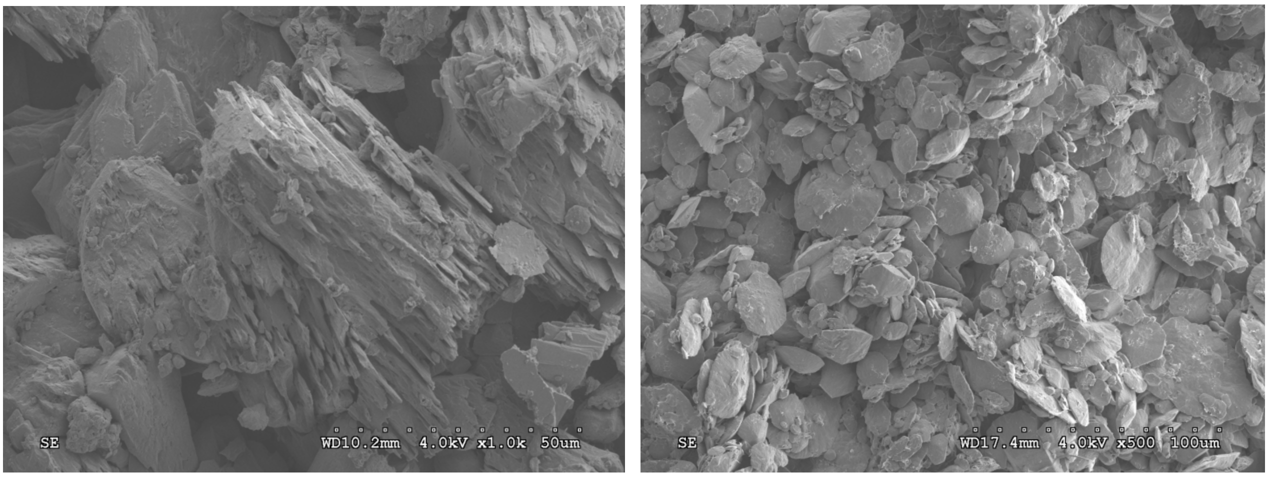

Figure 4. The image on the left clearly shows the dissolution of the original interlocking fabric of the Castile formation gypsum material. The image on the right shows the lenticular gypsum crystals which are commonly associated with pedogenic formation.

Pedogenic chromium and nickel fractionation in subtropical serpentine soils

Zeng-Yei Hseu[A], Shih-Hao Jien[B], Yoshiyuki Iizuka[c] , and Heng Tsai[D]

[A]Department of Environmental Science and Engineering, National Pingtung University of Science and Technology, Pingtung 91201, Taiwan, Email zyhseu@mail.npust.edu.tw
[B]Department of Soil and Water conservation, National Pingtung University of Science and Technology, Pingtung 91201, Taiwan, Email shjien@mail.npust.edu.tw
[C]Institute of Earth Sciences, Academia Sinica, Taipei 11529, Taiwan, Email yiizuka@earth.sinica.edu.tw
[D]Department of Geography, National Changhua University of Education, Changhua 50018, Taiwan, Email geotsaih@cc.ncue.edu.tw

Abstract

To elucidate the behavior of pedogenic Cr and Ni in serpentine soils at the scales of mineral, profile, and landscape, three pedons on the shoulder (Entisol), backslope (Inceptisol), and footslope (Alfisol) along a toposequence in Taiwan were chosen to explore these metals partition and their parent material origin by a combined approach of bulk soil analyses with selective sequential extraction (SSE) and direct mineralogical methods. Experimental results found deposits from the shoulder by surface erosion and runoff tended to be accumulated in the downhill, and thus total Cr and Ni were the lowest on the shoulder and highest on the footslope. Chromium and Ni were mainly concentrated in chromites and silicates respectively, but the metals were gradually transformed into easily mobile phases during the weathering of parent materials. The concentrations of acid soluble, reducible, and oxidizable fractions of Ni were higher than those of Cr, indicating Ni was more available than Cr. Bulk soil chemical composition supported the increase of extractability of Cr and Ni from the Entisol to Alfisol. The microscopic analyses identified chromites underwent a chemical modification and was a source of Cr in the soils. The chromites can be used as a pedogenic tracer for the soils.

Key Words

Availability, chromium, nickel, pedogenesis, serpentine, toposequence

Introduction

Serpentine soils are not derived from ultramafics only those with hydrothermal alternation of ultramafic minerals and a presence of serpentine minerals (Oze *et al*., 2004). However, serpentine soils are often of ecological or environmental importance due to high levels of potentially toxic metals, such as Co, Cr, Mn, and Ni (Becquer *et al*., 2006). Pedological studies of the parent material weathering in serpentine soils are numerous in the world. However, such studies on the ultramafic complexes in the island groups of the West Pacific Ocean are relatively rare, particularly in Taiwan (Hseu, 2006; Hseu *et al*., 2007; Hsiao *et al.,* 2009; Cheng *et al*., 2009). Due to the wide distribution and occurrence of serpentine soils, pedogenesis of these soils differed from location to location with varying climatic conditions as well as the nature of the parent material and other factors including topography, biota, and time. For serpentinitic parent materials, release of Cr and Ni to the ecosystems and particularly natural water systems during mineral weathering may occur, indicating the metals as a source of non-anthropogenic contamination. The influence of pedological conditions on the partition of metals is very important to the ecological functions of serpentine soils in the environment. Although most Cr and Ni in serpentine soils have been well known to be fixed by primary and secondary minerals corresponding to silicates and Fe oxides (Hseu, 2006), the release of these metals should be given increased attention during pedogenesis at the scales of mineral, profile, and landscape. An attractive question is “Is there any difference in partition between Cr and Ni from serpentine soils at the different scales under humid tropical conditions?” This study partitioned Cr and Ni into different fractions and assessed their mobility at the scales of mineral, profile, and landscape along a serpentine toposequence in eastern Taiwan using a combination of bulk soil analysis approach and mineralogical spectroscopy.

Methods

Area description and sample collection

The study area, Shih-Tao Mountain corresponding to a succession of landscape between 300 and 350 m of altitude, is located in southern section of the Coastal Range in eastern Taiwan (22°47’32’’ N, 121°09’30’’ E). The study area is composed of serpentinites and underlain mudstones that belong to the Lichi formation and crop out in the northeastern section. The serpentinitic rocks approximate 10 m thick are exotic blocks of ophiolite from the Philippine Sea Plate developed during the Late Pliocene epoch. Three pedons were selected from Shih-Tao Mountain on different landscapes along the serpentine toposequence within a distance of 500 m.

The reference pedons are pedon ST-1 on the shoulder, pedon ST-2 on the backslope, and pedon ST-3 on the footslope.

Physiochemical and mineralogical analyses

Soil samples from each pedon were subjected to physiochemical and mineralogical analyses. Total analysis of major element and Cr and Ni in soil samples utilized wavelength-dispersive X-ray fluorescence (XRF) (Spectro Xepos, USA). X-ray powder diffraction (XRD) patterns of rock and soil samples were obtained from 2^o to 70^o 2θ, at rate of $0.2^o 2\theta \mathrm{min}^{-1}$ (Rigaku D/max-2200/PC diffractometer with Ni-filtered Cu Kα radiation generated at 30 kV and 10 mA). Additionally, three undisturbed blocks from each C horizon were obtained in the field by aluminum boxes. After air drying, polished thin sections with a thickness of 30 μm were prepared. Selected thin sections were analyzed using backscatter electron microscopy (BSE) and energy dispersive x-ray spectroscopy (EDX) on an electron probe microanalyzer (JEOL JSM-6360LV). The microprobe was operated at the beam conditions of 15 kilo Volt (kV), and 18 pico Ampere (pA) for the acceleration voltage and beam current, respectively, in the vacuum condition of 25 Pa (Pascal) without carbon coating.

Sequential extraction of chromium and nickel

The three-step extraction procedure (SSE) was developed according to the Standards, Measurements and Testing Program (formerly the European Community Bureau of Reference, generally termed the BCR method). A detailed description of the BCR-protocol was given by using dilute acetic acid, a reducing agent and oxidizing agent. However, as an additional step, a mixture of $HF\text{-}HNO_3\text{-}HClO_4\text{-}H_2SO_4$ was used to dissolve Cr and Ni from the residue remaining following the three extraction steps. During the SEE procedure the four steps divided Cr and Ni into the following fractions: (1) acid extractable (F1), (2) reducible (F2), (3) oxidizable (F3), and (4) residual (F4).

Results and Discussion

The results from SSE demonstrated that the largest amounts of Cr in the soils were associated with the residual fraction, indicating the original Cr was primarily fixed in the primary and clay minerals of the serpentine soils (Table 1). The Cr-bearing minerals were identified by XRD in this work such as silicates and Cr-spinels (magnetite and chromite) which were only dissolved within the residual fraction, and thus supported the finding of F4 fraction with the SSE. Chromite, a common spinel in mafic and ultramafic rocks, was regarded as highly resistant to chemical weathering (Oze *et al*., 2004). However, Garnier *et al*. (2008) identified that the soil chromites, accumulated inside serpentine soil profiles, had undergone chemical weathering and led to the Cr enrichment during soil genesis under humid tropical conditions. Fig. 1 shows the chromite matrix is light gray; however, the edges of chromite, with white imperfections, are partly broken and are gradually altered along the cracks on the crystal surfaces in this work. Moreover, proportions of residual fraction decreased towards the surface to support the finding by Garnier *et al*. (2008).

Table 1. Chemical fractions (mg/kg) of Cr shown as a mean of triplication and its standard derivation in the study soils; recovery was obtained by sum of Cr content in each fraction divided by the Cr total content.

Pedon	Horizon	Depth	F1	F2	F3	F4	Recovery
		cm					%
ST-1	A	0-10	ND	1.63±0.12	8.96±0.34	959±12.1	91.4
	C1	10-40	ND	1.65±0.14	8.59±0.68	943±28.5	88.2
	C4	100-120	ND	1.49±0.11	4.22±0.34	1482±4.74	89.4
ST-2	A	0-10	0.15±0.05	3.34±0.11	57.9±1.93	2611±54.6	90.9
	Bw	10-30	0.14±0.05	3.05±0.11	72.6±2.25	2906±18.9	101
	C3	90-120	0.13±0.07	2.84±0.30	55.4±2.23	1538±29.4	85.7
ST-3	A	0-15	1.26±0.09	4.20±0.22	86.6±7.66	2951±98.2	95.3
	Bt	50-80	0.87±0.08	12.3±0.32	87.9±3.31	2975±20.5	97.7
	C	130-150	0.69±0.07	9.09±0.55	53.6±0.44	3092±32.6	95.8

Based on the bulk soil analyses by the SSE, the potential mobile Cr phases (e.g., F1, F2, or F3) increased with soil development from pedon ST-1 to pedon ST-3, and thus revealing the increased probability of chromite weathering in the contribution of Cr release in this study. The chromite matrix consisted of Cr 29.5±3.56 wt.%, Fe 25.4±6.55 wt.%, Si 7.61±2.22 wt.%, and Mg 7.53±1.13 wt.% by microprobe analysis (Figure 1). The composition of the imperfect edge toward the serpentine mineral matrix (dark gray veins with black striation) significantly decreased in Cr but increased in Si and Mg. Burkhard (1993) considered the presence of Si in the spinels as a relative index of their alteration degree. By the observation of polarized microscope for the serpentine soils in eastern Taiwan, opaque inclusions of magnetite and chromite stained the parent rocks black and dark brown and small amounts of weakly anisotropic light-yellow clay pseudomorphs were interpreted as hypogene neoformed clay minerals (Hseu *et al.*, 2007). Therefore, the microscopic analyses in this study verified that chromite underwent a chemical modification and led to an enrichment of available Cr in the soils during the rock weathering. The chromites can be used as a pedogenic tracer which was corresponding to the XRD finding.

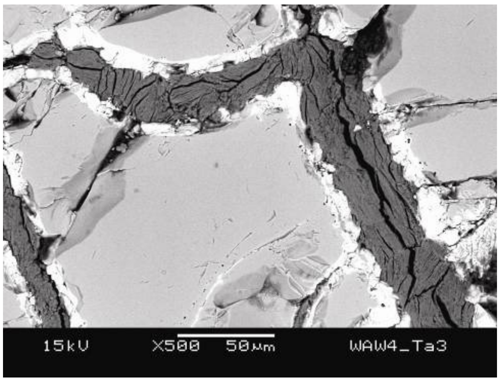

Figure 2. BSE image of Cr-spinels in the C horizons of ST-1 pedon.

Nickel was primarily recovered in the F4 compartment because large parts of Ni were primarily fixed in silicate lattices such as serpentines, smectites, and vermiculites in this study; while it was in minor extend in the reducible (F2) and oxidizable (F3) fractions of the soils (Table 2). The lowest concentrations of Ni existed in the acid extractable forms (F1). However, the concentrations of F1, F2, and F3 fractions of Ni always exceeded those of Cr. In comparison with the proportions of F1, F2, and F3 in total content of metals between Cr and Ni, this study found that Ni was more available than Cr in the toposequence during pedogenesis. Within single pedon, these propotions of Ni increased with decreasing soil depth, indicating that Ni was gradually transformed into easily mobile phases during the weathering of parent materials. Not any Ni-spinel has been found by XRD and BSE analyses in this study, revealing the major mineral origin of Ni in ultramafic soils was from silicates such as olivine, pyroxenes, and serpentine. Nickel released from the weathering of these primary minerals can substitute for magnesium in clay minerals such as smectites and vermiculite during the early stage of serpentine soil development. However, as the chemical weathering increases, these clay minerals became unstable (Hseu *et al.*, 2007). As a result, easily mobile elements like Si, Ca, and Mg were preferentially leached, whereas Cr and Ni remained in the profiles and accumulated along with iron and manganese (Garnier *et al.*, 2009). Nevertheless, nickel is not strongly held on clay and Fe oxide surfaces relative to other transition elements, even though a considerable amount of Ni can be adsorbed on the surfaces of Fe and Mn oxides at a pH ≥5 (Lee *et al.*, 2004). Therefore, the sustainable Ni was found in the F2 (Fe/Mn oxide-binding) fraction for this work.

From a pedological point of perspective, the order of soil development was pedon ST-1 (Entisol) → pedon ST-2 (Inceptisol) → pedon ST-3 (Alfisol). The parent materials of all pedons had similar chemical and mineral compositions. Due to leaching of Mg, the A horizons of pedons ST-1 and ST-2 and all horizons of ST-3 appeared relatively enriched SiO_2. Iron was leached from surface horizons and accumulated in subsurface horizons with soil development, whereas the DCB-extractable Fe was the highest in the argillic horizons (Bt) of pedon ST-3. At the landscape scale, the deposits from the shoulder by surface erosion and runoff were gradually accumulated in the downhill, so that total Cr and Ni were the lowest on the shoulder and highest on the footslope. At the profile scale, the SSE demonstrated that the largest amounts of Cr and Ni in the soils were associated with the residual fractions, but the metals were gradually transformed into easily mobile phases during the weathering of parent materials under the humid tropical condition. An exchangeable Ca/Mg ratio <0.7 is often used to relate the imbalance of these nutrient elements in serpentine soils (Brooks 1987). The bulk chemical composition of three pedons supported the findings in Ca/Mg ratio with soil development. In addition, it appears from this study that more than one soil mapping unit in the study area should be considered for land management.

Table 2. Chemical fractions (mg/kg) of Ni shown as a mean of triplication and its standard derivation in the study soils; recovery was obtained by sum of Ni content in each fraction divided by the Ni total content.

Pedon	Horizon	Depth	F1	F2	F3	F4	Recovery
		cm					%
ST-1	A	0-10	4.55±0.11	10.3±0.60	46.1±1.12	1314±96.8	95.4
	C1	10-40	4.75±0.23	33.8±1.13	53.4±1.13	1311±27.3	95.9
	C4	100-120	6.34±0.45	22.0±0.34	33.3±1.96	1173±35.7	93.6
ST-2	A	0-10	14.3±1.78	215±11.1	138±9.65	3289±68.7	101
	Bw	10-30	13.0±1.94	209±16.8	166±11.2	3212±16.4	101
	C3	90-120	9.70±0.43	238±22.3	159±11.0	1367±78.7	90.6
ST-3	A	0-15	32.9±4.77	327±12.9	275±16.4	2786±14.7	106
	Bt	50-80	31.8±2.92	395±14.6	283±11.0	2494±19.2	92.6
	C	130-150	49.9±1.92	220±18.3	314±11.1	3190±91.5	94.1

Conclusion

The order of soil development was Entisol on the shoulder → Inceptisol on the backslope → Alfisol on the footslope along the serpentine toposequence. Chromium and Ni were mainly concentrated in chromite and primary silicates, respectively. Despite of differences in parent material composition and in degree of soil development along the toposequence, similar partition of Cr and Ni was found in all soils. The microscopic analyses identified that chromite underwent a chemical modification and led to the enrichment of Cr in the soils during the parent material weathering. Nevertheless, nickel was more mobile than Cr in the soils, released mostly from silicates, and consequently adsorbed on the Fe oxides. The bulk chemical composition of all soils associated with the exchangeable Ca/Mg values supported the increase of extractability of Cr and Ni from the incipient to mature soils.

References

Becquer T, Quantin C, Rotté-Capet S, Ghanbaja J, Mustin C, Herbillon AJ (2006) Sources of trace metals in Ferralsols in New Caledonia. *European Journal of Soil Science* **57**, 200-213.

Brooks RR (1987) Serpentine and its Vegetation: a multidisciplinary approach. Croom Helm, London, UK.

Burkhard DJM (1993) Accessory chromium spinels: their coexistence and alteration in serpentines. *Geochimical et Cosmochimical Acta* **57**, 1297-1306.

Cheng CH, Jien SH, Tsai H, Chang YH, Chen YC, Hseu ZY (2009) Geochemical element differentiation in serpentine soils from the ophiolite complexes, eastern Taiwan. *Soil Science* **174**, 283-291.

Garnier J, Quantin C, Guimarães E, Becquer T (2008) Can chromite weathering be a source of Cr in soils? *Mineralogical Magazine* **72**, 49-53.

Garnier J, Quantin C, Guimarães E, Garg VK, Martins ES, Becquer T (2009) Understanding the genesis of ultramafic soils and catena dynamics in Niquelândia, Brazil. *Geoderma* **151**, 204-214.

Hseu ZY (2006) Concentration and distribution of chromium and nickel fractions along a serpentinitic toposequence. *Soil Science* **171**, 341-353.

Hseu ZY, Tsai H, His HC, Chen YC (2007) Weathering sequences of clay minerals in soils along a serpentinitic toposequence. *Clays and Clay Minerals* **55**, 389-401.

Hsiao KH, Bao KH, Wang SH, Hseu ZY (2009) Extractable Concentrations of Cobalt from Serpentine Soils with Several Single extraction Procedures. *Communications in Soil Science and Plant Analysis* **40**, 2200-2224.

Lee BD, Graham RC, Laurent TE, Amrhein C (2004) Pedogenesis in a wetland meadow and surrounding serpentinic landslide terrain, northern California, USA. *Geoderma* **118**, 303-320.

Oze C, Fendorf S, Bird DK, Coleman RG (2004) Chromium geochemistry of serpentine soils. *International Geological Review* **46**, 97-126.

Quantification of lessivage and impact of extreme climatic events on this process: An experimental approach

Laurence Quénard[A], Anatja Samouëlian[A], Isabelle Cousin[A], Sophie Cornu[B]

[A] INRA, UR 0272 Science du Sol, Centre de Recherche d'Orléans, CS 40001, 45075 Orléans cedex 2, France, Email laurence.quenard@orleans.inra.fr
[B] INRA Unité GSE, BP 80, 13545 Aix en Provence cedex 04, France, Email Sophie.Cornu@aix.inra.fr

Abstract

Understanding soil evolution requires characterising, quantifying, and modelling the major processes that govern pedogenesis. We proposed to study one of the most widespread processes in soils: lessivage, understood as the vertical transfer of fine particles from a horizon, called eluviated, to another horizon, called illuviated. Lessivage fluxes were never measured to our knowledge due to obvious technical difficulties. In addition, despite its description in many soil types, the existence of this process is somewhat controversial. We designed a laboratory experimental device to imitate the lessivage process and to test the impact i) of extreme events, as heavy rain, and ii) of the structure of the eluviated horizon on lessivage. We used a rainfall generator that allows the examination of the effect of rainfall on soil under controlled conditions. Two climatic modalities were tested: heavy rain on dry soil and small intensity rainfalls on wet soil. We present here the first results of these experiments.

Key Words

Clay translocation, eluviation, illuviation, loamy material, pedogenesis

Introduction

Many soils, particularly in temperate environments, exhibit superficial horizons depleted in fine particles (<2µm) compared to deeper horizons. Different processes can lead to this textural contrast. These soils may result from a geological contrast: weathering of different parent materials or surface deposit of coarser materials. Jamagne (1978) showed that some of these soils resulted thus from lessivage of fine particles from the upper-horizon to the sub-surface horizon: the upper horizon is then depleted (phenomenon of eluviation) in fine particles, while the underlying horizon is enriched (phenomenon of illuviation). The diagnostic features of this process are the presence of clay coatings and clay enrichment in sub-surface horizons (or in some major or trace elements, which are preferentially bound to these particles). Baize (1989, 1995) and others described that some of the soils characterized by a strong textural differentiation as Planosols or clayey soils with surface depleted horizons, result from the lateral departure of clay particles and their export out of the solum via a temporary hypodermic groundwater. For Legros (2007) and Presley *et al.* (2004), accumulation of clay in the underlying horizon results from the in situ weathering of primary minerals. For Phillips (2007), bioturbation also plays a role in the formation of texturally contrasted profiles. However the action of the soil macrofauna is also described as a homogenizing effect of the upper horizons (e.g. Faivre and Chamorro, 1995).
Finally, the lessivage is usually the most common way to explain textural contrast. It is the major process responsible for the formation of Luvisols, which are well spread in the northern half of Europe, in Quaternary Loess, this material being favourable to the development of these soils. Nevertheless it has never been measured by experiments due to technical difficulties.

The objective of this study is to implement a laboratory experiment to quantify the vertical transfer of particles (departure and accumulation) under different climatic conditions: a typical winter rain train on wet soil and a heavy rain event on dry soil. We performed this experiment on soil horizons sampled in different Luvisols with contrasted mineralogical and physico-chemical properties.

Principle of the experiment

Two laboratory experiments were designed. The first one focuses on eluviation and the second one on illuviation. Two factors governing the lessivage were tested: climate and soil structure. For climate, we chose to simulate i) a summer heavy rain on a dry soil monolith and ii) a low intensity winter rain on a wet soil monolith. The structure is tested only for eluviation by using either undisturbed soil horizons or remoulded soil sample. Eluviation was simulated on a column made of the superposition of a loamy soil horizon (called L1) on a bed of pure quartz and of silt size (called LQ) (Figure 1). We followed the gradual release of L1 particles and their trapping in the LQ after several rain events. Free drainage was applied at the basis of the quartz bed.

During rain events, we avoided long duration waterlogging phenomenon by rainfall interruption in order to not introduce other processes as oxydo-reduction. Between two rain events, the soil columns were allowed to dry up in order to recover their initial water content. The water content in the column was monitored by tensiometers placed at different depths in the column. After several rain events, two monoliths were removed from the experiment and sub-sampled. The incorporation of particles to the quartz bed was quantified by sorting the mobile fraction from the quartz bed and characterizing the clay particles by X-ray diffraction, measurement of the CEC and measurement of the specific surface of this fraction. Indeed, as the quartz used for the quartz bed (LQ) was pure, any clay particle detected in LQ would come from the L1 eluviation.

The associated porosity evolution was also quantified by X-ray tomography.

Illuviation was simulated on a column made of a loamy soil horizon (L1) lying on a second monolith of a loamy soil horizon (called L2) having contrasting mineralogical and physico-chemical properties (Figure 1). The two superposed monoliths were laid on a quartz bed (LQ) to avoid free drainage at the base of L2.

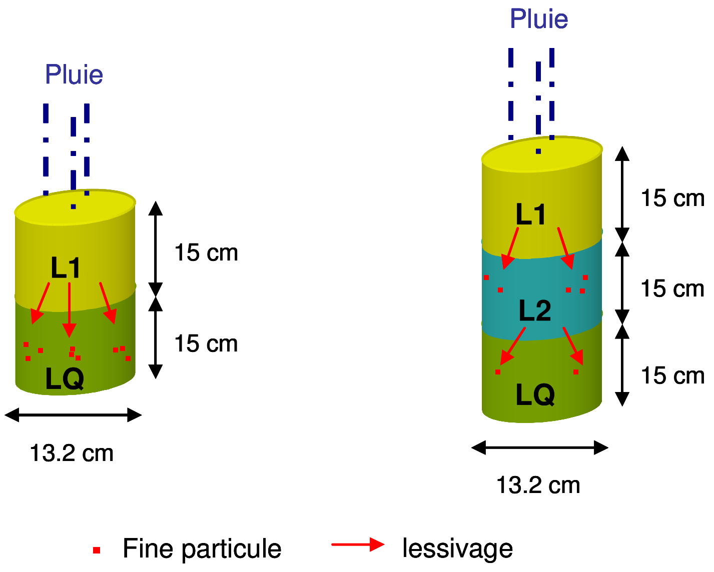

Figure 1. Schematic diagrams of the two experiments: a) Eluviation, b) Illuviation.

Dimensioning of the experiment

Characteristics of the chosen loamy materials and of the repacked columns

As mentioned above the two loamy materials were chosen for their contrasted characteristics in terms of mineralogy, CEC and specific surface of the fraction less than 2 µm. In addition, L1 physico-chemical characteristics were chosen to favour eluviation, say a pH comprised between 5.5 and 6.5; the L2 chemical characteristics were chosen to favour illuviation, say a pH higher than 7.

The chosen L1 was sampled at "Heurtebise" 10km from Chateau-Thierry in the Paris Basin. Its clay mineralogy is largely dominated by smectites, its water pH is of 5.80 and its CEC measured by the cobaltihexamine methods of 10.8 cmol$^+$/kg.

The soil and quartz cylinders height has been set at 15 cm. The undisturbed soil cylinders were sampled in the field and stored at 4°C to avoid evolution of the soil structure by biological activity. The remoulded cylinders were build by repacking soil aggregates dried at 40°C and sieved at 4mm, at a bulk density equal to 1.45 g.cm^{-3}, which was a bulk density close to the one observed in the field.

Climatic conditions

The heavy rain event had an intensity of 20mm/h and occurred on a dry soil whose water content was equal to 10%. The classical winter rain event had an intensity of 6 mm/h and occurred on a moist soil with a water content of 20%. These conditions were determined on the basis of climatic records.

We decided to apply rainfall of 40 mm that was equivalent to the porosity volume of the repacked L1. For the heavy rain intensity (20mm/h), 40mm were applied in 4 rains of 30 minutes, separated each by 30 minutes to avoid pounding at the surface of the columns. Under these conditions, only limited pounding occurred. The columns were let to dry for three weeks to return to their initial water content (10% water). After that drying period, a new period of rainfall was applied in the same conditions. These successive operations (wetting by

rainfall and drying by evaporation) were repeated at least ten times.
For small intensity rainfalls (6 mm/h), we applied 40 mm in 3 rains of 2 hours separated each by 24 hours. As for the 20mm/h intensity, only limited pounding occurred on the monolith surface. In one week of drying, the column returns to its initial water content (20% water). As for the other rainfall intensity, the whole process was repeated ten times.

Expected results and conclusions

Three rain events were applied for the heavy rain conditions. One column was the removed from the experiment and sub-sampled. Analyses are ongoing. Result will allow determining the quantities and the nature of the eluviated materials. Longer series of rain events will be conducted to monitor the evolution within time of the eluviated quantities and of its nature, first on disturbed soil and then on soils collected in situ.
This experiment allowed quantifying eluviation and its kinetics. We will then quantify illuviation and its kinetic. The combination of the two experiments allowing quantifying lessivage will help in characterizing the temporal evolution of this process in order to model it and ultimately integrate this lessivage model into a larger model of soil evolution.

References

Baize D (1989) ‘Guide des analyses courantes en pédologie’. (INRA édition: Paris).

Baize D (1995) Les sols argileux appauvris en argile sous climat tempéré humide. Planosol texturaux, Pélosols différenciés et autre solum. *Etude et Gestion des Sols* **4**, 227-240.

Faivre P, et Chamarro C (1995) Facteurs biotiques et mécanismes de lessivage particulaire dans les sols. L’exemple des toposéquences caractéristiques des Andes de Columbie. *Etude et Gestion des Sols* **1**, 25-42.

Jamagne M (1978) Les processus pédogénétiques dans une séquence évolutive progressive sur formations limoneuses loessiques en zone tempérée froide et humide. *Comptes Rendus hebdomadaires des Séances de l’Académie des Sciences* **286**(1), 25-27.

Legros JP (2007) ‘Les Grands Sol du Monde’. (Presses Polytechniques et Universitaires Romandes: Suisse).

Phillips JD (2007) Development of texture contrast soils by a combination of bioturbation and translocation. *Catena* **70**, 90-104.

Presley DR, Ransom MD, Kluitenberg GJ, Finnell PR (2004) Effect of thirty years irrigation on the genesis and morphology of two semiarid in Kansas. *Soil Science Society of America Journal* **68**, 1916-1926.

Ratios and ranges of soil-forming factors influence on pedogenesis

Alexander Gennadiyev, James Bockheim, John Kimble

Faculty of Geography, Moscow State University, Moscow, Russia, Email gennad@geogr.msu.ru

Abstract

The issue of ratios and ranges of soil-forming factors influence on pedogenesis was discussed during the whole history of genetic soil science. Most of opinions were that all soil-forming factors are, in effect, of the same importance and take equal part in soil formation. At the same time, any of factors could become leading one in the development of soils under certain situations limited in time and/or space. Different bioclimatogenic, lithogenic, volcanogenic, palaeohydrogenic and other macrostructures of soil cover were described. An attempt was made to formulate the ratios and ranges of soil-forming factors influence on pedogenesis in the form of laws. There were shown numerous situations when, along with relief, other factors, such as hydromorphism, parent materials, etc., acquire prime importance in the catenary differentiation of soil cover. Three cycles of soil development in time (biological, biogeomorphologic and bioclimatic) were described. The alternation of evolutionary phases of convergence and divergence between the components of soil cover caused by the domination of lithogenic, biogenic, topogenic or climatogenic factor was revealed. It is possible to assert rather reasonably that there are certain ratios between factors in terms of their influence on different aspects of a soil-forming process: energy; substantive; and process-dynamic.

Key words

Soil zonality, soil catenas, soil evolution.

Introduction

The issue of ratios and ranges of soil-forming factors influence on pedogenesis was discussed during the whole history of genetic soil science. Sometimes it was put in the form of a special theoretical problem, but more often it arose as an adjacent problem during soil geography studies or while making soil maps and determining soil classifications. There is an established opinion that Dokuchaev considered climate to be a leading factor of soil formation. This is inconsistent with the fact that, Dokuchaev constantly underlined that «all soil-forming factors are, in effect, of the same importance and take equal part in formation of a normal soil» (1889). This approach was an essential part of the Dokuchaev's paradigm. On the other hand, in his works Dokuchaev spoke about predominance of this or that soil-forming factor at different levels of soil cover organization. For example, he considered horizontal and vertical zonality of soils to be a result of global or regional bioclimatic zonality (Dokuchaev 1899), but he also paid attention to «topography of soils» meaning that local features of soil cover depend on the morphological variability of terrain. Nevertheless, there were attempts in soil science to identify leading factor of soil formation, namely climate (Sibirtsev 1951, Hilgard 1892, Coffey 1912), biota (Viliams 1949), parent materials (Lyon *et al.* 1915; Shaw 1930), and to insist on its universal predominance, i.e. the «leadership» of this factor under all conditions and at all stages of soil formation process. It is obvious that such point of view contradicts both the essence of the genetic concept of soil-forming factors, and the actual regularities of soil distribution and evolution of soils on the Earth's surface. At the same time, any of soil-forming factors could really become leading one in the development of soils and soil cover under certain situations limited in time and/or space.

Results and Conclusion

The factors limiting the development of soils

The limiting role of soil-forming factors can be found in various classifications of soils. For example, climatic (arctic, desert) and non-climatic (eroded, alluvial) imperfectly developed soils with (A)C or AC profiles are identified in the French classification system which is based on an evolution-genetic principle (Duchaufour 1965). Their immaturity is the result of climatic features, erosion processes or intensive accumulation of deposits. In this case the soil-forming potential of other factors, for example, rocks, remains unrealized.

The concept of "zonal soils" dominating in the Russian soil science for a long time understood them as soils which are formed on flat surfaces built of moderately water-permeable sediments (loams) without any specific chemical or mineralogical features, without influence of ground waters, in the absence of both washing-off and deposition. According to this concept zonal soils reflect a certain balance of soil-forming factors which means that the difference between soils is only due to climatic features. The soils which do not meet the above-mentioned conditions, are not "zonal", therefore they have been classified as biolithogenic, biohydrogenic and biohalogenic. Later Liverovskii (1987) formulated the law of plurality of zonal soils according to which a variety of combinations of bioclimatic factors with lithological and historic-genetic factors results in the occurrence of several zonal types of soils within the same soil zone.

In the modern US Soil Taxonomy the presence of less developed diagnostic horizons (histic, cambic, ochric) and the absence of well developed ones (argillic, oxic, etc.) in soils are considered to be the result of the limiting influence of climatic (Aridisols), lithological or chronological factors (Inceptisols, Entisols). Within these orders relatively more developed soils occur at the levels of suborders and soil great groups reflecting the total results of the "opposition" of this or that soil-forming factor to the principal factor limiting soil development.

Domination of factors in the organization of soil cover

Ratios and ranges of soil-forming factors influence on pedogenesis can be revealed through the analysis of soil cover pattern at different levels of its organization. Birkeland (1974) collected and compared the materials on vegetation-soil, topography-soil and climate-soil relationships influencing on soil cover organization. The influences were ranged in terms of scale: from variation in soil with distance from trees and with tree species to regional soil trends related to climate.

It is a catenary approach to the analysis of soil formation phenomena that makes it possible to demonstrate the role of relief in the formation of soil cover and its structure. The works of Milne (1935), Bushnell (1942), Polynov (1953) and others describe diverse lateral genetic relations between soils, stemming from the leading role of geomorphologic factor. Classification of soil catenas by Kasimov and Perelman (1992) shows numerous situations when, along with relief, other factors, such as hydromorphism, lithogenic base etc., acquire prime importance in the catenary differentiation of soil cover.

Fridland (1986) has found out that there are several genetic types of climatic zonality of soil cover and the transition of one zone into another is governed by the change of this or that climatic parameter. He distinguished zonality of soils caused by thermal factor changes for a) the areas with high humidification and b) the extremely arid areas. Zonality based on the changes of climatic humidification was distinguished for the situations when a) the spatial trends of humidification coincide with the changes of thermal conditions, and b) the spatial trends of humidification differ markedly from those of thermal conditions. Each of these types of zonality manifests itself in specific forms on the Earth’s surface.

Bockheim (2005) elucidated the concept of soil endemism and ranged soils according to degree of their “uniqueness” and distinguishing soil-forming factors such as unusual parent materials (volcanic ash, smectitic clays, paralithic contacts), extreme soil climate conditions (aridic soil moisture regime), specific local topography (closed depressions), etc. Sokolov (2004) made an attempt to formulate different ratios and ranges of soil-forming factors influence on pedogenesis in the form of laws. He introduced the law of maximum lithogenic divergence of soil formation under humid climatic conditions and the law of maximum topogenic divergence of soil formation under arid ones. In the first case (under humid climate) soil-forming processes differ on different parent rocks whereas the soils of various geomorphologic positions (autonomous and heteronomous) are quite similar in soil-forming processes. In the second case (under arid climate) the variety of soils and contrasts in the soil cover are caused by relief features. Autonomous and heteronomous soils usually differ in water regime and, consequently, in the type of soil formation.

Domination of factors in the evolution of soils

Ratios and ranges of soil-forming factors influence on pedogenesis can be revealed through studying the evolution of soils. Rozov (1956) suggested three cycles of soil development in time, i.e. biological, biogeomorphologic and bioclimatic. This means that under the invariance of other factors the balance between soil and the environment could be destabilized by changes of either biota, or relief, or climate. Similarly, any factor could become a driving force of evolution not only for particular soils, but also the multicomponent structure of the soil cover. Thereupon a principle of “stages discrepancy of co-evolving elements of soil combinations” has been suggested (Gennadiyev 2001). The stages discrepancy means alternation of evolutionary phases of convergence and divergence between the components of soil cover, and it could be biogenic, lithogenic, topogenic and climatic according to the leading factor of soil evolution.

As geographers-soil scientists pointed out over and over again, the results of soil formation in various bioclimatic and topolithological conditions could be correctly interpreted only if soils of rather similar absolute age are considered. Thereupon a concept of «time correction of soil-forming potential of the environment» was suggested (Gennadiyev 2001). It postulates that it is expedient to find and compare soils of the same age in order to evaluate the role of climate, biota, rocks and relief in the evolution of soils. It is this approach that makes it possible to avoid erroneous attributing to these soil-forming factors the influence which actually relates to the duration of soil formation. The results obtained on the basis of this approach were used for a hypothetical modeling of two isochronous soil cover patterns formed within the modern and Late Holocene stages of pedogenesis (about the last 1000 and 3000 years, respectively) in the Russian Plain and the Great Plains of North America.

Contribution of factors to the components of soil-forming process.

It is possible to assert rather reasonably that there are certain ratios between factors in terms of their influence on different aspects of a soil-forming process: energy; substantive; and process-dynamic. The general scheme illustrates differentiated contribution of various factors to the energy, material base and dynamics of soil formation (Figure 1).

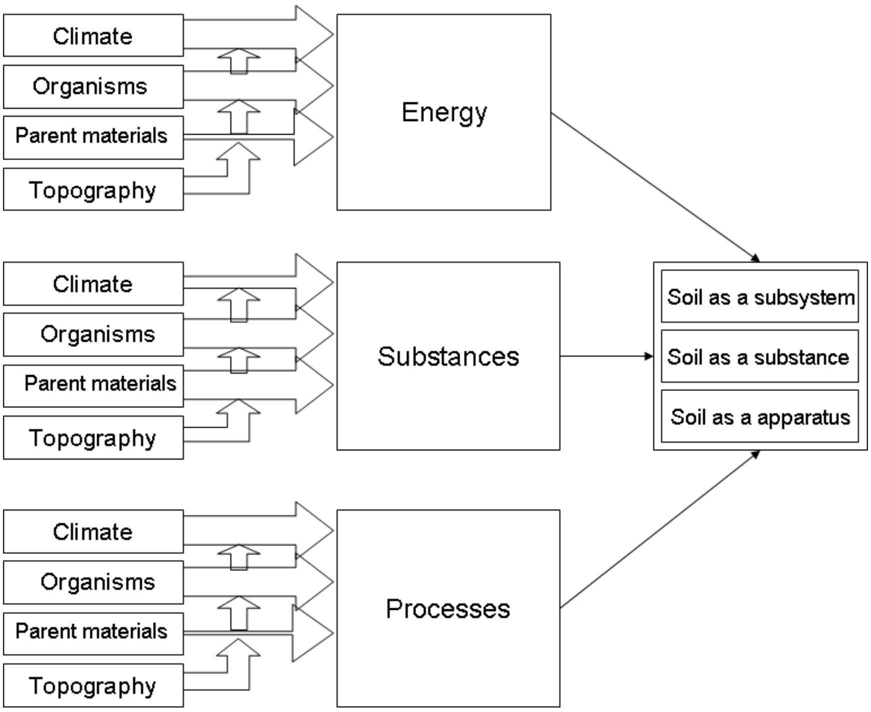

Figure 1. The general scheme of soil formation: contribution of factors to the components of soil-forming process.

The most powerful energy source of soil formation is solar radiation which is a main component of climatic factor. Coming as direct flows on the Earth's surface, it is transformed into thermal and other kinds of energy. The solar energy is mainly spent for the processes of heat and water exchange in the system of "soil-vegetation-atmosphere". Considerable input of energy into soil occurs during dying off of organisms, especially plants which contain solar energy bounded through photosynthesis. The energy contribution of the geological factor results, mainly, from the gravitational influence on soil and, accordingly, on the processes of radial and lateral migration of soil matter. Energy which comes to soil from the deep layers of the lithosphere, or as a result of disintegration of radioactive elements, is insignificantly small. Thus, there are certain ratios between the amounts of energy delivered into soils by climatic, biological and geological factors. The geomorphologic factor provides no direct energy contribution; it just supports energy redistribution over the surface of soil cover.

The material base of soil formation appears mainly due to two factors - geological and biological. Rocks deliver various mineral components which during each given moment of time usually account for more than 90% of the total soil mass. Organic compounds account for a smaller part of soil mass; however in the course of time the cycles of biomass production and decomposition considerably increase total participation of organic substances in the interaction with the substances of geological origin (which form rather inert mineral part of soils).

The contribution of climatic factor to the material base of soil formation is the enrichment of soil with atmospheric water, air and dust. The influence of relief in this aspect is only the redistribution of material soil components.

The contribution of factors to soil-forming processes is also rather differentiated. Needless to say, both energy and substantive contributions of factors influence the dynamic phenomena in soils. However in this case we mean the direct transfer of those mechanisms of functioning which are inherent in the factors of soil formation. So, rocks and relief are generally rather inert as functioning systems. On the contrary, the biological factor is very variable. The most universal mechanism of soil formation, related to the functioning of biota, is the biological cycle, first of all in the system of soil-living plants-litter-soil. The climatic factor of soil formation is no less dynamic than the biological one. Water, thermal and air regimes of soils (which are also fundamental mechanisms of soil formation) are interrelated with water, air and heat exchange cycles between the atmosphere and soil. Cyclic and reversible dynamic phenomena in soils are soil microprocesses. They naturally fit four groups: 1) an exchange of matter and energy between soil and other natural bodies; 2) transformations of matter and energy within soil; 3) changes of substance consistence in soil; 4) movement of matter and energy in soil. Certain combinations of simultaneously occurring soil microprocesses are characterized by incompleteness of their cycles and the accumulation of residual effects. This does result in the elementary soil-forming macroprocesses, or specific soil-forming macroprocesses (Rode, 1984) which lead to the evolutionary changes of soils. All three aspects of the notion of "soil" (soil as a substance, as a set of dynamic phenomena, i.e. a functioning apparatus, and as a part of a system) and their relation to the substantive, functional and energy aspects of soil formation are shown at Figure 1.

References

Birkeland PW (1974) Pedology, weathering, and geomorphological research (Oxford university press: New York-London-Toronto)

Bockheim JG (2005) Soil endemism and its relation to soil formation theory. *Geoderma* **129,** 109-124.

Bushnell TM (1942) Some aspects of the catena concept. *Soil Science Society of America Proceedings* **7,** 466-476.

Coffey GN (1912) A study of the soils of the United States. (USDA Bureau of Soils: Washington).

Dokuchaev VV (1899) A contribution to the theory of natural zones: horizontal and vertical soil zones. (St. Petersburg).

Duchaufour P (1965) Precis de pedologie. (Deuxieme edition: Paris).

Fridland VM (1986) Problems of soil geography, genesis and classification (Nauka: Moscow).

Gennadiyev AN (2001) Soil formation stages in relation to ecosystem development. *Eurasian Soil Science* **34** (Supplementary issue), 13-20.

Gerasimov, Glazovskaya (1960) Fundamentals of soil science and soil geography (Geografgiz: Moscow).

Kasimov NS, Perelman AI (1992) Geochemistry of soils. *Eurasian Soil Science* **24** (4), 59-76.

Milne GA (1935) Some suggested units of classification and mapping particularly for East African soils. *Soil Resources* **4**, 183-198.

Hilgard EW (1892) A report on the relations of soil to climate. *USDA. Weather Bulletin* **3**, 1-59.

Liverovskii Yu A (1987) Problems of soil genesis and geography. (Nauka: Moscow).

Lyon TL, Fippin EO, Buckman HO (1915) Soils, their properties and management. MacMillan. New York.

Polynov BB (1953) Doctrine of landscapes (USSR Academy of Sciences Press: Moscow).

Rode AA (1984) Soil genesis and soil-forming processes. (Nauka: Moscow).

Rozov NN (1956) Principles of soil classification development. *Soil Science (Pochvovedenie)* **6,** 24-31.

Shaw CF (1930) Potent factors in soil formation. *Ecology* **11:** 239-245).

Sibirtsev NM (1951) Soil Science. In ‘Selected works’. pp. 110-128. (Sel’hozgiz: Moscow).

Sokolov IA (2004) Theoretical problems of Pedology. (Humanitarian technologies: Novosibirsk).

Viliams VR (1949) Fundamentals of soil science and Earth science. (Sel’hozgiz: Moscow).

Regional distribution of the Loess-like Red Clay in Subtropical China and its Paleoclimatic implications

Xue-Feng Hu, Xu Cao, Ji Wei, and Liang-Feng Xu

Department of Environmental Science and Engineering, School of Environmental and Chemical Engineering, Shanghai University, Shanghai 200444, China, Email xfhu@shu.edu.cn

Abstract

Grain-size and geochemical characteristics of 18 Quaternary Red Clay (QRC) profiles in the lower and middle reaches of the Yangtze River between 25°N - 31°N in subtropical China were studied. The results showed that the QRC, distributed along the Yangtze River between 29°N - 31°N, shares the loess-like characteristics with the Xiashu Loess, which may originate from aeolian dust deposits. The QRC, mainly distributed between 28°N - 29°N, however, is in double-part structure: The upper part also shows the loess-like characteristics; the lower part indicates alluvial features. The loess-like QRC is mainly distributed along the Yangtze River, but gradually declines southwards and is rarely seen to the south of 28° N. The existence of the loess-like QRC is strong evidence for the occurrence of heavy dustfalls in the modern red-soil areas in subtropical China during the Quaternary glacial periods. The loess-like QRC is located approximately 3° latitude south of the Xiashu Loess, implying that the loess/red clay boundary in the Yangtze Valley had frequently oscillated with the alternations between glacial and interglacial climates during the Quaternary period. This leads to multiple or overlapped soil parent materials in the region. Soil properties are not totally determined by modern climate. The possible influence of paleoclimate on soil genesis should also be considered.

Key Words

Quaternary Red Clay (QRC), Xiashu Loess, Loess-like characteristics, Quaternary glacial and interglacial climates

Introduction

The dustfall has continuously occurred in northern China at least since the beginning of the Quaternary period (Liu 1985). The loess-like deposits widely distributed in the lower and middle reaches of the Yangtze River in southern China are called the Xiashu Loess. Recent studies (Li *et al.,* 2001; Yang *et al.,* 2004) believed that the Xiashu Loess shares the similar source provenance with the loess in the Chinese Loess Plateau. The typical Xiashu Loess is mainly distributed along the Yangtze River approximately north of 31°N latitude. The landscape, south of the Xiashu Loess, is gradually changed into red clay. The red clay in southern China is acidic and strongly weathered, resulting from long-term warm and humid climate (Gong, 1985). The transition of the Xiashu Loess to the red clay reflects a great change of geographical zone in the Yangtze Valley. The sedimentary red clay in southern China, without any pedogenic relationships with underlying rocks, is conventionally called the Quaternary red clay (QRC) (Gong, 1985; Hu *et al.,* 2003, 2009). Yang (1991) found that the red clay along the Yangtze River is extremely similar to the Xiashu Loess, and then proposed that it is really old loess formed in the Early or Middle Pleistocene. So far, only the QRC in Xuancheng and Jiujiang was deeply studied and believed to be in aeolian dust origin (Hu *et al.,* 1998; 2005; Xiong *et al.,* 1999; 2002; Hu and Gong, 1999; 2001). Further study is needed to scrutinize whether the loess-like QRC really exists and what spatial range it is distributed in. In this study, 18 typical QRC profiles mainly located in the lower and middle reaches of the Yangtze River in subtropical China between 25°N and 31°N were selected, the grain size and geochemistry of which were measured, aiming to prove the existence of the loess-like QRC further, and then to reveal its regional distribution and paleoclimatic implications.

Methods

18 QRC profiles with typical morphological features located in subtropical China approximately between 25° N - 31° N were selected (Fig. 1), coded with the abbreviation of geographical names (e.g. a profile in Jiujiang was coded as P-JJ) . The soil samples were collected at an interval of 10 cm in all the profiles, and then air-dried, ground and passed through a 2 mm sieve. As previously described (Hu *et al.,* 2005; 2009), the grain-size distributions of the soil samples (<2mm) were measured by a Laser Grain-size Analyzer (LS13320), with a measuring range from 0.04-2000 μm, after being pretreated. 10 major elements and 19 trace elements were determined by the X-ray Fluorescence Spectroscopy (XRF) (Hu *et al.,* 2008).

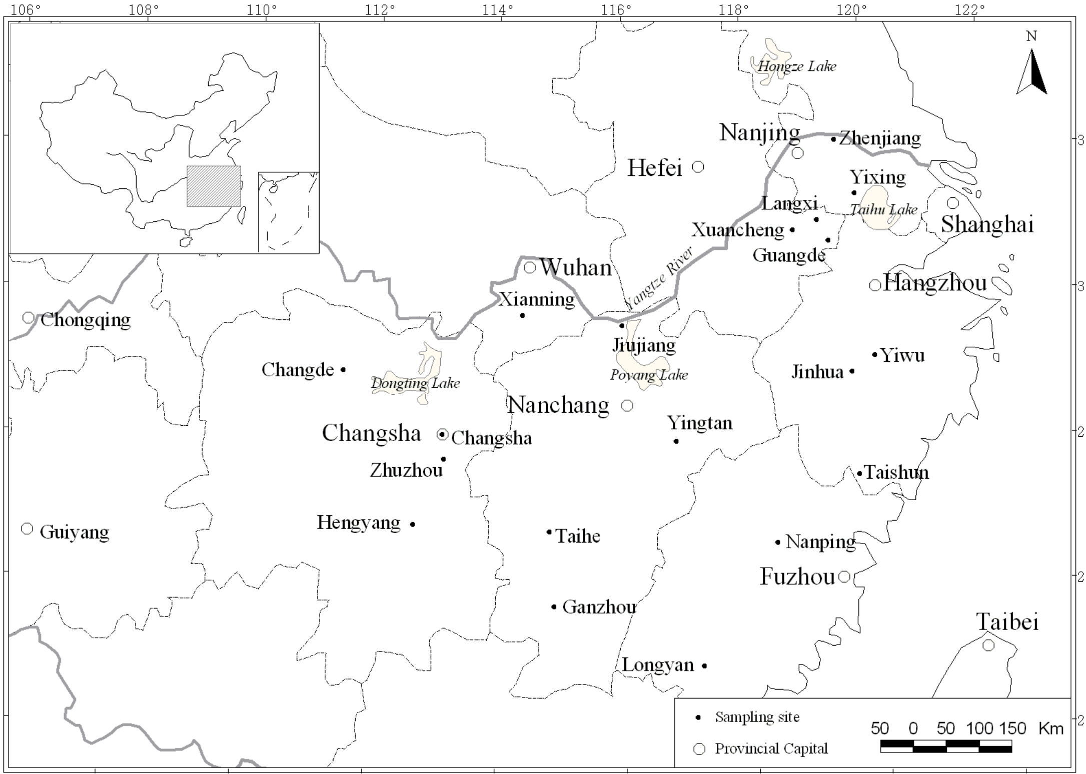

Figure 1. Sketch map showing the locations of the 18 QRC profiles in subtropical China. A shadow square in the inset map shows the location of the study areas in mainland China.

Results

Grain-size distribution of the QRC

The 18 study profiles can be classified into three types according to their grain-size characteristics: The grain sizes of Type A, including P-JJ, P-XC, P-YX, P-LX, P-GD and P-XN and mainly distributed along the Yangtze River between 29° - 31° N latitude, are characterized by fine and uniformity (e.g. Figure 2.), with no gravel (>2mm) and low sand (>63μm), mostly < 5%, but high content of basic dust fraction (10μm - 63μm), which are much comparable to those of the Xiashu loess and hence called the loess-like QRC. The grain sizes of Type B, including P-YT, P-TH, P-GZ, P-NP, P-TS, P-HY and P-LY and mainly distributed to the south of 28° N, are significantly different from Type A, which show alluvial features, with gravel layers, low content of basic dust fraction and vertically instable grain-size distribution. Type AB, including P-CS, P-CD, P-ZZ, P-YW and P-JH and mainly distributed between 28° - 29°, show double-layer structure: The upper part is identical with Type A and belongs to the loess-like red clay; the lower part shows water-reworked alluvial features like Type B.

Geochemical characteristics of the QRC

Major element contents of the QRC profiles are excellently correlated with their grain-size distributions: The curves of major elements of Type A are vertical stable and uniform (e.g. Figure 2.) and comparable to the Xiashu Loess. In contrast, these of Type B often vertically fluctuate, implying the material inconsistency and alluvial features. These of Type AB also show the dualistic properties: The upper part is vertically uniform and similar to Type A and the Xiashu loess; the lower part vertical fluctuates like Type B. Trace element distributions of the QRC profiles were also study. These of the typical layers of Type A are extremely similar to the Xiashu Loess, suggesting their similar source provenance. These of Type B show different patterns from Type A and the Xiashu Loess, implying its different source provenance from the aeolian loess. These of Type AB are also dualistic as studied above.

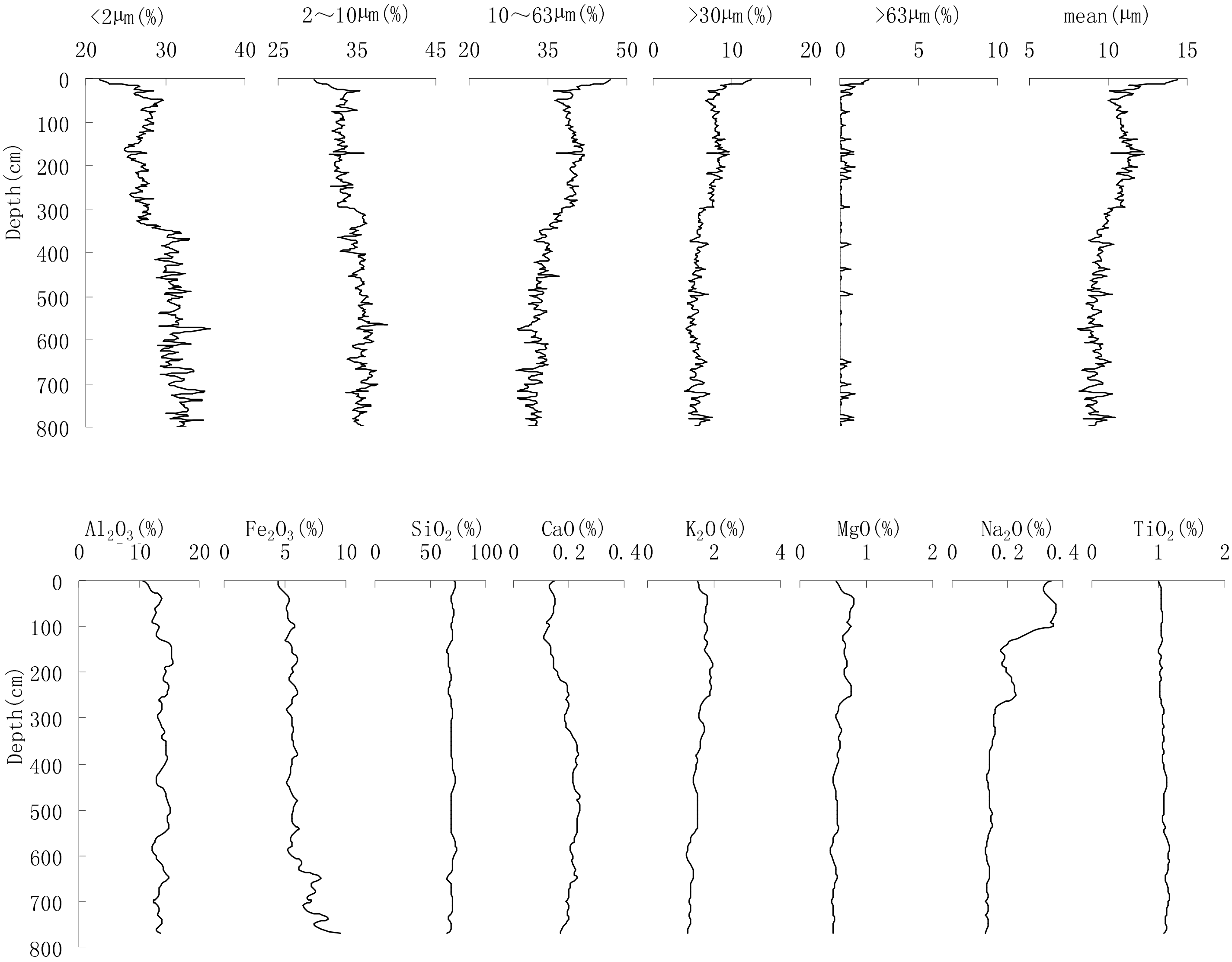

Figure 2. Vertical distributions of grain-size fractions (above) and major element contents (below) of P-XC in Xuancheng, Anhui province, China.

Conclusions

The study of the grain size and geochemistry of the QRC has fully suggested that the QRC with the aeolian dust characteristics like the Xiashu Loess really exists in subtropical China, which originated from aeolian dust deposits. This loess-like QRC is mainly distributed along the Yangtze River between 29° N - 31° N, but gradually declines southwards and is rarely seen to the south of 28° N.

The region distributed with the loess-like QRC is approximately 3° latitude south of the Xiashu Loess. This strongly suggests that the dust deposits had ever extended to the modern red soil areas, south of the Xiashu Loess. It is believed that the boundary between the highly weathered red clay and the aeolian loess in the Yangtze Valley had oscillated to and fro with a range of about 3° latitude corresponding to the multi-cyclical paleoclimatic changes during the Quaternary period: Under the glacial climates, the stronger winter monsoon drove aeolian dust southwards at least till 28° N latitude and formed loess-like soils there; under the interglacial climates, however, the dustfall was weakened and replaced by the laterized processes in the southern areas, which caused the northward shift of the loess/red clay boundary.

The existence of the loess-like QRC suggests that the QRC with highly weathered property was not a product of a long consecutive warm-humid climate. At least, its parent material, which is believed to be dust deposits, was formed under a cold and warm climate.

Therefore, the loess-like QRC had actually experienced both cold-dry and warm-humid climates, implying that some great paleoclimatic changes had ever occurred in the Yangtze Valley during the Quaternary period.

The loess-like QRC profiles are believed to consist of the cyclical alternations between loess deposits and pedogenesis, like the loess – paleosol sequences in the Loess Plateau, but such cyclical information was severely overlapped and combined and cannot be clearly distinguished any more.

The loess-like QRC also was formed during multiple stages. The weathering degree of the red clay developed in the Middle Pleistocene is more intensive than that in the Late Pleistocene. The old red clay can also be a parent material of modern soil due to water erosion. This leads to the co-existence of different zonal soils, such as ultisols and alfisols, in the region. Therefore, soil properties are not totally determined by modern climate, and the possible influence of paleoclimate on soil genesis and types should also be considered.

Acknowledgements

We sincerely thank Mr. Hong-Bo Wang for his great help in the field and laboratory work. This work was supported by the National Natural Science Foundation of China (Nos. 40971126 and 40571067).

References

Gong ZT (1985) Bio-geochemistry of the red weathering crusts. In 'Red Soils in China' (Ed Li QK) pp. 24-40. (Science Press: Beijing) (in Chinese).

Hu XF, Yuan GD, Gong ZT (1998) Origin of Quaternary red clay of southern Anhui Province. *Pedosphere* 8(3), 267-272.

Hu XF, Gong ZT (1999) A "yellow cap"on Quaternary red clay in Jiujiang, Jiangxi Province. *Pedosphere* 9(4), 311-318.

Hu XF, Gong ZT (2001) Comparative study on the origin of Quaternary red earth in Jiujiang and Taihe, Jiangxi Province. *Acta Pedologica Sinica* **38**(1), 1-9 (in Chinese).

Hu XF, Cheng TF, Wu HX (2003) Do multiple cycles of aeolian deposit-pedogenesis exist in the reticulate red clay sections in southern China? *Chinese Science Bulletin* **48**(12), 1251-1258.

Hu XF, Zhu Y, Shen MN (2005) Grain-size evidence for multiple origins of the reticulate red clay in southern China. *Chinese Science Bulletin* **50**(9), 910-918.

Hu XF, Jiang W, Ye W, Shen MN, Zhang WG, Wang HB, Lu CW, Zhu LD (2008) Yellow-brown Earth on Quaternary Red Clay in Langxi County, Anhui Province in Subtropical China: Evidence for Paleoclimatic Change in late Quaternary period. *Journal of Plant Nutrition and Soil Science* **171**(4), 542-551.

Hu XF, Wei J, Xu LF, Zhang GL, Zhang WG (2009) Magnetic susceptibility of the Quaternary Red Clay in subtropical China and its paleoenvironmental implications. *Palaeogeography, Palaeoclimatology, Palaeoecology* **279**, 216-232.

Li XS, Yang DY, Lu HY (2001) Grain-size features and genesis of the Xiashu Loess in Zhenjiang. *Marine Geology and Quaternary Geology* **21**(1), 25-32 (in Chinese).

Liu TS (1985) Loess and the Environment. (China Ocean Press: Beijing).

Xiong SF, Ding ZL, Liu TS (1999) Comparisons of grain size characteristics of red earth from southern China with that of loess and dune sand from Beijing region. *Chinese Science Bulletin* **44**(18), 1690-1693.

Xiong SF, Sun DH, Ding ZL (2002) Aeolian origin of the red earth in southeast China. *Journal of Quaternary Science* **17** (2), 181-191.

Yang DY (1991) The Quaternary dust-fall accumulation and the monsoon variability in eastern China. *Quaternary Sciences* **11**(4), 354-360 (in Chinese).

Yang SY, Li CX, Yang DY, Li XS (2004) Chemical weathering of the loess deposits in the lower Changjiang Valley China, and paleoclimatic implications. *Quat. Int.* **117**, 27-34.

Role of microbial processes in the functioning (Fe mobilization and redistribution) of a representative tropical soil sequence

S.J. Stemmler[A], E. Fritsch[B,C], N. R. do Nascimento[D] and J. Berthelin[A,E]

[A]Laboratoire des Interactions Microorganismes-minéraux-matières Organiques dans les sols (LIMOS), UMR 7137 CNRS-Université Henri Poincaré (Nancy I), BP 239, 54506 Vandœuvre lès Nancy Cedex, jacques.

[B]IRD, Institut de Recherche pour le Développement (IRD), 213 rue La Fayette, 75480 Paris Cedex 10, France.

[C]Institut de Minéralogie et de Physique des Milieux Condensés (IMPMC), UMR CNRS 7590, Université Paris 6 et 7 and IPGP, 4 place Jussieu, 75252 Paris Cedex 05, France.

[D]DEPLAN/IGCE/UNESP, Instituto de Geociências e Ciências Exatas, Rua 10, n°2527, 13500-230 Rio Claro, SP, Brazil.

[E]Corresponding author. Email berthelin@limos.uhp-nancy.fr

Abstract

Field studies and laboratory experiments have been performed to determine the main processes and the parameters involved in the weathering and soil evolution in a tropical soil sequence from ferralsols to gleysols. The work considers mainly the redox interfaces of a soil sequence located in Brazil, looking at the interactions between minerals – soil organic matter and microorganisms.

Results show that the bacterial activity (mainly of iron reducing bacteria, IRB) located at the redox interfaces of the hill-side sequences and under the dependence of water movement, soil organic matter and iron availability is the major agent of these weathering processes.

Key Words

Tropical soils, microbial soil functioning, critical zone, iron reducing bacteria.

Introduction

In humid tropical countries, strong weathering of soil materials and, in particular of ferric oxyhydroxides (hematite, goethite), occurs on very large areas. It leads to fundamental changes in soil properties, involving yellowing, bleaching and consistency of soils (Schwertmann and Kämpf 1985; Peterschmitt *et al.* 1996; Fritsch *et al.* in press) (e.g. from Ferralsols-Cambisol to Gleysols), and also metal dispersion and redistribution (Quantin *et al.* 2002). The redistribution (solubilization-accumulation) of iron is a major process, strongly dependant on topographic criteria, drainage conditions (Tardy 1993) and microbial activity (Berthelin 1982; Stemmler and Berthelin 2003). It corresponds to the more common process acting in the tropics (Fritsch *et al.* in press). Formerly in such soils, the weathering and evolution were considered as based mainly on geochemical processes. Now biological parameters are recognized through interactions between microbial, chemical, and physical phenomenons (Macedo and Bryant 1987; Stemmler and Berthelin 2003). Very few data exist on the hydrobiogeochemical and geomicrobiological conditions that promote the mobilization and transfer of iron in tropical soil landscapes. To study and better define the role of such biological factors, we have selected a sequence of well drained to poorly-drained soils (Acrisols-Cambisols - Gleysols) of the humid region (2 300 mm per year) representative of the upper Amazon basin. In such sequence, iron mobilization has played and is still supposed to play an important role in the vertical and lateral soil differentiation.

The purpose of the study was (1) to determine in laboratory experimental conditions, close to the field conditions, the iron reducing bacterial (IRB) (Lovley 1997; Bousserrhine *et al.* 1999) activities in different soil profiles and horizons of the soil sequence, and to show their possible involvement in the evolution of soil sequences as observed in the fields (2) to connect the laboratory results with the physico-chemical and geochemical analysis performed on soils and waters.

Material and methods

The soil sequence (100 m long, 3 m depth) was located at Humaita, upper Amazon basin (Brasil) and was equipped of lysimeters from the soil F6 to F1 (Figure 1). Soil samples (F1 to F6) were collected near the lysimeters in horizons of reference profiles of the sequence from the plateau (red-yellow Acrisols) to the depression (Gleysol).

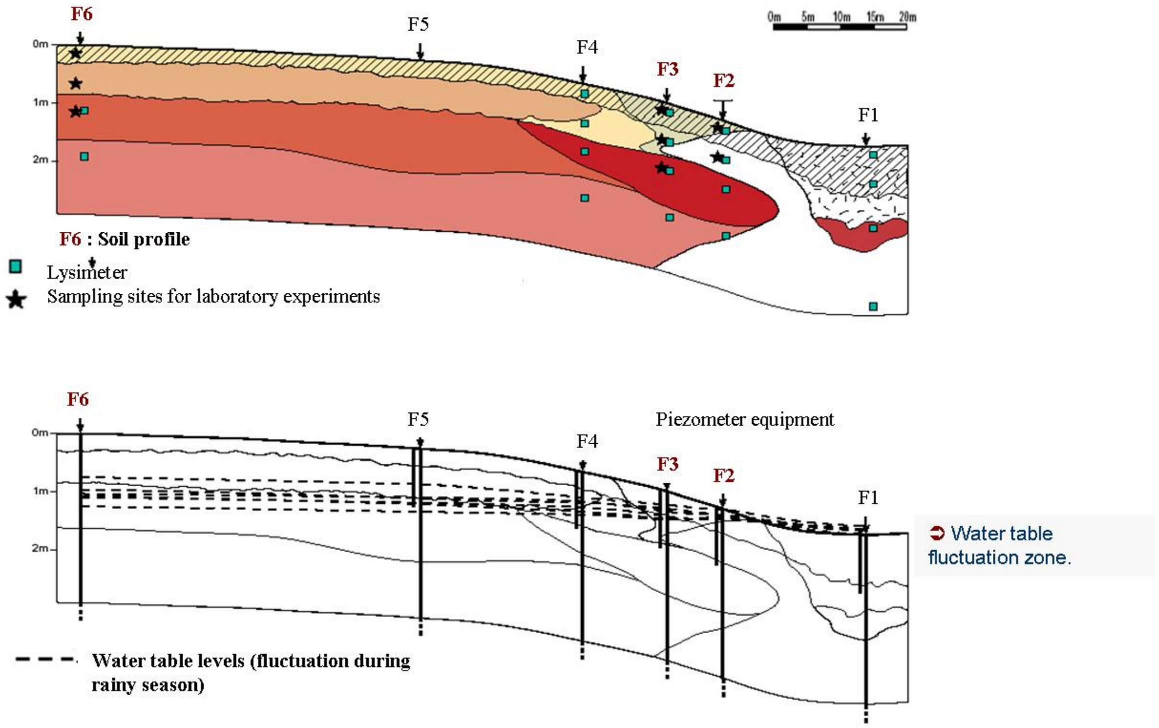

Figure 1. Studied tropical soil sequence of Humaita (Brazil).

The soils were characterized by particle size distribution, elemental analysis, pH, C, N, mineralogy (XRD-TEM). Soil waters were analyzed for Eh, pH, ferrous and total iron, nitrates and ammonia dissolved organic carbon (DOC) in different periods of the year. To determine the bacterial processes, experiments were performed by incubation of soil samples in laboratory devices without addition of nutrients except those from soils. Abiotic controls were also performed. At least 3 replicates were done per treatment Measurements concerned Eh, pH, organic matter biodegradation and mineralization (CO_2, DOC, NO_3^-, NH_4^+, ferrous and total iron, bacterial counting, screening, isolation and identification (biochemical and molecular biology methods: PCR, TGGE).

Results and discussion

Field measurements in soil waters and ground waters (decrease and low values of Eh, production of NH_4^+, decrease and reduction of NO_3^-, high content of Fe^{2+} and of DOC…, screening of microorganims), suggested occurrence of reducing bacterial mediated processes much more in the transition zone of water table and the occurrence of aero-anaerobic and anaerobic bacterial activities involving iron reducing bacteria (IRB).
Results of laboratory experiments performed in different devices simulating different environmental conditions and using soil samples originating from different sites and horizons, underline the involvement of iron reducing bacteria both in the biodegradation of soil organic matter (SOM) and the weathering of minerals (mainly ferric oxyhydroxides) which are dissolved as Fe^{2+}. High yields of bacterial iron reduction were observed in aero-anaerobic and anaerobic conditions, but also in nonwaterlogged soils when available organic matter was present to be use by bacteria to develop anoxic conditions and reducing processes. Correlations between mineralization of SOM and solubilization of iron were very significant. Fermentative and non fermentative bacteria appeared to be concerned. Their occurrence was confirmed by molecular biology (PCR-TGGE) indicating Shewanella, Enterobacter, Clostridium, Bacillus). SOM biodegradation and mineralization concerned mainly fulvic compounds. The reduction and dissolution of iron modified also the distribution of iron in their geochemical compartments. A relative decrease of well crystallized ferric iron (Fe_d) and an increase of not well crystallized ferric iron (Fe_0) were observed. Calculation of weathering coefficients has shown that, depending on soils, type of horizons, incubation time… (i.e. bioavailability of SOM and iron) the mineralization of one organic carbon allowed to solubilise from 0.06 to 1.29 iron (Fe). The stronger iron reducing bacterial activities were also located in samples originating from transition zones and fluctuation zones of water table in the surface and subsurface horizons.

Conclusion

The bacterial activity of iron reducing bacteria (IRB) is well correlated with the reduction and dissolution of ferric oxyhydroxides and the release and redistribution of iron in the soil sequence. IRB communities located at the redox interfaces of the hill-side sequences and under the dependence of water movement, organic matter and iron availability are the major agents of the weathering processes and of the redistribution of iron in the soil sequence. However further characterization of bacterial communities and of the factors of control of bioavailability of SOM and of iron is required to aid our understanding of the soil sequence functioning and to better quantify the parameters for modelling.

References

Berthelin J (1982) Processus microbiens intervenant dans les sols hydromorphes en régions tempérées. Incidence sur la pédogénèse. *Pédologie Gand* **XXXII**, 313-328.

Bousserrhine N, Gasser U, Jeanroy E, Berthelin J (1999) Bacterial and chemical reductive dissolution of Mn, Co, Cr and Al substituted goethites. *Geomicrobiol. J.* **16,** 245-258.

Fritsch E, Herbillon AJ, Nascimento (do) NR, Grimaldi M, Melfi MJ (2010) From Plinthic Acrisols to Plinthosols and Gleysols. Soil and landscape evolution on the Solimões sediments of the upper Amazon basin. *European Journal of Soil Science* (in press)

Kämpf N, Schwertmann U (1983) Gœthite and hematite in a climosequence in Southern Brazil and their application in classification of kaolinitic soils. *Geoderma* **29,** 27-39.

Lovley DR (1997) Microbial Fe(III) reduction in subsurface environments. *FEMS Microbiol. Rev.* **20**, 305-313.

Macedo J, Bryant RB (1987) Morphology, mineralogy and genesis of a hydrosequence of oxisols in Brazil. *Soil Sci. Soc. Am. J.* **53,** 1114-1118.

Peterschmitt E, Fritsch E, Rajot JL, Herbillon AJ (1996) Yellowing, bleaching and ferritisation processes in soil mantle of the Western Ghâts, South India. *Geoderma* **74,** 235-253.

Quantin C, Becquer T, Rouiller JH, Berthelin J (2002) Redistribution of metals in a New Caledonia Ferralsol after microbial weathering. *Soil Sci. Soc. Am. J.* **66,** 1797-1804.

Schwertmann U, Kämpf N (1985) Properties of goethite and hematite in kaolinitic soils of southern and central Brazil. *Soil Science* **139,** 344-350.

Stemmler SJ, Berthelin J (2003) Microbial activity, a major parameter of iron mobilisation in a typical watershed of humid tropical countries (Nsimi, Cameroon). *European Journal of Soil Science* **54,** 725-733.

Tardy Y (1993) 'Pétrologie des latérites et des sols tropicaux'. (Masson: Paris).

Soil development indices in a soil chronosequence formed on Lower Pleistocene terraces in the north-western Duero basin (León, Spain)

Manuel Vidal[A]; Eduardo Villa[A]; Sara Alcalde[A]; Eduardo Alonso[A]; Juan A. Robles[A]

[A]School of Agricultural Engineering, University of León, Spain, Email mavidb@unileon.es

Abstract

A study was carried out in a soil chronosequence developed on alluvial deposits, comprising six terraces displaying marked variations due to altitudinal differences. Many of their morphological properties, such as their original red colour, have become obscured beneath a variety of colours as a result of the intense hydromorphism acting upon the impermeable Miocene clay substrate which underlies these formations. The accumulation indices (AI) for total clay and fine clay, and most especially those corresponding to the iron oxides (Fed/Fet), were found to be good indicators, highlighting developmental and evolutionary differences between the six soils.

Key Words

Terraces, chronosequence, clay, iron oxides, accumulation indices

Introduction

The majority of soil properties change according to the length of time other formation factors are active. Nevertheless, due to the high number of edaphic properties, it is difficult to assess a soil's development stage from a single property. Thus, many authors have established indices based on comparing variations in the properties of a given soil with corresponding variations in the soil's parental materials. To this end, some researchers have concentrated primarily on morphological properties (Bilzi and Ciolkosz, 1977; Harden, 1982), whilst others have used analytical laboratory data (Walker and Green, 1976; Birkeland, 1984; Levine and Ciolkosz, 1983; Harrison *et al.*, 1990). Soil sequences spread over a system of river terraces comprise the most frequently studied type of chronosequence.

The aims of the present work were to assess the changes in some properties over time and establish the relative age of the edaphic formations corresponding to the six levels of river terraces spread over the soil chronosequence of the mid-upper reaches of the Orbigo River (NW Duero basin, León, Spain).

Methods

Over geological time this river has left a typical scaled relief, with abundant horizontal surfaces placed between sharp scarps. A representative profile was chosen from each of the six geomorphological surfaces distinguished. The fluvial deposits have thicknesses ranging between 4 and 5 m and are composed mainly of gravels, cobbles and stones and sand originating from the erosion of quartzites and slates.

The study area is characterised by a mean annual temperature of 10.4° C, mean annual rainfall of 521 mm and mean annual ETP of 645 mm. Soil temperature and moisture regimes are mesic and xeric, respectively. The sequum comprises an A horizon (normally umbric), and an AB transition horizon followed by a thick argillic horizon (Bt). Due to the intense hydromorphism acting upon the underlying Miocene clay substrate, this latter horizon generally displayed high colouring with fading of the original red, presenting intensive migration of iron and manganese. According to the WRB classification (FAO, 2006), the six soils comprised Umbric Acrisols, corresponding to Typic Palexerults according to the Soil Taxonomy (USDA, 1999).

In order to carry out the characterisation proposed as the aim of the study, three accumulation indices (AI) were estimated: the accumulation index of total clay, the corresponding accumulation index of fine clay and the accumulation index associated with intensity of mineral alteration, represented by the accumulation of iron oxides (Fed/Fet). Total iron (Fet) was determined using the method proposed by Pratt (1965), whilst free iron oxides (Fed) were extracted using the method developed by Merha and Jackson (1960).

Results

The six soils studied in the river chronosequence comprised old evolved edaphic formations of a marked superacid nature as shown by the mean pH values in KCl of 3.5 – 3.7, base satutation percentages of 20-30% and Al saturation of 50-75%. The gravels and quartzite blocks corresponding to the three upper terrace levels presented intensive desintegration. Height between the highest terrace T6 and the following terrace T5 was 23 m; between T5 and T4, 19 m; between T4 and T3, 51 m; between T3 and T2, 36 m, and between T2 and T1, 35

m. In total, a height of 164 m was recorded between the upper and lower terraces.

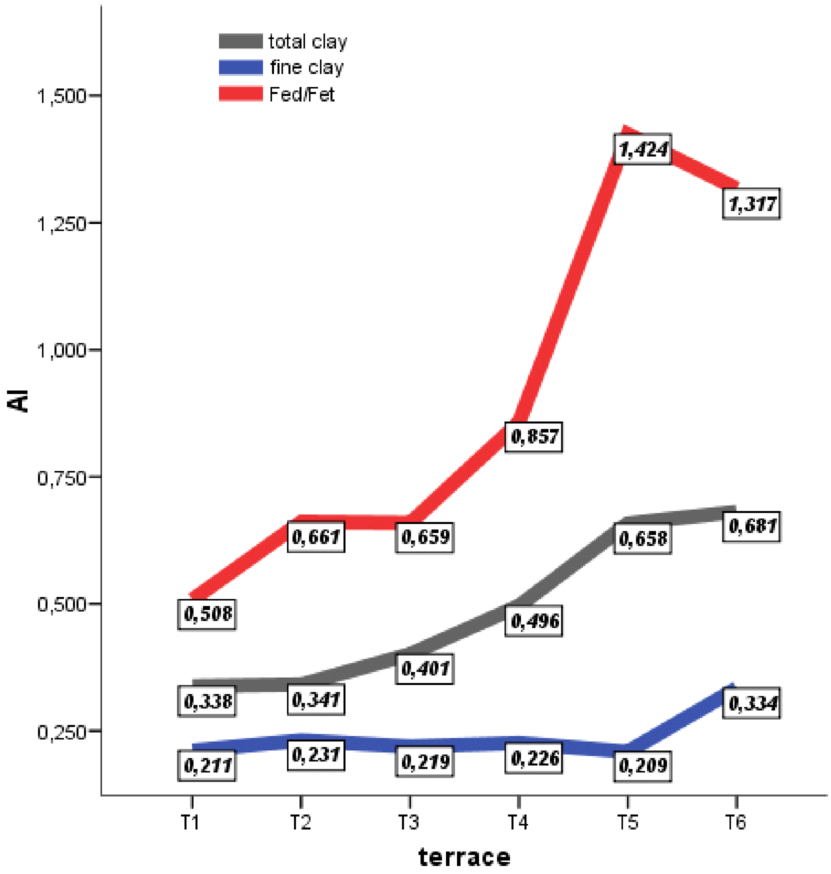

Figure 1. Accumulation Indices (AI) of total clay, fine clay and Fed/Fet.

The AI corresponding to total and fine clay respectively were estimated from differences between clay content (%) in the Bt horizons and the A and AB horizons; this difference was divided by the sum of Bt horizon thicknesses (cm).The AI of free iron oxides (Fed/Fet) was calculated in the same way.

The evolutionary and developmental level of the six soils comprising the chronosequence can be seen in Figure 1, where the AI obtained for each terrace is given. The total clay AI were highest on levels T6 and T5, whilst T4 and T3 presented medium values and lowest and very similar values were recorded for T2 and T1. However, the fine clay AI did not present such clear differences, and variations in the AI corresponding to the Fed/Fet ratio were found to be a much better indicator of the development of this soil chronosequence. For a given intensity of weathering, the free Fe content (Fed) should increase in proportion to total Fe content (Fet). On this basis, T6 and T5 presented greater development and mineral alteration than the lower terraces T4, T3, T2 and T1.

Conclusion

In the soil chronosequence studied, comprising highly evolved soils with thick argillic horizons where the hydromorphism hinders the expression of significant morphological features. The accumulation indices (AI) corresponding to total clay content and proportion of crystallized iron Fed/Fet were found to be excellent indicators of degree of edaphic evolution and development. These indices enable evolutionary differences to be established and the relative age of these edaphic formations to be determined.

References

Bilzi AF, Ciolkosz EJ (1977) A field morphology scale for evaluating pedological development. *Soil Science* **24,** 45-48.

Birkeland PW (1984) Holocene soil chronofunctions, Southern Alps, New Zealand. *Geoderma* **34,** 115-134.

FAO (2006) World Reference Base for Soil Resources. A framework for international classification, correlation and communication. (Food and Agriculture Organization of the United Nations Publishing: Rome).

Harden J (1982) A quantitative index of soil development from field description: exemples from a chronosequencein central California. *Geoderma* **28,** 1-28.

Harrison JBJ, McFadden LD, Weldon RJ (1990) Spatial soil variability in the Cajon Pass chronosequence: implications for the use of soils as a geochronological tool. In "Soils and landscape evolution. Geomorphology". (Eds. Knuepfer PLK, McFadden LD), pp. 93-108.

Levine ER, Ciolkosz EJ (1983) Soil development in till of various ages in Northeastern Pennsylvania. *Quaternary Research* **19**, 85-99.

Merha OP, Jackson ML (1960) Iron oxide removal from soils and clays by dithionite-citrate system buffered with sodium bicarbonate. In "Proceedings of the 7th Natl. Conference Clays and Clays Minerals" **7**, 317-327.

Pratt PF (1965) Digestion with hydrofluoric and percchloric acids for total potassium and sodium. In "Methods of soils Analysis, I". (Ed. Black CA *et al.*), pp. 1019-1021 Agronomy series No.9, (Society of Agronomy: Madison, Wisconsin).

USDA (1999) Soil Taxanomy: A basic system of soil classification for making and interpreting soil survey. Agricullture Handbook No.436, 2nd edition, (Eds U.S.D.A. Gov. Print Office, Washington).

Walker PH, Green P (1976) Soil trends in two valley fill sequences. *Australian Journal of Soil Research* **14,** 291-303.

Soil distribution relationships as revealed by a global soil database

Jonathan Gray[A], Geoff Humphreys[B] and Jozef Deckers[C]

[A]NSW Department of Environment, Climate Change and Water, PO Box 3720, Parramatta (Sydney), NSW 2124 Australia, Email jonathan.gray@environment.nsw.gov.au
[B]Department of Physical Geography, Macquarie University (Sydney), NSW 2109 Australia (deceased)
[C]Catholic University of Leuven, Vital Decosterstraat 102, 3000 Leuven, Belgium.

Abstract

Broad quantitative relationships between the environmental factors of climate, parent material and topography and a range of important soil properties and World Reference Base (WRB) soil types were developed using the ISRIC WISE Global soil database Three different analytical approaches were used in the analysis, involving (i) multiple linear regressions, (ii) fitted decision trees and (iii) categorical analysis with median values. Despite the relatively low to moderate strengths of the derived relationships, they can provide useful first approximations of soil character under different environmental conditions and could be applied in broad quantitative soil modelling and mapping programs. They have the potential for widespread application as they should be universally applicable, are based on readily available data and do not require sophisticated quantitative modelling techniques. Most relationships are in accord with accepted pedological thinking and support the state factor model of soil formation, but some anomalies are observed and deserve further examination. The results reveal the dominant influence of climate and parent material in controlling the distribution of many soil properties, with the influence of topography being less evident, at least at the global scale. The WRB soil classification scheme is shown to be least partly guided by genetic factors.

Key Words

Digital soil survey, soil prediction, environmental correlation, modelling, soil genesis.

Introduction

Soil data is increasingly being relied upon in ecological, hydrologic, climatic and other environmental applications in addition to its traditional role in agriculture and natural resource management. There is a need for precise quantitative relationships between soil and key environmental factors to aid soil data collection and soil modelling around the globe. Such relationships form the basis of digital soil mapping techniques, which are widely considered to be where the future of soil survey lies (Lagacherie and McBratney 2007, Hartemink 2006; Grunwald 2006). However, most published information on soil-environment relationships is of a qualitative form, and even these are often not clearly enunciated. Few universally applicable quantitative relationships have been published and widely accepted to date. Most that have been published relate to specific regions rather than to continental or global scales. Heuvelink (2005) laments that most of our knowledge on soil forming processes is available only in a conceptual or descriptive form and that so far we have not succeeded in building a generic, quantitative, reproducible model that predicts the soil from its controlling factors in a satisfactory way. Soil-environment relationships are generally based on the principles inherent in the now widely accepted State Factor model of soil formation and the associated fundamental soil equation. This model, sometimes referred to as the *clorpt* model, maintains that the soil or soil property is a function of the factors of climate (*cl*), organism or biota (*o*), relief or topography (*r*), parent material (*p*) and time (*t*) (Jenny 1941). The equation has been described as “a general statement implying that soils are natural bodies that are distributed in a predictable way in response to a systematic interaction of environmental factors” (Hudson 1992).

Methods

The ISRIC WISE Global Datasets (2002 and 2008 versions) were examined to extract relationships that could be used to model soil behaviour at the global level. The datasets contain several thousand geo-referenced soil profiles from up to 149 countries (Batjes 2002, 2008). It was established by the International Soil Reference and Information Centre using the framework of the World Inventory of Soil Emission Potential (WISE) project. Climatic data was derived from a world climatic dataset contained in FAO/IIASA (2002).

Multiple queries were created in the Access databases to extract key soil properties, WRB soil types and the associated environmental variables relating to topography, parent material and climate. These variables were divided into classes as outlined below. Age and biotic activity could not be included in the query process due to their lack of meaningful indicators.

Topography – slope percent in conjunction with landform features, two classes
Parent material – broad silica (SiO_2) content; five classes with one based on calcareous character
Climate – annual rainfall (R) and rainfall/ potential evapotranspiration (R/EV); eight classes.
Only 1646 profiles within the datasets matched the final query requirements, comprised of 1108 in near level sites and 538 in sloping sites. The combination of two topographic, five parent material and eight climatic classes resulted in the creation of 80 different environmental regimes, which provided a basis for presenting categorical analysis results.

Exploratory statistical analysis was undertaken using S-Plus (2003) software, including: (i) multi-variate linear regressions (ii) fitted decision trees, and (iii) a categorical approach giving soil types and median soil property values in each of 80 different environmental regimes. Standard statistical techniques were applied to test the performance of the relationships and the relative contributions of each variable. Graphical plots were prepared for all relationships. Predictions of soil properties derived using the three approaches were tested for accuracy against actual values from 100 random samples drawn from the ISRIC database prior to the development of the relationships.

Results

Soil-environment relationships were derived using the different approaches for a wide range of soil properties (pH, sum of bases, CEC, base saturation, organic carbon, ESP, EC_e, clay and sand content) for both topsoil and subsoil horizons, and for WRB soil types. Full results are reported in Gray *et al.* (2009) and Gray *et al.* (in press).

Multiple linear regression approach

Regression relationships between the numerous soil properties and the three environmental variables were established. Results for pH and sum of bases are presented in Figure 1.

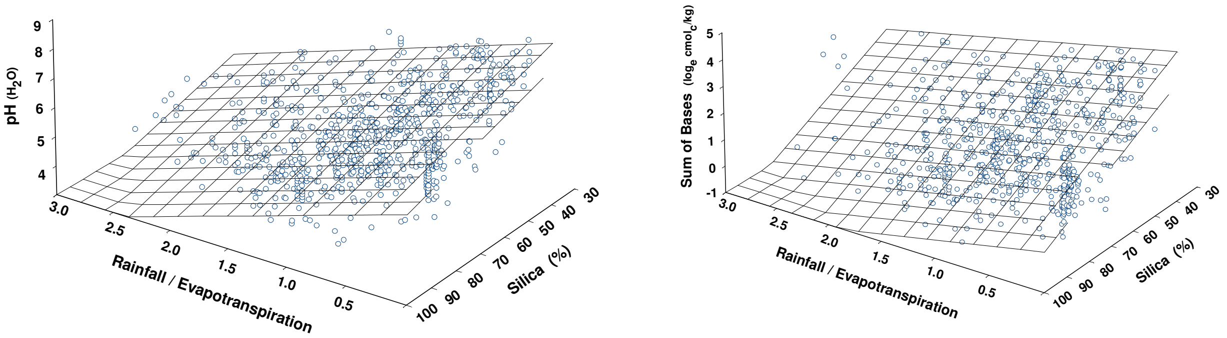

$pH = 8.69 - 1.22(R/EV) - 0.025(silica\%) - 0.0072(slope\%)$

$N = 490, R^2 = 0.40, F\ model = 106.0, p = <0.0000$

$\ln(SumBase) = 5.57 - 0.81(R/EV) - 0.051(silica\%)$

$N = 781, R^2 = 0.30, F\ model = 88.3, p = <0.0000$

Figure 1. Regression planes of key topsoil properties v R/EV and silica%.

Coefficient of determination (R^2) values are generally in the low to moderate range for most properties. For pH they are moderate (~0.30-0.40), indicating a moderate correlation and that these regression relationships are at least moderately effective in accounting for the variation of this property in the database. R^2 values are low to moderate for sum of bases and clay (~0.30-0.35) and only low for organic carbon (~0.10-0.25), indicating that these relationships are of only low to moderate effectiveness in accounting for the variation of these properties.

Decision tree approach

Decision trees were fitted to the data for each of the key soil properties. For the purposes of simplicity and ease of presentation, the sensitivity of the trees was set so as to finish with approximately 10-12 leaves at the base. The tree for topsoil pH is presented in Figure 2. It can be seen that for a hypothetical site with very wet climate (G), highly siliceous parent material (HS) and sloping topography (S), the topsoil may be expected to have a pH of 5.2.

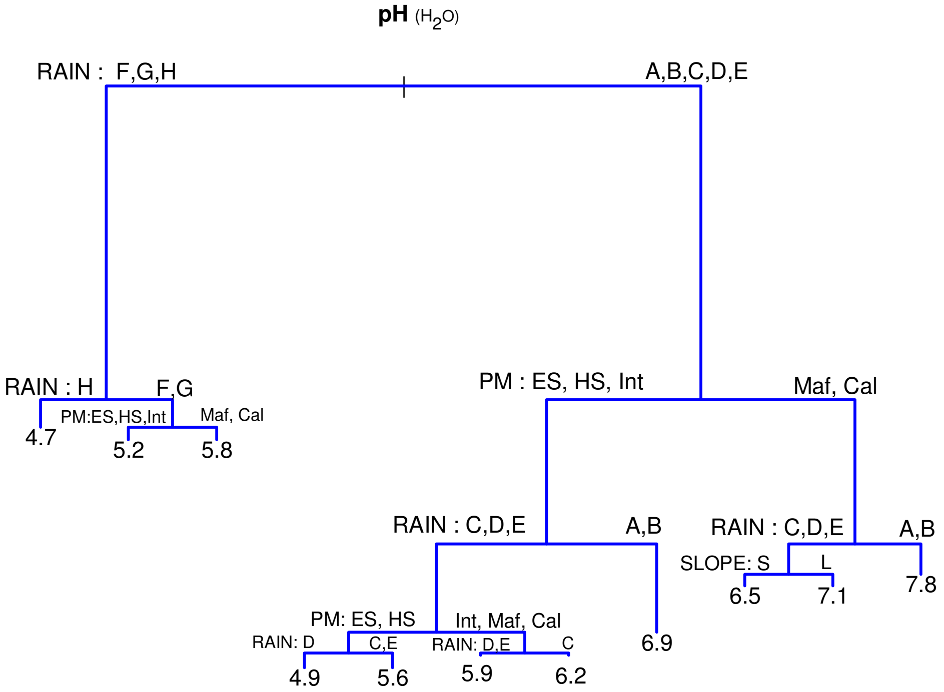

Legend

Rainfall (mm pa)

A	<250 (extremely dry)
B	250-500 (very dry)
C	500-750 (dry)
D	750-1000 (mod. dry)
E	1000-1250 (mod. wet)
F	1250-1500 (wet)
G	1500-2000 (very wet)
H	>2000 (extremely wet)

Parent Material

ES	extremely siliceous
HS	highly siliceous
Int	intemediate
Maf	mafic
Cal	calcareous

Topography

L	near level sites
S	sloping sites

Figure 2. Fitted decision trees for topsoil pH.

The models all reveal a generally consistent change in soil properties as the environmental factors vary, eg, decreasing pH with increasing wetness and increasing siliceous character. However, some minor anomalies occur, which may be due to low sample numbers or other sources of error as discussed later.

Categorical median value approach

The median values of the various soil properties in each of the 80 different environmental regimes were derived. These were presented in a series of tables and box plots for key properties in Gray *et al.* (2009). The plots and tables reveal the broad trends in behaviour of the soil properties with changing conditions.

World Reference Base soil pie charts

Data on WRB soil types were extracted for each of the topographic-parent material-climate regimes and presented in a series of pie charts. Each chart presents the dominant WRB soil types (up to seven) and the three most dominant qualifiers, together with their percentages and sample numbers. The associated percentages give an indication of the likely probability of occurrence of each soil type or qualifier in that regime. Three example charts are shown in Figure 3. Full results are presented in Gray *et al.* (in press).

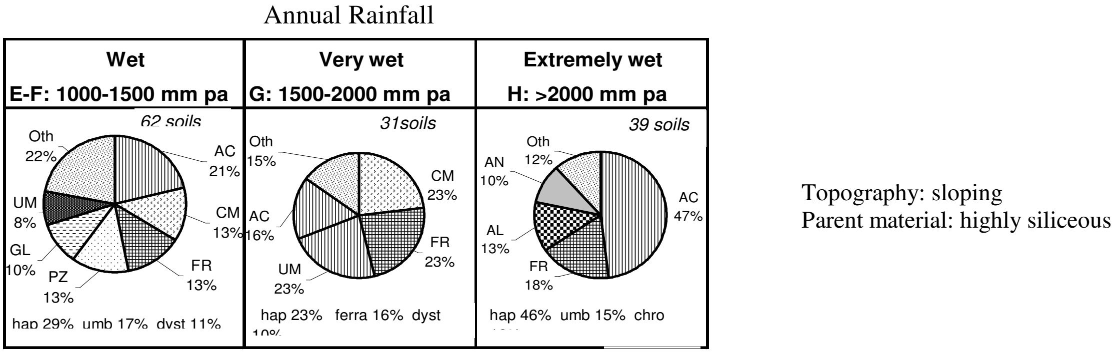

Figure 3. WRB pie charts for three environmental regimes.

Discussion

Despite the relatively low to moderate strengths of the predictive relationships developed, they may assist in the collection and modelling of soil data as required to meet the growing demands for this information in many earth, environmental, climatic and other scientific modelling programs. More specifically, the relatively simple and pragmatic relationships may:

- provide useful first approximations of soil character under different environmental conditions that could be applied in broad quantitative soil modelling and mapping programs.
- have the potential for widespread application as they should be universally applicable, are based on readily available data and do not require sophisticated quantitative modelling techniques. They may thus facilitate an increased application of digital techniques in addition to conventional techniques in soil survey organisations and in the broader soil science community.
- assist in our understanding of soil formation and soil distribution. Most relationships revealed are in accord with accepted pedological thinking and support the state factor model of soil formation, but some anomalies are observed and deserve further examination.

The relatively low to moderate effectiveness of the relationships reflects the inherent complexity of soil property–environmental factor relationships. A high variability in soil properties is demonstrated even in samples within generally similar environmental condition. Factors that may contribute to this high variability include: the relatively small number of usable samples in the database, influence of other environmental factors not considered here including biotic and age factors; the simplification of climatic, parent material and topographic factors, the polygenetic nature of many soils with influence by past climates; and the influence of "intrinsic" rather than traditionally accepted extrinsic" factors (Phillips 2001). The WRB relationship results suggest that this classification scheme is at least moderately guided by soil forming factors and that it may represent a scheme with an appropriate balance between genetic factors and purely diagnostic features in its underlying principles.

The project has demonstrated the potential value of large world soil databases for the understanding, modelling and mapping of soil distribution around the globe. Further analyses of the ISRIC and other large soil databases with more sophisticated data mining techniques would undoubtedly help to refine the predictive tools and shed further light on factors influencing soil distribution.

References

Batjes NH (2002) 'A homogenised soil profile dataset for global and regional environmental research' (WISE, vers. 1.1), Report 2002/01. (International Soil Reference and Information Centre: Wageningen).

Batjes NH (2008) 'ISRIC-WISE harmonized Global Soil Profile Dataset (version 3.1), Report 2008/02'. (International Soil Reference and Information Centre: Wageningen).

Gray JM, Humphreys GS, Deckers JA (2009) Relationships in soil distribution as revealed by a global soil database, *Geoderma* **150**, 309-323.

Gray JM, Humphreys GS, Deckers JA (2010) Distribution patterns of World Reference Base soil as revealed by a global soil database. (in press)

Grunwald S (2006) What Do We Really Know about the Space-Time Continuum of Soil-Landscapes? In 'Environmental Soil-Landscape Modelling - Geographic Information Technologies and Pedometrics'. (Ed S Grunwald) pp. 3-36. (Taylor and Francis)

Hartemink AE (2006) 'The Future of Soil Science'. (International Union of Soil Sciences (IUSS): Wageningen).

Heuvelink GBM (2005). Foreword. In 'Environmental Soil-Landscape Modelling - Geographic Information Technologies and Pedometrics'. (Ed S Grunwald) (Taylor and Francis).

Hudson BD (1992). The soil survey as paradigm based science. *Soil Science Society of America Journal* **56**, 836-841.

Jenny H (1941) 'Factors of Soil Formation.' (McGraw-Hill Book Company Inc.: New York).

Lagacherie P, McBratney AB (2007) Spatial Soil Information Systems and Spatial Soil Inference Systems: Perspectives for Digital Soil Mapping. In 'Digital Soil Mapping'. (Eds P Lagacherie, AB McBratney, M Voltz) pp. 3-22. (Elsevier: Amsterdam).

Phillips JD (2001) The Relative Importance of Intrinsic and Extrinsic Factors in Pedodiversity. *Annals of the Association of American Geographers* **94**, 609-621.

Soil genesis along a paddy soil chronosequence in a millennium scale

Gan-Lin Zhang[A, B] and Liu-Mei Chen[A, B]

[A]State Key Laboratory of Soil and Sustainable Agriculture, Institute of Soil Science, Chinese Academy of Sciences, Nanjing, China, Email glzhang@issas.ac.cn
[B]Graduate School of the Chinese Academy of Sciences, Beijing, China.

Abstract

A paddy soil chronosequence consisting of five profiles derived from calcareous marine sediments ranging in paddy cultivation history from 0 to 1000 years was studied. The general soil physical and chemical properties, magnetic properties, clay mineral and major elements of the soil samples were measured, in order to investigate the dynamic change of different soil properties, and to understand the response rate of soil properties over different time scales. The results showed that soil properties including surface soil organic carbon, $CaCO_3$, MS(magnetic susceptibility), IRM_s(soft isothermal remanent magnetization), had notable changes within the initial stage (50 yrs) of paddy cultivation. Clay content, free iron oxides, and IRM_h (hard isothermal remanent magnetization), change notably when paddy cultivation history reach 700 years. However, clay mineralogy shows few changes even if the cultivation time reaches 1000 years. The results of gains and losses of major elements indicate Ca, Mg, and Na are strongly lost in the initial stage (50 yrs) of paddy cultivation and gradually depleted with increasing paddy cultivation time, Si and Al remain basically constant, while, Fe has large depth variation. In conclusion, our data demonstrate that different soil components and properties have quite different changing process and rate under paddy cultivation condition.

Key Words

Paddy soils, chronosequence, pedogenesis, mass balance, dynamic change, time scale.

Introduction

Soil chronosequences are valuable tools for investigating rates and directions of pedogenic evolution (Huggett 1998). Brantley (2008) indicated that different soil components have different response times that vary from hundreds of millions of years to minutes in regolith and suggested that learning how soils will change in the future will require observations and models that cross time scales. Paddy soils are an important soil resource for food production in Asia. Knowledge of rates and processes of geochemical and pedogenic changes under wet cultivation is useful for the improvement and sustainable use of these important soil resources. As anthropogenic soils, paddy soils provide a good basis for soil change study over a millennium scale. The objectives of this study are to investigate the dynamic change of various soil properties over a fairly well quantified time scales, using a well-dated paddy chronosequence under human cultivation condition.

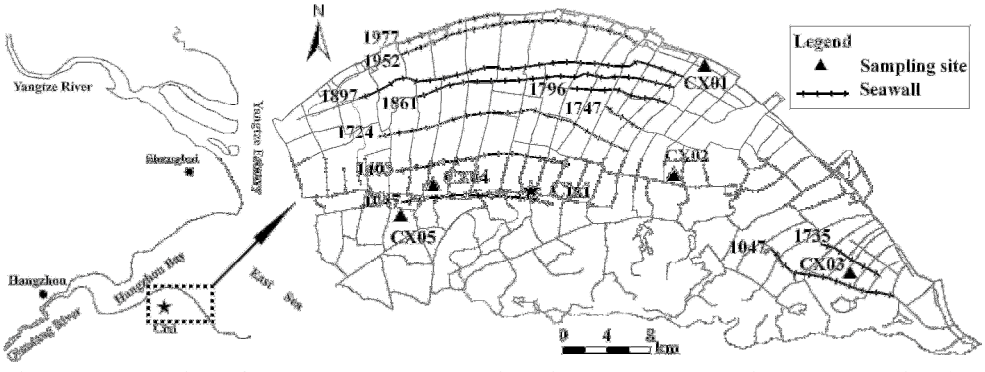

Figure 1. Location of study area and sampling sites. Numbers beside the dark line (seawall position) represent the calendar (AD) year when the seawall was built.

Materials and methods

Study area and soil chronosequence recognition

The studied area is located in Cixi, Zhejiang Province, facing the East China Sea (Figure 1). The region belongs to the southern fringe of northern subtropics and has a mean annual temperature of 16.3°C and a mean annual rainfall of 1325 mm. The sampling area is a marine deposit plain. Parent materials are mainly marine sediments with some river alluvium derived from East Sea and Qiantang River. With sedimentation, the land becomes free from tides and followed by building seawall for paddy cultivation. Along the coastline extension, seawalls were built in different stages successively. Wang (2004) collected and compiled a series of Cixi County Annals that records chronologically the significant natural, social and economical events. The detailed records of seawall construction and rice cultivation history are available. A paddy soil chronosequence consisting of four profiles were sampled. The age data, i.e., approximately 300, 700, and 1000 years of paddy cultivation history, was determined based on the time of seawall constructions, while the profile with 50 years of paddy cultivation was determined by local farmers. In addition, we selected an uncultivated mud beach profile as the original soil (Gleyic Fluvisols) (time zero).

Field sampling and 1aboratory analyses

Within each identical paddy cultivation history area, three paddy fields are chosen based on historic information, specific location, fresh irrigation water availability and current land uses, and one representative profile is chosen for sampling. All soil samples were collected when the fields were drained after rice harvest. Soil profiles were described and sampled according to genetic horizons following standard field study methods. Figure 2 show the image of the five studied profiles. Soil samples were dried at room temperature and gently crushed using a wooden pestle and mortar, and then passed through a 2 mm nylon sieve. Soil organic carbon, $CaCO_3$, particle size distribution, free iron oxides, clay mineral, and major element concentrations were measured according to ISSAS (1978). Magnetic parameters were measured and calculated according to Evans and Heller (2003). Chen and Zhang (2009) indicated that no lithological discontinuities occur both within and among the studied soils, by using various indicators determining lithological discontinuities (LDs) (Schaetzl 1998).

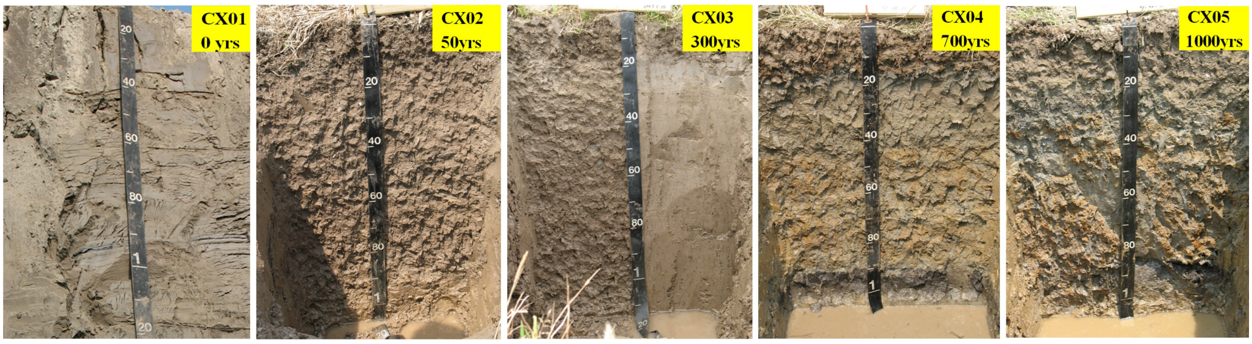

Figure 2. The studied pedons of the paddy soil chronosequence, with age varying from 0 to 1000 years of paddy cultivation history.

Results and discussion

Physical and chemical properties

The vertical distribution of soil organic carbon (SOC), $CaCO_3$, clay content and free iron oxides (Fe_d) in the uncultivated soil is relatively uniform over 0-120 cm soil depth, as compared with that in paddy soils (Figure 3), showing that no pedological changes occur. SOC value in A horizons (roughly 0-16 cm depth) in paddy soils (range from 14.2g/kg to 24.3g/kg) was consistently higher than that in uncultivated soil (4.0g/kg). Vertical distribution of SOC in the lower horizons is generally uniform and the contents in majority of horizons are around 4.0g/kg, except the Ahb horizon in 700yrs paddy profile (90-112cm) and 1000yrs paddy profile (85-100cm), which is a buried layer rich in humus and partially degraded plant debris. SOC in any horizons in paddy soil profiles does not show increasing or decreasing trend against paddy cultivation age. This indicates that paddy cultivation significantly increases the SOC in surface horizons, but SOC does increase constantly and would reach an equilibrium stage in a relatively short time span (around 50 years) under a given ecosystem conditions. The mean value of $CaCO_3$ content (averaged over 0-120cm depth) is 58.3g/kg in the uncultivated soil. $CaCO_3$ content decreases gradually with increasing paddy cultivation age within 300yrs. In the pedons of paddy cultivation age more than 300 yrs, i.e. 700yrs and 1000yrs no $CaCO_3$ is found over 0-120 cm soil depth. The leaching loss of $CaCO_3$ in the calcareous soil increases with increasing paddy cultivation age due to the artificial periodic irrigation and drainage in rice planting system. Clay content in overall depth in paddy soils is consistently higher than that in uncultivated soil. Clay content in the profiles with 50 and 300 years of cultivation history show slightly higher, however, in the 700 and 1000-year paddy profiles have obviously higher clay content, compared with uncultivated soil. The increased clay content is mainly found in depth within about 40 cm and 80cm of paddy profiles. The depth distribution of clay content in paddy soils suggest clear clay illuviation occurred in older paddy soils, i.e.700 and 1000 years paddy profiles in the depth about below 40cm for 700 years paddy pedons, 20cm for 1000 years one. Deposition of suspended material from irrigation water (generally fine particles) and mechanical leaching probably favors clay accumulations and differentiation. Distribution pattern of Fe_d was similar to that of clay contents. The Fe_d in paddy profiles showed obvious sequential trend with time. The differentiation of Fe_d between surface horizon and subsurface horizon is stronger with paddy cultivation time, especially in those older soils (700 and 1000 yrs paddy cultivation history) in which the Fe_d of surface horizon to Fe_d of subsurface horizon ratio is more than 2.0. The illuviation depth of maximum Fe_d content of 300, 700, and 1000 years paddy profiles over 0-120 cm depth occurs at 30 cm, 50 cm and 80 cm respectively. The amount of Fe_d in illuviation horizon increases gradually with increasing rice cultivation age. The results indicate that the illuviation of Fe_d increases in quantity and the depth of illuviation lower gradually with the increasing of paddy cultivation age.

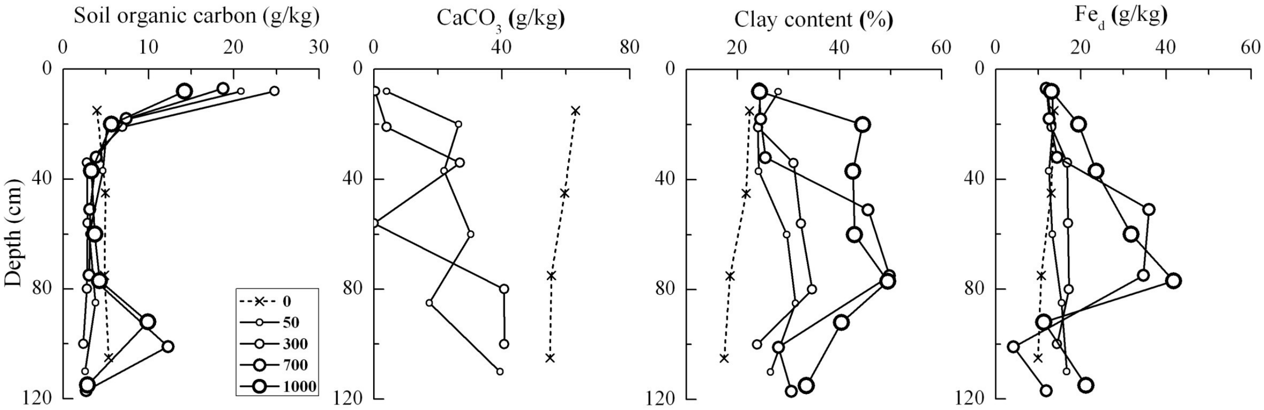

Figure 3. Depth distribution of soil organic carbon, $CaCO_3$, clay (<2μm) and Fe_d (free iron oxides) in the chronosequential soils.

Magnetic properties

The depth distribution of magnetic susceptibility (MS), soft and hard isothermal remanent magnetization (IRM_s and IRM_h) in all pedons is relatively uniform over 0-120cm soil depth, as compared with S_{-100mT} (Figure 4). Three stages could be divided for the changes of the magentic parameters with paddy cultivation age. The first stage (from uncultivated soil to 50 years paddy soil) is characterized by the remarkable decrease of MS and IRM_s resulting from reductive dissolution of ferrimagnetic minerals. The second stage (50~700 years) is characterized by the profile differentiation of S_{-100mT}. The third stage (700~1000 years) is characterized by significant decrease of IRM_h and relatively stable MS, indicating that antiferromagnatic mineral (goethite) remarkably decreases and paramagnetic minerals (lepidocrocite) are formed in the illuviation horizon when the paddy cultivation age reach to 700yrs in which $CaCO_3$ have been leached out completely from the overall pedons. The results reveal that magnetic parameters can both respond to and reflect iron oxides minerals change in paddy soils and have a quite different change pattern in submerged environment compared with that in non-paddy soils (Singer *et al.* 1996).

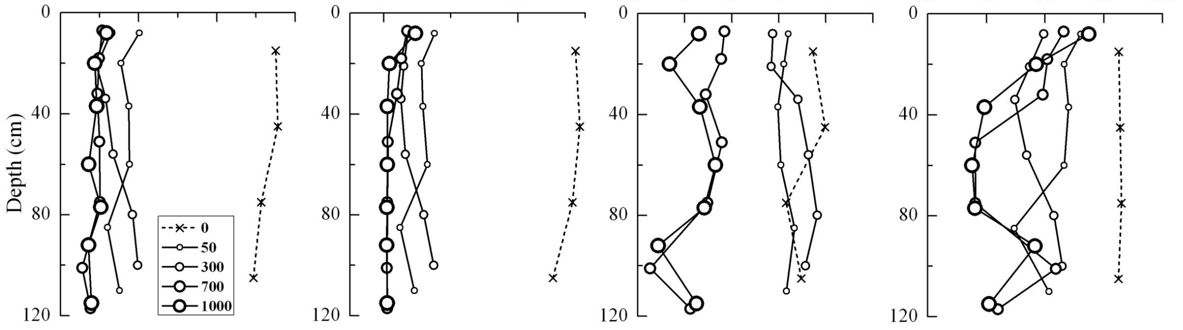

Figure 4. Depth distribution of magnetic parameters in the chronosequential soils.

Clay minerals

The clay mineral assemblage (detailed data are not shown due to page limit) mainly consists of illite (40-50%), chlorite (20-30%), and kaolinite (10-20%) with a few amounts of smectite and quartz. In comparison with the uncultivated soil and the paddy soils with different cultivation history, the clay mineralogy shows few change, even if the cultivation time reaches 1000 years.

Mass-balance calculations of major elements

Gains and losses of nine major elements (mean value in each paddy soil pedons over 0-120cm depth) in chronoseqnential paddy soils are calculated (using Ti as immobile element and using uncultivated soil as the original soil) and shown in Figure 5. Ca, Na, and Mg are characterized by the remarkable loss in the paddy cultivation initial stage (50 yrs) and gradually depleted with increasing paddy cultivation time. P and Mn are characterized by the slightly enriched in the paddy cultivation initial stage (50 yrs) and remarkable loss in the cultivation age more than 700 years. Comparatively, Si and Al have small migration rates. Fe and K are characterized by basically constant mean value in overall profiles and large depth variation with loss in the surface horizon and gain in the subsurface horizon (mainly between 40 cm and 80cm).

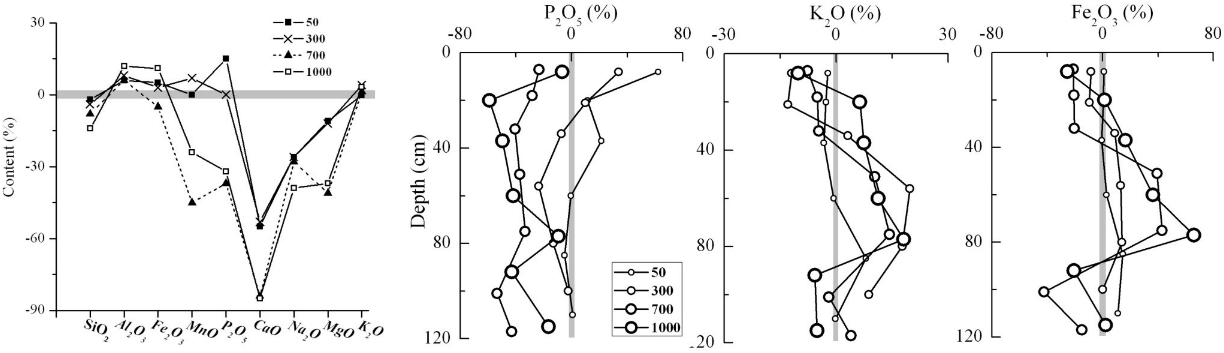

Figure 5. Gains and losses of major elements in paddy soils compared with uncultivated soil.

Conclusion

The studied paddy chronosequence developed on fairly uniform parent materials under nearly identical climate conditions and landscape provides a good opportunity to study the time-dependent changes in soil development. Soil properties including SOC, $CaCO_3$, MS, IRM_s, show notable changes within paddy cultivation initial stage (50 yrs). To clay content, free iron oxides, and IRM_h, notable changes occur when paddy cultivation history reach 700yrs. However, clay mineralogy shows few changes even if the cultivation time reaches to 1000 years. The mass balance of major elements indicate Ca, Mg, and Na are strongly lost in the paddy cultivation initial stage (50 yrs) and gradually depleted with increasing paddy cultivation time, Si and Al are basically constant, while, Fe has large depth variation. Although the total amount of iron has no dramatic change during paddy cultivation, it translocated to form an iron-rich layer with time and it transformed drastically as shown by the evolution of magnetic parameters.

Acknowledgement

The study was supported by the Natural Science Foundation of China (grant no. 40625001) and Chinese Academy of Sciences (KZCX2-YW-409).

References

Brantley SL (2008) Understanding soil time. *Science* **321**, 1454-1455.

Chen LM, Zhang GL (2009) Parent material uniformity and evolution of soil characteristics of a paddy soil chronosequence derived from marine sediments. *Acta Pedologica Sinica* **46**, 753-763.

Evans ME, Heller F (2003) 'Environmental Magnetism.' (Academic press: San Diego, CA).

Huggett RJ (1998) Soil chronosequences, soil development, and soil evolution: a critical review. *Catena* **32**, 155–172.

ISSAS (Institute of Soil Science the Chinese Academy of Sciences) (1978) 'Methods for Soil Physical and Chemical Analysis.' (Shanghai Sci. and Tech. Press: Shanghai).

Schaetzl RJ (1998) Lithologic discontinuities in some soils on drumlins: Theory, detection, and application. *Soil Science* **163**, 570-590.

Singer MJ, Verosub KL, Fine P, TenPas J (1996) A conceptual model for the enhancement of magnetic susceptibility in soils. *Quaternary International* **34-36**, 243–248.

Wang QY (2004) 'Evolution history of seawall in Cixi county, Zhejiang province.' (Fang Zhi press: Beijing).

Stable Fe isotopes - a prospective tool for investigating soil processes

Zuzana Fekiacova[A], Sylvain Pichat[B] and Fabienne Trolard[A]

[A]INRA UR1119 Géochimie des Sols et des Eaux, Aix-en-Provence, France, E-mail: Zuzana.Fekiacova@aix.inra.fr
[B]Laboratoire de Sciences de la Terre, Ecole Normale Supérieure de Lyon, UCB Lyon 1, France, E-mail: spichat@ens-lyon.fr

Abstract

Soil preservation for the future is one of the major objectives of the present-day research. Variations of the isotopic signatures of major elements recorded in soils can bring information about the nature and behaviour of major soil constituents in response to climatic changes and human-induced pressures. We have analysed variations of the Fe isotopic compositions in soils with the objective of (i) investigating mechanisms that control soil development and (ii) examining the impact of various factors, such as climate, topography and intensive human activity on the soil evolution. Our results show significant vertical variations of Fe isotopic composition within redoximorphic soils (Luvisol-Gleysol and Gleysol) but only limited variations within the well-drained Cambisol. No simple relationship can be established between the Fe isotopes variations and pedogenic Fe transfer. Although redox-controlled Fe-mobilization appears to be the main process, additional mechanisms (i.e., primary mineral alteration or other in situ transformations) and factors (i.e. topography) need to be examined, in order to decipher and interpret the Fe isotopes record in soils.

Key Words

Soil conservation, iron isotopes, agriculture, climate

Introduction

Soil durability is continually tested by ongoing climatic changes and by human-induced pressures. In order to insure soil preservation for the future, understanding mechanisms and processes that control soil evolution is among the major scientific challenges. In addition to frequently used methods, isotopes of major elements represent a powerful tool for studying soil processes and can bring helpful information about the nature and dynamics of major soil constituents and their behaviour in response to climatic and anthropogenic changes. Iron is the fourth most abundant element on Earth, it is present in all geological and biological materials and plays an important role in soil structure. Studies of the Fe isotopic compositions of various materials have been made possible by recent progress in analytical techniques, such as multi-collector inductively coupled-plasma mass spectrometry (MC-ICP-MS) (e.g., Beard *et al.,* 2003; Albarède and Beard, 2004; Dauphas and Rouxel, 2006). Thus, investigation of the Fe isotopes variations in soils can help shed light on the mechanisms that play dominant roles in the behaviour of soil constituents in response to various human- and climate-induced pressures.

Fe isotopes variations in redoximorphic soils

Among the most important mechanisms that control Fe isotope fractionation in soils are: modification of the oxidation-reduction state, complexation with organic matter, dissolution and precipitation of Fe minerals. Previous studies demonstrated that there exist systematic variations of Fe isotopic compositions in soils (e.g., Fantle and DePaolo, 2004; Thompson *et al.,* 2007; Wiederhold *et al.,* 2007a; Wiederhold *et al.,* 2007b; Johnson *et al.,* 2008). However, the relationship between the Fe isotopes variations and pedogenic Fe-translocation remains unclear and is complicated by further biochemical mechanisms such as plant uptake and production, and transfer and biodegradation of organo-metallic complexes.

Redox-related transformations and Fe transfer are important processes in redoximorphic soils. We have studied vertical and lateral variations of the Fe isotopic composition of the soils affected (i) by seasonal modifications of water-saturation conditions and (ii) by human activity (intensive agriculture). The aim of our work is to shed light on the dominant mechanisms that control the evolution of redoximorphic soils and to examine the impact of various factors, such as climate, topography and intensive human activity on soil evolution.

Sampling area

Soil samples were collected in the Kervidy-Naizin catchment basin located in Brittany, western France. The sampling area belongs to the Environmental Research Observatory AgrHyS (ERO) designed to study the response time of hydro-chemical fluxes to the evolution of agro-hydrosystems (ORE AgrHyS, 2007a). The region is characterised by oceanic, humid and temperate climate with mean annual precipitation of 909 mm and monthly mean temperature ranges from 5.4°C to 17.4°C (ORE AgrHyS, 2007b). The soils developed on weathered upper Proterozoic schists. They are locally dominated by silt, clay or sandstone materials and contain a large number of secondary minerals such as Fe-oxides and oxi-hydroxides (hematite, goethite), Mn-oxides, illite, smectite, kaolinite, etc. Soil evolution in the area was influenced mainly by climate with an important short-term variability and by human activity through an intensive agriculture.

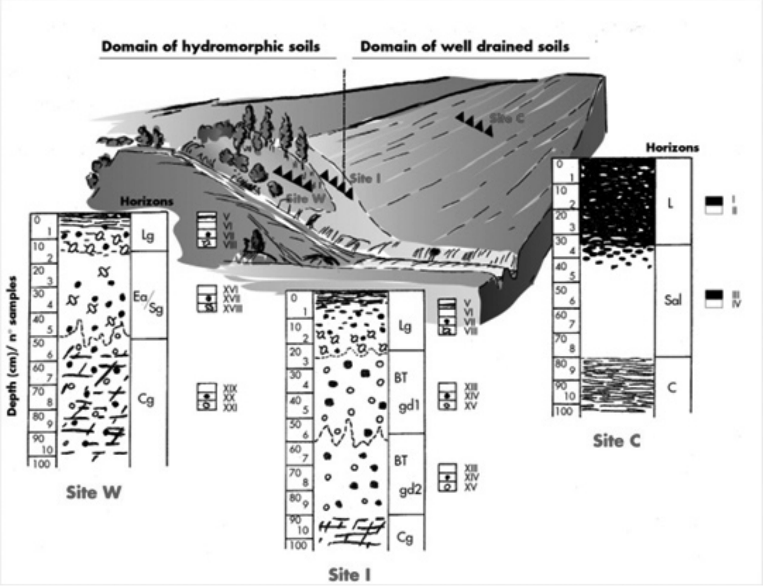

Figure 1. Drawing of the sampling area (from Trolard and Bourrié, 2008).

Three dominant soil types were described in the Kervidy-Naizin catchment site (e.g., Jaffrezic, 1997):
(i) Cambisol located on the hill slope (site C, Figure 1) is used as cropland and is characterised by dominantly well-drained, oxic conditions. It consists of three horizons: Ap-B-C.
(ii) Luvisol-Gleysol located in the transition zone (wasteland) between the well-drained cropland and poorly-drained lowermost part of the landscape (site I, Figure 1). The soil consists of a horizon sequence Apg-Btg-Cg and contains redoximorphic features such as mottling and rust accumulations in root spaces.
(iii) Gleysol located in the bottomland (wasteland) (site W, Figure 1), at proximity to a small river. It is characterised by poorly-drained conditions, shallow water table and waterlogged environment. The soil consists of a horizon sequence Apg-E-Cg and is characterised by typical redoximorphic features that have developed due to an excess of water of topographical origin.

Samples and methods

We collected samples using an auger from profiles in the Cambisol (cropland on the hill slope), in the Luvisol-Gleysol (transition zone) and in the Gleysol (downslope redoximorphic zone). One sample was taken every 10 cm in order to obtain high spatial vertical resolution. An aliquot of each sample was dried and ground into fine powder using an agate mortar. For the isotopic measurements, approximately 300 mg of sample powder was treated with 30% H_2O_2 in order to eliminate organic matter and then dissolved using a mixture of concentrated HF-HNO_3 acids, at high temperature (~130°C). Iron and other trace metals (Cu, Zn) were separated and further purified using ion exchange resins (AG MP1, AG1X8). Iron concentrations were analysed using ICP-AES (Icap 6300) at the Laboratoire de Sciences de la Terre, Ecole Normale Supérieure de Lyon, France. Iron isotopic compositions were analysed using high-resolution MC-ICP-MS Nu1700 (national instrument at the Laboratoire de Sciences de la Terre, Ecole Normale Supérieure de Lyon, France). A standard-bracketing approach was used to correct for instrumental mass bias and isotope data are reported in delta notation: $\delta^{56}Fe = [(^{56}Fe/^{54}Fe)_{sample}/(^{56}Fe/^{54}Fe)_{IRMM\text{-}014} - 1]*10^3$ (‰).

Results and discussion

The iron concentration remains constant within the Cambisol profile (hill slope), indicating no significant vertical transfer of iron with depth (Figure 2 a). Moreover, the Fe isotopic compositions are uniform, within the analytical error, but we observe a slight increase in $\delta^{56}Fe$ in the B-horizon. In contrast, the Luvisol-Gleysol (transition zone) and Gleysol (bottomland) show significant variations of the Fe concentrations and Fe isotopic compositions with depth (Figure 2 b, c). The surface horizons (Apg) of both the Luvisol-Gleysol and Gleysol are depleted in Fe compared to the surface horizon of the Cambisol and the Fe content increases with depth. The $\delta^{56}Fe$ ranges vertically from -0.1 to +0.2 ‰ within the Luvisol-Gleysol (Figure 2 b) and from -0.2 to 0.2 ‰

within in the Gleysol (Figure 2 c).

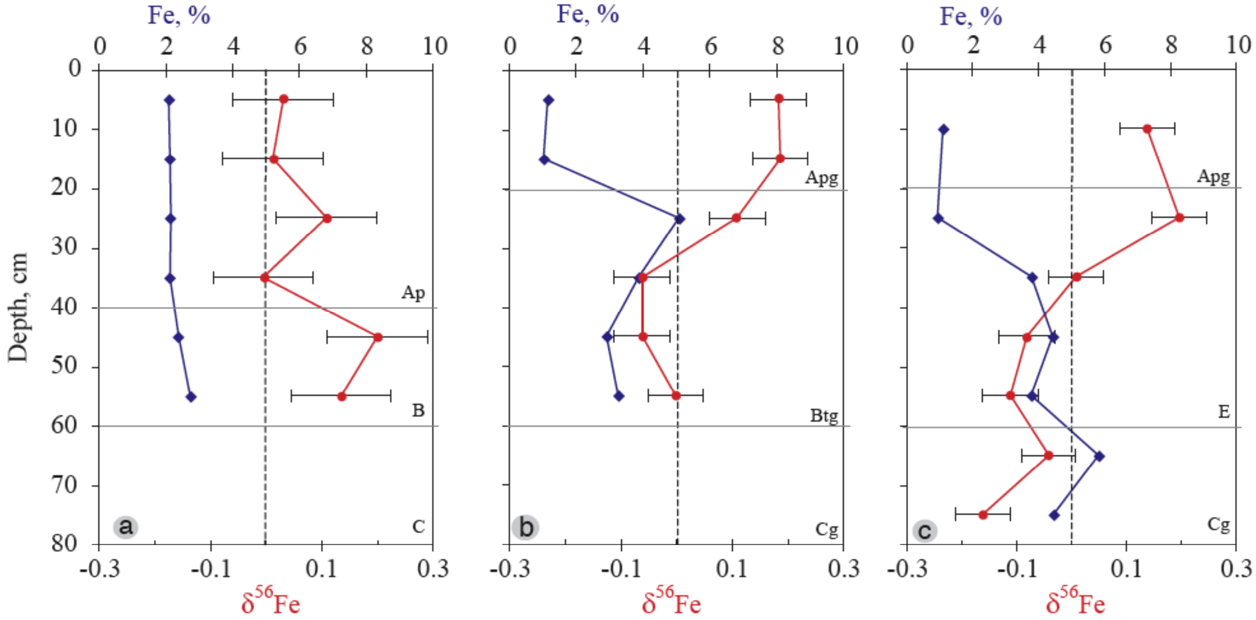

Figure 2. Vertical variations of the Fe concentration (blue diamonds) and Fe isotopic composition (red circles) in the three soils: (a) Cambisol (hill slope), (b) Luvisol-Gleysol (transition zone) and (c) Gleysol (bottomland). Error bars indicate 2σ for the Fe isotopic analyses and range from 0.05 to 0.09 ‰. Grey horizontal lines with abbreviations indicate horizon limits.

Uniform Fe concentrations and Fe isotopic compositions were previously described by Wiederhold *et al.* (2007a) in a freely drained Cambisol and indicated that Fe remained immobile due to dominant oxic conditions in well-aerated soils. Our results are consistent with the absence of vertical Fe transfer in the Cambisol (Figure 2 a). However, we observe a slight increase of δ^{56}Fe in the B-horizon, which suggests enrichment in heavy Fe isotopes at depth. This enrichment is likely to be linked to the in situ mineral transformation, rather than to Fe mobilization.

Significant vertical variations in the Fe concentrations and Fe isotopic compositions observed in the Luvisol-Gleysol and Gleysol (Figure 2 b, c) are consistent with a soil development influenced by important seasonal variations of the water regime, and consequently, by modifications of the oxidation-reduction conditions. The lowest Fe concentrations observed in the surface horizons (Apg) are associated with the highest δ^{56}Fe within both, Luvisol-Gleysol and Gleysol profiles. In waterlogged environment, increased accumulation of organic matter and weathering of clay minerals lead to remobilization of Fe as organo-metallic complexes or dissolved Fe^{II} (e. g., Fritsch *et al.,* 2009). Light Fe isotopes preferentially released during bacterially mediated dissolution in reducing conditions or during ligand-controlled dissolution are transferred either vertically or laterally, by the excess runoff water. Our results, i.e. high δ^{56}Fe in the topsoil and low δ^{56}Fe in depth, are consistent with the preferential release of the light Fe isotopes during Fe-oxi-hydroxides dissolution and depletion of light Fe in the surface horizons of the waterlogged soils. Iron content increases gradually with depth indicating accumulation of the Fe removed from the upper horizons. At the same time, the δ^{56}Fe decreases with depth and show progressive enrichment of deeper horizons in light Fe isotopes. Furthermore, we observe several particularities in the soil affected by waterlogging. In the Luvisol-Gleysol (Figure 2 b), there is a peak of Fe concentration on the top of the Btg horizon corresponding to the seasonal water table-level variations. However, the lowest δ^{56}Fe does not correspond to the maximum Fe content but is located deeper in the soil profile, suggesting that processes other than Fe translocation are involved in the Fe isotopes fractionation within this soil.

In addition, in the Gleysol we observe development of the eluvial (E) horizon, which should show depletion in Fe because of Fe-leaching under reducing conditions. Instead we observe a gradual increase of Fe content with depth associated with a decrease of δ^{56}Fe. The light Fe accumulation within E horizon might indicate temporary oxidizing conditions leading to Fe fixation (lateral input from the uphill and Fe accumulation).

Conclusions

Vertical and lateral variations of the Fe isotopic composition (i) record spatial and temporal changes of soil conditions and (ii) reflect dominant mechanisms that play a role in the soil evolution. Thus, the Fe isotope studies could bring helpful information for understanding the soil processes. However, mechanisms that fractionate Fe isotopes in soils are complex (modification of redox conditions, complexation, plant uptake, etc.) and the relationship between Fe isotope fractionation and pedogenic Fe transfer is not straightforward. In order to interpret the Fe isotope record in soils, we need to decipher small-scale variations (e. g. sampling and analyses of individual soil minerals and redoximorphic features), and particularly those related to in situ mineral transformations. Also, additional comprehensive investigations are necessary on soils developed under different conditions. Alternatively, combined studies using isotopes of other metallic elements with geochemical behaviour differing from that of Fe (Zn or Cu) should help discriminate between dominant soil processes.

Acknowledgments

We thank the Institut National de la Recherche Agronomique, Rennes (INRA, UMR SAS, Rennes) and the ERO AgrHyS for technical support during the soil sampling.

References

Albarède F, Beard BL (2004) Analytical methods for non-traditional isotopes. *Reviews in Mineralogy and Geochemistry* **55**, 113-152.

Beard BL, Johnson CM, Skulan JL, Nealson KH, Cox L, Sun H (2003) Application of Fe isotopes to tracing the geochemical and biological cycling of Fe. *Chemical Geology* **195**, 87-117.

Dauphas N, Rouxel O (2006) Mass spectrometry and natural variations of iron isotopes. *Mass Spectrometry Reviews* **25**, 515-550.

Fantle MS, DePaolo DJ (2004) Iron isotopic fractionation during continental weathering. *Earth and Planetary Science Letters* **228**, 547-562.

Fritsch E, Allard Th, Benedetti MF, Bardy M, do Nascimento NR, Li Y, Calas G (2009) Organic complexation and translocation of ferric iron in podzols of Negro River watershed. Separation of secondary Fe species from Al species. *Geochimica et Cosmochimica Acta* **73**, 1813-1825.

Jaffrezic A (1997) Géochimie des éléments métalliques, des nitrates et du carbone organique dissous dans les eaux et les sols hydromorphes. Thèse de Doctorat, Géosciences Rennes, pp 296.

Johnson CM, Beard BL, Roden EE (2008) The iron isotope fingerprints of redox and biogeochemical cycling in modern and ancient earth. *Annual Reviews of Earth and Planetary Science Letters* **36**, 457-493.

ORE AgrHyS (2007a) www.inra.fr/ore_agrhys_eng/presentation/objectifs.

ORE AgrHyS (2007b) http://www.inra.fr/ore_agrhys/presentation/site_et_equipement/site_de_kervidy_naizin/climate_and_hydrology.

Thompson A, Ruiz J, Chadwick OA, Titus M, Chorover J (2007) Rayleigh fractionation of iron isotopes during pedogenesis along a climatic sequence of Hawwaiian basalts. *Chemical Geology* **238**, 72-83.

Trolard F, Bourrié G (2008) Contamination des sols et des formations superficielles, In ‘Les formations superficielles‘. (Eds Y Dewolf Y, G Bourrié), pp. 767-774. (Ellipses Edition: Paris).

Wiederhold JG, Teutsch N, Kraemer M, Halliday AN, Kretzschmar R (2007a) Iron isotope fractionation in oxic soils by mineral weathering and podzolization. *Geochimica et Cosmochimica Acta* **71**, 5821-5833.

Wiederhold JG, Teutsch N, Kraemer M, Halliday AN, Kretzschmar R (2007b) Iron isotope fractionation during pedogenesis in redoximorphic soils. *Soil Science Society of America Journal* **71**, 1840-1850.

Systematization of the topsoil fabrics in soils of the arid lands in northwest of central Asia

Marina Lebedeva[A], Maria Gerasimova [B] and Dmitry Golovanov [B]

[A]V.V. Dokuchaev Soil Institute, Moscow; Russia, Email m_verba@mail.ru
[B]Faculty of Geography, Lomonosov Moscow State University, Moscow; Russia, Email etingof@glasnet.ru, dm_golovanov@mail.ru

Abstract

The micromorphological data concerning aridic soils are far from being numerous; therefore, the information presented contributes to the development of pedogenetic ideas and characterization of diagnostic horizons and genetic properties in the substantive-genetic classification systems. The diversity, functioning and resilience of aridic soils are basically determined by the properties of their topsoils, which are regarded as recent dynamic formations opposite to the subsoils mostly formed under different paleoclimatic environment; topsoil properties are more important for soil classification. Each of two upper horizons in the new Russian system of soil classification (the light-humus and xero-humus) has the same micromorphological features in different soils; however, in a sequence of soils, some individual micromorphological properties were revealed that indicate the increasing aridity. The micromorphological properties of the topsoils make it possible to identify the mechanisms of some phenomena: aeolian deposition, structural re-arrangement, dynamics of secondary carbonates, and cryptosolonetzic manifestations.

Key Words

Micromorphological analysis, genesis, classification of aridic soils.

Introduction

Micromorphology of aridic soils has been so far examined insufficiently because of problems with preparing thin sections of their friable and brittle topsoils. Nonetheless, most common soils of the USSR deserts and semideserts were described (Minashina 1966; Romashkevich and Gerasimova 1977; Gubin 1984; Gerasimova 2008). In other countries, the studies of desert soil pedofeatures started later (Figueira and Stoops 1983; Mills *et al.* 2008; Williams *et al.* 2008). As for classification purposes, the micromorphological properties of aridic soils have been thoroughly characterized by Allen (1985) in a special issue of Proceedings of American Soil Science Society. The objective of our research is to categorize the topsoil fabrics inherent to aridic soils in Russia and adjacent countries in compliance with the diagnostic elements of substantive classification systems.

Materials and methods

1. Soils. Objects of research are diagnostic horizons and pedofeatures inherent to virgin arid soils derived from non-saline parent materials. Under consideration is a wide spectrum of arid soils developed under conditions of increasing aridity in Russia, Uzbekistan. Particular fabrics of Aridic Calcisols and Yermic Regosols as exemplified by soils of Mongolia were discussed earlier (Golovanov 2005).

2. Diagnostic horizons and diagnostic (genetic) properties have similar functions in the new Russian system and in the WRB system. In different versions of both systems their taxonomic significance slightly changed, whereas the definitions remained the same. *Diagnostic horizons* in the Russian system comprise: *light-humus, eluvial-solonetzic* and *xero-humus* horizons.

The *light-humus (AJ)* horizon occurs in brown aridic (Aridic Calcisols), part of Solonetzes and Gypsic Kastanozems in Russia; its central image was derived from the Siltic Calcisols of Central Asia. *Eluvial-solonetzic (SEL)* horizon is regarded as indicative of degrading Solonetzes.

In the former version of the Russian classification system (RCS) (2004), the *xero-humus*, or *crusty-subcrusty horizon* (AKL) was introduced. It was defined as a paragenetic association of thin subhorizons: porous crust and platy ‘subcrust’. In Russia, it was identified only in the brown semidesert soils (Gypsic Calcisols), where it was discontinuous, rather weakly expressed, or its thickness was insufficient to fit criteria for a diagnostic horizon. That’s why, its diagnostic significance was reduced in the version of RCS-2008, and it was qualified for a diagnostic property, or microprofile – [akl]. The crusty subhorizon is rather compact although porous, brownish light gray, effervescent, its depth does not exceed 2-4 cm. The subcrusty subhorizon is loose, light in color, and has a lenticular-platy structure; both subhorizons are salt-free.

Irrespectively of the taxonomic significance, the described formation has much in common with the *yermic horizon* in the WRB system. By definition, the yermic horizon has the same ingredients – the porous crust with

1 – 6 August 2010, Brisbane, Australia. Published on DVD.

stony inclusions of desert pavement underlain by a fragile platy layer (WRB-1998), while in WRB-2006 this sequence was indicated as being not obligatory. In both WRB definitions, aeolian phenomena and aridic properties are included in the definition.

In the Russian system, the elements of aridic environments and soils are recorded at the level of diagnostic properties, which is justified by the geographic reasons. The following diagnostic properties are specified: takyric (kt), pendent-carbonate (ic), gypsic (cs), saline (s); aeolian-accumulative (ael).

Sampling from soil pits was done at small intervals to characterize the subhorizons. Thin sections were prepared by M.A. Lebedev in the laboratory of Dokuchaev Soil Institute; synthetic resins were used for the impregnation procedure under vacuum, which provides the preservation of crystalline pedofeatures.

Results

Light-humus AJ horizon is characterized based on the data for Siltic Calcisols, Gypsic Kastanozems and Gypsic Calcisols soils, moderately Deep Mollic Solonetzes. The topsoil of a typical Siltic Calcisols (Uzbekistan, piedmont plain of the Turkestanskii Ridge) is light brown, weakly compact, with moderate crumb structure, many fine roots and faunal chambers. It has the following set of micromorphological properties: high pedality and porosity, carbonate-clay plasma; mostly rounded aggregates, 0.1-0.2 mm in diameter, the largest are faunal castings; 'loessic microaggregation' (according to Minashina 1966) with aggregates 0.02-0.05 mm in size, is recognized in some parts of thin sections. Plasma is weakly anisotropic, b-fabric is crystallitic. Packing voids with clear walls are predominant among pores. Fine organic residues including root remains in voids are few, as the fine-dispersed organic matter. These characteristics of serozems are typical for the upper horizons of soils on loess and they may be regarded as composing a 'central image', or micromorphotype (Gerasimova 2003) of the light-humus horizon. The transformation of parent rock (loess) fabric into that of the AJ horizon is due to soil fauna, effects of roots and microbial transformation of organic residues during the short period of spring rains.

The light-humus horizon of Gypsic Kastanozem (Gerasimova *et al.* 1996) has a dark color as compared to AJ horizon in other soils, the strongest crumb structure with a higher proportion of biogenic aggregates, the most abundant root residues; it may be even partially free of carbonates. The light-humus horizon was also studied in moderately deep Deep Mollic Solonetzes of Dzhanybek experimental station, northwest of the Caspian Lowland (Lebedeva and Gerasimova 2009). It was found out recently that properties of AJ horizon in this area are not stable because of changing microrelief and activity of burrowing mammals bringing calcareous and saline material to the surface. Therefore, they range from those in light-colored and highly calcareous variants to rather dark, structured and leached ones. In the moderately Deep Mollic Solonetzes, the AJ horizon merges into the eluvial-solonetzic (SEL) one followed by the solonetzic (natric) subsoil. The SEL horizon displays micromorphological evidences of clay and humus depletion in the uppermost parts of columnar peds.

In terms of micromorphology, the AJ horizon has the following properties: brown disperse humus, predominance of moderately decomposed plant residues, specific microstructures: rounded aggregates arranged in fine plates. Admixtures of apedal micrite-enriched material were also found; they testify to the translocation of subsoil substrate into the AJ horizon (Lebedeva and Gerasimova 2009). Episalic Solonetzes (Yermic) were also studied in microcatenas in Dzhanybek experimental station; they are confined to the driest microhighs almost without vegetation, and their surface is dissected by fissures into small polygons. They differ of other Solonetzes by shallow topsoil above the solonetzic horizon composed of crusty and subcrusty subhorizons, 2 to 4 cm thick each. The lower part of the porous crust is gradually acquiring a horizontal stratification and merges in the subcrusty subhorizon. Presumably, this stratification may be maintained by freezing/thawing cycles. No features of SEL horizon were identified. In thin sections, the crusty K subhorizon is homogeneous and compact, has silty-plasmic elementary fabric, isolated isometric pores, including the rounded ones, mostly vesicular. The subcrusty L subhorizon is of the same texture, but has elongated or horizontal voids, partially fine planes.Gypsic Calcisols and Yermic Calcisols have their AJ horizons basically corresponding to its central image (Gubin 1984), and with inclusions of morphons of the crusty-subcrusty microprofile (akl). The latter may be either complete – composed of both layers, or represented by one of its ingredients. Our observations in the Caspian Lowland have shown that the proportion between the AJ and akl morphons depends on texture: the lighter the texture, the lower is the share of akl morphons. In other words, the akl morphons are rather confined to loamy plots with sparse vegetation, while under the bunch grasses they are replaced by the AJ morphons.

Micromorphology of Gypsic Calcisols in the southern Caspian Lowland was studied by one of the authors in the near-coastal hummocky area. The light-humus horizon has a c/f related distribution close to gefuric: sand-size grains are interconnected by clay braces or coatings; packing voids prevail, plasma is carbonate-clay with clear micrite concentrations, very few plant residues are weakly decomposed, and black tissue residues occur as well;

faunal casts are very few. Vesicular pores were recorded only once in an AJ of heavier texture. Grain coatings are laminated: the inner layers are clay, while the outer ones are carbonate-impregnated. There were no evidences of platy microstructure, which may be explained by light texture.

The xero-humus AKL horizon (or akl property) is inherent to desert soils. In the sequence of soils with increasing aridity up to the Yermic Regosols of Mongolia, the akl property is gradually replaced by the AKL horizon, as the latter is described in (Lebedeva *et al.* 2009). Moreover, the depth of the xero-humus horizon increases and its differentiation into crusty and subcrusty subhorizons becomes more distinct. The Yermic Calcisols of Uzbekistan is affected by current aeolian accumulation of loessic weakly calcareous material with inclusions of rounded aggregates. The crusty subhorizon abounds in voids – vesicular and packing voids among weakly separated aggregates; the void system is basically open. The clay plasma is impregnated by carbonates, although there are few fine and discontinuous grain coatings. The skeleton grains are weakly sorted, sand- and silt-sized, few of them are weakly rounded, they produce a porphyric c/f ratio. The subcrusty subhorizon has a horizontal stratification – fine platy or scaly-platy microstructure with horizontal packing voids; in some soils, weak rounded aggregates included in the plates may be recognized; the impregnation by carbonates is low in some parts, no evidence of clay plasma mobility, few fresh castings of woodlouses.

Aeolian accumulation is an additional mechanism contributing to the formation of xero-humus horizon, or overlain upon it. Aeolian aggregates are easily identified in the in-blown silt by their shape, distinct boundaries, higher clay content and c/f ratio different of that of enclosing material. Such rounded aeolian aggregates participate in the fabric of the AKL horizon; they are more distinct in the subcrusty ingredient, where they form primary peds in platy microstructures. In the crusty ingredient, they coalesce; packing voids between them may be mitigated by the infillings. Thus, major elements of the AKL horizon being well expressed macro- and micromorphologically in the Yermic Calcisols of Uzbekistan are complemented by aeolian phenomena (*ael* property).

Table 1. Diagnostic elements of aridic topsoils identified at a micromorphological level.

Soil (WRB-2006)	Diagnostic horizons 1)				Genetic features 2)					
	AJ	*AKL*		*Desert pavemen*	*[akl]*	*ael*	*ic*	*dc*	*s*	*cs*
		K	L							
Siltic Calcisols	+2)									
Gypsic Kastanozems	+									
Deep Mollic Solonetz	+									
Gypsic Calcisols	(+)	+		(+)	+	(+)				(+)
Episalic Solonetz (Yermic)		+	+		+	(+)				
Aridic Calcisols		+	+	(+)		+	+	(+)		(+)
Yermic Calcisols		+	+	+		+		(+)		(+)
Yermic Regosols		+	+	+		+		+	+	(+)

1) Symbols for horizons: *AJ* – light-humus; *AKL* – xero-humus, *K* – crusty and *L* –subcrusty subhorizons.

2) Genetic features: microprofile - *[akl]*; aeolian-accumulative – *ael;* dispersed-carbonate – *dc;* pendant-carbonate – *ic;* saline – *s;* gypsum-containing – *cs.*

3) Conventions: + diagnostic horizon or genetic feature is present; (+) – horizon or feature is optionally manifested; empty column – horizon or feature has no manifestation.

Conclusion

In a soil sequence with increasing aridity, the diagnostic horizons and properties are combined in a regular way corresponding to the changes in soil formation conditions and soil-forming processes; in the same time, the sequence is in good agreement with diagnostic elements of substantive classification systems (Table 1). Thus, the soils studied form two groups: with a distinct light-humus AJ horizon, and with a xero-humus AKL horizon composed of K and L subhorizons; these groups correspond to two types of pedogenesis, respectively. The former is the dry-steppe humus-accumulative type (minimal variant), the latter – the desertic "crust formation" manifested in the structural re-arrangement of the solid phase. With this approach, Gypsic Calcisols soils may be regarded as intergrades between steppe and desert pedogenesis types; Episalic Solonetz (Yermic), despite their occurrence in the dry steppe, seem to be closer to the desert type unlike Deep Mollic Solonetz.

References

Allen BL (1985). Micromorphology of Aridisols. In 'Soil Micromorphology and Soil Classification', (Eds LA

Douglas, ML Thompson). pp. 197-216. (SSSA Special Publication 15: Madison)
Classification and Diagnostics of Soils of Russia (2004) (Eds L Shishov, V Tonkonogov, I Lebedeva M Gerasimova). (Oecumene Publ.: Smolensk). (in Russian)
Field Guide for Russian Soils (2008) (DokuchaevSoil Inst.: Moscow) (in Russian)
Figueira H, Stoops G (1983) Application of micromorphometric techniques to the experimental study of vesicular layer formation. *Pedologie* **33**, 77 - 92.
Gerasimova MI, Gubin SV, Shoba SA (1996) 'Soils of Russia and Adjacent Countries: Geography and Micromorphology'. (Wageningen: Moscow).
Gerasimova MI (2003) Higher levels of description – approaches to the micromorphological characterisation of Russian soils. *Catena* special issue 319-339.
Gerasimova MI, Lebedeva MP (2008). Contribution of Micromorphology to Classification of Aridic Soils. *Catena* 197-216.
Golovanov DL, Lebedeva (Verba) MP, Dorokhova MF, Slobodkin AI (2005) Micromorphological and Microbiological Characteristics of Elementary Pedogenetic Processes in Desert Soils of Mongolia. *Eurasian Soil Scienc* **5**, 1290-1300.
Gubin SV (1984) Micromorphological diagnostics of brown and grey-brown soils of northern Ust'-Urt. In 'Nature, Soils and Reclamation of the Ust'-Urt desert'. pp. 127-134. (Pushchino) (in Russian)
Lebedeva (Verba) MP, Golovanov DL, Inozemtsev SA (2009) Microfabrics of Desert Soils of Mongolia. *Eurasian Soil Science* **42**, 1204-1217.
Mills A, Fox S, Poch RM (2008) Micromorphology of surface crusts in the Knevrsvlakte, South Afrika In 'Soil micromorphology. Micro-investigation on the Earth's critical zone'. (Chengdu: China).

Minashina NG (1966) Micromorphology of loess, serozems, hei-loo-too and some problems of their paleogenesis. In 'Micromorphological Method in the Studies of Soil Genesis'. pp. 76-93. (Nauka Publ.: Moscow) (in Russian)
Romashkevich AI, Gerasimova MI (1977) Major aspects of micromorphology of arid soils in the USSR. In 'Aridic Soils, their Genesis, Geochemistry, Reclamation'. pp. 239-254. (Moscow) (in Russian).
Stoops G (2003) 'Guidelines For Analysis and description of soil and regolith thin sections'. (Soil Science Society of America: Madison)
World Reference Base for Soil Resources (1998) 'IUSS/ISRIC/FAO, Technical paper, iss. **84'**. (FAO: Rome).
World Reference Base for soil Resources (2006) 'A framework for international classification, correlation and communication'. IUSS/ISRIC/FAO, Technical paper, iss. **103**, (FAO: Rome).
Williams AJ, Buck BJ, Soukup D (2008) Models of biological soil crust development, Mojave Desert, USA. In 'Soil micromorphology. Micro-investigation on the Erth's critical zone'. Conference Abstracts. (Chengdu: China).

The story of O: The dominance of organisms as a soil-forming factor from an integrated geologic perspective and modern field and experimental studies

Stephen T Hasiotis[A] & Alan F Halfen[B]

[A]Department of Geology, University of Kansas, 1475 Jayhawk Blvd., Rm. 120, Lawrence, Kansas, USA, Email hasiotis@ku.edu;
[B]Department of Geography, University of Kansas, 1475 Jayhawk Blvd., Rm. 213, Lawrence, Kansas, USA, Email afhalfen@ku.edu

Abstract

Geological and neoichnological evidence demonstrates the dominance of organisms through their life histories and behaviors as a major soil-forming factor since the Late Ordovician (~460 million years of Earth history). Continental deposits since that time preserve an abundance of paleosols that contain a great variety of trace fossils (i.e., krotovina) of microbes, plants, and animals. Trace fossils produced by animals preserve the burrows, nests, tracks, and trails that are intimately associated with a range of sedimentary and pedogenic structures indicative of immature to mature soil development in fluvial, alluvial, lacustrine, and eolian depositional systems. Neoichnological studies of organisms—field and experimental research on their tracemaking activity—in terrestrial environments confirm their tremendous influence on sediment mixing, soil formation, and soil turnover. Burrowing animals displace sediments by diffusive (mm-scale particle movement) and advective (cm- to m-scale particle movement) methods via a combination of carrying, pulling, pushing, raking, breaking or cutting, and forcing that result in traces. These traces have distinct three-dimensional shapes and volumes that are repeated in space and time, resulting in soil formation. Many of these traces have changed little through 100's of millions of years of evolution based on comparisons between modern and ancient animal traces.

Key Words

Ichnofossils, ichnology, nests, paleosols, bioturbation, biomantle

Introduction

Organisms, particularly animals, have been and currently are one of the most important of all the soil-forming factors (Figure 1) for most the Phanerozoic, at least since the Late Ordovician (~460 million years ago) (e.g., Wallwork, 1970; Hole, 1981; Hasiotis, 2003, 2007). Research of modern soils and soil biota shows that animals are extremely effective at mixing sediment and soils within the subsurface, acting to help build and destroy pedogenic structures and voids, and playing a major role in nutrient cycling via the work of detrivores and saprovores (e.g., Darwin, 1881; Wallwork, 1970; Hole, 1981; Halfen and Hasiotis, this volume). Recent research on continental deposits shows that trace fossils—the study of tracks, trails, burrows, nests, rooting patterns, borings, and biolaminates—abound in immature to very mature paleosols that can be attributed to a variety of microbial communities, plants, and animals, based on the comparisons of three-dimensional (3D) morphology to modern burrows (krotovina) and their tracemakers (e.g., Hasiotis, 2003, 2007, and references therein).

The purpose of this paper is to summarize the significance of animal bioturbation as a major soil-forming factor and ecosystem maintenance through the mixing of sediment and formation of soils, soil turnover, regulation and modulation of ecosystems as ecosystem engineers, and a major contributor to the evolution of terrestrial ecosystems since the Ordovician. The relationship between the effects of modern animals and that of their work preserved in the geologic record is demonstrated through the perspective of neoichnological and geological research. Neoichnology—the study of traces produced by modern organisms—provides the basis for understanding traces that result from a variety of behaviours from different organisms, so that those 3D structures produced can be related to: (1) particular behavior(s); (2) the physicochemical conditions—the effects of climate, topography, parent material—under which they were produced; (3) the time it took to produce the structure and how long it was used; and (4) the groundwater profile and greater hydrologic system of the landscape in which they occur (e.g., Hasiotis, 2007). Neoichnological field and laboratory research provides the detailed information that allow trace fossils in the geological record to be used as proxies for: 1) biodiversity of soil biotic communities not recorded by body fossils in that strata or geologic time interval; 2) soil moisture and water table level and it seasonal fluctuations; 3) early stages in soil formation (Entisols, Inceptisols) for which there are few abiotic pedogenic features; and 4) climatic setting relating to the amount of precipitation or through by analogy of occurrence in modern settings and its average temperature and precipitation.

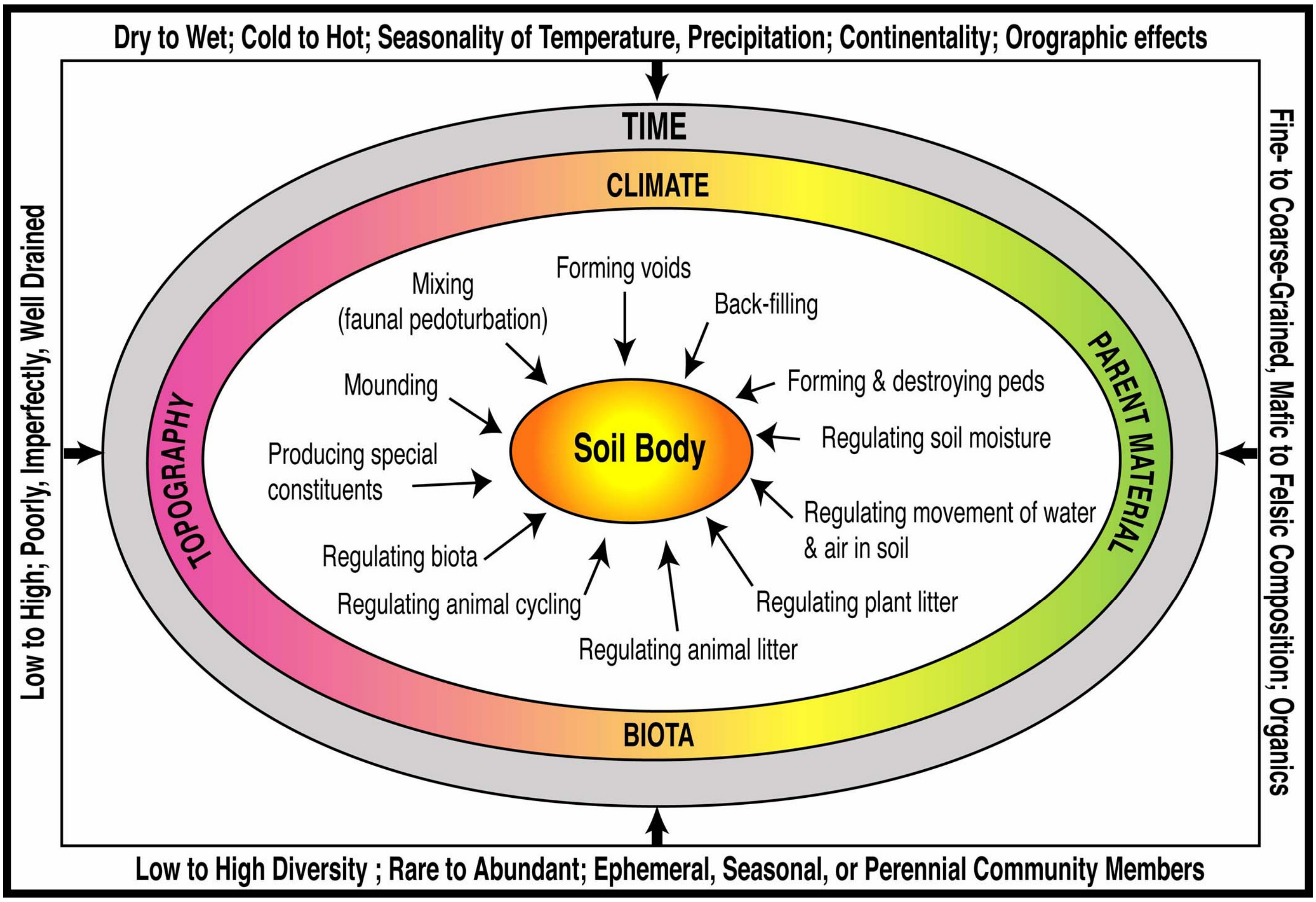

Figure 1. The effects of the five major soil-forming factors on the soil body (modified from Hole, 1981; Hasiotis, 2007). Note that at any one time, the biota, climate, topography, and parent material will vary. Time is also the only variable that proceeds at a relatively constant rate and is predictable when reconstructing deep time Earth history.

Linking the Work of Animals to Soil Formation

The presence of animals categorized as geophiles and geobionts in soils (Figure 2) has been defined based on the amount of time and portion of their life cycle spent within subsurface: transient, temporary, periodic, permanent, and accidental—listed in order from the least amount of time and effect on the subsurface to the most time and effect (Wallwork, 1970; Hole, 1981; Hasiotis, 2007). The impact of animals on sediments and soils is through the work of adults and juveniles (=nymph [incomplete metamorphosis], larva [complete metamorphosis], or juvenile) of invertebrates and vertebrates. In general, the more time spent within the subsurface, the greater degree and depth of bioturbation and mixing and, therefore, the greater effect on soil formation. Bioturbation, which produces burrows and nests, produces macrochannels and macropores that will impact the rate and degree of such soil processes as translocation, transformation, and the additions and losses of constituents to soils (Hole, 1981; Hasiotis, 2003, 2007). Bioturbation, in combination with the abiotic effects of shrink-swell clays, cryoturbation, haloturbation, and gravitational draining and movement of material, is considered pedoturbation. The role of bioturbation is significant to pedoturbation in that the work of animals produces the channels and voids in which abiotic pedoturbation can take place, as well as allowing for greater exchange between the soil atmosphere and Earths atmosphere, greater infiltration of precipitation and overland flow, and greater incorporation of organic matter into the subsurface (Wallwork, 1970; Hole, 1981; Hasiotis, 2007).

Overall, the rate and depth of work conducted by animals is much greater than that of plants via root penetration and tree throw. Although plants contribute the vast majority of organic matter and that their organic acids assist in the breakdown of lithic constituents, their roots displace very little material in comparison to the material displaced upward and downward by animals (e.g., Hole, 1981; Hasiotis, 2003, 2007; Halfen and Hasiotis, this volume; and references therein). The burrows and nests of animals can penetrate to ~100 m below the surface, and modify over 1 km^3 to as much as ~10 km^3 for an individual nest of some social insects (Hasiotis, 2003, 2007).

Animals displace sediments by diffusive (mm-scale particle movement) and advective (cm- to m-scale particle movement) methods via a combination of carrying, pulling, pushing, raking, breaking or cutting, and forcing that result in traces (Hasiotis, 2003, 2007; Halfen and Hasiotis, this volume; and references cited within these works). The depth of penetration and amount of mixing will also depend on the amount of soil moisture in the vadose zone and the position of the phreatic zone (e.g., Wallwork, 1970; Hasiotis, 2007). Through 10^1 to 10^6 years this work on a landscape will result in vegetable moulds, biomantles, and features that define soil orders (e.g., Darwin, 1881; Hole, 1981; Johnson, 1981; Hasiotis, 2007).

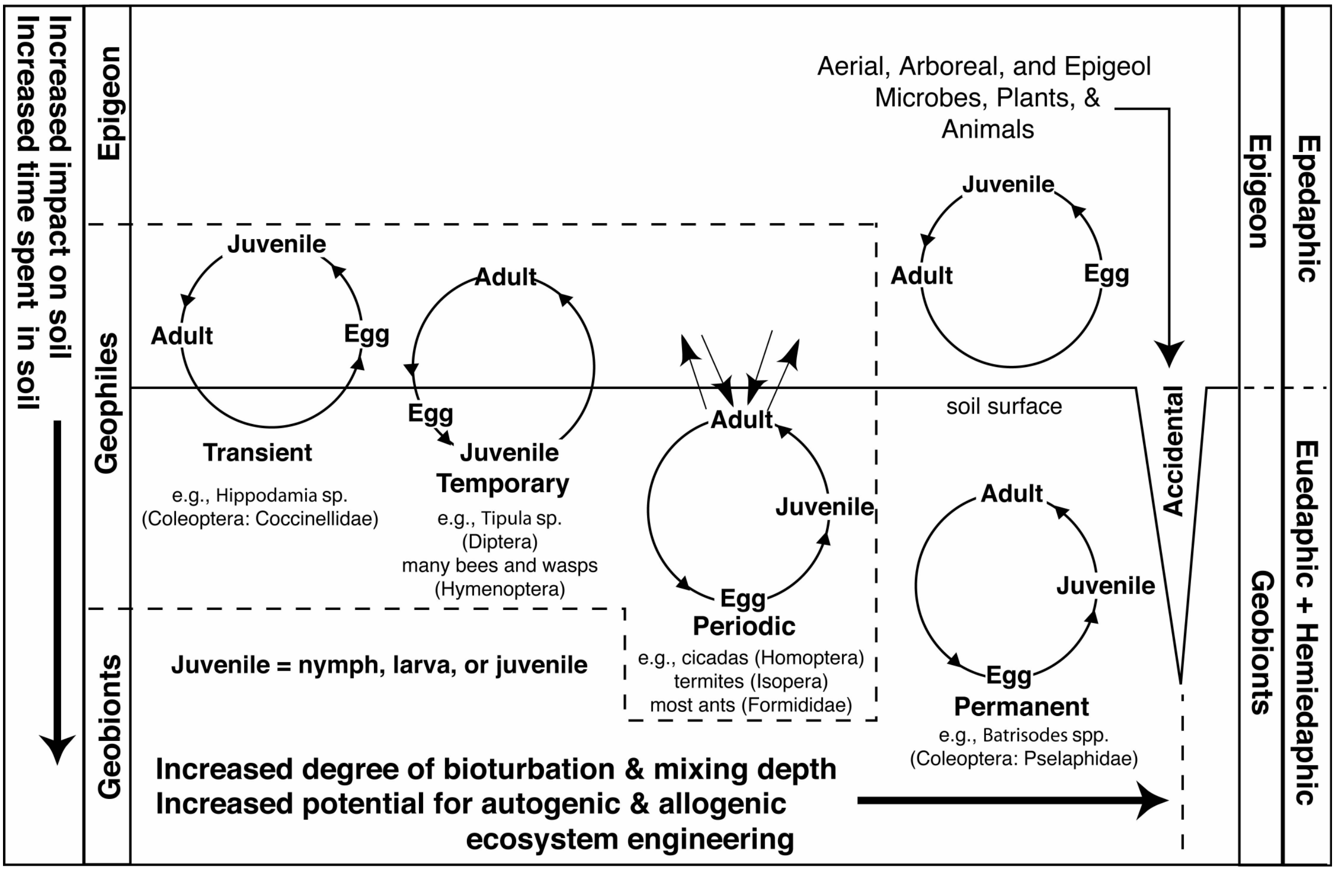

Figure 2. The presence of animals in soil and their impact on bioturbation, pedogenesis, and potential to act as ecosystem engineers (modified from Wallwork, 1970; Hole, 1981; Hasiotis, 2007).

Linking Trace Fossils to the Work of Animals in Paleosols in the Geological Record

Animals that inhabit modern terrestrial settings and play a role in soil formation are the result over 460 Ma of years of evolution. Many of stem groups of these organisms have their evolutionary roots in the mid- to late Paleozoic and early Mesozoic (Triassic) (Hasiotis, 2003, 2007; and references therein). Trace fossils of these animals, therefore, represent their activity and work in the same way that krotovina. Trace fossils, studied via their architectural and surficial morphologies and the material that fills them, record information about the tracemaker and the physicochemical conditions of its surroundings. Interpretation of the tracemaker is often inferred from the trace fossil and its relationship to the strata. Most importantly, these interpretations are also made via comparison to similar structures found in modern depositional systems and environments that are analogous to the geologic deposits. Such actualistic studies of the effects of termites, ants, dung beetles, wasps, crayfish, spiders, earthworms, and mammals on soil formation (e.g., Darwin, 1881; Wallwork, 1970; Johnson, 1981; Halfen and Hasiotis, this volume) have been used to interpret similar structures and their significance in the rock record, including earlier extensions of their fossil records (Hasiotis, 2003, 2007). For example, crayfish burrows have been identified in Triassic and possibly Permian rocks, and can be used to interpret the paleo-water table level. Meniscate backfilled burrows attributed to beetle larvae and cicada nymphs, by comparison to neoichnological experiments have been identified in Permian and Triassic paleosols (Counts and Hasiotis, 2009). The advantage to studying animal behavior and its effects on pedogenesis in paleosols is that diagenesis has enhanced the redoximorphic characteristics of biogenic and biogenically mediated pedogenic features.

Ecosystem Engineers and Geoengineers

Jones *et al.* (1994) defined ecosystem engineers as those organisms that create, modify, and maintain habitats by directly or indirectly modulating the availability of resources to other species. Two types of ecosystem engineers are defined: autogenic engineers that change the habitat via their own physical structures, and allogenic engineers that change the environment by shifting living or nonliving material from one physical situation to another. A variety of macro- and mesoscopic soil animals can be classified as both autogenic and allogenic ecosystem engineers because they bioturbate and redistribute soil material, create and destroy pedogenic structures and macrochannels-pores, and ventilate and irrigate soils. The result of this work is the creation of dynamic landscapes composed of soil mosaics, increase oxygenation of sediments, stimulate microflora and decomposition rates, and change and regulate the biophysicochemical properties of the sediment (e.g., Wallwork, 1970; Johnson, 1980). Animal trace fossils and their intimate association with the paleosols also preserve how their activity shaped the ancient landscapes in which they lived, and how above- and belowground ecosystems and soils evolved through time. Such soil animals as termites, ants, crayfish, burrowing mammals, and earthworms, therefore, should be considered geoengineers as they have well-documented trace fossil records in paleosols as far back as the Triassic and Jurassic, and in some cases as early as the late Paleozoic.

Conclusions

Terrestrial ecosystems, soil-forming factors, and the animals that bioturbate, turnover soil, and engineer the landscape are the result of nearly 4 Ga of evolution. The evidence that links the modern studies of soil formation and ecosystem nutrient cycling to the geological record of paleosols and the evolution of terrestrial ecosystems is preserved as microbial, plant, and animal trace fossils. Trace fossils in paleosols preserve the results of extensive bioturbation of sediments that lead to paleosols in which the animals continue to bioturbate. Results of neoichnological and soil biologic studies demonstrate that the structures and mixing produced by animals can be attributed to similar structures and fabrics preserved in paleosols. Future research should focus on work of modern animals and it produces pedogenic features, and its linkage to terrestrial trace fossils in continental deposits. Geologic studies should focus on the linkage between trace fossils and paleosols, and how those they can be used to interpret the biophysicochemical conditions under which those paleosols formed.

References

Counts JW, Hasiotis ST (2009) Neoichnological experiments documenting burrowing behaviors and traces of the masked chafer beetle (Coleoptera: Scarabaeidae: *Cyclocephala* sp.): Behavioral significance of extant soil-dwelling insects to understanding backfilled trace fossils in the continental realm. *PALAIOS* **24**, 75-92.

Darwin C (1881) 'The formation of vegetable mould through the action of worms, with observations on their habits.' (John Murray, London).

Halfen AF, Hasiotis ST (2010) Downward Thinking: Rethinking the "Up" in Soil Bioturbation. In 19th World Congress of Soil Science. (This volume).

Hasiotis ST (2003) Complex ichnofossils of solitary to social soil organisms: under- standing their evolution and roles in terrestrial paleoecosystems. *Palaeogeography, Palaeoclimatology, Palaeoecology* **192**, 259-320.

Hasiotis ST (2007) Continental ichnology: fundamental processes and controls on trace-fossil distribution. In Trace Fossils Concepts, Problems, Prospects. (Ed W Miller III), pp. 268-284. (Amsterdam, Elsevier Press).

Hole FD (1981) Effects of animals on soil. *Geoderma* **25**, 75-112.

Johnson DL (1990) Biomantle evolution and the redistribution of earth materials and artifacts. *Soil Science* **149**, 84-102.

Jones CG, Lawton JH, Shachak M (1994) Organisms as ecosystem engineers. *Oikos* **69**, 373-386.

Wallwork JA (1970) Ecology of Soil Animals. (McGraw Hill, London).